博 士 論 文

MULTI-CRITERIA EVALUATION OF A DISTRIBUTED ENERGY SYSTEM FOCUSING ON GRID STABILIZATION AND CARBON EMISSION REDUCTION

系統電力の安定化と炭素排出削減に焦点を当てた分散型エネルギーシステムの多基準評価に関する研究

北九州市立大学国際環境工学研究科

2021 年 2 月

張 麗婷

LITING ZHANG

Doctoral Thesis

MULTI-CRITERIA EVALUATION OF A DISTRIBUTED ENERGY SYSTEM FOCUSING ON GRID STABILIZATION AND CARBON EMISSION REDUCTION

February 2021

ZHANG LITING

The University of Kitakyushu
Faculty of Environmental Engineering
Department of Architecture
Gao Laboratory

Preface

DESs can save energy cost, reduce environmental impact and improve the reliability of the power grid. However, its high investment and improper capacity caused poor economic benefits. Moreover, the current evaluation method with a single criterion is relatively simple and one-sided, which cannot reflect the comprehensive benefits of the DES. Therefore, this research proposed a distributed energy system (DES) composed of photovoltaic, energy storage and gas engine, and its grid stabilization and carbon reduction potentials were analyzed. Focusing on these advantages, a multi-criteria evaluation method was established to optimize the system. Finally, different case study scenarios of the DES utilization were demonstrated. It is hoped to improve the core competitiveness of the DES and promote its development.

Acknowledgements

This work could not have been completed without the support, guidance, and help of many people and institutions, for providing data and insights, for which I am very grateful.

First, a special acknowledgment is given to my respectable supervisor, Professor Weijun GAO, for his support in many ways over the years and for giving me the opportunity to study at the University of Kitakyushu. He has exquisite academic skills and a rigorous work style, and friendly and amiable. His patient instruction and constructive suggestions are beneficial to me a lot. The thesis could not be finished without his guidance and help.

Second, particular thanks go to all the teachers and professors who have taught me for their instruction and generous support during these years. Also, I would also like to thank all university colleagues, Dr. Fanyue QIAN, who gives me guidance and research supports; and Ms. Dan Yu, Ms. Tingting XU, Ms. Xueyuan Zhao, and Ms. Zhonghui Liu from whom I get tremendous love and encouragement as well as technical instruction; moreover, Dr. Jinming JIANG, Mr. Daoyuan Wen also give me the help, cooperation, and supports of research and daily life in Japan.

Finally, I would like to express my deepest thanks to my parents for their loving considerations and great confidence in me that made it possible to finish this study.

Multi-criteria evaluation of a distributed energy system focusing on grid stabilization and carbon emission reduction

ABSTRACT

With the rapid growth in energy demand and concerns about climate change coupled with the depletion of fossil fuels, the countries around the world are looking forward to an alternative approach of more clean, efficient, and reliable energy consumption. As a clean and low emissions system located at or near its end-users characterized with poly-generation systems, the distributed energy system (DES) attracts increasing attention. However, the implementation of DES is still hindered mainly due to the high investment cost and improper design, caused by lack of a comprehensive evaluation. At present, the evaluation method of the DES is relatively simple and one-sided, which cannot reasonably and accurately evaluate the comprehensive benefits of the DES. Therefore, this study proposed a DES composed of photovoltaic, energy storage and gas engine, and its grid stabilization and carbon reduction potentials were analyzed. After that, a multi-criteria evaluation method is established and proposed to optimize the design of the proposed DES focusing on the grid stabilization and carbon emission reduction. Finally, two different case study scenarios of the DES utilization were demonstrated. It is hoped to improve the core competitiveness of the DES and promote its development.

In Chapter 1, RESEARCH BACKGROUND AND PURPOSE OF THE STUDY. Firstly, the significance of the DES for addressing the energy shortage and the environmental problem is expounded through the advantages of the DES. In addition, the current development status of the DES is investigated and the technologies that can be applied to distributed energy systems are introduced. The promotion difficulties of the distributed energy system are discussed as well. And the research purpose and structure process of this study are described in the final.

In Chapter 2, LITERATURE REVIEW OF THE DISTRIBUTED ENERGY SYSTEM. The research in the design and evaluation of the distributed energy system were reviewed. The DES is a complex system composed of multiple devices and can supply multiple energy sources, its configuration design and operation strategy determine the achievements of the system, which is the main research focus of the DES. Moreover, different evaluation methods will have a significant impact on the configuration and operation strategy of the distributed energy system. Therefore, the evaluation methods of the DES proposed by previous literature were sorted out.

In Chapter 3, THEORIES AND METHODOLOGY OF THE STUDY. In this part, the methodological research and the mathematic models were presented. Firstly, the

research motivation in this study was expounded. Then, the models of the proposed energy system were established. At the same time, the reliability, economic and environmental performance of the DES were quantitative analyzed. Moreover, the simulation models and algorithms used in the follow-up study were provided.

In Chapter 4, ECONOMIC AND ENVIRONMENTAL ANALYSIS OF DISTRIBUTED ENERGY SYSTEM FOCUSING ON GRID STABILIZATION. In order to explore the grid stabilization impact of distributed energy systems, two novel indices of the DES were proposed called “independence ratio” and “peak shaving ratio” to analyze the ability of self-supply and the effect of peak load reduction. And a DES model composed of photovoltaic, gas internal combustion engine and battery energy storage systems was established. Then, the impact of DESs with different combinations on the grid stabilization is analyzed by taking the Smart Community in Higashida, Japan as an example. After that, the economic and environmental performance of the DES with the economic optimal combinations were analyzed under different independence ratios and peak shaving ratios.

In Chapter 5, MULTI-CRITERIA ASSESSMENT FOR OPTIMIZING DISTRIBUTED ENERGY SYSTEM. Different configurations of the equipment will profoundly affect the performance of the distributed energy system, especially the grid stabilization and CO_2 emission reduction effect. A reasonable and comprehensive evaluation method is helpful to improve the core competitiveness of the DES. In this part, a multi-criteria evaluation method based on economic, reliability and environmental performance was proposed, and the effect of different evaluation criteria on the configuration optimization of each equipment in the distributed energy system was compared and analyzed. Firstly, the PV penetration is used as the variable to establish different configuration application scenarios of the DES. By introducing peak load price and carbon tax, the grid stabilization and carbon emission reduction effect were converted into economic benefits, and a configuration optimization model of the DES with the objective of minimizing the total cost was established based on the Genetic Algorithm. Then, compared with the obtained optimal combinations of the DES under different evaluation criteria, the impact of grid stabilization and emission reduction effect on the configuration optimization of equipment in the DES was analyzed.

In Chapter 6, PROMOTION AND UTILIZATION OF THE DISTRIBUTED ENERGY SYSTEM: A CASE STUDY OF COMBINED COOLING, HEATING AND POWER SYSTEM. As a typical DES, the utilization of the CCHP system and the impact of different factors on promoting the system were discussed. Firstly, according to the actual configuration of a CCHP system in an amusement park, three CCHP systems with different penetration were proposed and simulated by TRNSYS simulation software. Secondly,

the economic and environmental performance of these different penetration CCHP systems were evaluated based on the dynamic payback period and carbon dioxide emissions. Then, the impacts of investment cost, energy prices, investment subsidy, and a carbon tax on the promotion of the DES were discussed through the sensitivity analysis. Some advice on developing the DES were suggested according to the analysis results.

In Chapter 7, PROMOTION AND UTILIZATION OF THE DISTRIBUTED ENERGY SYSTEM: A CASE STUDY OF EMERGENCY POWER SYSTEM. The utilization of the DES as emergency power system was analyzed. The study is divided into two parts. Firstly, the integration of the stand-alone emergency power systems was optimized to improve the regional reliability with the least cost. Secondly, when the power failure in the whole region, the distributed generation was considered as emergency power to integrate with the emergency power system. The impact of different connected modes on the reliability and economic benefits of the overall power system is compared through four case studies. The reliability and cost-saving after application of the DESs were improved.

In Chapter 8, CONCLUSION AND PROSPECT. The conclusions of whole thesis were deduced, and the future work of distributed energy system was put forward.

張 麗婷 博士論文の構成

MULTI-CRITERIA EVALUATION OF A DISTRIBUTED ENERGY SYSTEM FOCUSING ON GRID STABILIZATION AND CARBON EMISSION REDUCTION

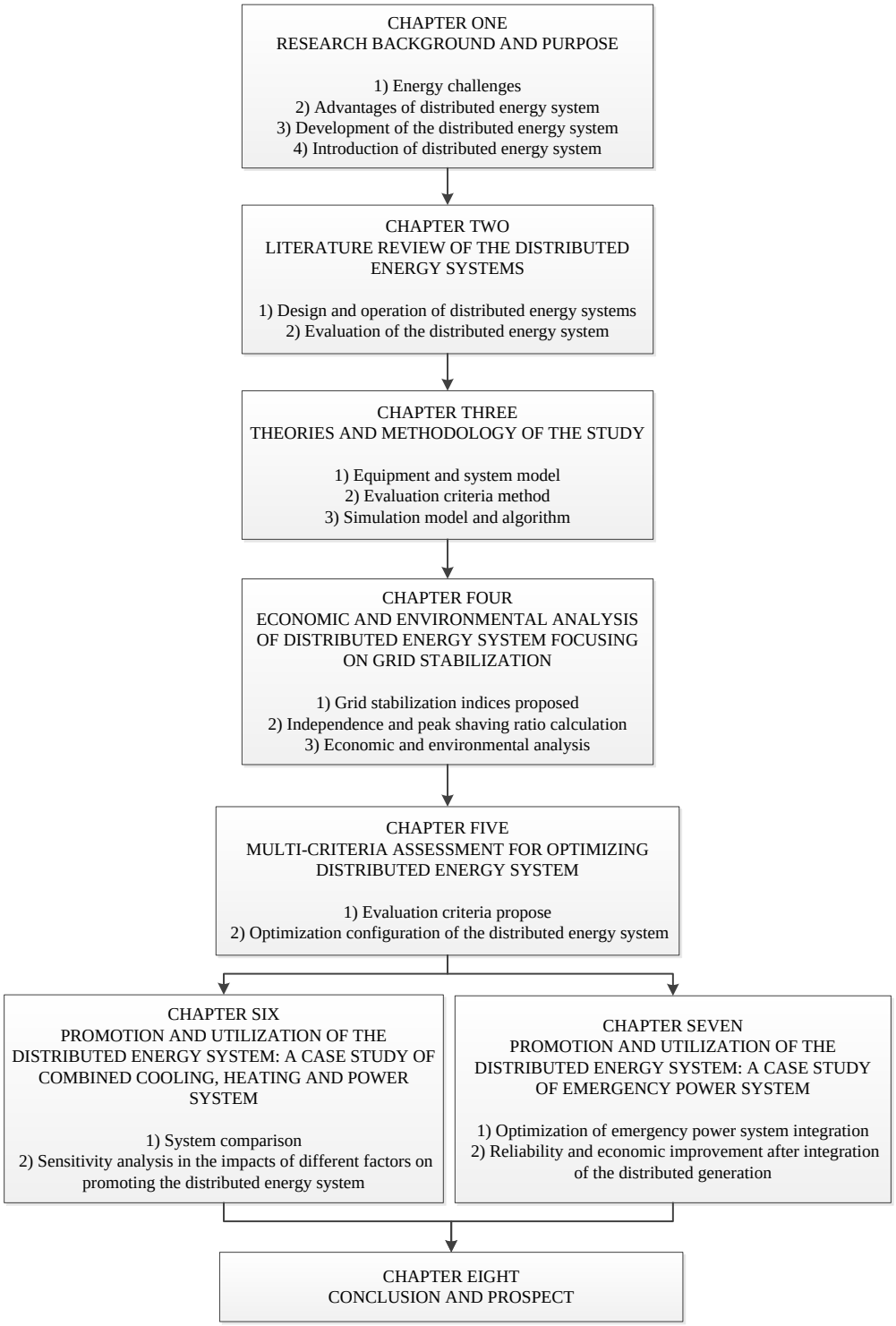

TABLE OF CONTENTS

ABSTRACT I
STRUCTURE OF THIS PAPER IV

CHAPTER 1: RESEARCH BACKGROUND AND PURPOSE OF THE STUDY

1.1 Background 1-1
1.1.1 Energy challenges 1-1
1.1.2 Advantages of distributed energy system 1-5
1.1.3 Development of distributed energy system 1-9
1.2 Distributed energy system 1-15
1.2.1 Technology of the distributed energy system 1-15
1.2.2 Promotion difficulties of the distributed energy system 1-19
1.3 Research structure and logical framework 1-20
Reference 1-24

CHAPTER 2: LITERATURE REVIEW OF THE DISTRIBUTED ENERGY SYSTEM

2.1 Overview of distributed energy system 2-1
2.2 Design and operation analysis of the distributed energy system 2-7
2.2.1 Optimal configuration design of the distributed energy system 2-7
2.2.2 Operation strategy of the distributed energy system 2-13
2.3 Evaluation of the distributed energy system 2-19
2.3.1 Economic performance of the distributed energy system 2-20
2.3.2 Environmental performance of the distributed energy system 2-23
2.3.3 Reliability performance of the distributed energy system 2-25
Reference 2-29

CHAPTER 3: THEORIES AND METHODOLOGY OF THE STUDY

3.1 Motivation 3-1
3.2 Model establishment 3-2
3.2.1 Devices and distributed energy systems model 3-2
3.2.2 Performance analysis 3-15
3.2.3 Simulation model and algorithm 3-20
Reference 3-24

CHAPTER 4: ECONOMIC AND ENVIRONMENTAL ANALYSIS OF THE DISTRIBUTED ENERGY SYSTEM FOCUSING ON GRID STABILIZATION

4.1 Content 4-1
4.2 Methodology 4-2
4.2.1 Distributed energy system model 4-2
4.2.2 The independence and peak shaving performance of distributed energy systems 4-4
4.2.3 The economic and environmental analysis of the distributed energy systems 4-5
4.3 Research object introduction and basic data 4-7
4.3.1 Research object 4-7
4.3.2 PV production 4-9
4.3.3 Study cases 4-10
4.4 The comparison results of the study cases 4-12
4.5 The economic and environmental analysis focusing on grid stabilization 4-14
4.5.1 Distributed energy system with PV and ICE 4-14
4.5.2 Distributed energy system with PV, ICE and BESS 4-16
4.6. Summary 4-21
Appendix 4-22
Reference 4-24

CHAPTER 5: MULTI-CRITERIA ASSESSMENT FOR OPTIMIZING THE DISTRIBUTED ENERGY SYSTEM

5.1 Content 5-1
5.2 Methodology 5-3
5.2.1 Operation strategy model of the distributed energy system 5-3
5.2.2 Evaluation criteria 5-5
5.2.3 Configuration optimization model 5-6
5.3 Research object and PV penetration prediction 5-8
5.4 Optimal design and comparison 5-12
5.4.1 The results under objective function of annual basic cost 5-12
5.4.2 The results under objective function of annual basic cost and peak load cost 5-16
5.4.3 The results under objective function of annual basic cost, peak load cost and CO_2 emission cost 5-19
5.4.4 The results comparison under three objective functions 5-21
5.5 Sensibility analysis 5-26
5.5.1 Peak load price change 5-26

5.5.2 Carbon tax change 5-27
5.6 Summary 5-30
Reference 5-31

CHAPTER 6: PROMOTION AND UTILIZATION OF THE DISTRIBUTED ENERGY SYSTEM: A CASE STUDY OF COMBINED COOLING, HEATING AND POWER SYSTEM

6.1 Content 6-1
6.2 Methodology 6-1
6.2.1 Establishment of the CCHP system model 6-1
6.2.2 Evaluation criteria 6-4
6.3 Case study 6-6
6.3.1 Introduction of the research case 6-6
6.3.2 Simulation model 6-9
6.4 Results and discussion 6-12
6.4.1 Simulation results of the energy consumption and generation 6-12
6.4.2 Comparison of economic and environment performance in three systems 6-16
6.4.3 Impact of different factors on the economic performance of CCHP system 6-18
6.4.4 Sensitivity analysis 6-23
6.5 Summary 6-24
Appendix 6-26
Reference 6-30

CHAPTER 7: PROMOTION AND UTILIZATION OF THE DISTRIBUTED ENERGY SYSTEM: A CASE STUDY OF EMERGENCY POWER SYSTEM

7.1 Content 7-1
7.2 Reliability and economic analysis of emergency power system integration 7-2
7.2.1 Overview of the Issues 7-2
7.2.2 Methodology of emergency power system optimization 7-3
7.2.3 Application of the emergency power system integration 7-11
7.2.4 Impact of characteristics parameters of EPSs on the total cost 7-16
7.3 Reliability and economic analysis of distributed generation as emergency power ... 7-18
7.3.1 Reliability analysis of power system 7-18
7.3.2 Case comparison 7-19
7.3.3 Results and discussion 7-23
7.4 Summary 7-28

Appendix 7-29
Reference 7-32

CHAPTER 8: CONCLUSION AND PROSPECT

8.1 Conclusion 8-1
8.2 Prospect 8-5

Chapter 1

RESEARCH BACKGROUND AND PURPOSE OF THIS STUDY

CHAPTER ONE: RESEARCH BACKGROUND AND PURPOSE OF THIS STUDY

RESEARCH BACKGROUND AND PURPOSE OF THIS STUDY *1-1*

1.1 Background 1-1

1.1.1 Energy challenges 1-1

1.1.2 Advantages of distributed energy system 1-5

1.1.3 Development of distributed energy system 1-9

1.2 Distributed energy system 1-15

1.2.1 Technology of the distributed energy system 1-15

1.2.2 Promotion difficulties of the distributed energy system 1-19

1.3 Research purpose and core content 1-20

Reference 1-24

1.1 Background

1.1.1 Energy challenges

Energy is an important material basis for human survival and civilization development, which is related to the national economy and people's livelihood and national strategic competitiveness. At present, economic globalization is facing a new situation, and the global energy production and consumption revolution is booming, in which energy science and technology innovation play a core leading role. The rational development of energy and scientific utilization are the necessary guarantee to realize sustainable development. With the development of human civilization, the demand for energy is sharply increasing. The energy consumption structure, which is mainly based on fossil fuels like coal and oil, has caused a series of energy crisis while promoting the progress and development of society.

1) Rapid depletion of fossil fuels

Since the dawn of the industrial revolution, fossil fuels have been the driving force behind the industrialized world and its economic growth. According to the Statistical Review of World Energy, the primary direct energy consumption of the fossil fuels from insignificant levels in 1800 to an output of nearly 140,000 TWh in 2019 (Fig.1-1). At present, about 85% of all primary energy in the world is derived from fossil fuels with oil accounting for 33.06%, coal for 27.04% and natural gas for 24.23% [1]. Global fossil fuel consumption is on the rise, and new reserves are becoming harder to find. Fig.1-2 shows the future energy reserves for coal, gas and oil.Those that are discovered are significantly smaller than the ones that have been found in the past. Oil reserves are a good example: 16 of the 20 largest oil fields in the world have reached peak level production – they're simply too small to keep up with global demand [2].

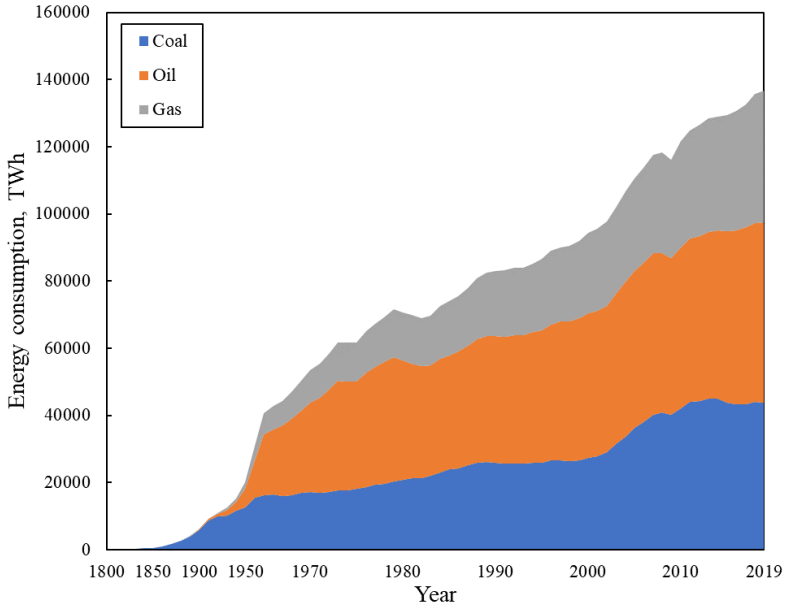

Fig.1-1 Global coal consumption, measured in terawatt-hours. (Resource: BP Statistical Review of World Energy: All data has normalised to terawatt-hours (TWh) using a conversion factor of 277.778 to convert from exajoules (EJ) to TWh.)

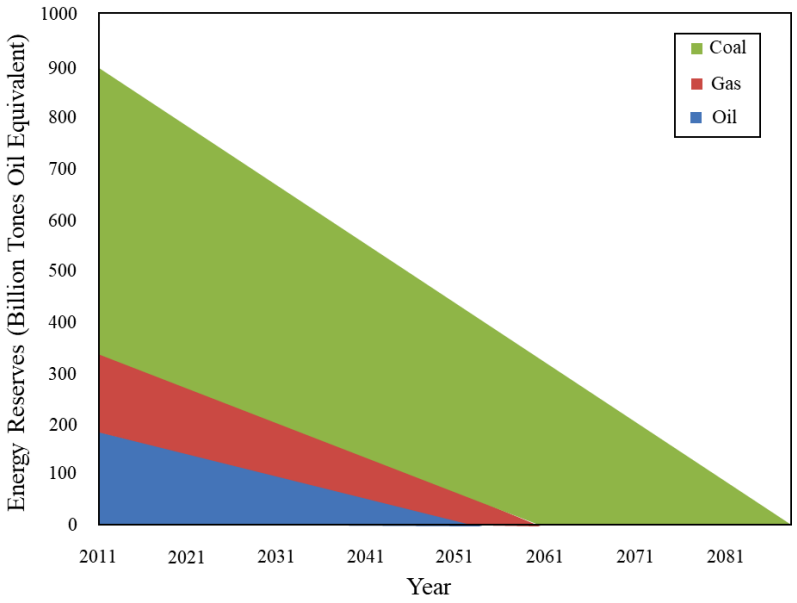

Fig.1-2 Future reserves for coal, gas and oil (Source: CIA World Factbook and Statista).

Globally, we currently consume the equivalent of over 11 billion tonnes of oil from fossil fuels every year. Crude oil reserves are vanishing at a rate of more than 4 billion tonnes a year – so if we carry on as we are, our known oil deposits could run out in just over 53 years. If we increase gas production to fill the energy gap left by oil, our known gas reserves only give us just 52 years left.Although it's often claimed that we have enough coal to last hundreds of years, this doesn't take into account the need for increased production if we run out of oil and gas. If we step up production to make up for depleted oil and gas reserves, our known coal deposits could be gone in 150 years [2].

2) Environmental deterioration

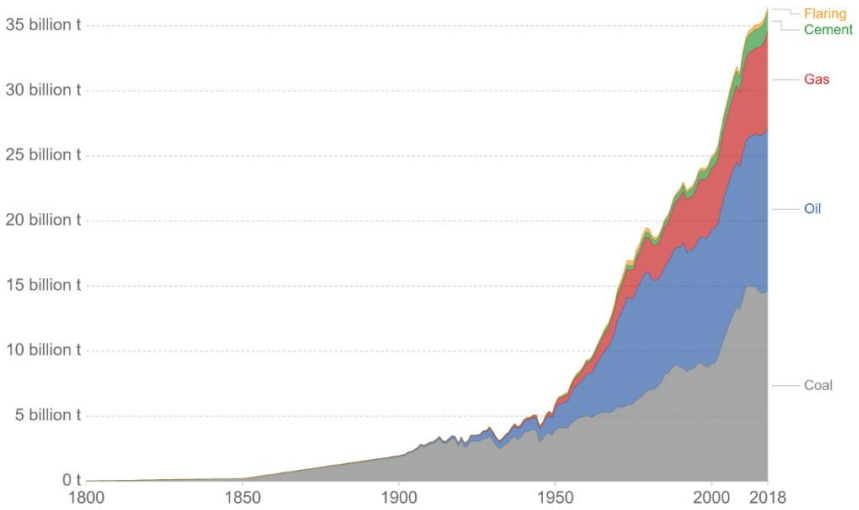

Fig.1-3 CO_2 emission trends from 1800 to 2018 by fuel type (Source: Global Carbon Project (GCP);CDIAC)

Global reliance on fossil energy is causing serious environmental deterioration. Fig.1-3 shows the CO_2 emission trends from 1800 to 2018 by fuel type [3]. The CO_2 emission from fossil fuel combustion is the largest largest contribution [4]. In 2018, nearly 35 billion tons of CO_2 were emitted from fossil fuel consumption and this has 3.5 times since 1950.

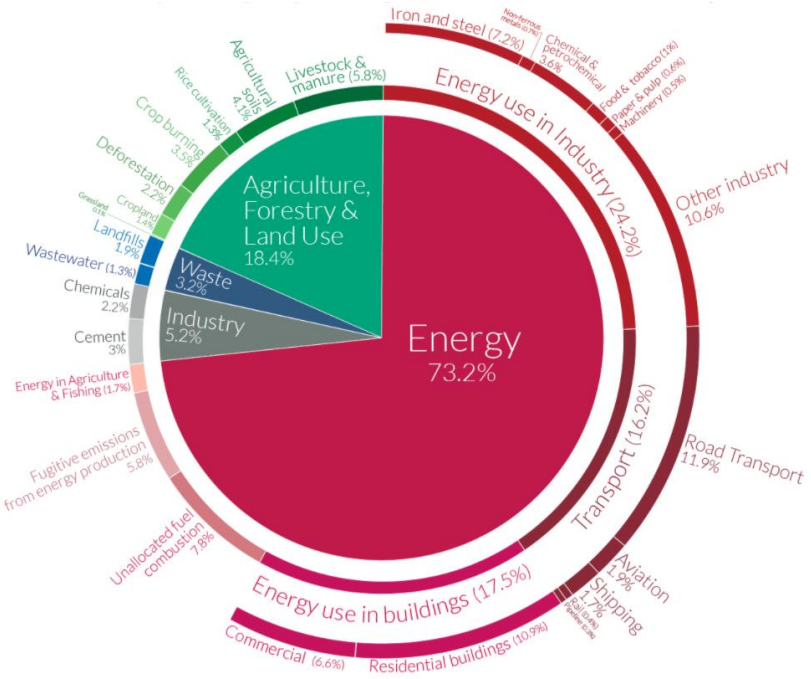

a) Global CO2 emissions by sector

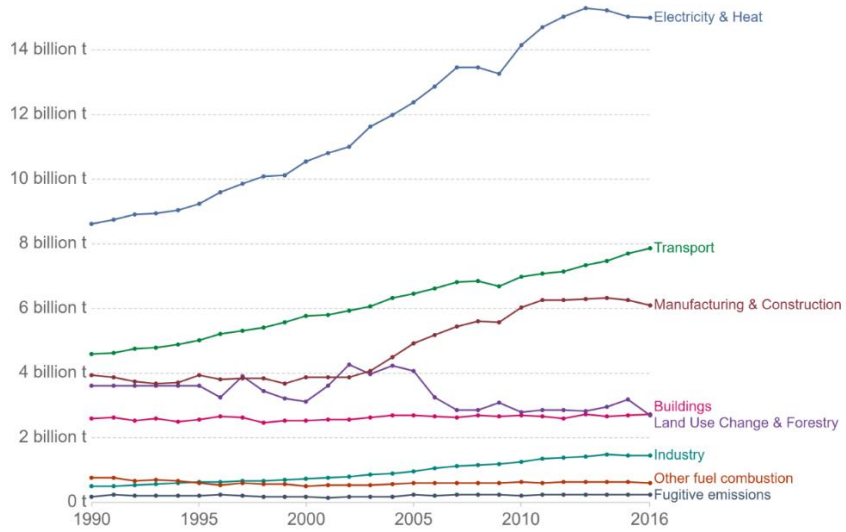

a) Annual CO_2 emissions by sector

Fig.1-4 Global CO_2 emissions (Source: (Source: CAIT Climate Data Explorer via. Climate Watch).

In fact, energy production is the dominating source of CO_2. Roughly 73% of all anthropogenic

CO_2 emissions derive from the energy sector, of which the energy consumption for electricity and heat is the main source of emissions (Fig.1-4) [5]. However, the current high-speed development of the economy will result in the continuous growth of power and heat demand. Energy demand will double by 2050. If the current proportion of fossil fuels remains the same, carbon emissions will certainly exceed the upper limit allowed to keep the global average temperature rise below 2℃. Such high emissions will have a disastrous impact on the global climate. The CO_2 emission increasing caused by excessive consumption of fossil energy leads to a series of environmental pollution problems such as air pollution, acid rain, greenhouse effect [6]. There is a growing body of evidence indicating that there will be challenges with supplying enough fossil energy for continued growth of economies and related emissions. The depeletion of fossil fuel has often been identified as a major challenge for the world in the 21st century together with anthropogenic climate change [7]. Therefore, there is a desperate need to find alternatives to fossil fuels and take advantage of state-of-the-art techniques to enhance energy efficiency and reduce emission.

3) Power grid insecurity

Electricity is at the heart of modern economies and it is providing a rising share of energy services. Demand for electricity is set to increase further as a result of rising household incomes, with the electrification of transport and heat, and growing demand for digital connected devices and air conditioning. The power systems based on fossil fuels, has the characteristics of large-scale and centralized. The network needed for its transmission and distribution is relatively complex. Most of the users are concentrated in a specific area, so the flexibility of load change and the safety of energy supply are poor. Once a small failure is happened in the supply chain, all users in the area are suffering electricity loss. This is troublesome because it could lead to supply inadequacy risks that cause more power outages, which can affect everything from national security and the digital economy to public health and the environment. For example, in 2003, a large-scale blackout occurred in Manhattan, New York City, USA, and then affected the eastern part of the United States and parts of Canada. The subway was shut down, the airport was closed, and even some people were trapped in elevators, which had a serious impact on people's normal life and industrial safety. Table 1-1 shows the large-scale power grid outages that have occurred over the years in the world [8,9]. It is indicated that the traditional energy supply has technical and security disadvantages.

Moreover, it is also a challenge for many countries that the existing power structure cannot support the rapid growth of power demand. For example, Japan's energy situation presents an unprecedented and severe situation after the 2011 East Japan Earthquake. The widespread shutdown of nuclear power plants has led to planned power rationing in parts of Japan during the peak period, and the problem of insufficient power supply in the power system has become increasingly prominent. Recognising the importance of rethinking Japan’s energy and power supply policies in the post-Fukushima era, the Government of Japan adopted an updated Strategic Energy Plan (the 4th Basic Energy Plan) in April 2014. This Plan provides a new course for Japan’s energy policy. Two basic principles are reflected in this Plan [10]. First, it reiterates the so-called “3E+S” focus of the nation’s energy policy, emphasising energy security, economic efficiency, and environmental protection without compromising safety. Second, it emphasises the need to look at both supply and demand side options by creating a supply-demand structure that is multi-layered, diversified, and flexible [11].

Table 1-1 Large-scale power grid blackouts and causes that have occurred over the years [8,9]

Time	Blackouts	Cause of accident	Load loss (GW)
August 10, 1996	Blackout in the western United States power system grid	High voltage line discharges to trees	30.5
August 14, 2003	Blackout in interconnected North America power system grid	Single line failure	61.8
September 28, 2003	blackout in Italy power system grid	Lightning strikes the tree causing a short circuit	14.21
July 1, 2006	Huazhong (Henan) Power Grid Accident	Substation differential protection device misoperation	2.6
November 4, 2006	Blackout in Western Europe power system grid	Exceeding the predicted trend and the overload caused by multiple network breaks	16.72
March 7, 2009	Shanghai grid short circuit event	Maintenance personnel misuse	1.435
2019.7.13	New York blackout	Transformer Fire	Lasts about five hours.

Facing the challenges of resource shortage, environmental pollution, energy insecurity and other energy crises, countries around the world are constantly exploring new areas of energy development. There are two key to reliaze the energy structure transition. One is to change the energy structure based on fossil energy, accelerate the development and utilization of renewable energy, and strive for diversified, cleaned, efficient energy supply and consumption; the second is to greatly improve the comprehensive utilization efficiency of energy to achieve the goal of a low-carbon and safe energy system estabilishment.

Distributed energy system (DES), a clean and low emissions system located at or near its end-users can accommodate high shares of renewable resources and is characterized with high-efficiency poly-generation systems. Currently, identified as an alternative approach of energy utilization to solve energy problems, the DES attracts increasing attention over these years.

1.1.2 Advantages of distributed energy system

Distributed energy system (DES) is the use of small-scale power generation technologies such as renewable energy resources, energy storage and so on located close to the load being served. meanwhile, multiple technologies are combined and complement each other,as shown in Fig.1-5. In different countries, the definition of DER system is different, for instance, the definition in China is “the DES is an energy system that intelligently combines distributed energy resources close to the consumer side, increases the reliability and economy of energy services, and reduces environmental

impact" [12]. The broader definition also includes other resources linked to the distribution network, such as combined heat and power (CHP) system or combined cooling heating and power (CCHP) system. As for the specific forms of distributed energy, it includes: natural gas distributed energy connected to the distribution network or located near the load center, distributed renewable energy and distributed energy storage, demand side response, energy efficiency technology and so on. Compared with the conventional energy supply system, the DES has several advantages.

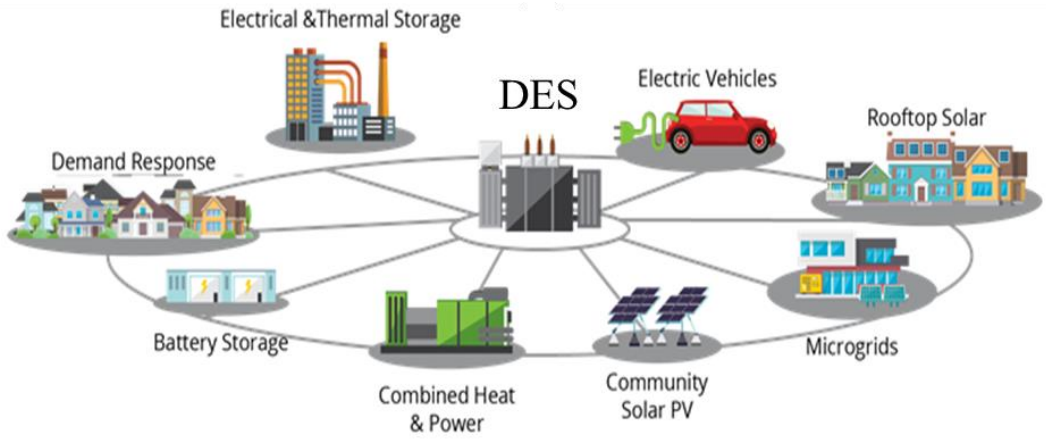

Fig.1-5 Schematic diagram of distributed energy system [13]

1) Close to the consumer side and variable capacity

As the general definition of the DES, the system is close to the consumer side or the energy resources. That is the electricity come form rather than another region or city, the resources located in the business, the hospitals, college campuses or the communities which near the them serve. The distributed energy sits at different position on the grid. Maybe it not at the center of the electricity supply system, but it can at any position that the customers need. The capacity of power generation devices can be changed according to the demand of the customers or other needed. Distributed generation allows me to use a variety of power generating technologies, decreasing my dependence on any one resource. With stock portfolios, organizations, and energy, there is strength in diversity.

2) Energy conservation and high-efficiency

Distributed energy system is considered to be an effective energy saving system. First of all, renewable energy can be widely used in distributed energy system to reduce the dependence on traditional fossil energy. Secondly, equipment such as combined heating and power (CHP) can be used to improve the efficiency of primary energy. Third, because the system is sited close to the customer and other characteristics can reduce energy waste in the transport process to save energy. Fig.1-6 depicts the comparison of the energy efficiency of separate power and heat supply and centralized supply. It can be seen that the natural gas distributed energy system will increase the separate supply from 55% to 87% through the cascade utilization of energy.

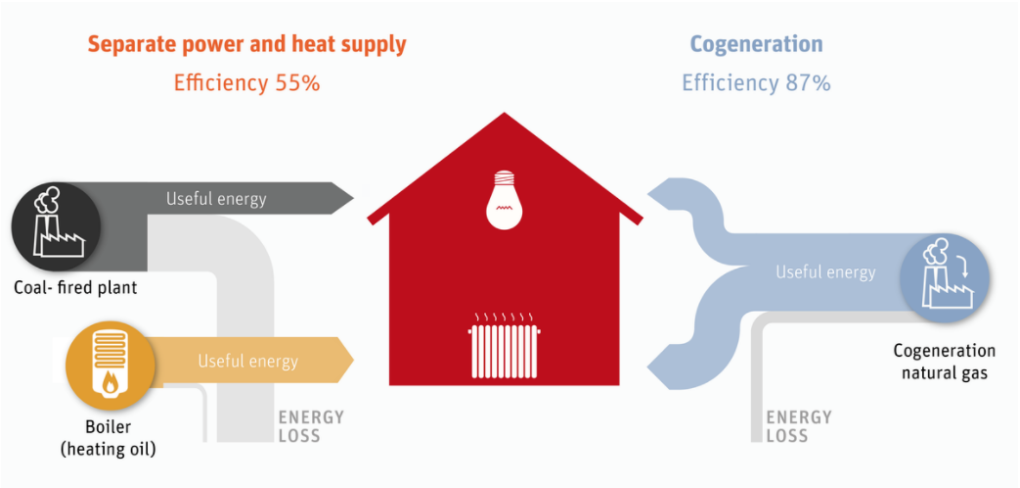

Fig.1-6 Comparison of the energy efficiency of cogeneration with conventional coal power plant and heating system [14]

3) Maximizing clean energy

In order to combat climate change effectively, the IEA promotes the use of renewable energies for electricity production as one important solution. Next to being just as reliable, renewables have two advantages in comparison to traditional fossil fuels: they are flexible and variable in use. As centralised fossil fuel utilities and nuclear plants start to phase out, they will make room for sustainable resources like solar power, wind and biofuels (and gas as a transition resource). Although both wind and solar are used for centralised power generation (e.g., offshore wind or solar farms), they have great potential to be employed as distributed source across any country. An intelligent grid architecture of combined and interconnected micro, mini and medium-sized grid structures allows the coexistence of many different electricity generating utilities. The distributed energy is more efficient than centralised generation and provides the appropriate architecture for the change to renewable energy supplies in the future. Looking ahead a few years, as old power plants become obsolete, this system would enable electricity generation to fall back into the hands of consumers, who also become producers (or prosumers). Policy-making in the energy sector should take this into account and make an informed choice for a more efficient, more reliable, cleaner and economically efficient future of electricity. Consumers and the environment will appreciate it.

4) Flexible controlling

Distributed energy system is considered as one of the effective controls means to adjust peak power consumption and reduce grid load. Power can be stored during peak hours through storage or other technologies, released during peak hours or replenished to balance the grid with power generation equipment. This management control is called peak shaving, one of the most important control of the DES. This helps the facility to reduce the demand charges and the utility by maintaining a constant demand during the day and at night.

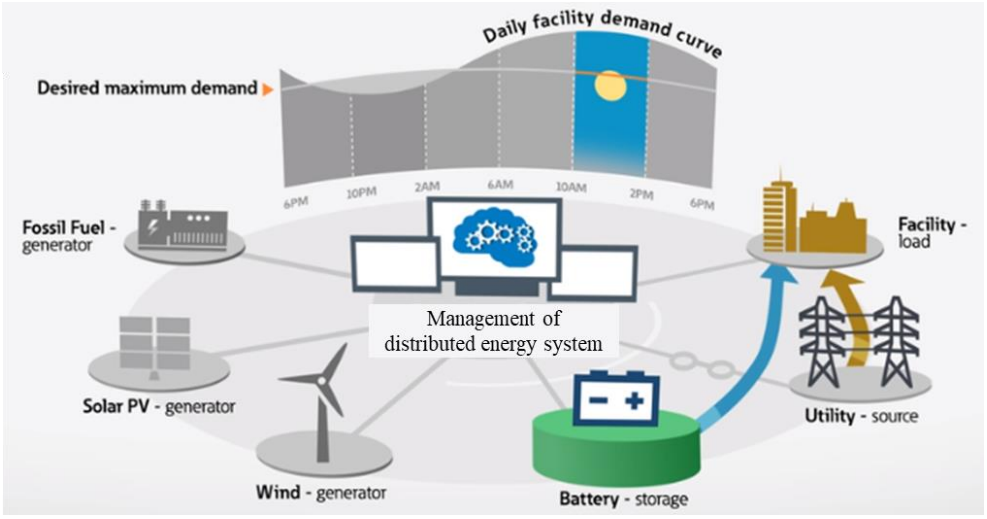

Fig.1-7 Schematic diagram of peak shaving of the DES [15]

5) Improving reliability

Distributed energy system can effectively improve the reliability of the power grid. And another contribution is to improve the energy resilience. The difference between energy reliability and energy resilience is that energy reliability refers to the ability to prevent system interruption, while energy resilience refers to the ability of the system to recover from an interruption. Massive power plants have to remain on-grid for most of their lifetime, distributed power generators can be used more flexibly and provide electricity when and where it is needed–if circumstances change, decentralised utilities offer much greater flexibility to adapt. This comes at great benefits for the overall resilience of the grid: distributed generation systems are able to “provide power to critical facilities during times of large-scale power disruptions and outages”. Distributed energy systems can have the ability to sell excess power to the grid or to provide the electricity to the grid in an emergency. As shown in Fig.1-8, the distributed energy system shows less vulnerable than centrilized energy system [16]. Storms, falling tree branches, brownouts, and acts of terror all threaten the grid, and when it fails, it typically leaves tens of thousands of customers (or millions in extreme cases) without power for long periods of time.

Distributed energy is distributed to the nearby load end, which can form an effective supplement to the traditional large power grid. The establishment of distributed energy microgrid in the load center of disaster prone areas can improve the power supply reserve, facilitate the black start after fault, and improve the overall disaster resistance and emergency power supply capacity of the power grid. As a supplementary form of large-scale power grid, in special cases (such as earthquake, snowstorm, flood, hurricane and other unexpected disasters), distributed energy microgrid can be used as backup power supply to support the receiving end grid; at the same time, distributed energy microgrid system can be quickly separated from the large power grid to form an isolated network, so as to ensure the uninterrupted power supply of important users. In natural disaster prone areas, through the layout and construction of different forms and scales of distributed energy microgrid, the power supply to important loads can be quickly restored on site after disasters[37].

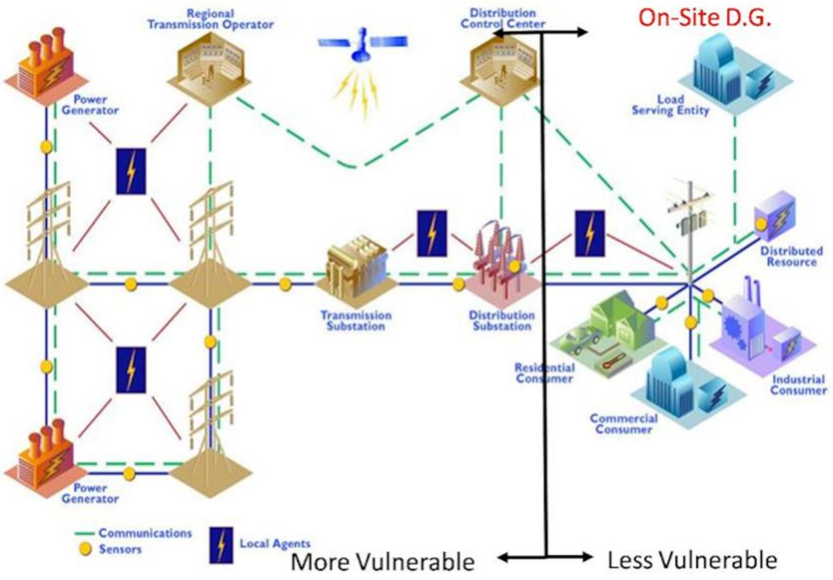

Fig.1-8 The vulnerablitiy comparison of centrilized and distributed energy system. (Source: US Department of Energy) [16]

1.1.3 Development of distributed energy system

Distributed energy is an efficient way to use distributed resources to meet the energy consumption demand of users nearby [17]. Due to the different user demand and energy development strategy in different periods, the development process of distributed energy can be divided into three stages: cogeneration, renewable energy integration and smart grid [18].

1) Cogeneration. Cogeneration started in the 1970s to improve the efficiency of energy utilization. The typical form of energy utilization is distributed natural gas cogeneration. In 1978, the United States promulgated the public utility management policy act to encourage the development of high-efficiency small-scale cogeneration power supply. In 1979, Denmark promulgated the "heating law" to develop cogeneration with natural gas and biomass as fuel. In 1981, Japan built the first gas multi generation project in the Tokyo National arena [19].

The combined cooling heating and power (CCHP) system can effectively improve the efficiency of energy utilization by cascade utilization of energy and providing electricity, heat, cold energy and domestic hot water to users. If the grid connected power energy complementary mode is adopted, the overall economic benefits and utilization efficiency of the system can be increased. Therefore, the development and application of CCHP is in line with the general trend of coordinated development of energy and environment [20]. CCHP is applied in developed countries such as the United States, Japan and the United Kingdom The CCHP system is different from the traditional centralized energy supply system and the primary energy is mainly natural gas. The comprehensive benefits in energy saving, environment improvement and power supply are more obvious. Therefore, through decades of development, the comprehensive energy efficiency and air quality of these countries have been improved unprecedentedly [21].

The U.S. government began to develop CHP/CCHP plants since 1978, when the Public Utility

Regulatory Policy Act (PURPA) was proposed. In the PURPA, utilities are required to interconnect with and purchase electricity from cogeneration systems, in order to give industrial and institutional users access to the grid and allow excess electricity to be sold back. With the help of the PURPA and the federal tax credit for CHP investment, the installed capacity of CHP/CCHP systems grew to 45 GW in 1995 from 12 GW in 1980 [22]. Due to the intense competition and instability in the electricity market, the development of CHP/CCHP plants slowed down in 1990s. Only 1 GW installed capacity increased from 1995 to 1998. To boost the development, together with the Environmental Protection Agency (EPA), the U.S. Department of Energy (DOE) proposed the "Combined cooling heating & power for buildings 2020 vision", which aimed to double the installed capacity in 2010. Following the proposed document, the installed capacity grew significantly to 56 GW in 2001. The mid-term goal of 2010 is to reduce the generation cost of distributed energy system, improve the energy comprehensive utilization efficiency and reliability of distributed energy system, and make the distributed energy system account for 20% of the newly installed generating capacity . Then in 2004, with a total installed capacity of 80 GW, the goal of 92 GW has been almost achieved. In 2009, after the Energy Policy Act in 2005, the installed capacity has achieved 91 GW . According to "the White Paper on CHP in a Clean Energy Standard" [23], the U.S. DOE aims to have an 11% increase, from current 9%, of CHP share of the U.S. electric power by 2030.. By 2020, the United States will achieve the goal of the world's most clean, efficient and safe country in terms of power production and transmission through the maximum use of distributed energy systems with good revenue. According to statistics, there are more than 6000 distributed cooling, heating and power generation stations in the United States, including more than 200 University distributed energy stations. According to the plan of the Department of energy, by 2020, more than 50% of the newly-built office buildings or shopping malls in the United States will adopt the mode of CO generation of cooling, heating and electricity. At the same time, 15% of the existing building energy supply systems will be retrofitted.

In the United Kingdom, the number and installed capacity of CHP/CCHP plants increased dramatically from 1999 to 2000, during which the UK government took methods of fiscal incentives, grant support, regulatory framework, promotion of innova- tion, and government leadership and partnership to support the development of CHP/CCHP. Before 2000, the installed capacity kept around 3.5 GW, while in 2000, it increased to 4.5 GW. From then on, the UK government continuously drafted a series of policies to target at achieving 10 GW of good quality installed CHP plants. In the end of 2010, the total installed capacity in the UK reached 6 GW [22].

Due to its geographical location, Japan is in short supply of domestic energy, so it pays special attention to the development and utilization of new energy and the improvement of energy utilization. In 1981, Japan's first domestic cooling, heating, and power cogeneration system was completed in Tokyo National Arena. Since then, Japan has also begun to vigorously develop distributed energy projects. In December 2005, the Kyoto Economic Energy Project was put into operation. This distributed energy supply system includes 50KW photovoltaic power generation, 50KW wind power generation, 5×80kW biological power generation and a 250kW fuel cell and 100KW battery. The system is reliable and safe, and has achieved good economic and environmental benefits.

2) Renewable energy. At the beginning of the 21st century, the average proportion of distributed

energy in the electricity market of EU is as high as 10%. According to the energy development plans of European countries, the utilization of distributed new energy is mainly promoted [24]. In 2000, Germany promulgated the renewable energy law to promote the development of new energy through flexible pricing mechanism. The scale of distributed new energy generation has exceeded that of distributed combined heat and power system. With the maturity of technology and the increase of clean and low-carbon demand, distributed new energy as an important way of new energy utilization has been widely concerned.

Renewable energy has the characteristics of clean, natural regeneration, wide area distribution, low energy density, intermittency and so on, and has the characteristics of obvious distributed energy in nature. Renewable energy does not exist the possibility of energy exhaustion. Therefore, the development and utilization of renewable energy has been paid more and more attention by many countries, especially in the countries with energy shortage. With the recovery of nuclear energy and the rapid development of renewable energy in the world, the development of clean energy is growing year by year, and its growth rate is second to natural gas. According to statistics, the global renewable energy consumption in 2017 increased by 16% compared with 2016, and maintained a double-digit growth rate. Among them, solar energy growth rate is 29.6%, wind energy growth rate is 15.6%. Taking nuclear, hydropower and natural gas into account, the global clean energy consumption ratio in 2017 reached 38%, which exceeded 28% of coal consumption and 34% of oil consumption. Fig.1-9 present the renewables share of power generation by region [1].

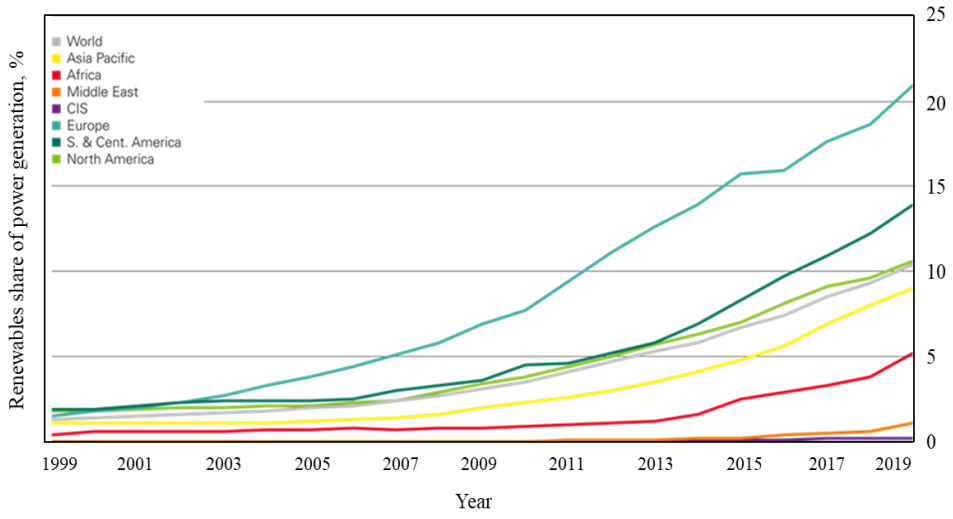

Fig.1-9 Renewables share of power generation by region (Percentage) (Source: BP Statistical Review of World Energy 2020)

At the same time, electricity generation structures also changed with the renewable energy development. Among the renewable energies, the solar and wind electricity generation is regarded as an important party in hybrid distributed energy resource (HDER) system. The photovoltaic (PV) and wind farms (WFs) can constitute a part of the power generation of HDER system, to meet the peak demand or storage the produced electricity to energy storage system for future utilization. Therefore, the development and application of solar PV and wind can promote the development of DES. The PV and wind electricity generation in some countries in 2016 and a predictive value in

2022 is shown in Fig.1-10. Fig.1-10 shows that only a few countries' electricity generation by the PV and wind is more than 10%, but the additional PV and wind share in 2022 present a good increasing of the two energy [25].

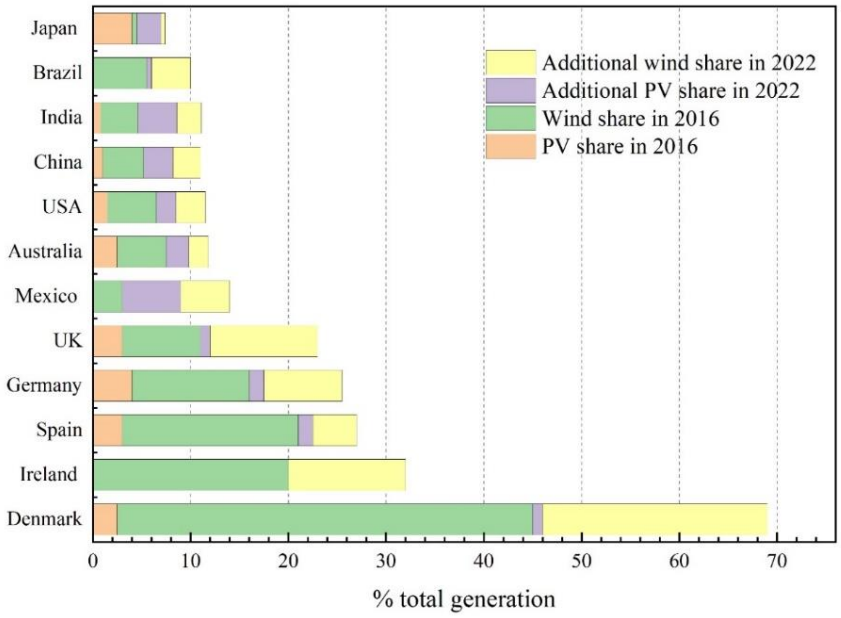

Fig.1-10 The PV and wind electricity generation in some countries in 2016 and a predictive value in 2022 (Source: RENEWABLES 2017. 2016 generation data for OECD countries based on IEA (2017b), World Energy Statisticsand Balances 2017, www.iea.org/statistics/)

Note: The shares represent variable renewable electricity generation as a percentage of total electricity output, not of total electricity consumption. In countries with high shares of variable generation, such as Denmark, generation and consumption differences may be large as a result of electricity trading.

Prior to the 2011 Fukushima earthquake, Japan's energy mix was highly dependent on coal and nuclear power, with minimal contributions from renewable energy technologies. In years preceding 2011, the renewable energy mix consisted mainly of hydropower and biomass. Following the Great East Japan Earthquake, Japan saw a major shift to oil and natural gas. In 2012, Japan implemented a Feed-in Tariff (FiT) for renewable energy production. The policy states that electric power companies are obliged to purchase electricity generated from renewable energy sources, on a fixed period contract at a fixed price. The implementation of the FiT has allowed capital investment for renewable energy supply to increase greatly. Fig.1-11 shows the renewable generation of Japan. This in turn has resulted in a major increase in the installation of solar photovoltaic. So much so that in both 2014 and 2015, Japan was one of the three largest solar installation markets [26]. Implemented in 2015, the Long-term Energy Supply and Demand Outlook provides a more detailed look into the consequences of the 2011 earthquake, and the future of Japan's energy mix. The policy also looks into the continued diversification of Japan's energy supply; away from fossil fuels and towards renewable energy technologies. The target states that by 2030, Japan's self-sufficiency rate aims to increase to approximately 24.3% [27]. The main aim of this target is to increase self-

sufficiency to levels greater than they were, prior to the 2011 earthquake. The 2015 Outlook also emphasises the importance of a well balanced power mix being implemented in order to achieve environmental suitability, economic efficiency, safety and a stable supply.

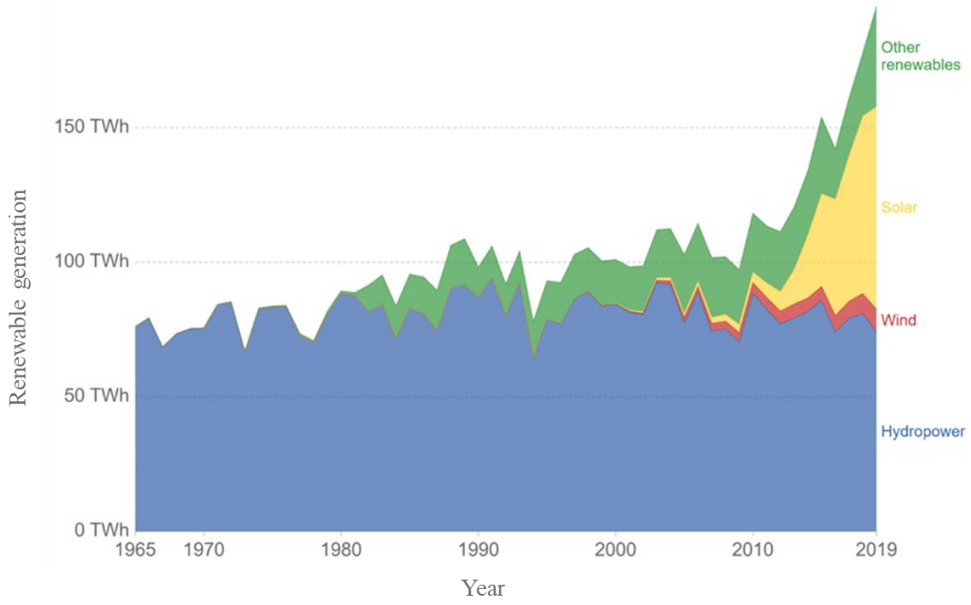

Fig.1-11 Renewable energy generation of Japan (Source: bp Statistical Review of World Energy 2020)

China has become a global leader in renewable energy. It has vast resources and great potential for future development. In 2013, China installed more new renewable energy capacity than all of Europe and the rest of the Asia Pacific region. China currently has the world's largest installed capacity of hydro, solar and wind power. The share of renewables in China's energy mix was 13% in 2010, including an estimated 6% traditional use of biomass, and 7% modern renewables. Hydro power (3.4%) and solar thermal (1.5%) accounted for most of China's modern renewable energy use. In 2015, the renewable sources provided 24% of its electricity generation, with most of the remainder provided by coal power plants. In 2017, renewable energy comprised 36.6% of China's total installed electric power capacity, and 26.4% of total power generation, the vast majority from hydroelectric sources [28]. Nevertheless, the share of renewable sources in the energy mix had been gradually rising in recent years. Fig1-12 shows the renewable generation of China. The main drivers for this shift are the increasing cost-competitiveness of renewable energy technologies and other benefits such as improved energy security and decreased air pollution. According to Energy Production and Consumption Revolution Strategy 2016-2030, by 2030, 50% of total electric power generation will be from non-fossil energy sources, including nuclear and renewable energy. Renewable energy will shift from meeting new electricity needs to replacing existing electricity needs that have been traditionally satisfied by thermal power productions. It is expected that renewable energy will become the main power source by 2030 [29].

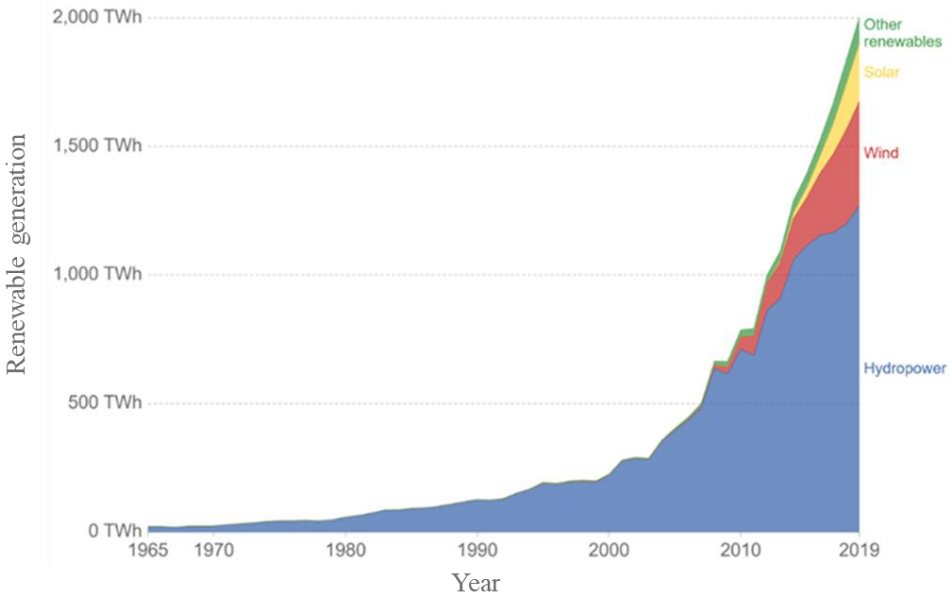

Fig.1-12 Renewable energy generation of China (Source: bp Statistical Review of World Energy 2020)

3) Smart grid. A report of the Navigant Research proposed that the DES will be a core role for the future deployment of energy infrastructure which is refer to the technology advances, business model innovation, changing regulations, and sustainability and resilience concerns [30]. Although sometimes controversial, distributed energy systems have had a significant impact on the popularity of the power industry. According to the report from the Navigant Research that the global DES investment capacity is expected to grow from 132.4 GW in 2017 to the 528.4 GW in 2026. With the continuous development of renewable energy and internet technology, distributed generation is developing towards the direction of multi energy complementary and integrated energy system. Smart grid are modern, localized, small-scale grids integrated use of digital technology with power grids[31,32]. Contrary to the traditional, centralized electricity grid (macrogrid), it can effectively integrate various sources of DES, especially Renewable energy sources. Germany has focused on the issue of multi-organic coordination. Australia has provided subsidies for the photovoltaic and energy storage system in rural and remote areas [33]. China has issued documents in recent 2 years to support the pilot projects of multi-energy complementary, integrated optimization, "Internet +", and intelligent energy. In recent years, Japan has proposed building a regional self reliance energy system and smart communities.

1.2 Distributed energy system

As we all known, distributed energy refers to a comprehensive energy utilization system distributed at the user end. It is a system that determines the unit configuration and capacity scale by optimizing the resources, environment and economic benefits. It pursues the maximization of terminal energy utilization efficiency, adopts demand-responsive design and modular combination configuration, which can meet various energy needs of users and optimize and integrate the supply and demand of resource allocation. The DES is a complex system, which is mainly reflected in the following points. 1) Multiple energy resources input and multiple energy output is a reason of the complex, for instance, the input resources can include fossil energy (oil, coal, natural gas, etc.), hydrogen (H2), biomass, solar energy, wind energy and so on; the multiple energy output may include the electricity, heating (for space heating, hot water and so on) and cooling. That may the DER system is more complex than the conventional power plant only uses one resource for power generation, or the thermal plant only uses one resource for the thermal generation. 2) The DES may consist of multiple devices and components. For instance, the power generation can adopt a variety of devices, like gas engine, gas turbine, fuel cell, reciprocating engine and so on; if the system should meet the heating and cooling demand, the heart recovery devices, absorption chiller, adsorption chiller, electrical chiller, solar thermal, geothermal thermal gas engine and so on; in order to overcome the fluctuation of energy supply, the power system must have certain energy storage capacity, the storage device can classify to electrical storage device and thermal storage device. In addition to the power generation device, thermal generation, thermal convention and energy storage devices, some auxiliary devices and components also constitute the complexity of system, like DC-DC converter, DC-AC converter, pump, fans, pipe, wire and so on.

We can understand distributed energy systems from the perspective of distributed energy conversion and classification of distributed energy systems, as shown in Fig.1-13.

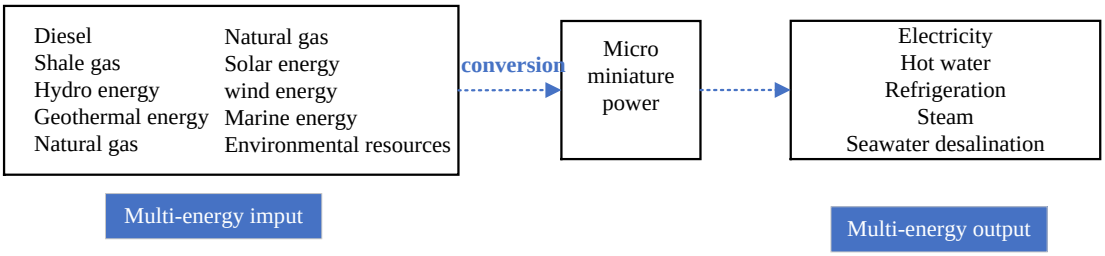

Fig.1-13 Flow chat of distributed energy conversion

1.2.1 Technology of the distributed energy system

Mudathir Funsho Akorede et al. [34] presented a block diagram of the main technologies of DER system is shown in Fig.1-14.

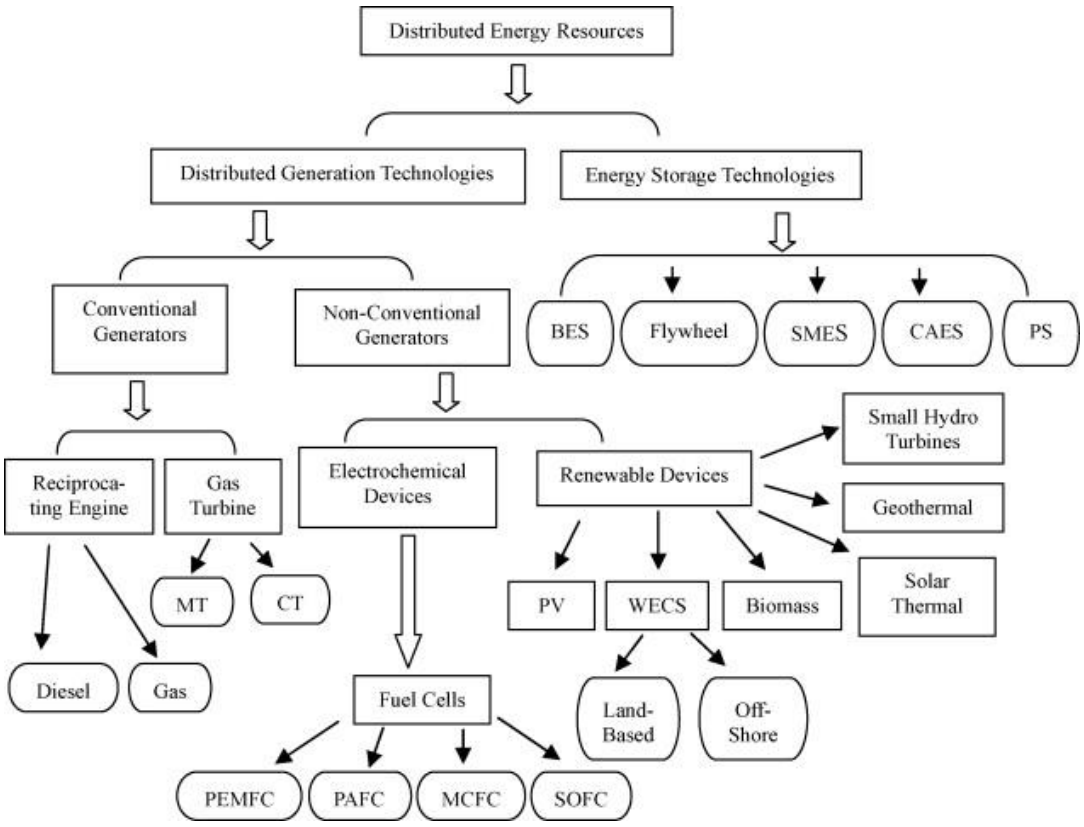

Fig.1-14 The main technologies of DER system [34]

(Notes: MT: Micro-turbines; CT: Combustion turbines; WECS: Wind energy conversion system; BESS: Battery energy storage system; SMES: Superconducting magnetic energy storage; CAES: Compressed air energy storage; PS: Pumped storage; PEMFC: proton exchange membrane fuel cell; AFC: alkaline fuel cell; PAFC: phosphoric acid fuel cell; SOFC: solid oxide fuel cell; MCFC: molten carbonate fuel cell)

(1) Solar energy power generation

Conversion of solar energy directly to electricity has been technologically possible since the late 1930s, using photovoltaic systems (PVs). These systems are commonly known as solar panels. PV solar panels consist ofdiscrete multiple cells, connected together either in series or parallel, that convert light radiation into electricity. PV technology could be stand-alone or connected to the grid. Solar photovoltaic power generation is a power generation method that uses the photovoltaic effect of solids (semiconductors) to directly transfer light energy to electrical energy. The solar photovoltaic power generation system consists of three parts: solar panels, batteries, and controllers. The continuous reduction of manufacture cost, solar photovoltaic power generation will present a good development prospect.

(2) Wind power generation

Power generation is the main form of wind energy utilization. Wind turbines can be powered either individually or in combination with other forms of power generation, such as diesel generators or micro-gas turbines, to supply power to a unit or an area, or to integrate power into conventional

grid operations. Windmills or wind turbines convert the kinetic energy of the streaming air to electric power. Investigation has revealed that power is produced in the wind speed of 4–25 m/s range [35]. The size of the wind turbine has increased rapidly during the last two decades with the largest units now being about 4 MWcompared to the 1970s in which unit sizes were below 20 kW. For wind turbines above 1.0 MW size to overcome mechanical stresses, they are equipped with a variable speed system incorporating power electronics. Single units can normally be integrated to the distribution grid of 10–20 kV, though the present trend is that wind power is being located off shore in larger parks that are connected to high voltage levels, even to the transmission system. The power quality depends on the system design. Direct connection of synchronous generators may result in increased flicker levels and relatively large active power variation. At present, wind energy has been found to be the most competitive among all renewable energy technologies.

(3) Gas turbines (GT)

A gas turbine, otherwise known as a combustion turbine, is a rotary engine that extracts energy from a flow ofcombustion gas. It has a combustion chamber in-between the upstream compressor coupled to a downstream turbine. Gas turbines are generally divided into three main categories, namely: heavy frame, aeroderivative, and micro-turbine. The technology is largely based upon aircraft auxiliary power units and automotive style turbo chargers [36]. Energy is added to the gas stream in the combustor, where air is mixed with fuel and ignited. Combustion increases the temperature, velocity and volume ofthe gas flow. This is directed through a nozzle over the turbine's blades, spinning the turbine and powering the compressor. Energy is extracted in the form of shaft power, compressed air and thrust, in any combination, and used to power aircraft, trains, ships, generators, and even tanks [9].

(4) Fell cell

Fuel cell is a kind of power generation device which can convert the chemical energy of hydrogen and other fuels into electrical energy directly through electrochemical reaction without combustion. Because fuel cell does not involve combustion and is not limited by Carnot cycle, the energy conversion rate is high [37]. In addition, the fuel cell does not use mechanical transmission parts and has no noise pollution; the reaction products are mainly electricity, heat and water, and the emission of harmful gases is very little. Therefore, fuel cell is an efficient, environment-friendly, high reliability, quiet energy conversion mode, which is one of the research hotspots in the field of energy. Fig.1-14 is a system block diagram of fuel cell power plant.So far, many types of fuel cells have been developed, and there are many classification methods. According to the types of electrolytes, they can be divided into five categories: alkaline fuel cell, phosphoric acid fuel cell, proton exchange membrane fuel cell, molten carbonate fuel cell and solid oxide fuel cell [38].

(5) Energy storage

Energy storage technology can meet the demand of electric energy or thermal / cold energy for a period of time by storing electric energy, which has the functions of peak shaving and valley filling, frequency and voltage regulation, smooth transition and reducing grid fluctuation [39]. Energy storage technology can solve the problem of intermittent renewable energy limited by environmental factors, and ensure the balance of supply and demand of energy system [40]. According to the

different energy storage principles of energy storage technology, energy storage technology can be divided into physical energy storage, electrical energy storage and heat storage technology [41]. Fig.1-15 shows the statistical results of the relative development of different energy storage technologies. At present, more energy storage technologies are in the stage of technology development and market demonstration. By the end of 2017, the total installed capacity of energy storage projects has reached 175.4gw. Among them, the most mature commercial pumped storage accounts for the largest proportion of installed capacity, accounting for 96%; the installed capacity of electrochemical energy storage is 2.93GW, accounting for only 1.7%.

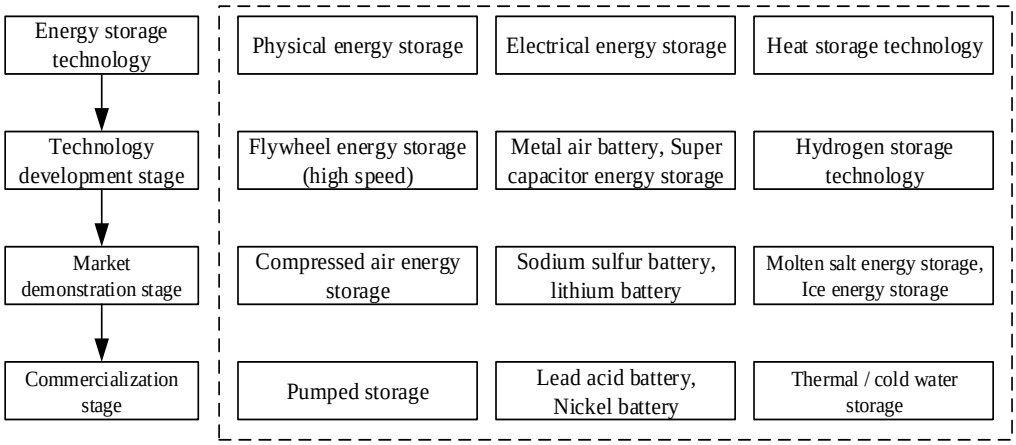

Fig.1-15 Development of different energy storage technologies.

(6) cooling, heating and power (CCHP) distributed energy system

The cooling, heating and power (CCHP) distributed energy system is mainly composed of power generation equipment, waste heat utilization equipment, peak shaving equipment and relevant main and auxiliary equipment, which is the use of heat engine or power station from a single fuel or energy source near the user side at the same time to produce electricity and heat to meet the changing needs of users [42]. The power generation unit (PGU) provides electricity for the user. Heat, produced as a by- product, is collected to meet cooling and heating demands via the absorption chiller and heating unit. If the PGU cannot provide enough electricity or by-product heat, additional electricity and fuel need to be purchased to compensate for the electric gap and feed the auxiliary boiler, respectively. In this way, three types of energy, i.e., cooling, heating and electricity, can be supplied simultaneously. A well-designed gas cooling, heating and power distributed energy system should balance the cost saving, improve the comprehensive utilization efficiency and energy saving rate of primary energy, and reduce pollutant emissions.

This kind of combined systems can exhibit excellent energy, environmental and economic performance. Indeed, feeding different technologies with different fuels for producing different energy vectors gives birth to a variety of alternatives for more effective design and planning of the energy systems. In addition, the possibility of co-generating hydrogen and of using it as a storage energy vector, in case exploiting volatile electricity production from renewable sources such as wind or sun, represents a further variable that could be advantageously exploited. Hence, the possible benefits from the combined production of multiple energy vectors (e.g., electricity, heat, cooling, hydrogen, or other chemical products) paves the way to future scenarios focused on the development

of multi-generation (or poly- generation) solutions [43].

1.2.2 Promotion difficulties of the distributed energy system

Due to the advantages of high efficiency, energy conservation and environmental protection, distributed energy system has been vigorously developed by the government. However, the practices of DES have shown that the actual operation performance is not as good as expected in many cases. Nearly half of the more than 40 DES projects in China have been out of service due to economic problems [44]. There are some main barriers:

1) Economic aspect:

Even though lower fuel and operating costs may make the DES cost competitive on a life-cycle basis, higher initial capital costs can mean that the DES provides less installed capacity per initial dollar invested than conventional energy system. Thus, investments of the DESs generally require higher amounts of financing for the same capacity. Depending on the circumstances, capital markets may demand a premium in lending rates for financing the DES projects because more capital is being risked up front than in conventional energy projects [45].

2) Technology aspect:

The unreasonable capacity of the system equipment is the most important issue. Distributed energy supply system has a wide range of optional system forms, main and auxiliary equipment and their capacity. There is no universally applicable technical scheme. Its configuration is closely related to the climate characteristics, load demand, energy price and supply of the user's area, which puts forward high requirements for the system configuration determination. For the optimal configuration of regional distributed energy supply system, the main task is to determine the system structure and form reasonably, optimize the type, capacity and number of main equipment, and obtain the comprehensive performance of economic, environmental and other aspects of the whole year, so as to provide decision-making reference for owners, provide selection basis for design, and provide guidance for operation strategy formulation. Improper configuration of distributed energy supply system will lead to waste of equipment investment, failure to give full play to economic benefits, low system operation efficiency and other problems, and even lead to system failure in extreme events .

3) Evaluation aspect:

The economic performance of the DES can be directly reflected through quantitative indicators such as annualized cost or payback period, but the social benefits brought by the advantages of energy-saving, environmental protection and improving the reliability of the power grid can not be directly compared with the economic benefits. As a result, the current evaluation method of the DESs usually uses energy-saving or economic benefits only, which is relatively simple and one-sided [46,47]. The single criterion cannot reasonably and accurately reflect the comprehensive benefits of the DESs. Energy efficiency, economic sustainability and environmental protection are the most important aspects of the distributed energy system. However, as they often mutually influence each other, how to reach a reasonable compromise is critical [44]. A considerate evaluation method from multiple perspectives is needed for helping the promotion of the DESs.

1.3 Research purpose and core content

1.3.1 Research purpose and core content

The research purpose and logic of the article is shown in Fig.1-16 below. From the energy challenges of the energy shortage, environmental problems, and insecurity of power grid, this research explores the application potential in the grid stabilization and carbon emission reduction of distributed energy system. And a multi-criteria evaluation is proposed to optimize the design of the distributed energy system to improve the core competitiveness of the distributed energy system. Finally, different case study scenarios of the DES utilization are demonstrated. It is hoped to provide help for the promotion of distributed energy system.

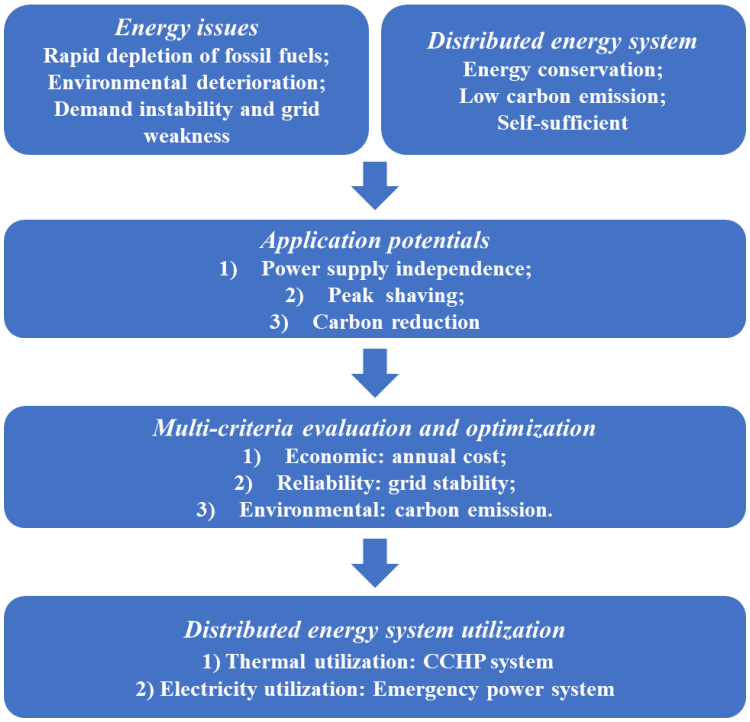

Fig. 1-16 Research logic of the article

1.3.2 Chapter content overview and related instructions

The chapter names and basic structure of the article are shown in Fig.1-17. The brief chapters introduction are shown in Fig.1-18.

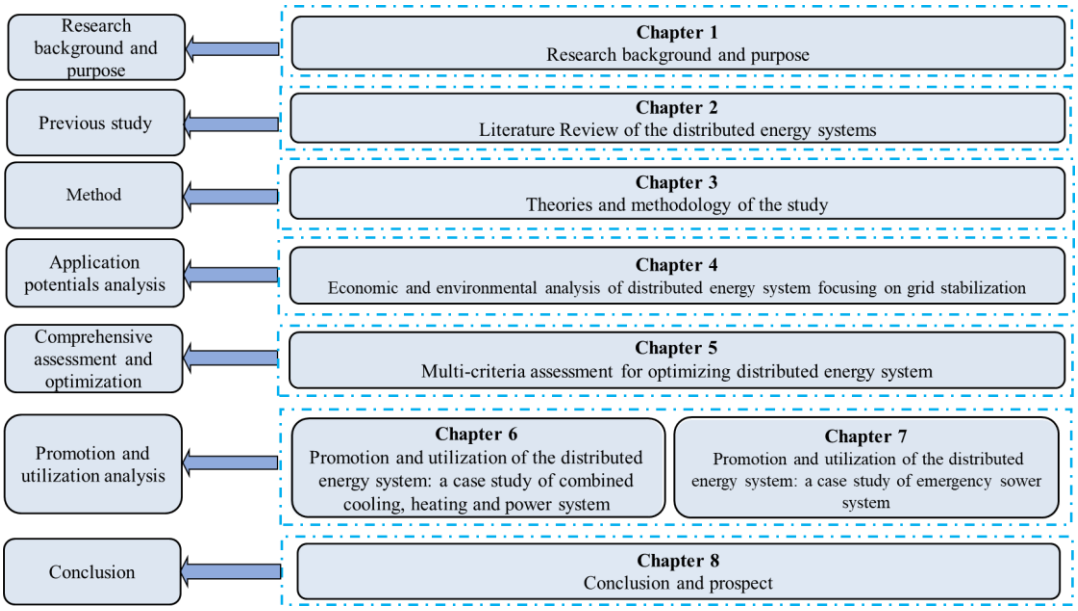

Fig.1-17 Chapter name and basic structure

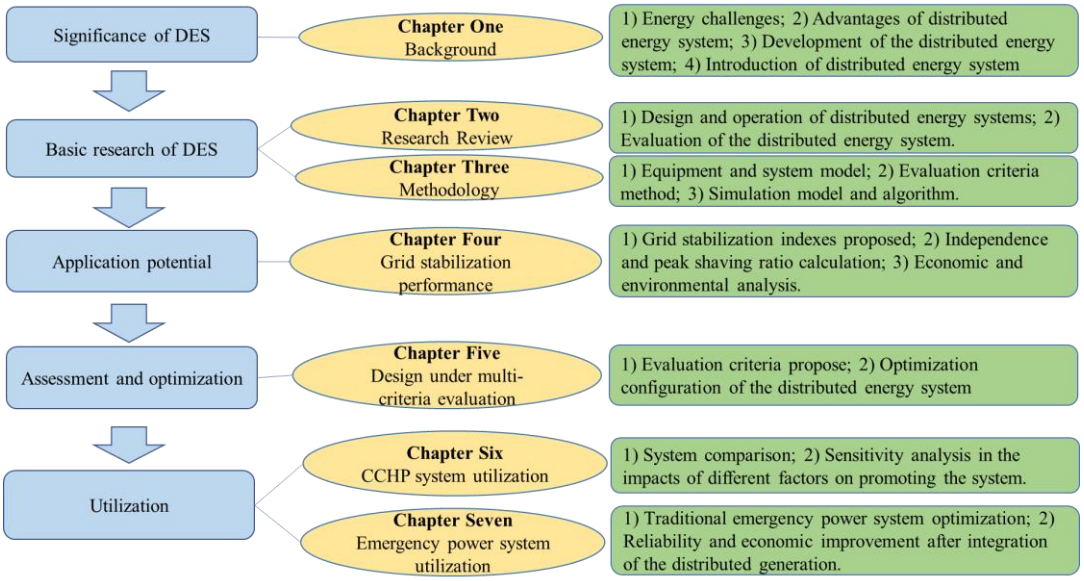

Fig.1-18 Brief chapter introduction

In Chapter 1, Research Background and Purpose of the Study:

With the rapid growth in energy demand, concerns about climate change, high prices of fossil fuels and the depletion of fossil fuels, the distributed energy system has been playing proactive roles in sustainable energy development. In view of the current energy problems, the significance of the distributed energy system for future energy development is discussed in this chapter. In addition, the current development status of the distributed energy system is investigated and the technologies that can be applied to distributed energy systems are introduced. The promotion difficulties of the distributed energy system are discussed as well.

In Chapter 2, Literature review of the distributed energy system:

This part is mainly to sort out the research status of the distributed energy system. Design and evaluation are the most important aspects for application of the distributed energy system. Because the distributed energy system is a complex system composed of multiple devices and can supply multiple energy sources, its configuration design and operation strategy determine the achievements of the system. Moreover, different evaluation method will have a significant impact on the configuration and operation strategy of the distributed energy system. A reasonable evaluation method can accelerate the development of the distributed energy system. Therefore, the research in design and evaluation of the distributed energy system are reviewed.

In Chapter 3, Theories and methodology of the study:

This chapter presents the methodological research and established the mathematical model. Firstly, the research motivation in this study is expounded. Then, the equipment models of the proposed energy system are established. At the same time, the reliability, economic and environmental performance of the DES were quantitative analyzed to evaluate the application effect and optimize the configuration of the equipment in the distributed energy system. Moreover, the simulation models and algorithms used in the follow-up study are provided.

In Chapter 4, Economic and environmental analysis of distributed energy system focusing on grid stabilization:

In this chapter, two novel indices of the distributed energy system on the grid stabilization effect are proposed called “independence ratio” and “peak shaving ratio” to analyze the ability of self-supply and the effect of peak load reduction. In order to explore the impact of distributed energy systems on the grid, this chapter establishes a distributed energy system model composed of photovoltaic, gas internal combustion engine and battery energy storage systems. Then, the impact of distributed energy systems with different combinations on the independence ratio and peak shaving ratio is analyzed by taking the Smart Community in Higashida, Japan as an example. After that, the economic and environmental performance are analyzed under different grid stabilization indices under the optimal combination of the distributed energy system with the least cost.

In Chapter 5, Multi-criteria assessment for optimizing distributed energy system:

A multi-criteria evaluation method of the distributed energy system is proposed taking the economy, reliability and environment into consideration, and the effect of different evaluation criteria on the configuration optimization of each equipment in the distributed energy system is compared and analyzed. Different configurations of the equipment will profoundly affect the grid stabilization and CO_2 emission reduction effect of the distributed energy system. Therefore, the PV penetration is used as the variable to establish different configuration application scenarios of the distributed energy system. After converting the grid stabilization and carbon emission reduction effect into the economic benefits by introducing peak load price and carbon tax, a configuration optimization model of the distributed energy system with the objective of minimizing the total cost is established based on the Genetic Algorithm. Then, the optimal combination of the distributed energy system under different evaluation criteria is obtained and compared to analyze the impact of grid stabilization and carbon emission reduction effect on the configuration optimization of

equipment in the distributed energy system.

In Chapter 6, Promotion and utilization of the distributed energy system: a case study of combined cooling, heating and power system:

The combined cooling, heating and power system (CCHP system) is a typical DES, which is identified as a sustainable energy development with its high efficiency. The utilization of the CCHP system and the impact of different factors on promoting the system were discussed in this chapter. A actual CCHP system of an amusement park is used as an example. Firstly, according to the actual configuration of the system, three CCHP systems with different penetration are proposed and simulated by TRNSYS simulation software. Secondly, the economic and environmental performance of these different penetration CCHP systems are evaluated based on the dynamic payback period and carbon dioxide emissions. Then, the impacts of investment cost, energy prices, investment subsidy, and a carbon tax on the promotion of the distributed energy system are discussed through the sensitivity analysis.

In Chapter 7, Promotion and utilization of the distributed energy system: a case study of emergency power system:

The utilization of the DES as emergency power system under the power outage scenario in the improvement of the reliability and cost saving is analyzed. The study is divided into two parts. Firstly, the integration of the stand-alone emergency power systems is optimized to improve the regional reliability with the least cost. To achieve this purpose, an integration and dispatch model is proposed by connecting the stand-alone emergency power subsystems with the micro-network and backing up each other. Secondly, when the power failure in the whole region, the distributed generation is considered as emergency power to integrate with the emergency power system. The impact of different configurations and connection modes of the gas internal-combustion engine and diesel generators on the reliability and economic benefits of the overall power system is compared through four case studies.

In Chapter 8, Conclusion and Prospect:

This part summarizes the research of previous chapters. And based on the conclusions, the future development of distributed energy system and the prospect of further research are put forward.

Reference

[1] BP. Statistical Review of World Energy, 2020. Bp 2020:66.

[2] When will fossil fuels run out? Ecotricity 2020. https://www.ecotricity.co.uk/our-green-energy/energy-independence/the-end-of-fossil-fuels (accessed November 1, 2020).

[3] Hannah R, Roser M. Emissions by sector. Our World Data 2020. https://ourworldindata.org/emissions-by-sector (accessed November 1, 2020).

[4] Höök M, Tang X. Depletion of fossil fuels and anthropogenic climate change-A review. Energy Policy 2013;52:797–809. https://doi.org/10.1016/j.enpol.2012.10.046.

[5] Hannah R, Roser M. CO_2 and Greenhouse Gas Emissions. Our World Data 2020. https://ourworldindata.org/co2-and-other-greenhouse-gas-emissions (accessed November 1, 2020).

[6] Liu K, Lin B. Research on influencing factors of environmental pollution in China: A spatial econometric analysis. J Clean Prod 2019;206:356–64. https://doi.org/10.1016/j.jclepro.2018.09.194.

[7] Fantazzini D, Höök M, Angelantoni A. Global oil risks in the early 21st century. Energy Policy 2011;39:7865–73. https://doi.org/10.1016/j.enpol.2011.09.035.

[8] Pina A, Ferrão P, Fournier J, Lacarrière B, Corre O Le, Andri AI. ScienceDirect ScienceDirect ScienceDirect ScienceDirect Literature Review of Power System Blackouts Literature Review of Power System Blackouts Yuan-Kang Assessing the feasibility of using the a heat demand-outdoor Yuan-Kang Yi-Liang function for a long-t. Energy Procedia 2017;141:428–31. https://doi.org/10.1016/j.egypro.2017.11.055.

[9] Khattak MA, Mohamad T, Tuan H, Mohd MW, Izzuan M, Ghazali M, et al. Energy Security Policy Shift of North America and Ontario , Canada Following 2003 Power Blackout : A Review. Prog Energy Environ 2018;4:14–24.

[10] Moinuddin M, Kuriyama A. Japan 2050 Low Carbon Navigator: Possible application for assessing climate policy impacts. Energy Strateg Rev 2019;26:100384. https://doi.org/10.1016/j.esr.2019.100384.

[11] IGES. Japan's 3E+S; Energy Policy Objectives 2015:3–5.

[12] I.E.Agency. PROSPECTS for DISTRIBUTED in CHINA. IEA 2017.

[13] Tame the Impacts of Distributed Energy Resources n.d. https://www.oati.com/Solution/Smart-Energy/distributed-energy-resource-management (accessed November 1, 2020).

[14] Cogeneration. Wikipedia n.d. https://en.wikipedia.org/wiki/Cogeneration (accessed November 1, 2020).

[15] Facility Peak-shaving. Worldw Powering Bus n.d. http://videos.eaton.com/microgrid/detail/videos/microgrid-videos/video/5339682985001/peak-shaving?autoStart=true (accessed November 1, 2020).

[16] Tom L. Technical Benefits of Distributed Energy Generation. EngineeringCom 2013.

https://www.engineering.com/ElectronicsDesign/ElectronicsDesignArticles/ArticleID/5924/Technical-Benefits-of-Distributed-Energy-Generation.aspx (accessed November 1, 2020).

[17] Perera P. Constraints and Barriers to Deployment of Distributed Energy Systems and Micro Grids in Southern China. Energy Procedia 2016;103:201–6. https://doi.org/10.1016/j.egypro.2016.11.273.

[18] Abazari A, Monsef H, Wu B. Coordination strategies of distributed energy resources including FESS, DEG, FC and WTG in load frequency control (LFC) scheme of hybrid isolated micro-grid. Int J Electr Power Energy Syst 2019;109:535–47. https://doi.org/10.1016/j.ijepes.2019.02.029.

[19] Wu G, Xiang Y, Liu J, Shen X, Cheng S, Hong B, et al. Distributed energy-reserve Co-Optimization of electricity and natural gas systems with multi-type reserve resources. Energy 2020;207:118229. https://doi.org/10.1016/j.energy.2020.118229.

[20] Ju L, Tan Z, Li H, Tan Q, Yu X, Song X. Multi-objective operation optimization and evaluation model for CCHP and renewable energy based hybrid energy system driven by distributed energy resources in China. Energy 2016;111:322–40. https://doi.org/10.1016/j.energy.2016.05.085.

[21] Wang J, Ye X, Li Y, Gui X, Guo H. An energy efficiency evaluation method of distributed CCHP system based on attribute theory for optimal investment strategy. Energy Procedia 2018;152:95–100. https://doi.org/10.1016/j.egypro.2018.09.065.

[22] Liu M, Shi Y, Fang F. Combined cooling, heating and power systems: A survey. Renew Sustain Energy Rev 2014;35:1–22. https://doi.org/10.1016/j.rser.2014.03.054.

[23] Sclafani A, Beyene A. Sizing CCHP systems for variable and non-coincident loads. Cogener Distrib Gener J 2008;23:6–19. https://doi.org/10.1080/15453660809509144.

[24] Ma W, Fang S, Liu G, Zhou R. Modeling of district load forecasting for distributed energy system. Appl Energy 2017;204:181–205. https://doi.org/10.1016/j.apenergy.2017.07.009.

[25] IEA. Market Report Series: Renewables 2017 - Analisys and Forecast to 2022 2017:30.

[26] Gain N, Share M. Japan’s Energy Transformation 2016.

[27] Ministry of Economy Trade & Industry. Long-term Energy Supply and Demand Outlook 2015:13.

[28] Dong W, Ye Q. Utility of renewable energy in China’s low-carbon transition. 2018.

[29] Renewable I, Agency E. Renewable Energy Prospects: China, summary 2014.

[30] NAVIGANT R. Global Capacity of Distributed Energy Resources Is Expected to Reach Nearly 530 GW in 2026. 2017.

[31] Saleh M, Brandauer W. Design and implementation of CCNY DC microgrid testbed How does access to this work benefit you ? Let us know ! 2016.

[32] Reuters E. China’s solar capacity overtakes Germany in 2015, industry data show. 2016.

[33] Han J, Ouyang L, Xu Y, Zeng R, Kang S, Zhang G. Current status of distributed energy system in China. Renew Sustain Energy Rev 2016;55:288–97. https://doi.org/10.1016/j.rser.2015.10.147.

[34] Akorede MF, Hizam H, Pouresmaeil E. Distributed energy resources and benefits to the environment. Renew Sustain Energy Rev 2010;14:724–34. https://doi.org/10.1016/j.rser.2009.10.025.

[35] Méndez VH, Rivier J, De La Fuente JI, Gómez T, Arceluz J, Marín J, et al. Impact of distributed generation on distribution investment deferral. Int J Electr Power Energy Syst 2006;28:244–52. https://doi.org/10.1016/j.ijepes.2005.11.016.

[36] Willis H, Lee E. Distributed power generation: planning and evaluation. Crc Press 2018.

[37] Gigliucci G, Petruzzi L, Cerelli E, Garzisi A, La Mendola A. Demonstration of a residential CHP system based on PEM fuel cells. J Power Sources 2004;131:62–8. https://doi.org/10.1016/j.jpowsour.2004.01.010.

[38] Ren H, Wu Q, Gao W, Zhou W. Optimal operation of a grid-connected hybrid PV/fuel cell/battery energy system for residential applications. Energy 2016;113:702–12. https://doi.org/10.1016/j.energy.2016.07.091.

[39] Das CK, Bass O, Mahmoud TS, Kothapalli G, Masoum MAS, Mousavi N. An optimal allocation and sizing strategy of distributed energy storage systems to improve performance of distribution networks. J Energy Storage 2019;26:100847. https://doi.org/10.1016/j.est.2019.100847.

[40] Das CK, Bass O, Mahmoud TS, Kothapalli G, Mousavi N, Habibi D, et al. Optimal allocation of distributed energy storage systems to improve performance and power quality of distribution networks. Appl Energy 2019;252:113468. https://doi.org/10.1016/j.apenergy.2019.113468.

[41] Ali AY, Basit A, Ahmad T, Qamar A, Iqbal J. Optimizing coordinated control of distributed energy storage system in microgrid to improve battery life. Comput Electr Eng 2020;86. https://doi.org/10.1016/j.compeleceng.2020.106741.

[42] Karmellos M, Mavrotas G. Multi-objective optimization and comparison framework for the design of Distributed Energy Systems. Energy Convers Manag 2019;180:473–95. https://doi.org/10.1016/j.enconman.2018.10.083.

[43] Chicco G, Mancarella P. Distributed multi-generation: A comprehensive view. Renew Sustain Energy Rev 2009;13:535–51. https://doi.org/10.1016/j.rser.2007.11.014.

[44] Wei D, Chen A, Sun B, Zhang C. Multi-objective optimal operation and energy coupling analysis of combined cooling and heating system. Energy 2016;98:296–307. https://doi.org/10.1016/j.energy.2016.01.027.

[45] Beck F, Martinot E. Renewable Energy Policies and Barriers. Encycl Energy 2004:365–83. https://doi.org/10.1016/b0-12-176480-x/00488-5.

[46] Wang JJ, Jing YY, Bai H, Zhang JL. Economic analysis and optimization design of a solar combined cooling heating and power system in different operation strategies. Proc 2012 7th IEEE Conf Ind Electron Appl ICIEA 2012 2012:108–12. https://doi.org/10.1109/ICIEA.2012.6360706.

[47] Wang J, Mao T, Dou C. Configuration Optimization with operation strategy of solarassisted building cooling heating and power system to minimize energy consumption. Energy Procedia 2016;88:742–7. https://doi.org/10.1016/j.egypro.2016.06.063.

Chapter 2

LITERATURE REVIEW OF THE DISTRIBUTED ENERGY SYSTEM

CHAPTER TWO: LITERATURE REVIEW OF THE DISTRIBUTED ENERGY SYSTEM

LITERATURE REVIEW OF THE DISTRIBUTED ENERGY SYSTEM *2-1*

2.1 Overview of distributed energy system 2-1

2.2 Design and operation analysis of the distributed energy system 2-7

2.2.1 Optimal configuration design of the distributed energy system 2-7

2.2.2 Operation strategy of the distributed energy system 2-13

2.3 Evaluation of the distributed energy system 2-19

2.3.1 Economic performance of the distributed energy system 2-20

2.3.2 Environmental performance of the distributed energy system 2-23

2.3.3 Reliability performance of the distributed energy system 2-25

Reference 2-29

2.1 Overview of distributed energy system

At present, the practice shows that DES has great advantages. It can reduce greenhouse gas emission, make environment friendly and improve energy utilization efficiency, and it is mainly reflected in three aspects [1]. First, DES can greatly improve energy efficiency compared to centralized power generation plus remote power transmission. Because of its no transmission loss, DES has the advantage of 90% energy utilization, which is far more than the large coal-fired power plants whose terminal utilization rate is 30% ~ 47% after deducting the auxiliary power and line loss rate. Second, distributed energy systems can greatly reduce CO_2 emissions. From 2000 to 2005, the United States adopted CCHP systems for all types of buildings, increasing the proportion from 4%to 50% and reducing CO_2 emissions by 19% in 2010. The forecast result shows that if 8% of the existing buildings can use DES technology, the CO_2 emission will be reduced by 30% by 2020. Third, distributed energy system uses a variety of thermal equipment for distributed power supply, which is easy to get involved in small hydropower, solar energy, nuclear energy or other new energy technologies, and is one of the most promising technologies for sustainable development. Meanwhile, CCHP system is the most popular application in DES.

There is no consensus definition of distributed energy system yet. However, based on the relationships among CCHP, distributed energy resources (DER), on-site renewable energy system and distributed CCHP system offered by Wu et al. [2]. Consideration of the change of energy production ways caused by the advancement of renewable energy utilization technologies, the relationship among multi-generation system (including CHP and CCHP), renewable energy system and DES is clarified in Fig.2-1 [3]. The coverage of DES is various: it can be a typical residential home and the small DES used combines rooftop solar PV cells, CHP and battery. It also can be an industrial site and the DES under construction considers the use of rooftop PV, GSHP, CHP unit, waste heat-based heat pump, etc. In summary, DES includes the multigeneration system and renewable energy system.

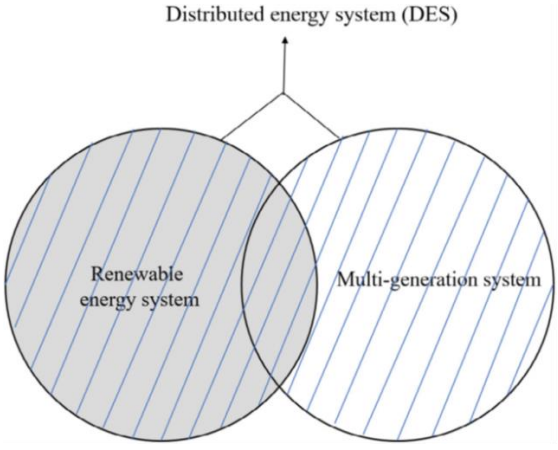

Fig.2-1 Relationships among renewable energy system, multi-generation system and DES [3].

The UK government has been developing distributed energy technology for many years and has designed the best plan for energy efficiency. Over the past 20 years, more than 1000 DES have been installed in hotels, leisure centers, hospitals, universities and colleges, horticulture, airports, public

buildings, commercial buildings, shopping malls and other corresponding places in the UK. Fig.2-2 shows the distribution of electricity demand in the UK in 2012, in which residential and commercial electricity consumption belong to the part of building energy consumption and account for a large proportion. According to the International Energy Agency, building energy consumption accounts for 35% of the world's total terminal energy consumption, which is the largest end use energy sector. After the adoption of CCHP, the annual CO_2 and SO_2 emissions in the UK are reduced by 50000t and 1000t, respectively.

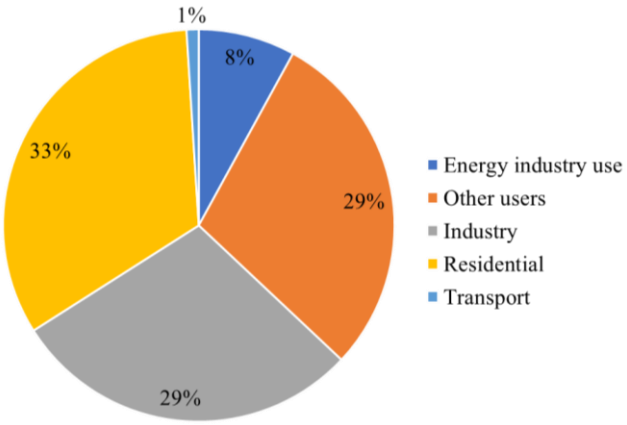

Fig.2-2 The demand for electricity distribution of England in 2015 [4]**.**

In China, optimizing the energy structure and increasing the proportion of renewable energy is the only way for energy development. In August 2007, the development and Reform Commission of the Chinese government issued the natural gas utilization policy, which has listed the distribution of CHP and CCHP users as the priority of natural gas utilization [5]. By the end of 2015, there were 288 natural gas distributed energy projects (single unit scale less than or equal to 50 MW and total installed capacity less than 200 MW), with a total installed capacity of more than 11.12 million kW. It is estimated that by 2020, the installed capacity of natural gas power generation will reach more than 110 million kW [6]. Fig.2-3 shows the structure chart of China's power generation installed capacity and China's generating capacity in 2017.

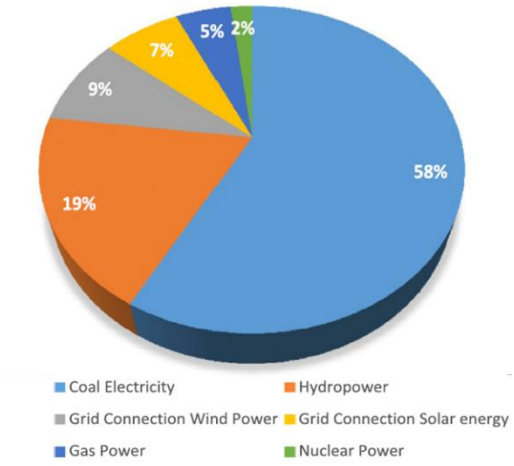

Fig.2-3 The structure chart of China's power generation installed capacity in 2017 [7]**.**

As of the end of 2017, the cumulative installed capacity of China's distributed photovoltaic was 29.66 GW, an increase of 190% over the previous year. In 2017, the new installed capacity of China's distributed photovoltaic was 19.5 GW, an increase of 350% over the previous year, accounting for nearly 40% of the total new installed capacity of photovoltaic. The cumulative grid-connected capacity of distributed photovoltaic in eight provinces exceeded 1 GW, of which Zhejiang and Shandong exceeded 4 GW, Jiangsu and Anhui exceeded 3 GW. The relevant data is displayed in Fig.2-4 and 2-5 [8,9].

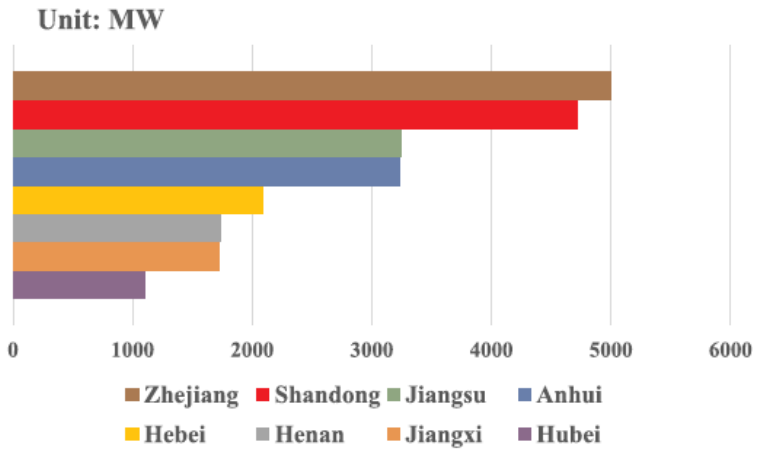

Fig.2-4 Provinces with cumulative grid-connected capacity of more than 1000 MW in distributed photovoltaic power generation in 2017 [8]**.**

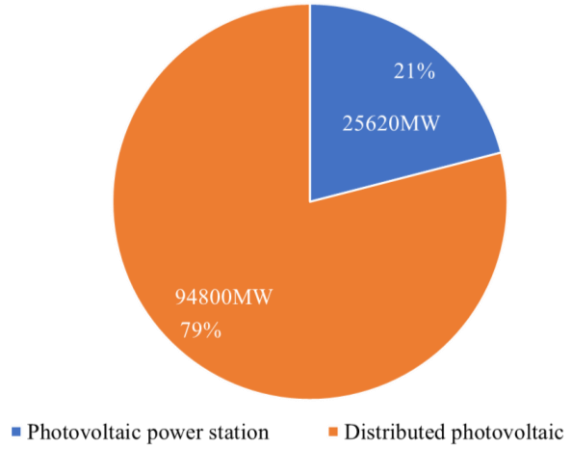

Fig.2-5 The proportion of China's photovoltaic power generation installed capacity by the end of September 2017 [9]**.**

The United States is one of the first countries in the world to develop distributed energy technology. Since 1978, the United States has advocated the development of small-scale cogeneration. In 1999, the industry put forward "CCHP creativity" and "CCHP 2020 program", and vigorously promoted the implementation of distributed energy technology in general commercial buildings. At the same time, the Ministry of energy has also formulated various relevant laws and regulations, tax and other preferential policies to support the promotion of the cogeneration system. The United States is rich in natural gas resources, which greatly promotes the development of natural

gas distributed energy utilization. By 2000, there were 980 natural gas distributed energy projects in commercial and public buildings in the United States, with a total installed capacity of 4.9 million kW, and 1016 industrial natural gas distributed energy projects with a total installed capacity of 45.5 million kW, totaling more than 50 million kW. After the "9.11" incident in 2001, the United States vigorously developed the distributed energy system of combined cooling, heating and electricity to ensure the security of energy supply. In 2003, the total installed capacity of natural gas distributed energy was 56 million kW, accounting for 7% of the total electricity installed in the United States and 9% of the power generation. At present, there are more than 6000 distributed CCHP systems in the United States, most of which use natural gas as fuel, and use gas turbine combined cycle CCHP technology to mainly solve heating, cooling, domestic hot water supply and part of power supply.

Over the past 20 years, Denmark's GDP has doubled, but energy consumption has not increased, and environmental pollution has not intensified [10]. The reason lies in Denmark's active development of CO generation of cold, heat and electricity, advocating scientific use of energy, supporting distributed energy, and supporting the development of national economy by improving energy utilization rate. Since 1999, the Danish government has carried out electric power reform, committed to increasing the application proportion of distributed Cogeneration in central heating, and explicitly proposed the heat supply bill. Before 2013, there was no thermal power plant in Denmark that did not provide heat, and no heating boiler room did not generate electricity. At present, Denmark has transformed the production of cold, hot and electric products into high-tech co production of cold, heat and electricity, making the progress of science and technology into real productivity, cogeneration supplies 90% of Denmark's regional load demand.

Japan is a big country of energy consumption, but it is also a country lacking in energy. The rapid economic development is inseparable from the application of energy, so it is particularly important to make efficient use of limited resources [11]. Japan set up the thermal energy technology association in 1972 and set up the "energy conservation center" in 1978, and started to launch "solar juice plan" and "Moonlight project". The energy conservation law was promulgated in 1979 and further revised in 1998 and 2002. In addition, distributed energy, mainly represented by renewable energy and cogeneration, has been vigorously promoted in Japan. Especially with the rapid development of gas-fired generating units, fuel cells, solar power generation and other technologies, the proportion of distributed energy in Japan's overall energy system has also increased to more than 13%. Since 1980s, with the operation of the No.1 Thermal Power Unit in Tokyo National arena, Japan has begun to vigorously develop natural gas distributed energy, with an average annual installed capacity of 300000 kW [12]. From 1990's to 2007, the annual installed capacity of distributed energy in Japan was 400000-500000 kW. In terms of planning, in June 2010, the Japanese government issued a plan to promote the introduction of natural gas cogeneration system, and put forward the development plan of the total installed capacity of 8 million kW by 2020 and 11 million kW by 2030 (accounting for about 15% of the total installed power generation capacity in Japan).

Blackhall et al. [13] discusses some of the important technical, economic and social opportunities and challenges of optimizing the value of DER integration into electricity networks and markets. Global energy systems are transitioning from fossil fuel-fired generation to renewable generation and this trend is set to accelerate over coming decades and the result is presents in Fig.2-6. It is vital

to ensure that we decarbonize our energy system to limit dangerous climate change to below 2 degrees (IPCC, 2018) and preferably below 1.5 degrees. One dimension of this transition is the increasing adoption of distributed energy resources (DER) such as solar PV, small-scale energy storage, demand response mechanisms and electric vehicles (EVs). As DER adoption increases, global electricity systems will demonstrate increasing levels of decentralization, with this change currently occurring faster in Australia than any other nation as seen in Fig.2-7.

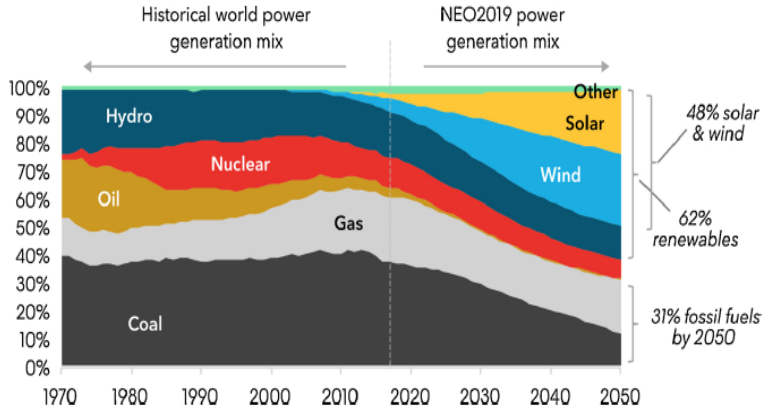

Fig.2-6 Historical and forecast share of global electricity generation by source (Source: BNEF (2019)).

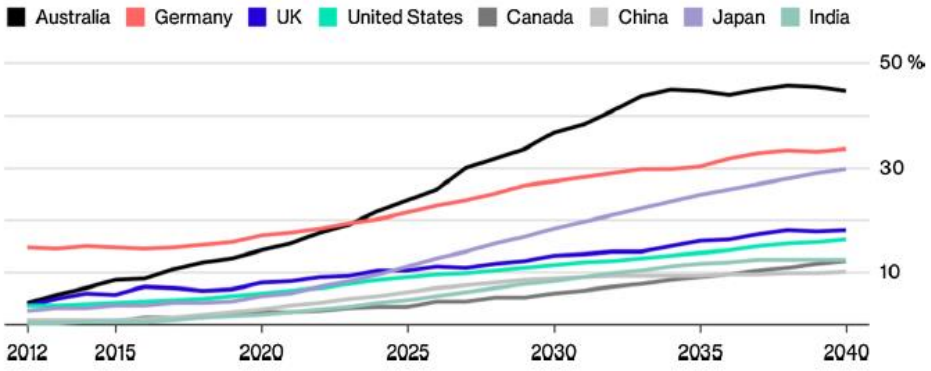

Fig.2-7 Forecast ratio of behind-the-meter electricity capacity to total installed capacity in the coming decades (Source: BNEF (2017)).

At present, the world energy structure is in the double replacement period of oil and gas replacing coal and non-fossil energy replacing fossil energy [3]. However, solar energy, wind energy and other renewable energy are affected by resources, technology, region, and other conditions, so it is difficult to achieve large-scale replacement in the short term. As a strategic choice of energy transformation, the development of distributed energy has the advantages of high energy efficiency, clean and environmental protection, good security, peak shaving and valley filling, and good economic benefits. It is the best way to use natural gas efficiently [14]. Distributed energy realizes scientific energy use and energy cascade utilization, and the energy comprehensive utilization efficiency reaches 70% - 90% [15]. It is a modern energy supply mode to realize energy supply nearby the load center, which meets the requirements of energy conservation and environmental protection and

the construction of a conservation-oriented society. Chittum et al. [16] examine how decision makers can more precisely assess the costs of disruptive weather events and the value of resilient distributed energy systems such as combined heat and power (CHP) and propose a framework for a metric called the Distributed Energy Resource Resiliency Value (DERRV) and discuss how such a metric might be applied to CHP.

Recently some reviews of DES development have been done. Han et al. [17] reviewed the DES status in China from four aspects including system optimization, development influence factor, application, and polices. The energy consumption structure of China and the world in 2014 is shown by Fig.2-8. It can be found that the ratio of coal is still higher than the average level of the world and the clean energies vice versa. Ma et al. [18] focused on the district load forecast modeling for a distributed energy system. However, neither the level of DES application nor the method of performance evaluation has been discussed clearly. Besides, DES also has been developing rapidly in some African countries, apart from China and the developed countries.

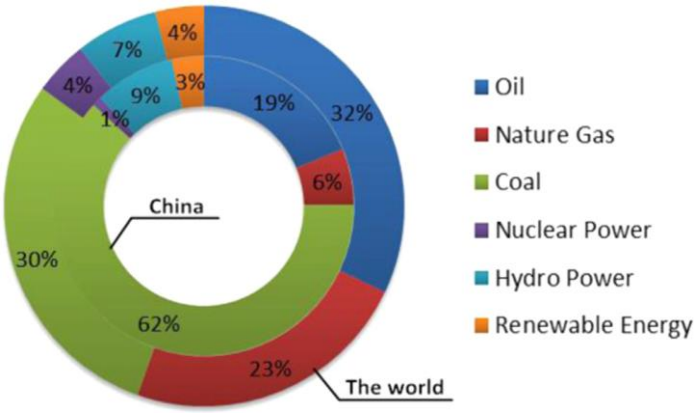

Fig.2-8 Energy consumption structures of China and the World [17]**.**

Recently some reviews of DES development have been done, and the research of the DES has attracted increasing attention, as illustrated by Fig.2-9. It shows that the sum of the published articles is 311 and the sum of citations is up to 2885 in Web of Science when “distributed energy system” is set as search and timespan is set as 2010–2019. Specifically, the sum of published articles within 2014–2019 is up to 222, accounting for 71% of the total articles published within 2010–2019 [3].

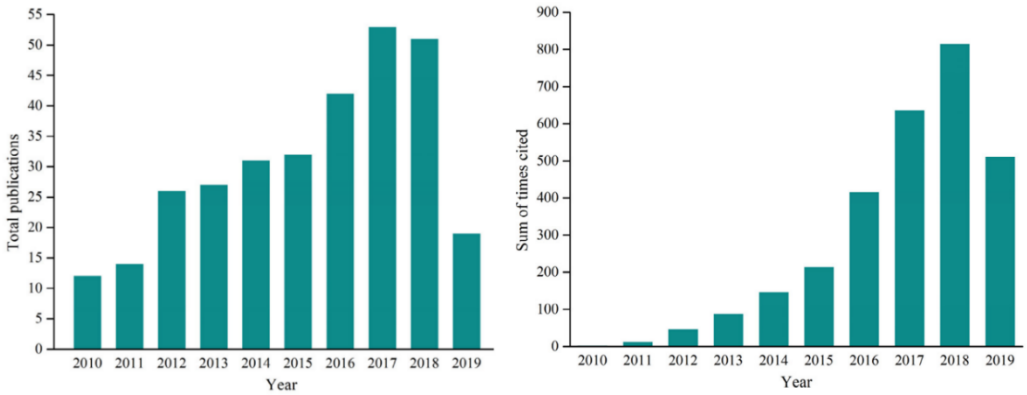

Fig.2-9 Distribution of SCI papers with the topic of “distributed energy system” [2].

2.2 Design and operation analysis of the distributed energy system

2.2.1 Optimal configuration design of the distributed energy system

Distributed energy system can utilize many kinds of energy, including natural gas, biomass, wind energy, solar energy, geothermal energy and so on. It can also be coupled with waste heat, residual pressure, residual gas, and other energy forms. Due to different energy forms, distributed energy systems have various forms and structures. According to the classification standard of prime mover, distributed energy system mainly includes the following technologies: cogeneration, renewable energy, energy storage and fuel cell, etc. the technical block diagram is shown in Fig.2-10.

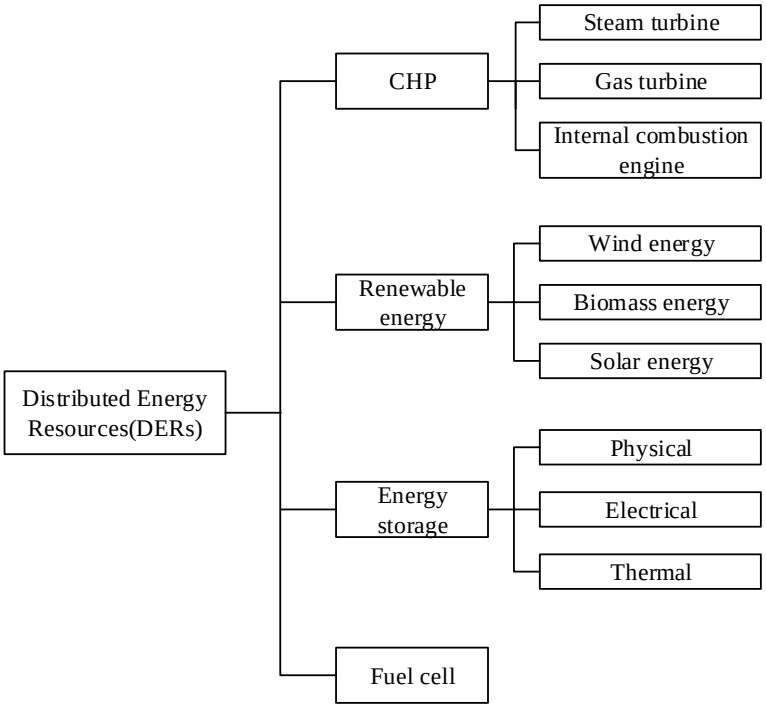

Fig.2-10 Technical block diagram of DESs.

As a systematic and complex energy-saving and emission reduction scheme, since the concept of distributed energy was put forward, the problem of system optimization planning and design has attracted enough attention of researchers. With the continuous deepening of the connotation and extension of the distributed energy system, the scope of its system optimization is also expanding, at the same time, the optimization level is also deepening, and the optimization methods are constantly innovating [19,20].

Wu et al. [20] propose an energy-reserve co-optimization model for electricity and natural gas systems with multi-type reserve resources.

Li et al. [21] explore bidirectional interactive behaviors among multi-stakeholder energy systems and seek energy management strategies in neighboring communities. Multiple independent optimization problems for decentralized stakeholders are obtained and solved based on an analytical target cascading algorithm, in which Lagrangian penalty terms are considered to ensure consistency in energy bidirectional interaction.

Cortes et al. [22] considers the case study of a smart microgrid district and obtained results allow advancement of the net-zero energy neighborhood concept in all the evaluated scenarios within a daily horizon and a positive energy balance in wider horizons.

Tooryan et al. [23] presents an optimization solution to reduce the operational cost for a hybrid residential microgrid consisting of diesel generator, wind turbine and photovoltaic array, and battery energy storage system. The proposed method results are shown that there is about a 35% reduction in CO2 emission in the optimal configuration in comparison with the scenario in which only diesel generators provide the total demand of the MG system.

Das et al. [24] explores the feasibility of using local renewable options to meet the local load demand with a minimum cost of electricity (COE). HOMER simulation and MCDM approach is used for an optimized decentralized hybrid renewable energy solution (wind-hydro-battery) with minimum DG support. A minimum COE ($0.63/kWh) and CO2 emissions (481 kg/year) are estimated for optimum uninterrupted power supply.

Luo et al. [25] presents a mixed integer linear programming model for optimizing the structure and operation of a distributed energy resource system with district energy networks on a virtual island. A cost allocation analysis based on cooperative game theory is performed to distribute the system cost between individual stakeholders. The results highlight that the energy networks effectively reduce the system cost.

Wu et al. [26] proposes a two-stage stochastic mixed-integer programming method for jointly determining optimal sizes of various DERs, considering both economic benefits and resilience performance. The results found that the proposed method can effectively determine the optimal DER sizes to meet a required resilience goal at the maximum net-benefit. Impacts of several key factors including tariff rates, discount rate, and survivability level on optimal DER sizes are analyzed through case studies.

Wu et al. [27] proposes a measurement-based online distributed optimization framework for coordinating networked distributed energy resources (DERs) in distribution networks, focusing on the security-constrained optimal dispatch of networked DERs. The results show that all DERs adjust their outputs independently to realize the optimal dispatch of ADNs while responding to variations in system conditions and satisfying the necessary constraints.

Guo et al. [28] presents a new method of optimizing the distributed energy of AC/DC hybrid microgrids with power electronic transformer. The results show that: as the application of power electronic transformer in AC/DC hybrid system, the power transfer between the AC network and the DC network is controlled by the power regulation function of the power electronic transformer, which can effectively realize the full disposition of distributed generation.

Ranjbar et al. [29] presents a new robust co-planning model for transmission investment and merchant distributed energy resources (DERs). The proposed model is a tri-level min-max-min optimization problem where the upper, middle, and lower levels are investment decision of transmission lines and DERs, worst case realization of uncertain parameters, and the best actions in order to minimize the operation costs. Results of a case study based on the IEEE RTS 24-bus test system show the usefulness of the proposed model.

Luo et al. [30] constructs a DES driven by solar, geothermal, aerothermal, natural gas and power grid with energy conversion devices modeled based on part load performance. Results indicate that constant efficiency/COP of equipment yields an 11.7% drop in annual total cost (ATC), a 10.4% increment in annual total CO2 emission (ATE) and a 12.5% reduction in coefficient of energy performance (CEP). ATC and ATE of the optimal solution acquired under a conventional operation strategy increase by 6.8% and 3.7%, while CEP decreases by 66.9%.

Karmellos et al. [31] presents two multi-objective models for the design of Distributed Energy Systems (DES) for satisfying local needs in heating, cooling and electricity. The results show that each optimal solution in both methods has a different system configuration and operational profile of the technologies.

Ali et al. [32] presents a control strategy for distributed BESS in a centrally controlled microgrid to enhance the calendar life of BESS. The proposed strategy controls the charging and discharging of individual batteries based on state of charge (SOC), state of health (SOH) and maximum capacity. The controller selects the BESS with better health and higher capacity for operation on priority resulting in better calendar life of the energy storage system. The simulations results for the test system indicates an overall improvement in calendar life of BESS by 57%.

Hamada et al. [33] proposes integrated system of residential DERs which secure the supply reserve internally. The results of case study show that the operation which secures internal reserve of 20% of PV generation can be performed by about 2% increase of the total cost.

Perera et al. [34] introduces a novel optimization algorithm, coupling an existing energy hub model with a hybrid surrogate model in order to reduce computational time in the optimization process.

Das et al. [35] proposes a strategy for optimal allocation of distributed ESSs in distribution networks to simultaneously minimize voltage deviation, flickers, power losses, and line loading. The optimization results are verified through the application of the conventional artificial bee colony algorithm. Detailed simulation results imply that the proposed ESS allocation technique can successfully minimize voltage deviation, flicker disturbance, line loading, and power losses, and thereby significantly improve performance and power quality of a distribution network.

Mavromatiis et al. [36] examines the design of autonomous Distributed Energy Systems (DES) under energy demand and solar radiation uncertainty. The results reveal that the most cost-effective DES solutions achieve an electrical autonomy of 20% relying on renewable PV electricity generation.

Karmellos et al. [37] presents an application of a multi-objective optimization model for designing a DES, using total annual cost (TAC) and carbon emissions as objective functions. To investigate solutions' robustness, four methods are used, (a) objective-wise worst-case uncertainty, (b) minimax regret criterion (MMR), (c) min expected regret criterion (MER) and (d) Monte Carlo simulation, in order to compare the differences in values of objective functions and resulting DES configuration. The proposed methods are presented through a case study and the results show that DES configuration varies when uncertainties in parameters are considered, enabling a decision maker (DM) to make a more informed choice.

Kang et al. [38] developes a robust optimal method for distributed energy system (DES) design considering uncertainties. It is found that, compared with other schemes, the optimum DES has least life-cycle total cost and better robustness of performance under different operating conditions. The DES identified by this method achieves economic benefits and higher total system energy efficiency in the latter years of its life-cycle compared with the DES identified by optimal design method without considering the life-cycle performance.

Gil et al. [39] proposes a distributed model predictive controller for the efficient operation of a distributed energy system comprising a solar-powered membrane distillation facility and a greenhouse, which is the most widespread type of crop cultivation. The result shows that the application of the DMPC strategy allows us to reduce the specific thermal energy consumption of the SMD plant by 5 % compared to manual operation.

Chen et al. [40] proposes a method to optimize the location and capacity of the embedded distributed energy storage system (DESS) to meet the needs of ADN and DGs. In this paper, the optimization model of ESS's capacity is solved by GA with good researching ability and convergence. The forward and backward substitution method is used in the algorithm, which is suitable for calculation of the power flow in the radial distribution network. The analysis of examples shows that the optimal allocation method and model on DESS in ADN based on GE can get the reasonable scheme considering the economy and safety. And the influence of different DG output cases on the optimal allocation of ESS are also obtained in this process.

Ren et al. [41] develops a simulation framework of the distributed energy system while considering the two operating forms, namely, heat tracking operation mode and electricity tracking operation mode. Fig.2-11 shows the simulation diagrams of the DER system under the heat tracking mode and electricity tracking mode, respectively. According to the simulation results, compared with the conventional centralized energy system, the economic, energy and environmental performances of distributed energy systems are better regardless of heat tracking or electricity tracking model.

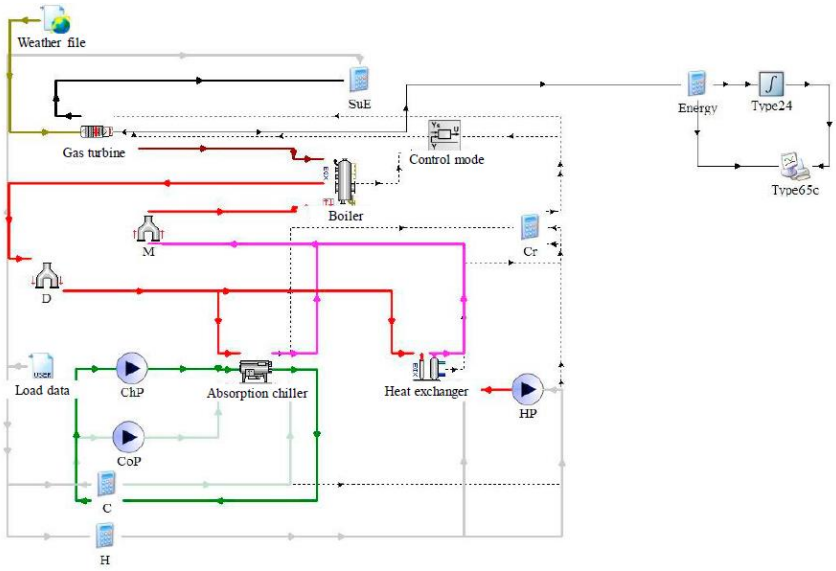

Fig.2-11 The simulation diagram of the heat tracking mode [41].

Xing et al. [42] establishes a multi-objective mathematical programming (MOMP) model to minimize the total construction investment and operation costs of each industrial park considering emission, energy balance and other technical constraints. Fig.2-12 gives the energy flow chart of DES. In detail, the cooling demand is satisfied by an electric refrigerator (ER) or a steam chiller (SC), electricity demand is provided by a gas turbine (GT) and local grid, and the heating demand is satisfied by a GT, a gas boiler (GB), and a biomass boiler (BIO). The results show that electricity price has the strongest impact on the economic performance of the industrial parks, followed by natural gas price and biomass price, but natural gas price does not affect the gas allocation ratio. Moreover, when the total input natural gas is increased by 10–90%, the total cost can be reduced by 0.69%–7.83%.

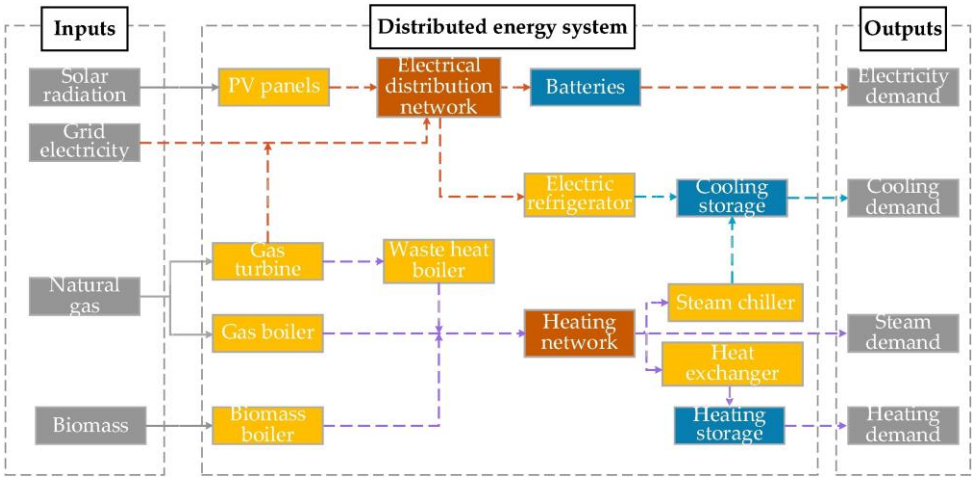

Fig.2-12 Energy flow chart of DES in industrial park [42]**.**

Kang et al. [43] proposes new configuration of distributed energy system (DES), which integrates a district cooling system as a new energy-efficient technology to be used in cooling dominated districts. Compared with the centralized energy system (CES), the DES allows electric chillers of larger capacities to be used and to operate at higher part load ratios, resulting in higher energy efficiency in operation.

Ren et al. [44] devised a combined cooling, heating, power and fuel (CCHPF) distributed energy system to improve the energy utilization efficiency and reduce the dependence on conventional fossil fuels. The optimal dispatch of the energy and the efficient economic operation. In comparison with existing CCHP systems, the energy utilization efficiency of the developed CCHPF system increases by 0.60% and 17.65%, CO2 emission decreases by 13.79% and 3.77%, as well as economic cost reduces 0.29% and 6.33% on a typical winter and summer days, respectively.

Blake et al. [45] introduces a model of an industrial microgrid with distributed energy resources (DERs). The model is applied to an existing manufacturing facility in Ireland. The test facility is connected to the main electricity grid but also has onsite generating units; a wind turbine and a combined heat and power (CHP) unit.

Yan et al. [46] proposed a life cycle economic and carbon emissions assessment framework by dividing the building distributed energy system into five stages. Fig.1-13 shows the framework of

the optimization process, which consists of four parts: (1) Parameter inputs, (2) Life cycle accounting approach, (3) MOMP model, (4) Results and discussions.

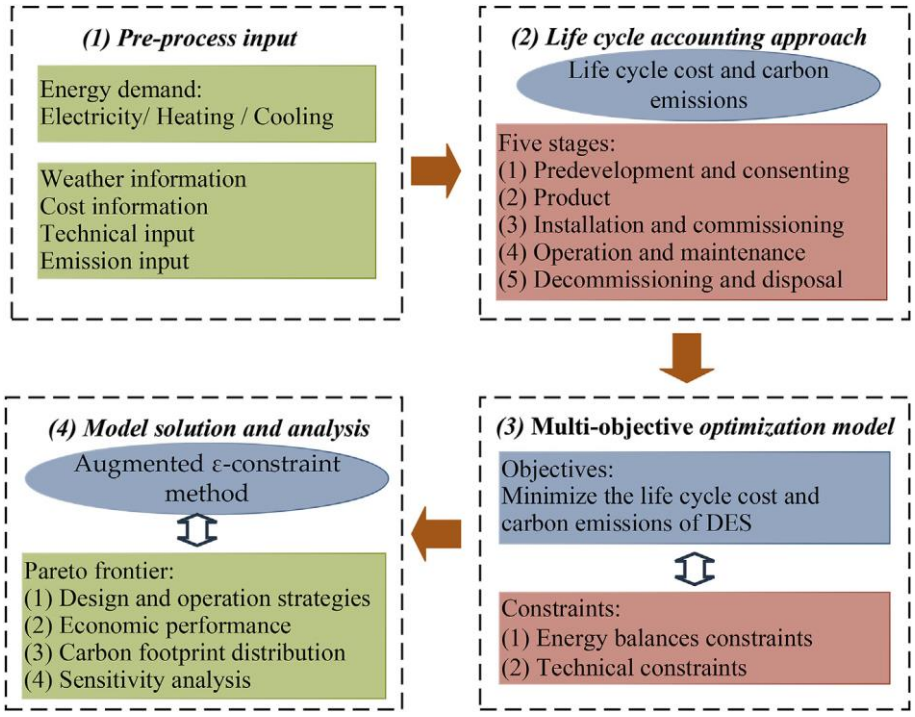

Fig.2-13 The overview of the optimization process.

In the first part, basic information should be prepared, consisting of energy demand, weather and cost information, and technical and emission inputs. In the second part, the detail life cycle cost and carbon emissions accounting approach is given by dividing the energy system life cycle into five stages: predevelopment and consenting stage, product stage, installation and commissioning stage, operation and maintenance stage, and decommissioning and disposal stage. In the third part, a MOMP model is set up to optimize the cluster and design of district buildings with DES taking the life cycle cost and carbon emissions as the objectives. Finally, the Pareto frontier is obtained by solving the model, and the economic performance and carbon footprint distribution under five stages are analyzed. It's found that the carbon emissions in the operation and maintenance stage accounts for the largest share in the entire life cycle. In addition, the proportion of carbon emissions from natural gas is the highest, accounting for 65–73% under environmental optimization and 85–88% under economic optimization.

Alzahrani et al. [47] encompasses a review of the recent optimization approaches for hybrid energy systems with PV, diesel turbine generators, and energy storage systems to give the basis for solving difficult and intricate real-world problems related to distributed energy system operation. The stochastic approaches have a variety of methods that have been widely used; they are presented in Fig.2-14. In contrast with the deterministic approaches, the stochastic approaches only depend on utilizing random operators to avert entrapment in local optima. The stochastic approaches also have the ability to highly accurately locate the global optimum solution to a problem.

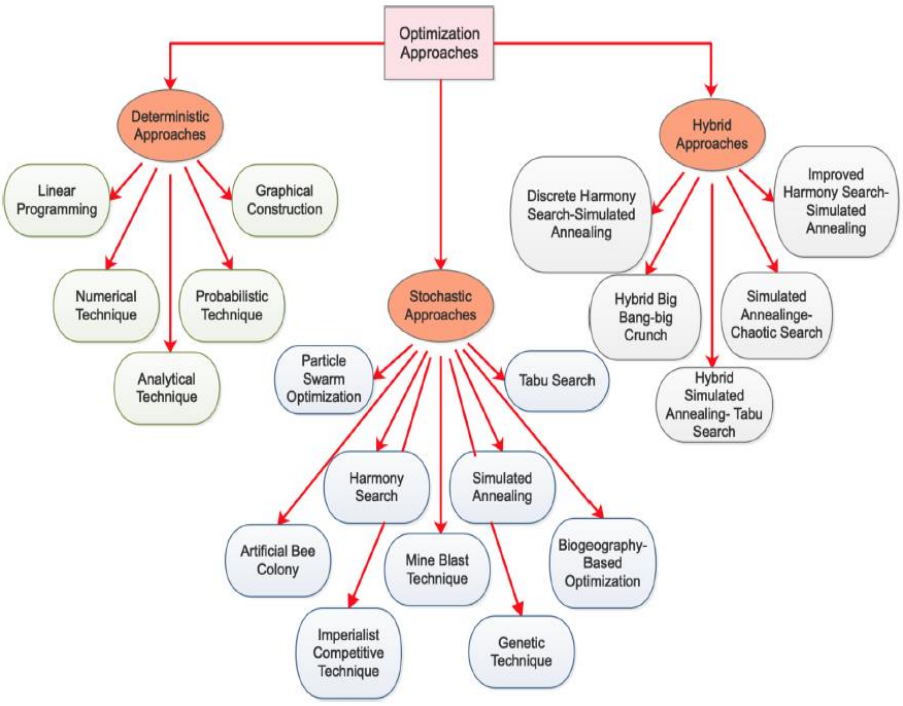

Fig.2-14 Diversity of optimization approaches

2.2.2 Operation strategy of the distributed energy system

The economic operation is essential for microgrid to expand its configuration. The peak shaving ability of microgrid is the most noteworthy. Many works have been studied in this field.

Levron et al. [48] optimized the peak shaving strategy and established a method to calculate the optimal peak value based on the load demand curve and storage capacity. The result reveals the lowest possible peak, given only the load's demand profile and the storage capacity. The effects of losses in the storage device are analyzed numerically, showing the increase of power peak associated with the increase of loss.

Plaza, J et al. [49] propose a new Peak Shaving algorithm in combination with a continuous battery peak power estimation algorithm for a battery energy storage system (BESS). Results show that the proposed Peak Shaving algorithm allows to easily limit power exchanges between the microgrid and the main grid.

Mehr et al. [50] established a grid-connected battery energy storage system by controlling lithium ion current for peak shaving and load balancing.

Li et al. [51] analyzed the performance of energy-efficiency appliances and distributed generators integrated with the grid by assessing the potential of load balancing in the public grid.

Kerestes et al. [52] achieved savings in system operating costs by using NaS battery storage and pumped storage to balance loads instead of gas turbine generators to meet peak load requirements.

Xu et al. [53] proposes a method to evaluate the performance of load leveling to evaluate different types of building load curves and demonstrate the benefits of load leveling on optimization of energy configuration by comparing the results before and after load leveling.

Yan et al. [54] focuses on stochastic daily operation optimization of multiple DESs with renewables in an Local energy communities (LECs). The detailed energy flows among the multiple DESs in the LEC under consideration in this paper are shown in Fig.2-15 below. And established a stochastic mixed-integer linear programming model with uncertain renewable generation modeled by a Markovian process to avoid the difficulties and drawbacks associated with scenario-based methods. The results show that the total expected cost of the LEC is reduced by the integrated management of the DESs as compared to the costs attained under other operation modes where there are no interconnections among DESs, demonstrating the potential benefits that can be achieved with LECs through the optimized management of local energy resources aiming to foster efficient use of the available energy.

Fonseca et al. [55] presents a modeling and multi-criteria optimization strategy for designing and operating decentralized power plants including different energy vectors. The objective functions are the total annualized cost, the CO_2 emissions and the grid dependence. According to optimization results, it is highlighted the influence of the assessed criteria upon the structure and the operating policy of the power plant. Additionally, by comparing the performance of the distributed energy system with respect to a centralized scenario, it is noted the significant potential of the decentralized generation. Indeed, depending on the optimization goal, CO_2 emission reduction up to 89%, and self-sufficiency up to 81% can be achieved.

Li et al. [56] studies the design and management of a distributed energy system incorporating renewable energy generation and heterogeneous end-users from residential, commercial and industrial sectors. The results show that with effective interactions among participants, electricity consumption of the entire energy system closely tracks the generation pattern of renewable resources, resulting in a significantly flattened schedule of grid electricity procurement.

Tian et al. [57] takes the DES of a scientific research station in Antarctica as an example when it comes to the optimization of its operation strategy, extracting the control logic for engineering applications from the optimized operation strategy. The results show that the primary energy consumption of the optimized operation strategy can be reduced by 11.8% when compared with the original operation strategy. By using the engineering control logic extracted from the optimized operation strategy to adjust the original operation strategy, the primary energy consumption of the system can be reduced by 9.6%.

Guan et al. [58] proposes an improved comprehensive evaluation model: the improved model comprehensively evaluates energy-saving, economic and environmental performance of the system, and factors including off-design condition performance and start-stop performance have also been considered. By comparing the improved model proposed with the simplified model, it can be found that the results obtained from the simplified one cannot meet the actual needs of the system and is unreasonable, thus validating the rationality of the improved model.

Malandra et al. [59] proposes an energy storage potential of electric Water Heaters for load balancing. The smart DESC architecture has been implemented in a simulator and tested on realistic case studies involving a homogeneous population of electric water heaters (EWHs) in a grid with renewable penetration. The simulation results showed that the smart DESC approach reduces the burden to power operators during peak hours with minimal impact on the comfort of customers.

Yu et al. [60] adopted to calculate the operating cost of heating season, the energy quality coefficient is used to evaluate the quality of different kinds of energy, and the exergy efficiency of heat exchange is analyzed to measure the energy utilization level. Operation cost and energy efficiency of the distributed energy system and conventional gas peak-shaving system are studied and compared. Results indicate that the distributed energy system based on the heating network can make full use of the waste heat generated by gas turbine, improve the exergy efficiency of heat exchange and decrease the fuel consumption.

Das et al. [61] presents a strategy for optimal allocation and sizing of distributed ESSs through P and Q injection by the ESSs to a distribution network. The obtained results suggest that the proposed PQ injection-based ESS placement strategy performs better than the P injection-based approach, which can significantly improve distribution network performance by minimizing voltage deviation, power losses, and line loading.

Many scholars have done a lot of research and Analysis on the operation optimization and maintenance of CCHP system. At present, the research on the optimization of CCHP system mostly belongs to the theoretical level [62]. Through the quantitative analysis of mathematical modeling, the advantages and disadvantages of CCHP system and the optimal operation state are evaluated. However, due to the limitation of system boundary conditions, the unpredictability of user load and the existence of defects in unit operation, there is a big difference between the theoretical research and the actual operation, even under the optimal setting conditions, the optimal operation can not be achieved [63,64].

In order to solve the problem of dealing with a variety of interconnected equipment and various types of energy flow, Gianfranco chicoo and other scholars used the matrix method to model the energy flow exchange between the internal equipment and external energy sources in the CCHP system and the energy between the devices [65]. Starting from the definition of the efficiency matrix of each specific equipment in the power station and the representation matrix of the related interconnection, the overall efficiency matrix representing the whole power station is constructed [66]. This structure is carried out through the original program, which is suitable for automation and symbolization. The concept of graph theory is used to explore the tree formed by the backward path from output to input. The proposed matrix formula maintains the separation of each energy vector, and each energy vector can be associated with its time-dependent price, which provides a basic framework for formulating the optimization problem of the management of the trigeneration system in the context of energy market [67]. This matrix formula provides an effective framework for establishing operational optimization problems, independent of the objective function and the chosen solution. Finally, a numerical example is given to illustrate the effectiveness of the proposed matrix formula.

The energy flow model of traditional distribution system is shown in Fig.2-15 [68]. The load required by general users includes electrical load, cooling load and heating load. The power load demand of users is directly met by the public grid, and the cooling load of users is provided by electric refrigerator. The boiler consumes fuel to generate heating steam, which provides heat for users through heat exchange equipment to meet the demand of heat load. In addition, as the whole distribution system needs to accumulate the auxiliary equipment such as fans for fluid transmission,

so the auxiliary equipment such as Juhe fan needs to consume a certain amount of electricity, and its energy consumption is also provided by the public grid. Typical distributed energy system generally includes prime mover (gas turbine, internal combustion engine, etc.), waste heat boiler, peak boiler, absorption chiller in steam desert, electric refrigerator, heat exchange equipment, etc., and its structure is shown in Fig.2-16 [68]. Natural gas is burned in the prime mover to drive the turbine or piston to work and drive the generator to generate electricity to meet the power demand of users and the system. When the power provided by the prime mover is insufficient, the insufficient power is obtained from the public grid. The high-temperature flue gas generated by the prime mover enters into the waste heat boiler to generate high-temperature steam. Part of the high-temperature steam provides heating load for users through heat exchange equipment, and the other part enters absorption chiller to supply cooling load for users. The electric refrigerator and absorption refrigerator operate at the same time to meet the whole refrigeration demand of users. When the heat required by the system is greater than the heat supplied by the HRSG, the insufficient heat is obtained by burning natural gas in the peaking boiler.

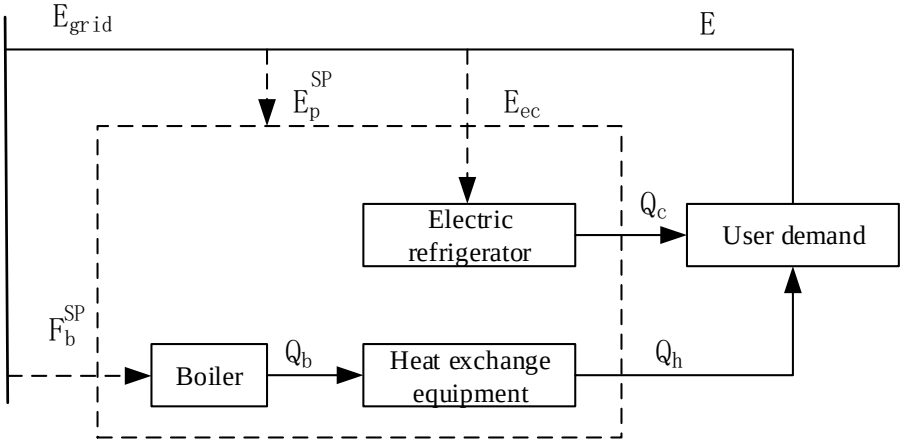

Fig.2-15 Energy flow model of distribution system [68]**.**

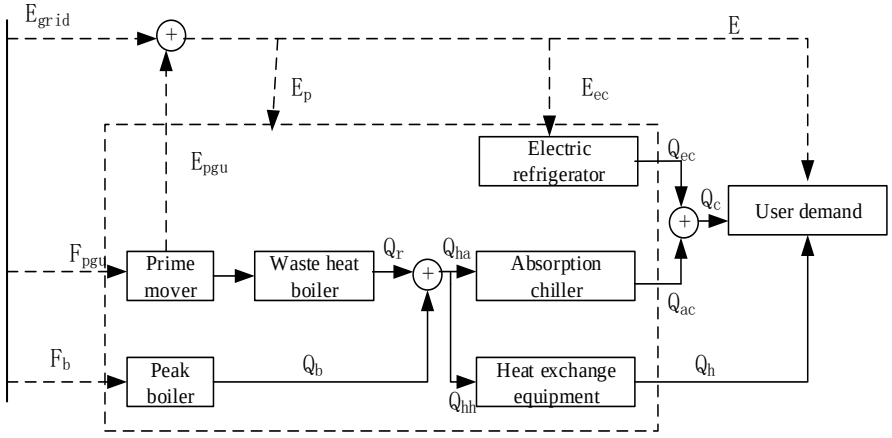

Fig.2-16 Typical distributed energy system structure [68]**.**

Kaikko et al. [69] studied the technical and economic analysis of gas turbine in cogeneration system. The micro gas turbine operates according to the heat load demand, replacing the purchased

power and the heat generated by the existing boiler. The purpose of the study is to analyze the impact of different load control methods on the overall economy of operation. The control parameters include turbine inlet temperature and shaft speed. Based on the analysis, the steady-state performance model of the actual component parameters is used to establish the micro gas turbine. The operation economy is determined by the combination of engine performance model and economic model. The economic model adopts NPV investment in micro gas turbine as the criterion. Therefore, the conditions of economical and effective operation of the engine are determined. In addition to the analysis of general effectiveness, the model is applied to the case of power supply and heat demand. The size range with the highest economic potential is determined for the micro turbine option. For the selected scale, determine the maximum cost allowed for the investment. In addition to the size of the micro gas turbine and the heat and power demand of specific cases, the results strongly depend on economic parameters. Finally, the sensitivity results to energy prices are presented.

Sundberg G et al. [70] analyzed the cost of gas and electricity, and pointed out that the lower gas electricity price ratio can make the cogeneration system more economical.

Gorsek A and others [71] calculated the net present value, investment payback period and other economic indicators of the cogeneration system, which proved the economic advantages of the cogeneration system over the split production system.

Rosen Ma et al. [72] compared the utilization rate of primary energy based on the first law of thermodynamics with that based on the second law of thermodynamics, and proved that the analysis results of the two indicators are different for different situations.

Biezma M V et al. [73] analyzed the economic evaluation indexes of cogeneration system and pointed out the advantages and disadvantages.

Ferreira et al. [74] propose a multi-objective optimization model applied to optimization the use of distributed energy resources in an energy system. The centralized control strategy is divided into three levels integrated into a master controller. The microgrid operation results demonstrate the effectivity of the proposed approach to steer grid power flow and prioritize active power injection or compensation of currents unbalance.

With the decline of natural gas price, gas-fired distributed energy has attracted more and more attention. More and more scholars have carried out in-depth research on distributed cogeneration and CCHP system [75,76]. Different CCHP schemes are compared by simulation. Through the analysis and comparison of the two schemes, the characteristics and basic laws of energy conversion of CCHP system are revealed, and the evaluation criteria for reasonable evaluation of CCHP system are also presented [77]. At the same time, the typical CCHP system is compared with the traditional CCHP system, and the results show that the energy consumption of CCHP system is reduced by 42% compared with the traditional CCHP system[78]. The energy consumption and energy saving of gas engine driven heat pump applied in CCHP system is analyzed, and compared with CCHP system, it is concluded that CCHP system is twice as high as the unified secondary energy utilization rate and the standard gas consumption is reduced by half [79].

The regional distributed energy combined cooling and heating system is used for energy

utilization and exergy analysis [80,81]. The influence of different load rates of gas turbine and boiler of prime mover on electric efficiency, primary energy utilization rate and exergy efficiency of distributed energy heating system is studied, and the comparable energy consumption and performance coefficient of cooling and heating are proposed, which are used to evaluate the heating performance of different heating modes and cogeneration [82]. On the premise of meeting the cooling and heating load of buildings, a multi-objective function is established to meet the requirements of annual cost, primary energy consumption and carbon dioxide emission, and the multi-objective optimization model is transformed into a single objective optimization model by using weight coefficient [83].

Based on the energy-saving mechanism of distributed cogeneration system, under the dynamic balance of power and heat on both sides of supply and demand, Ren and others [84] put forward the theoretical expression of energy-saving rate of distributed cogeneration system relative to different reference systems, aiming at the two general operation modes of "determining electricity by heat" and "determining heat by electricity" and five possible operating states under different heat to power ratios.

Liu et al. [85] proposed a distributed energy system with solar thermochemical recuperation. Results indicate that the proposed system achieves a primary energy ratio of 75.42%, and the net efficiency of solar to electricity is 23.26% on the design condition.

Gao et al. [86] investigated the distributed energy system with district cooling systems and studied Energy saving and impact on the grid in subtropical & high-density area. Results show that the DES&DCS can be energy efficient in subtropical and high-density areas. The energy saving is more than 10% and can be up to 19%. The control strategy following the cooling or electricity demand requiring more primary energy is recommended due to higher energy saving and more beneficial to the grid.

2.3 Evaluation of the distributed energy system

Compared with the traditional energy supply system, distributed energy system is a kind of energy solution which includes all kinds of power generation, energy storage and energy management. It has the characteristics of diversification and dynamic [87]. The system contains multi-level energy and a lot of information flow. It can not only deal with power failure and interruption freely, but also improve the flexibility of energy units, thus bringing better economic benefits and stability. Distributed energy system is compatible with different kinds of energy input. In addition to natural gas turbine (or internal combustion engine) power generation system, it also includes solar energy, wind energy and other renewable energy sources, and provides a variety of energy supply, such as electricity, heat, cold, etc. It provides building power supply and cooling and heating load mainly through the mutual supplement and coordination of various energy sources.

Distributed energy system has a wide prospect, so it is very important to evaluate the system comprehensively, systematically and effectively in order to evaluate its benefits more accurately. The current definition of energy efficiency focuses more on technology. However, for the system with different energy input, conversion, output and storage, only considering a certain energy utilization efficiency or the energy efficiency of a certain conversion link cannot truly and comprehensively reflect the efficiency level of the whole system, and more comprehensive indicators are needed to investigate the energy efficiency level of the whole system as a whole. This paper evaluates the distributed energy system through the performance of economy, environment and reliability, in order to promote the development and construction of multi energy complementary distributed energy system.

DES evaluation is often based on the comparison with a reference system, with consideration of multiple performances [88]. Further, when the evaluation involves several DES options, the evaluation becomes complex owing to the following two reasons [89]. The first is that the subjective evaluation based on experts' knowledge and experience is involved, apart from the objective evaluation. The second is that how the subjective evaluation is obtained and how the two types of evaluation are combined have a significant effect on the ranking of DES alternatives [90]. Therefore, based on the comparison with the reference system, research on the performance evaluation of diverse DESs also have been conducted to assist the decision-maker or engineer to identify the optimal DES. Jing et al. [91] applied a multicriteria assessment model that combines the improved gray relational analysis approach and entropy information approach to evaluate the performances of SOFC-CCHP used in five public buildings in China. In the combination model, the improved gray relational analysis approach was applied to determine the integrated gray incidence degree, based on the criteria weights determined by the entropy information approach. The larger gray incidence degree is, the better the option is. Yang et al. [92] also applied a combined approach to evaluate the DES applied in a university. Differently, in this combined approach, both subjective and objective evaluation were considered and the weights in each evaluation were determined by rank correlation analysis and entropy information method, respectively.

Many criteria have been used to evaluate DES performance in energetic, environmental, economic and other aspects. One or two evaluation criteria are commonly selected to show the DES performance in a certain aspect. Because DES is entirely or partially fired by renewable energies

and waste heat, there is a potential that primary energy is saved, and CO_2 emission and total cost are reduced by DES when compared with the reference system. Therefore, the primary energy saving ratio, CO_2 emission reduction ratio and annual total cost saving ratio are three of the most used criteria. Energy efficiency is usually proportional to environmental performance, but economic performance conflicts with them. Therefore, in the comprehensive performance analysis, economic, environmental, energy criteria, etc., are often integrated into one criterion by weights [141]. Reliability is also one of the most important advantages of the DES, which should be added into the evaluation. Trade-offs between different performances can be addressed by the comprehensive performance analysis. Among these evaluation performances, more attention is paid to economy, environment and reliability.

2.3.1 Economic performance of the distributed energy system

For any system, economic performance is an important part of whether it can be established and how to establish it reasonably. The economic evaluation of distributed energy system is usually reflected in investment cost and operation cost. For the part of investment cost, because the whole energy system is composed of a variety of equipment, it often needs a certain degree of investment support in the initial stage of construction, which is also an important standard to evaluate whether the whole distributed energy system meets the economic requirements. The investment cost consists of the total cost of each infrastructure. For the part of operation cost, in addition to the initial cost input, the energy system in the process of operation, for the needs of work and maintenance, will also produce a series of operating costs. The main factors include: the annual maintenance cost and annual operation cost of each infrastructure, the cost of fuel and energy consumption in a certain period of time, which can be followed according to different equipment.

Moradi et al. [93] evaluate the effects of microgrids on the consumers' energy costs and system reliability. The results indicate that the installation of distributed generation sources by forming a micro grid or with no micro grid will reduce the energy costs.

Zoka et al. [94] proposes a method for the economic evaluation of an autonomous independent network of distributed energy resources and estimates the total costs to consumers in a Microgrid with optimized operation of distributed generators and energy storage systems. The result presents that Microgrids have great technical and economic potential to become a new energy supply system.

Schröder et al. [45] investigated a grid-connected set of distributed energy resources that supply power for electric vehicle charging and hydrogen production through detailed simulation studies. The simulation results show that using the battery storage for peak shaving minimizes the distributed energy resources overall cost while simultaneously decreasing its dependence on the utility grid.

Horowitz et al. [95] present techno-economic analysis of three possible solutions for mitigating these effects on two real feeders: traditional infrastructure upgrades, autonomous volt-var controls, and a distributed energy management system (DERMS). And compare trade-offs for each solution in terms of effectiveness, upfront capital costs, operating costs, PV output curtailment, and distribution system losses. The results find that volt-var controls offer the lowest cost option for hosting capacity expansion but cannot mitigate all violations at high penetration levels.

Joshi et al. [96] provide a system consists of multiple solar PV modules, wind turbines, and

thermal generators. Fig.2-17 shows the implementation of PSO. Results have also been compared with the classical optimization technique QCP and other metaheuristic technique such as GA and one of the recently developed techniques, namely comprehensive TLBO (CTLBO), which indicates that the computational strength and quality of solution obtained from improved TLBO (TLBO–PSO) is superior to other four algorithms under consideration.

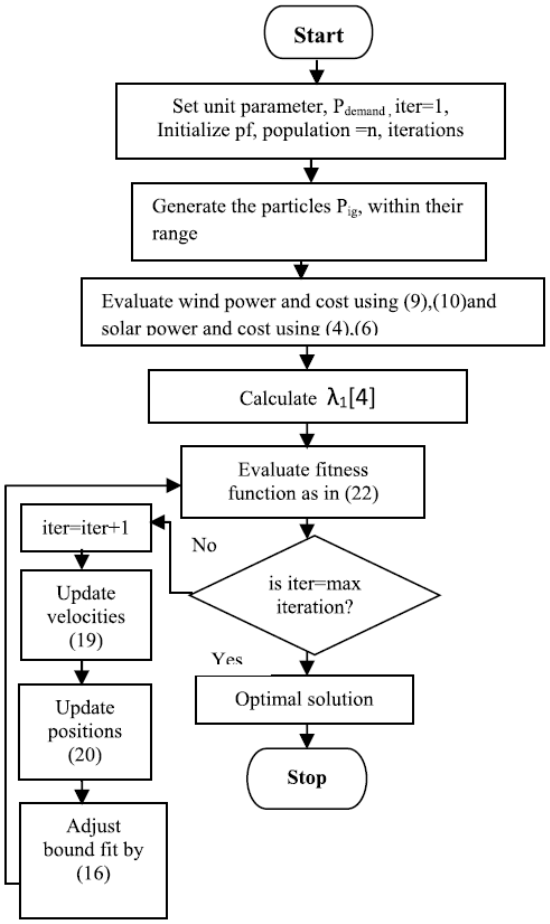

Fig.2-17 Flowchart of PSO based economic dispatch of power generation

Chang et al. [97] propose an improved distributed robust optimization approach with self-adaptive step-sizes based on the line search method and a polynomial filter, to minimize the overall costs of flexible resources including conventional generators, energy storage systems, renewable energy curtailments, deferrable loads and tie-line power exchanges, while considering various constraints, such as supply-demand power balance, line congestion constraints and power output limits. The results show that the proposed approach is effective and accurate compared to the traditional centralized gradient method.

Harder et al. [98] propose and develop a methodology for generic flexibility quantification. The result indicates the importance of realistically representing tariff structures for a proper flexibility quantification and cost estimation.

Kumamoto et al. [99] propose time-of-use (TOU) pricing that ensures every prosumer saves on energy costs. The results indicate that the proposed TOU pricing is economically efficient and

enables the aggregator to procure flexibility from its prosumers while increasing its own profit and reducing the energy cost of its prosumers.

Niu et al. [100] proposed a mixed-integer and linear programming model for optimizing the dispatch of a distributed energy system with minimum operational costs. A detailed case study is conducted in which three types of flexibility measures are modeled, and their effects on end-users and power grid are discussed. The optimal results show that each flexibility measure can well response to the time-of-use price.

Li et al. [101] proposed an energy storage economic dispatch strategy for deferring substation expansion considering the improvement of energy storage operation revenue to reduce the energy storage investment cost. the results show that the economic dispatching strategy proposed in this paper can greatly increase the operating income of energy storage, reduce the equivalent annual investment cost of energy storage equipment by $54,930 compared with the substation expansion scheme, and increase the annual availability rate of transformers to 32.8%, the annual availability hours of distributed generations increased by 267 h.

Bustos et al. [102] propose a robust framework based on a local and optimal microgrid combined with learning curves to assess the potential penetration of Distributed Energy Resources in households. Results show PV dominance with flat bundled volumetric tariffs and the increase of utility's bankruptcy risk if tariffs are not updated (47% revenue reduction).

Tao et al. [103] focus on the smart grid with integration of DE and storage devices and formulate the related real-time pricing (RTP) as a noncooperative game. With this approach, each user can schedule the optimal energy consumption, generation and/or storage strategies while preserving the privacies of the users and the provider. Numerical results illustrate that the RTP strategy can effectively reduce peak load, balance supply and demand and enhance the welfare of each user.

Ren et al. [104] proposed a Mixed Integer Nonlinear Programming (MINLP) model to deduce the optimal energy supply strategy of a DES. As a result, a systematic CBA framework is developed considering both multi-benefits and multi-stakeholders for a DES. According to the simulation results of a case study, the exploitation of various non-energy benefits is significant which may entirely reflect the social values of a DES. Also, the CBA from each stakeholder's viewpoint may increase their motivation to join the benefit-sharing union effectively. Furthermore, second benefit trade-off may be required to ensure the satisfied profit return for each stakeholder.

Eid et al. [105] presents an approach to determine the investment and short-term average costs of distributed energy resources to supply flexibility services in a local system, and compares those costs to the average costs in the Dutch markets for balancing and day-ahead flexibility. The analysis shows that local flexibility in many cases is much more expensive than centrally provided flexibility.

Liu et al. [106] conducted an economic evaluation among four EV-DRE coordination strategies. The coordination between EV and distributed energy, discussed in this paper, is described below in Fig.2-18. It finds that the cost of power supply from demand side PV plus storage systems could be lower than that of power grid supply before 2025. This paper also identifies the key barriers that EVs and distributed storage are facing in participating in the current electricity wholesale market in China and provides policy recommendations in terms of electricity time of use (TOU) tariffs, market

thresholds and metering issues.

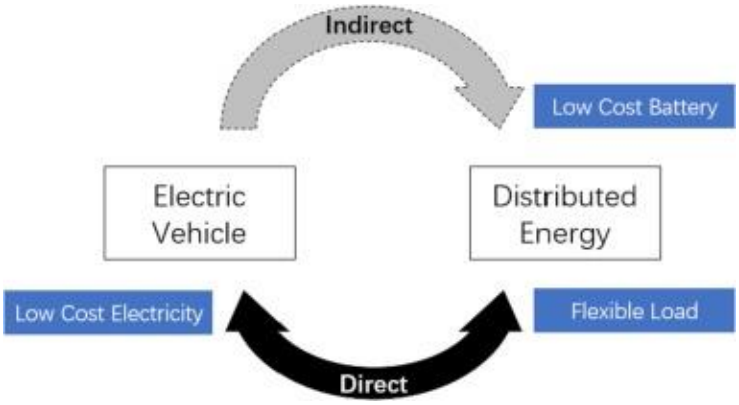

Fig.2-18 The bidirectional impacts of electric vehicles and distributed energy.

Kang et al. [107] aims to investigate the performance and benefits of the DES in Hong Kong. Based on the characteristic of energy demands, a DES, which integrates distributed generations and district cooling systems, is designed. Results denote that the DES can achieve a primary energy saving of 9.58%. Even the capital cost becomes higher, the DES is also economically beneficial due to the low operation cost.

2.3.2 Environmental performance of the distributed energy system

The environmental assessment of distributed energy system is usually reflected in the annual emissions of carbon dioxide and nitrogen-containing harmful gases. For the part of annual emission of harmful gases of carbon dioxide, the amount of carbon dioxide emitted in the process of work includes the pollution emission caused by the use of gas and the carbon dioxide emission caused by electric energy conversion, etc., and a variety of equipment operation may cause gas consumption. Therefore, there are many aspects involved, so we must take a more rigorous attitude and consider various factors to calculate the carbon dioxide emissions within a certain range. For the part of annual emissions of nitrogen-containing harmful gases, in order to investigate the impact of energy system on the surrounding environment, it is mainly based on the emissions of various harmful substances. In the infrastructure required for system operation, gas-fired boilers, gas engines, gas-fired batteries and other equipment may emit harmful gases containing nitrogen and carbon dioxide, thus threatening the air quality of the surrounding environment.

Obara et al. [108] show that introduction of the proposed microgrid can significantly reduce the environmental and economic impact. This study clarified the environmental capability and economic efficiency of the microgrid for cold regions under management of electric power quality. The optimal output of an independent microgrids consisting of natural gas combined cycle and large-scale photovoltaic was examined to achieve the CO_2 emission reduction.

He et al. [109] carried out a low-carbon economic scheduling model to improve the wind power and reduce CO2 emissions.

Ren et al. [110] proposed a residential energy system consists of the PV/Fuel cell/Battery and optimized it with the minimizing annual running cost or annual CO2 emissions.

Ju et al. [111] construct a CCHP and renewable energy based hybrid energy system driven by distributed energy resources (DERs CCHP) and proposes a multi-objective optimization model for DERs CCHP system under four optimization of energy rate (ER), total operation cost (TOC), carbon dioxide emission reductions (CER) and joint optimization. The result indicates the performance of the DERs CCHP system will become better with the increase of chiller COP, decrease of NG price and wind-photovoltaic equipment cost.

Wu et al. [112] investigated the impact of energy consumption, carbon and energy market regulations, energy density, and transaction rate in the low carbon transition for distributed energy systems through an agent-based model. Simulation results show that a single system cannot achieve low carbon transition, while a one-way climate policy linked system can realize low carbon transition. And also show that the larger high and low energy capacity is, the system is less likely to achieve low carbon transition in the circumstance of the same transaction rate with the constant emission policy bias.

Yan et al. [46] proposed a life cycle economic and carbon emissions assessment framework by dividing the building distributed energy system into five stages. Based on the theory of life cycle assessment (LCA), this research carried out the cost and carbon footprint analysis of DES by dividing the energy system life cycle into five stages: predevelopment and consenting stage, product stage, installation and commissioning stage, operation and maintenance stage, and decommissioning and disposal stage, the structure is presented in Fig.2-19. It's found that the carbon emissions in the operation and maintenance stage accounts for the largest share in the entire life cycle. In addition, the proportion of carbon emissions from natural gas is the highest, accounting for 65–73% under environmental optimization and 85–88% under economic optimization.

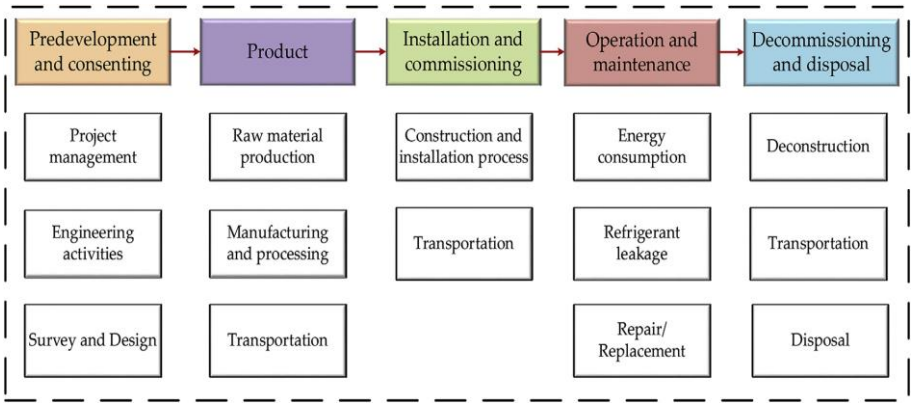

Fig.2-19 System framework of life cycle cost and carbon emissions of DES.

Wu et al. [113] regulates the low carbon transition in a distributed energy system and proposes a systematic scheme for different situations of countries. Simulation results show that under the condition of increased energy capacities with a positive feedback between supply and demand, low carbon transition can be facilitated by the combination of market adjustment favoring low carbon energies and the policy adjustment for low energy consumptions. By contrast, with low energy capacities and high energy consumptions, transitions from high-carbon economy to low-carbon economy inevitably render a catastrophic economic depression.

Liu et al. [114] proposes a new solar hybrid clean fuel-fired distributed energy system to increase the system thermodynamic efficiency and save fossil fuel, in which solar energy is upgraded into high-level chemical energy of syngas (H_2 and CO) by integrating solar-driven methanol decomposition based thermochemical conversion. Fig.2-20 illustrates a schematic view of the proposed DES and main components in this research. With the integration of solar energy utilization and tri-generation, the proposed system achieves a high net solar-to-electric efficiency, 24.66%, and results in high primary energy ratio, 83.86%, exergy efficiency, 38.81%, and carbon emission saving rate, 51.43%.

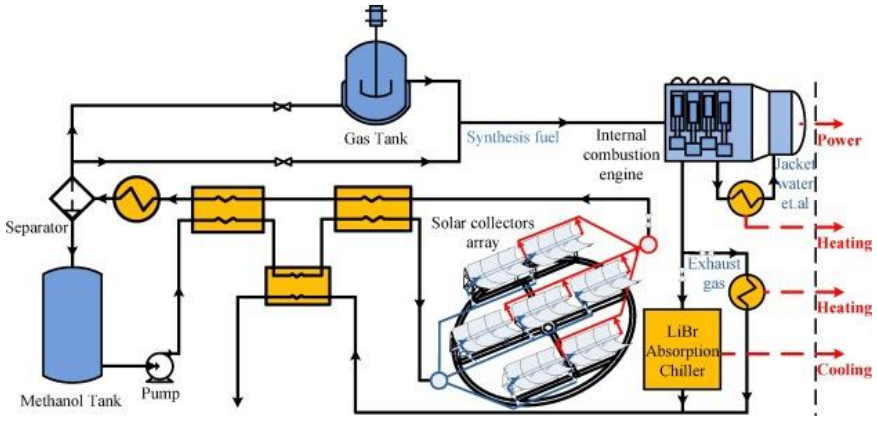

Fig.2-20 Schematic of the proposed DES.

2.3.3 Reliability performance of the distributed energy system

The main purpose of energy design and management research is to improve the reliability of power supply. Power system reliability refers to the ability of power system to resist the risk of outages in case of emergency event, which has always been the research focus of scholars and technicians in the field of electric power around the world. In this section, the reliability studies of the DER system and the technologies are reviewed.

As for the reliability analysis of distribution system, scholars at home and abroad have carried out a lot of research, and the methods used can be summarized into analytical method and Monte Carlo simulation method.

The analytical method directly analyzes the component and grid structure in the distribution network, so as to calculate the average performance index of the load point and the system [115]. The physical concept of the method is clear, and the results are relatively accurate, which is suitable for the distribution network with small scale. When the number of components in the distribution network increases and the network structure becomes complex, the analysis process of the analytical method becomes very complicated, and the amount of calculation increases greatly [116]. Analytical methods mainly include state space method and network method. The common methods in network method are: failure mode influence analysis method, minimum path method, minimum cut set method, network equivalence method, fault traversal method, etc. [117]. In recent years, some scholars have applied the method of artificial intelligence to the reliability analysis of distribution system. Fuzzy reliability evaluation method and artificial neural network reliability method have appeared [92]. The artificial neural network method is used to identify the failure state of the system

through the trained neural network. The load loss state is counted, and the reliability index of distribution system is calculated. Compared with the traditional state evaluation method, the artificial neural network analysis method has high efficiency and fast calculation speed, but the artificial intelligence algorithm is still in the initial stage of research and needs more in-depth research [118].

Adefarati et al. [119] evaluates the distributed generation (DG) system, which combines with the wind turbine generator (WTG), electric storage system (ESS) and photovoltaic (PV). A Markov model is proposed to access the stochastic characteristics of the major components of the renewable DG and compare the reliability with the conventional system. The result shown that the renewable resources can improve the reliability of the DG system and reduce the cost because the system reliability increased.

Binayak Banerjee et al. [120] analyzes the optimum value-based location of weak grid distributed system; this research point of this distributed system performance is reliable. The results of this analysis show that the location with the highest reliability of the weak grid distributed system occurs in the closest position to the customer, whether in terms of customer number, overall demand or customer priority. Neither the use of load reduction nor the use of renewable energy will change the location of the optimization. In addition, conventional resources are superior to intermittent resources based on an analysis of the maximum benefits that can be obtained from weak grid distributed system. This means that renewable energy will result in greater costs. The Markov model is a suitable approach to analyze the reliability of the system.

Borges et al. [121] proposes an optimization process which is solved by combining with the genetic algorithms (GA) to evaluate distributed generation impacts in the system reliability. The optimization process was applied to the hypothetical systems and an actual distribution system; the result shows that the presented method is suitable and robust.

In practical work, distributed energy system usually pursues economic benefits. Therefore, the reliability of the design scheme formulated under the social background has become one of the most important considerations [122]. The relationship between them can be expressed in the form of mathematical function model, which can more directly reflect the principles to be followed, and as a reference basis, it can play a greater role in the later optimization design of energy system [123]. Generally speaking, the cost of energy system should be composed of equipment maintenance cost, fuel resource consumption cost, basic configuration cost and other factors, which are in direct proportion to each other.

Moradi et al. [93] evaluates the effect of creating a microgrid and using of distributed generation resources to reduce costs and increase the reliability of supplying energy. The four scenarios are providing energy by main grid, main grid and distributed generation resources, isolated micro grid and a micro grid connected to an upstream network. Each scenario is considered in two cases for evaluating reliability. The results show that the energy supply using micro grid connected to upstream grid imposes the least energy cost with higher reliability for the consumers.

Due to the gradual development of power grid and the complexity of power system, Monte Carlo simulation method is used more and more in reliability research, which can greatly reduce the

calculation time of reliability evaluation [124]. Monte Carlo simulation method is a kind of probability simulation method which samples the states of components by random numbers generated by computer, and calculates the statistical characteristics of parameters through a large number of simulation experiments [125]. Compared with the traditional analytical method, Monte Carlo simulation method has many advantages and is widely used in the reliability evaluation of distribution network: first, the use of Monte Carlo simulation method can accurately simulate the random characteristics of system components, such as random load fluctuations, distributed generation fluctuations, component random failures, climate random changes and other random factors and system control strategies. Second, when the setting accuracy is fixed, the sampling times of Monte Carlo simulation method is independent of the scale of the system, which is especially suitable for the reliability evaluation of large and complex distribution networks with branches. Second, the simulation process of Monte Carlo simulation method is simple, intuitive, and easy to be used in practical operation. According to whether or not considering the time sequence characteristics, it can be divided into non sequential simulation method, sequential simulation method and pseudo sequential simulation flange class [126,127].

Wang et al. [128] adopted a binary particle swarm optimization (BPSO) to derive a set of meaningful system states, which significantly affects the adequacy indices of generation system including loss of load expectation (LOLE), loss of load frequency (LOLF), and expected energy not supplied (EENS).

Adefarati et al. [129] uses expected energy not served, loss of load expectation and loss of load probability to obtain the reliability performance indicators such as, in addition to utilizing an optimization tool in the MATLAB environment to investigate the environmental and economic effects of renewable energy resources in a power system.

Wang et al. [130] proposed a novel absorption thermal energy storage system together with electric energy storage for distributed energy systems. The results in a typical summer day indicate that the DG utilization rate increases from 80% to 92.9%, meanwhile the required capacities of electric chillers can be obviously reduced. The operating cost of DES also reduces by 12.9% compared with the DES without energy storage.

Zhu et al. [131] investigated the potential of distributed energy resources that can be used in Sichuan University (SCU). This research built 4 micro-grids with a total 156 Kw PV capacities to collect the power generation data. The total roof area of SCU Jiangan campus is 165701 m2, and the estimated installed capacity is 8.3MW-11.6MW. And based on this data, 33% ~ 46% power cost can be covered by PV power generation.

Li et al. [132] propose a systematic valuation process to quantify the value of distributed energy resources (DERs) in the active distribution networks (ADNs) context. The result show that the proposed valuation scheme will not only contribute to the proactive investment of DERs in ADN but also help enhance the role of DERs in offering affordable, reliable, resilient and sustainable electricity services to customers.

Nowadays, seeking a balance between reliability and economy is an important issue that power systems need to address today. The economics and reliability of power systems are mutually

constrained. In the process of power reliability assessment, the severity of accidents is determined by economic evaluation, rather than simply using electrical quantities such as load shedding and power outage duration [133]. The economics of sacrificing system operation in order to ensure the reliability of the system operation will be reconsidered. At present, many studies have proposed the customer damage function (CDF) [134], loss of load value (VOLL) [135], Expected un-served power (EUP) [136] and other indicators, combining reliability with economic for analysis. The Ref. [137] applies the EUP indicator to evaluate the system supply reliability, and the reliability cost of the system is allocated based on the EUP value expected by the user, representing the reliability level of the user. At the same time, the additional cost of meeting the supply reliability requirements of each user was also studied. In the case of changes in electricity prices, a new indicator for measuring the social value of the power system, called "Loss of Social Benefit Expectation" (LOSBE) came into being [138]. It refers to the difference between the social benefit of consuming a certain amount of electricity and the cost of providing the same amount of electricity, which is adjusted according to the power loss. Therefore, it is a more reasonable indicator under market conditions. The cost of energy not supplied (CENS) represents the average cost within the interruption interval. According to the expected energy not supplied (EENS), the power outage loss is estimated by modeling the outage cost as a function of the unprovided energy, regardless of the interruption duration and frequency [139]. In addition to the direct economic loss caused by power outages, it is also necessary to calculate the social indirect costs caused by power outages. The factors involved are complex and should be adjusted according to actual needs [140].

Previous research evaluated various DES from different points of view. Most of the papers use a single index economic performance to evaluate the DES. Some researchers also assessed the environmental performance to improve the advantage of the DES. There are few studies considering the grid stabilization performance when comparing various feasible combinations of DES technologies and their corresponding sizes. This research analyzed grid stabilization effect of the DES and used the multi-criteria evaluation to trade-off these different performances. The utilization of the DES as emergency power system to show the reliability improvement is also demonstrated in the research.

Reference

[1] Meng N, Li T, Wang J, Jia Y, Liu Q, Qin H. Synergetic cascade-evaporation mechanism of a novel building distributed energy supply system with cogeneration and temperature and humidity independent control characteristics. Energy Convers Manag 2020;209:112620. https://doi.org/10.1016/j.enconman.2020.112620.

[2] Wu DW, Wang RZ. Combined cooling, heating and power: A review. Prog Energy Combust Sci 2006;32:459–95. https://doi.org/10.1016/j.pecs.2006.02.001.

[3] Wen Q, Liu G, Rao Z, Liao S. Applications, evaluations and supportive strategies of distributed energy systems: A review. Energy Build 2020;225:110314. https://doi.org/10.1016/j.enbuild.2020.110314.

[4] Notice P, Release SP. UK Energy Statistics 2015:1–15.

[5] Du Q, Cui C, Zhang Y, Zhang C, Gang W, Wang S. Promotion of distributed energy systems integrated with district cooling systems considering uncertainties in energy market and policy in China. Energy Procedia 2018;149:256–65. https://doi.org/10.1016/j.egypro.2018.08.190.

[6] Perera P. Constraints and Barriers to Deployment of Distributed Energy Systems and Micro Grids in Southern China. Energy Procedia 2016;103:201–6. https://doi.org/10.1016/j.egypro.2016.11.273.

[7] The energy system of the People's Republic of China 2018. https://www.worldenergydata.org/china/ (accessed November 1, 2020).

[8] Hou J, Wang C, Luo S. How to improve the competiveness of distributed energy resources in China with blockchain technology. Technol Forecast Soc Change 2020;151. https://doi.org/10.1016/j.techfore.2019.119744.

[9] Zhang L, Qin Q, Wei YM. China's distributed energy policies: Evolution, instruments and recommendation. Energy Policy 2019;125:55–64. https://doi.org/10.1016/j.enpol.2018.10.028.

[10] Seidl R, von Wirth T, Krütli P. Social acceptance of distributed energy systems in Swiss, German, and Austrian energy transitions. Energy Res Soc Sci 2019;54:117–28. https://doi.org/10.1016/j.erss.2019.04.006.

[11] Garlet TB, Ribeiro JLD, Savian F de S, Siluk JCM. Value chain in distributed generation of photovoltaic energy and factors for competitiveness: A systematic review. Sol Energy 2020;211:396–411. https://doi.org/10.1016/j.solener.2020.09.040.

[12] Iliopoulos N, Esteban M, Kudo S. Assessing the willingness of residential electricity consumers to adopt demand side management and distributed energy resources: A case study on the Japanese market. Energy Policy 2020;137:111169. https://doi.org/10.1016/j.enpol.2019.111169.

[13] Blackhall L, Kuiper G, Nicholls L, Scott P. Optimising the value of distributed energy resources. Electr J 2020;33:106838. https://doi.org/10.1016/j.tej.2020.106838.

[14] Hou J, Wang J, Zhou Y, Lu X. Distributed energy systems: Multi-objective optimization and evaluation under different operational strategies. J Clean Prod 2021;280:124050.

https://doi.org/10.1016/j.jclepro.2020.124050.

[15] Hong B, Li Q, Chen W, Huang B, Yan H, Feng K. Supply modes for renewable-based distributed energy systems and their applications: case studies in China. Glob Energy Interconnect 2020;3:259–71. https://doi.org/10.1016/j.gloei.2020.07.007.

[16] Chittum A, Relf G. Valuing distributed energy resources: Combined heat and power and the modern grid. Electr J 2019;32:52–7. https://doi.org/10.1016/j.tej.2019.01.003.

[17] Han J, Ouyang L, Xu Y, Zeng R, Kang S, Zhang G. Current status of distributed energy system in China. Renew Sustain Energy Rev 2016;55:288–97. https://doi.org/10.1016/j.rser.2015.10.147.

[18] Ma W, Fang S, Liu G, Zhou R. Modeling of district load forecasting for distributed energy system. Appl Energy 2017;204:181–205. https://doi.org/10.1016/j.apenergy.2017.07.009.

[19] Ullah S, Haidar AMA, Hoole P, Zen H, Ahfock T. The current state of Distributed Renewable Generation, challenges of interconnection and opportunities for energy conversion based DC microgrids. J Clean Prod 2020;273:122777. https://doi.org/10.1016/j.jclepro.2020.122777.

[20] Wu G, Xiang Y, Liu J, Shen X, Cheng S, Hong B, et al. Distributed energy-reserve Co-Optimization of electricity and natural gas systems with multi-type reserve resources. Energy 2020;207:118229. https://doi.org/10.1016/j.energy.2020.118229.

[21] Li L, Yu S. Optimal management of multi-stakeholder distributed energy systems in low-carbon communities considering demand response resources and carbon tax. Sustain Cities Soc 2020;61:102230. https://doi.org/10.1016/j.scs.2020.102230.

[22] Cortés P, Auladell-León P, Muñuzuri J, Onieva L. Near-optimal operation of the distributed energy resources in a smart microgrid district. J Clean Prod 2020;252. https://doi.org/10.1016/j.jclepro.2019.119772.

[23] Tooryan F, HassanzadehFard H, Collins ER, Jin S, Ramezani B. Optimization and energy management of distributed energy resources for a hybrid residential microgrid. J Energy Storage 2020;30:101556. https://doi.org/10.1016/j.est.2020.101556.

[24] Das S, Ray A, De S. Optimum combination of renewable resources to meet local power demand in distributed generation: A case study for a remote place of India. Energy 2020;209:118473. https://doi.org/10.1016/j.energy.2020.118473.

[25] Luo X, Liu Y, Liu J, Liu X. Optimal design and cost allocation of a distributed energy resource (DER) system with district energy networks: A case study of an isolated island in the South China Sea. Sustain Cities Soc 2019;51:101726. https://doi.org/10.1016/j.scs.2019.101726.

[26] Wu D, Ma X, Huang S, Fu T, Balducci P. Stochastic optimal sizing of distributed energy resources for a cost-effective and resilient Microgrid. Energy 2020;198. https://doi.org/10.1016/j.energy.2020.117284.

[27] Wu J, Liu M, Lu W. Measurement-based online distributed optimization of networked distributed energy resources. Int J Electr Power Energy Syst 2020;117:105703. https://doi.org/10.1016/j.ijepes.2019.105703.

[28] Guo S, Mu Y, Jia H, Chen N, Pu T, Yuan X. Optimization of AC / DC hybrid distributed energy system with power electronic transformer. Energy Procedia 2019;158:6687–92. https://doi.org/10.1016/j.egypro.2019.01.021.

[29] Ranjbar H, Hosseini SH, Zareipour H. A robust optimization method for co-planning of transmission systems and merchant distributed energy resources. Int J Electr Power Energy Syst 2020;118:105845. https://doi.org/10.1016/j.ijepes.2020.105845.

[30] Luo Z, Yang S, Xie N, Xie W, Liu J, Souley Agbodjan Y, et al. Multi-objective capacity optimization of a distributed energy system considering economy, environment and energy. Energy Convers Manag 2019;200:112081. https://doi.org/10.1016/j.enconman.2019.112081.

[31] Karmellos M, Mavrotas G. Multi-objective optimization and comparison framework for the design of Distributed Energy Systems. Energy Convers Manag 2019;180:473–95. https://doi.org/10.1016/j.enconman.2018.10.083.

[32] Ali AY, Basit A, Ahmad T, Qamar A, Iqbal J. Optimizing coordinated control of distributed energy storage system in microgrid to improve battery life. Comput Electr Eng 2020;86. https://doi.org/10.1016/j.compeleceng.2020.106741.

[33] Hamada T, Matsuhashia R. Optimal Operation for Integrated Residential Distributed Energy Resources Considering Internal Reserve. Energy Procedia 2017;141:250–4. https://doi.org/10.1016/j.egypro.2017.11.101.

[34] Perera ATD, Wickramasinghe U, Nik VM, Scartezzini JL. Optimum design of distributed energy hubs using hybrid surrogate models (HSM). Energy Procedia 2017;122:187–92. https://doi.org/10.1016/j.egypro.2017.07.343.

[35] Das CK, Bass O, Mahmoud TS, Kothapalli G, Mousavi N, Habibi D, et al. Optimal allocation of distributed energy storage systems to improve performance and power quality of distribution networks. Appl Energy 2019;252:113468. https://doi.org/10.1016/j.apenergy.2019.113468.

[36] Mavromatidis G, Orehounig K, Carmeliet J. Designing electrically self-sufficient distributed energy systems under energy demand and solar radiation uncertainty. Energy Procedia 2017;122:1027–32. https://doi.org/10.1016/j.egypro.2017.07.470.

[37] Karmellos M, Georgiou PN, Mavrotas G. A comparison of methods for the optimal design of Distributed Energy Systems under uncertainty. Energy 2019;178:318–33. https://doi.org/10.1016/j.energy.2019.04.153.

[38] Kang J, Wang S. Robust optimal design of distributed energy systems based on life-cycle performance analysis using a probabilistic approach considering uncertainties of design inputs and equipment degradations. Appl Energy 2018;231:615–27. https://doi.org/10.1016/j.apenergy.2018.09.144.

[39] Gil JD, Álvarez JD, Roca L, Sánchez-Molina JA, Berenguel M, Rodríguez F. Optimal thermal energy management of a distributed energy system comprising a solar membrane distillation plant and a greenhouse. Energy Convers Manag 2019;198:111791. https://doi.org/10.1016/j.enconman.2019.111791.

[40] Chen M, Zou G, Jin X, Yao Z, Liu Y, Yin H. Optimal Allocation method on Distributed Energy Storage System in Active Distribution Network. Energy Procedia 2017;141:525–31. https://doi.org/10.1016/j.egypro.2017.11.070.

[41] Ren H, Lu Y, Zhang Y, Chen F, Yang X. Operation simulation and optimization of distributed energy system based on TRNSYS. Energy Procedia 2018;152:3–8. https://doi.org/10.1016/j.egypro.2018.09.050.

[42] Xing X, Yan Y, Zhang H, Long Y, Wang Y, Liang Y. Optimal design of distributed energy systems for industrial parks under gas shortage based on augmented ε-constraint method. J Clean Prod 2019;218:782–95. https://doi.org/10.1016/j.jclepro.2019.02.052.

[43] Kang J, Wang S, Yan C. A new distributed energy system configuration for cooling dominated districts and the performance assessment based on real site measurements. Renew Energy 2019;131:390–403. https://doi.org/10.1016/j.renene.2018.07.052.

[44] Ren T, Li X, Chang C, Chang Z, Wang L, Dai S. Multi-objective optimal analysis on the distributed energy system with solar driven metal oxide redox cycle based fuel production. J Clean Prod 2019;233:765–81. https://doi.org/10.1016/j.jclepro.2019.06.028.

[45] Schröder M, Abdin Z, Mérida W. Optimization of distributed energy resources for electric vehicle charging and fuel cell vehicle refueling. Appl Energy 2020;277:115562. https://doi.org/10.1016/j.apenergy.2020.115562.

[46] Yan Y, Zhang H, Meng J, Long Y, Zhou X, Li Z, et al. Carbon footprint in building distributed energy system: An optimization-based feasibility analysis for potential emission reduction. J Clean Prod 2019;239:117990. https://doi.org/10.1016/j.jclepro.2019.117990.

[47] Alzahrani AM, Zohdy M, Yan B. An Overview of Optimization Approaches for Operation of Hybrid Distributed Energy Systems with Photovoltaic and Diesel Turbine Generator. Electr Power Syst Res 2021;191:106877. https://doi.org/10.1016/j.epsr.2020.106877.

[48] Levron Y, Shmilovitz D. Power systems' optimal peak-shaving applying secondary storage. Electr Power Syst Res 2012;89:80–4. https://doi.org/10.1016/j.epsr.2012.02.007.

[49] García-Plaza M, Eloy-García Carrasco J, Alonso-Martínez J, Peña Asensio A. Peak shaving algorithm with dynamic minimum voltage tracking for battery storage systems in microgrid applications. J Energy Storage 2018;20:41–8. https://doi.org/10.1016/j.est.2018.08.021.

[50] Mehr TH, Masoum MAS, Jabalameli N. Grid-connected Lithium-ion battery energy storage system for load leveling and peak shaving. 2013 Australas Univ Power Eng Conf AUPEC 2013 2013. https://doi.org/10.1109/aupec.2013.6725376.

[51] Li Y, Gao W, Ruan Y, Ushifusa Y. Grid load shifting and performance assessments of residential efficient energy technologies, a case study in Japan. Sustain 2018;10. https://doi.org/10.3390/su10072117.

[52] Kerestes RJ, Reed GF, Sparacino AR. Economic analysis of grid level energy storage for the application of load leveling. IEEE Power Energy Soc Gen Meet 2012:1–9.

https://doi.org/10.1109/PESGM.2012.6345072.

[53] Xu L, Pan Y, Lin M, Huang Z. Community load leveling for energy configuration optimization: Methodology and a case study. Sustain Cities Soc 2017;35:94–106. https://doi.org/10.1016/j.scs.2017.07.017.

[54] Yan B, Di Somma M, Graditi G, Luh PB. Markovian-based stochastic operation optimization of multiple distributed energy systems with renewables in a local energy community. Electr Power Syst Res 2020;186:106364. https://doi.org/10.1016/j.epsr.2020.106364.

[55] Fonseca JD, Commenge JM, Camargo M, Falk L, Gil ID. Multi-criteria optimization for the design and operation of distributed energy systems considering sustainability dimensions. Energy 2021;214. https://doi.org/10.1016/j.energy.2020.118989.

[56] Li Y, Yang W, He P, Chen C, Wang X. Design and management of a distributed hybrid energy system through smart contract and blockchain. Appl Energy 2019;248:390–405. https://doi.org/10.1016/j.apenergy.2019.04.132.

[57] Tian Z, Fu F, Niu J, Sun R, Huang J. Optimization and extraction of an operation strategy for the distributed energy system of a research station in Antarctica. J Clean Prod 2020;246:119073. https://doi.org/10.1016/j.jclepro.2019.119073.

[58] Guan T, Lin H, Sun Q, Wennersten R. Optimal configuration and operation of multi-energy complementary distributed energy systems. Energy Procedia 2018;152:77–82. https://doi.org/10.1016/j.egypro.2018.09.062.

[59] Malandra F, Kizilkale AC, Sirois F, Sansò B, Anjos MF, Bernier M, et al. Smart Distributed Energy Storage Controller (smartDESC). Energy 2020;210. https://doi.org/10.1016/j.energy.2020.118500.

[60] Yu T, Wang X, Ji J, Zhao S. Energy efficiency of distributed energy system based on central heating network. Procedia Eng 2017;205:2171–5. https://doi.org/10.1016/j.proeng.2017.10.039.

[61] Das CK, Bass O, Mahmoud TS, Kothapalli G, Masoum MAS, Mousavi N. An optimal allocation and sizing strategy of distributed energy storage systems to improve performance of distribution networks. J Energy Storage 2019;26:100847. https://doi.org/10.1016/j.est.2019.100847.

[62] Abazari A, Monsef H, Wu B. Coordination strategies of distributed energy resources including FESS, DEG, FC and WTG in load frequency control (LFC) scheme of hybrid isolated micro-grid. Int J Electr Power Energy Syst 2019;109:535–47. https://doi.org/10.1016/j.ijepes.2019.02.029.

[63] Li B, Wan C, Yuan K, Song Y. Demand response for integrating distributed energy resources in transactive energy system. Energy Procedia 2019;158:6645–51. https://doi.org/10.1016/j.egypro.2019.01.040.

[64] Wang X, Tian H, Yan F, Feng W, Wang R, Pan J. Optimization of a distributed energy system with multiple waste heat sources and heat storage of different temperatures based on the energy quality. Appl Therm Eng 2020;181:115975. https://doi.org/10.1016/j.applthermaleng.2020.115975.

[65] Shin H, Lee B, Iba K. Power System Regional Dependency of Distributed Energy Resources:

Utilizing the Momentary Cessation Capability. IFAC-PapersOnLine 2019;52:1–5. https://doi.org/10.1016/j.ifacol.2019.08.145.

[66] Bahramara S, Mazza A, Chicco G, Shafie-khah M, Catalão JPS. Comprehensive review on the decision-making frameworks referring to the distribution network operation problem in the presence of distributed energy resources and microgrids. Int J Electr Power Energy Syst 2020;115:105466. https://doi.org/10.1016/j.ijepes.2019.105466.

[67] Liu G, Jiang T, Ollis TB, Zhang X, Tomsovic K. Distributed energy management for community microgrids considering network operational constraints and building thermal dynamics. Appl Energy 2019;239:83–95. https://doi.org/10.1016/j.apenergy.2019.01.210.

[68] Wen Q, Liu G, Wu W, Liao S. Multicriteria comprehensive evaluation framework for industrial park-level distributed energy system considering weights uncertainties. J Clean Prod 2020:124530. https://doi.org/10.1016/j.jclepro.2020.124530.

[69] Kaikko J, Backman J. Technical and economic performance analysis for a microturbine in combined heat and power generation. Energy 2007;32:378–87. https://doi.org/10.1016/j.energy.2006.06.013.

[70] Sundberg G, Henning D. Investments in combined heat and power plants: Influence of fuel price on cost minimised operation. Energy Convers Manag 2002;43:639–50. https://doi.org/10.1016/S0196-8904(01)00065-6.

[71] Goršek A, Glavič P. Process integration of a steam turbine. Appl Therm Eng 2003;23:1227–34. https://doi.org/10.1016/S1359-4311(03)00062-0.

[72] Rosen MA, Le MN, Dincer I. Efficiency analysis of a cogeneration and district energy system. Appl Therm Eng 2005;25:147–59. https://doi.org/10.1016/j.applthermaleng.2004.05.008.

[73] Biezma M V., San Cristóbal JR. Investment criteria for the selection of cogeneration plants - A state of the art review. Appl Therm Eng 2006;26:583–8. https://doi.org/10.1016/j.applthermaleng.2005.07.006.

[74] Ferreira WM, Meneghini IR, Brandao DI, Guimarães FG. Preference cone based multi-objective evolutionary algorithm to optimal management of distribuited energy resources in microgrids. Appl Energy 2020;274:115326. https://doi.org/10.1016/j.apenergy.2020.115326.

[75] Gilani MA, Kazemi A, Ghasemi M. Distribution system resilience enhancement by microgrid formation considering distributed energy resources. Energy 2020;191:116442. https://doi.org/10.1016/j.energy.2019.116442.

[76] Farrokhseresht M, Slootweg H, Gibescu M. Strategic bidding of distributed energy resources in coupled local and central markets. Sustain Energy, Grids Networks 2020;24:100390. https://doi.org/10.1016/j.segan.2020.100390.

[77] Guerrero J, Gebbran D, Mhanna S, Chapman AC, Verbič G. Towards a transactive energy system for integration of distributed energy resources: Home energy management, distributed optimal power flow, and peer-to-peer energy trading. Renew Sustain Energy Rev 2020;132.

https://doi.org/10.1016/j.rser.2020.110000.

[78] Zakernezhad H, Nazar MS, Shafie-khah M, Catalão JPS. Multi-level optimization framework for resilient distribution system expansion planning with distributed energy resources. Energy 2021;214. https://doi.org/10.1016/j.energy.2020.118807.

[79] Fridgen G, Halbrügge S, Olenberger C, Weibelzahl M. The insurance effect of renewable distributed energy resources against uncertain electricity price developments. Energy Econ 2020;91. https://doi.org/10.1016/j.eneco.2020.104887.

[80] Cho N, Yun S, Jung J. Shunt fault analysis methodology for power distribution networks with inverter-based distributed energy resources of the Korea Electric Power Corporation. Renew Sustain Energy Rev 2020;133:110140. https://doi.org/10.1016/j.rser.2020.110140.

[81] Rezvanfar R, Tarafdar Hagh M, Zare K. Power-based distribution locational marginal pricing under high-penetration of distributed energy resources. Int J Electr Power Energy Syst 2020;123:106303. https://doi.org/10.1016/j.ijepes.2020.106303.

[82] Lee GY, Ko BS, Lee JS, Kim RY. An off-line design methodology of droop control for multiple bi-directional distributed energy resources based on voltage sensitivity analysis in DC microgrids. Int J Electr Power Energy Syst 2020;118:105754. https://doi.org/10.1016/j.ijepes.2019.105754.

[83] Li S, Pan Y, Xu P. A decentralized peer-to-peer control scheme for heating and cooling trading in distributed energy systems. J Clean Prod 2020:124817. https://doi.org/10.1016/j.jclepro.2020.124817.

[84] Wu Q, Ren H, Gao W, Ren J. Multi-criteria assessment of combined cooling, heating and power systems located in different regions in Japan. Appl Therm Eng 2014;73:660–70. https://doi.org/10.1016/j.applthermaleng.2014.08.020.

[85] Liu T, Liu Q, Xu D, Sui J. Performance investigation of a new distributed energy system integrated a solar thermochemical process with chemical recuperation. Appl Therm Eng 2017;119:387–95. https://doi.org/10.1016/j.applthermaleng.2017.03.073.

[86] Gao J, Kang J, Zhang C, Gang W. Energy performance and operation characteristics of distributed energy systems with district cooling systems in subtropical areas under different control strategies. Energy 2018;153:849–60. https://doi.org/10.1016/j.energy.2018.04.098.

[87] Fang J, Liu Q, Liu T, Lei J, Jin H. Thermodynamic evaluation of a distributed energy system integrating a solar thermochemical process with a double-axis tracking parabolic trough collector. Appl Therm Eng 2018;145:541–51. https://doi.org/10.1016/j.applthermaleng.2018.09.046.

[88] do Nascimento ÁDJ, Rüther R. Evaluating distributed photovoltaic (PV) generation to foster the adoption of energy storage systems (ESS) in time-of-use frameworks. Sol Energy 2020;208:917–29. https://doi.org/10.1016/j.solener.2020.08.045.

[89] Wen Q, Liu G, Wu W, Liao S. Genetic algorithm-based operation strategy optimization and multi-criteria evaluation of distributed energy system for commercial buildings. Energy Convers Manag 2020;226:113529. https://doi.org/10.1016/j.enconman.2020.113529.

[90] Wang J, Ye X, Li Y, Gui X, Guo H. An energy efficiency evaluation method of distributed CCHP

system based on attribute theory for optimal investment strategy. Energy Procedia 2018;152:95–100. https://doi.org/10.1016/j.egypro.2018.09.065.

[91] Jing R, Wang M, Brandon N, Zhao Y. Multi-criteria evaluation of solid oxide fuel cell based combined cooling heating and power (SOFC-CCHP) applications for public buildings in China. Energy 2017;141:273–89. https://doi.org/10.1016/j.energy.2017.08.111.

[92] Yang K, Ding Y, Zhu N, Yang F, Wang Q. Multi-criteria integrated evaluation of distributed energy system for community energy planning based on improved grey incidence approach: A case study in Tianjin. Appl Energy 2018;229:352–63. https://doi.org/10.1016/j.apenergy.2018.08.016.

[93] Moradi MH, Khandani A. Evaluation economic and reliability issues for an autonomous independent network of distributed energy resources. Int J Electr Power Energy Syst 2014;56:75–82. https://doi.org/10.1016/j.ijepes.2013.11.006.

[94] Zoka Y, Sugimoto A, Yorino N, Kawahara K, Kubokawa J. An economic evaluation for an autonomous independent network of distributed energy resources. Electr Power Syst Res 2007;77:831–8. https://doi.org/10.1016/j.epsr.2006.07.006.

[95] Horowitz KAW, Jain A, Ding F, Mather B, Palmintier B. A techno-economic comparison of traditional upgrades, volt-var controls, and coordinated distributed energy resource management systems for integration of distributed photovoltaic resources. Int J Electr Power Energy Syst 2020;123:106222. https://doi.org/10.1016/j.ijepes.2020.106222.

[96] Joshi PM, Verma HK. An improved TLBO based economic dispatch of power generation through distributed energy resources considering environmental constraints. Sustain Energy, Grids Networks 2019;18:100207. https://doi.org/10.1016/j.segan.2019.100207.

[97] Chang X, Xu Y, Sun H, Khan I. A distributed robust optimization approach for the economic dispatch of flexible resources. Int J Electr Power Energy Syst 2021;124:106360. https://doi.org/10.1016/j.ijepes.2020.106360.

[98] Harder N, Qussous R, Weidlich A. The cost of providing operational flexibility from distributed energy resources. Appl Energy 2020;279:115784. https://doi.org/10.1016/j.apenergy.2020.115784.

[99] Kumamoto T, Aki H, Ishida M. Provision of grid flexibility by distributed energy resources in residential dwellings using time-of-use pricing. Sustain Energy, Grids Networks 2020;23:100385. https://doi.org/10.1016/j.segan.2020.100385.

[100] Niu J, Tian Z, Zhu J, Yue L. Implementation of a price-driven demand response in a distributed energy system with multi-energy flexibility measures. Energy Convers Manag 2020;208. https://doi.org/10.1016/j.enconman.2020.112575.

[101] Li C, Zhou H, Li J, Dong Z. Economic dispatching strategy of distributed energy storage for deferring substation expansion in the distribution network with distributed generation and electric vehicle. J Clean Prod 2020;253:119862. https://doi.org/10.1016/j.jclepro.2019.119862.

[102] Bustos C, Watts D, Olivares D. The evolution over time of Distributed Energy Resource's penetration: A robust framework to assess the future impact of prosumage under different tariff

designs. Appl Energy 2019;256:113903. https://doi.org/10.1016/j.apenergy.2019.113903.

[103] Tao L, Gao Y. Real-time pricing for smart grid with distributed energy and storage: A noncooperative game method considering spatially and temporally coupled constraints. Int J Electr Power Energy Syst 2020;115:105487. https://doi.org/10.1016/j.ijepes.2019.105487.

[104] Ren H, Wu Q, Zhu Q, Gao W. Cost–benefit analysis of distributed energy systems considering multi-benefits and multi-stakeholders. Energy 2019;189:116382. https://doi.org/10.1016/j.energy.2019.116382.

[105] Eid C, Grosveld J, Hakvoort R. Assessing the costs of electric flexibility from distributed energy resources: A case from the Netherlands. Sustain Energy Technol Assessments 2019;31:1–8. https://doi.org/10.1016/j.seta.2018.10.009.

[106] Liu J, Zhong C. An economic evaluation of the coordination between electric vehicle storage and distributed renewable energy. Energy 2019;186:115821. https://doi.org/10.1016/j.energy.2019.07.151.

[107] Kang J, Wang S, Gang W. Performance and Benefits of Distributed Energy Systems in Cooling Dominated Regions: A Case Study. Energy Procedia 2017;142:1991–6. https://doi.org/10.1016/j.egypro.2017.12.400.

[108] Obara S, Nagano K, Okada M. Facilities introduction planning of a microgrid with CO2 heat pump heating for cold regions. Energy 2017;135:486–99. https://doi.org/10.1016/j.energy.2017.06.154.

[109] He L, Lu Z, Zhang J, Geng L, Zhao H, Li X. Low-carbon economic dispatch for electricity and natural gas systems considering carbon capture systems and power-to-gas. Appl Energy 2018;224:357–70. https://doi.org/10.1016/j.apenergy.2018.04.119.

[110] Ren H, Wu Q, Gao W, Zhou W. Optimal operation of a grid-connected hybrid PV/fuel cell/battery energy system for residential applications. Energy 2016;113:702–12. https://doi.org/10.1016/j.energy.2016.07.091.

[111] Ju L, Tan Z, Li H, Tan Q, Yu X, Song X. Multi-objective operation optimization and evaluation model for CCHP and renewable energy based hybrid energy system driven by distributed energy resources in China. Energy 2016;111:322–40. https://doi.org/10.1016/j.energy.2016.05.085.

[112] Wu X, Cao J, Jiang C, Lou Y, Zhao S, Madani H, et al. Low Carbon Transition in Climate Policy Linked Distributed Energy System. Glob Transitions Proc 2020;1:1–6. https://doi.org/10.1016/j.gltp.2020.03.002.

[113] Wu X, Xu Y, Lou Y, Chen Y. Low carbon transition in a distributed energy system regulated by localized energy markets. Energy Policy 2018;122:474–85. https://doi.org/10.1016/j.enpol.2018.08.008.

[114] Liu T, Liu Q, Lei J, Sui J. A new solar hybrid clean fuel-fired distributed energy system with solar thermochemical conversion. J Clean Prod 2019;213:1011–23. https://doi.org/10.1016/j.jclepro.2018.12.193.

[115] Dai H, Wang J, Li G, Chen W, Qiu B, Yan J. A multi-criteria comprehensive evaluation

method for distributed energy system. Energy Procedia 2019;158:3748–53. https://doi.org/10.1016/j.egypro.2019.01.881.

[116] Sun C, Yuan K, Zhao T, Song G, Yang X, Song Y. Operational strategy based evaluation method of distributed energy storage system in active distribution networks. Energy Procedia 2019;158:1027–32. https://doi.org/10.1016/j.egypro.2019.01.249.

[117] Wang Y, Kuckelkorn J, Li D, Du J. Evaluation on distributed renewable energy system integrated with a Passive House building using a new energy performance index. Energy 2018;161:81–9. https://doi.org/10.1016/j.energy.2018.07.140.

[118] Jing R, Zhu X, Zhu Z, Wang W, Meng C, Shah N, et al. A multi-objective optimization and multi-criteria evaluation integrated framework for distributed energy system optimal planning. Energy Convers Manag 2018;166:445–62. https://doi.org/10.1016/j.enconman.2018.04.054.

[119] Adefarati T, Bansal RC. Reliability assessment of distribution system with the integration of renewable distributed generation. Appl Energy 2017;185:158–71. https://doi.org/10.1016/j.apenergy.2016.10.087.

[120] Banerjee B, Islam SM. Electrical Power and Energy Systems Reliability based optimum location of distributed generation. Int J Electr Power Energy Syst 2011;33:1470–8. https://doi.org/10.1016/j.ijepes.2011.06.029.

[121] Borges CLT, Falca DM. Optimal distributed generation allocation for reliability , losses , and voltage improvement 2006;28:413–20. https://doi.org/10.1016/j.ijepes.2006.02.003.

[122] Tan ZF, Zhang HJ, Shi QS, Song YH, Ju LW. Multi-objective operation optimization and evaluation of large-scale NG distributed energy system driven by gas-steam combined cycle in China. Energy Build 2014;76:572–87. https://doi.org/10.1016/j.enbuild.2014.03.029.

[123] Ren H, Gao W, Zhou W, Nakagami K. Multi-criteria evaluation for the optimal adoption of distributed residential energy systems in Japan. Energy Policy 2009;37:5484–93. https://doi.org/10.1016/j.enpol.2009.08.014.

[124] Ali Kadhem A, Abdul Wahab NI, Aris I, Jasni J, Abdalla AN. Computational techniques for assessing the reliability and sustainability of electrical power systems: A review. Renew Sustain Energy Rev 2017;80:1175–86. https://doi.org/10.1016/j.rser.2017.05.276.

[125] Ren H, Gao W. A MILP model for integrated plan and evaluation of distributed energy systems. Appl Energy 2010;87:1001–14. https://doi.org/10.1016/j.apenergy.2009.09.023.

[126] Ameli SM, Agnew B, Potts I. Integrated distributed energy evaluation software (IDEAS). Simulation of a micro-turbine based CHP system. Appl Therm Eng 2007;27:2161–5. https://doi.org/10.1016/j.applthermaleng.2005.07.019.

[127] Castagneto G, Zakeri B, Dodds PE, Subkhankulova D. Evaluating consumer investments in distributed energy technologies. Energy Policy 2020:112008. https://doi.org/10.1016/j.enpol.2020.112008.

[128] Wang L, Singh C, Tan KC. Reliability evaluation of power-generating systems including

time-dependent sources based on binary particle swarm optimization. 2007 IEEE Congr Evol Comput CEC 2007 2007:3346–52. https://doi.org/10.1109/CEC.2007.4424904.

[129] Adefarati T, Bansal RC. Reliability and economic assessment of a microgrid power system with the integration of renewable energy resources. Appl Energy 2017;206:911–33. https://doi.org/10.1016/j.apenergy.2017.08.228.

[130] Wang L, Xiao F, Cui B, Hu M, Lu T. Performance analysis of absorption thermal energy storage for distributed energy systems. Energy Procedia 2019;158:3152–7. https://doi.org/10.1016/j.egypro.2019.01.1017.

[131] Zhu Y, Wang F, Yan J. The Potential of Distributed Energy Resources in Building Sustainable Campus: The Case of Sichuan University. Energy Procedia 2018;145:582–5. https://doi.org/10.1016/j.egypro.2018.04.085.

[132] Li Z, Shahidehpour M, Alabdulwahab A, Al-Turki Y. Valuation of distributed energy resources in active distribution networks. Electr J 2019;32:27–36. https://doi.org/10.1016/j.tej.2019.03.001.

[133] Chao W, Zheng XU, Peng GAO, Yong C, Zhejiang U. Reliability Index Framework for Reliability Evaluation of Bulk Power System 2007;27.

[134] Chowdhury A. Application of customer interruption costs in transmission network reliability planning. IEEE Trans Ind Appl 2001;37:53–60.

[135] The Value of Lost Load (VoLL) in European Electricity Markets : Uses , Methodologies , Future Directions 2019.

[136] Okada K, Asano H, Yokoyama R, Niimura T. Reliability-based impact analysis of independent power producers for power system operations under deregulation. Can Conf Electr Comput Eng 1999;3:1325–30. https://doi.org/10.1109/ccece.1999.804885.

[137] Niioka S, Okada N, Yokoyama R. Evaluation and allocation of supply reliability cost in electricity market. PowerCon 2000 - 2000 Int Conf Power Syst Technol Proc 2000;2:703–7. https://doi.org/10.1109/ICPST.2000.897108.

[138] Yu Z, Nderitu G, Smardo F. A proposed LOSBE as a generation “reliability” index for deregulated electricity markets. 2000 IEEE Power Eng Soc Conf Proc 2000;3:1820–4. https://doi.org/10.1109/PESW.2000.847628.

[139] Adefarati T, Bansal RC. Reliability assessment of distribution system with the integration of renewable distributed generation. Appl Energy 2017;185:158–71. https://doi.org/10.1016/j.apenergy.2016.10.087.

[140] Xiuguang Y, Chun H. Risk Assessment of Distribution Network Involving Fault Outage Economic Losses. Proc CSU-EPSA 2016;8:7–12.

[141] Zhang X, Li H, Liu L, Bai C, Wang S, Song Q, et al. Optimization analysis of a novel combined heating and power system based on biomass partial gasification and ground source heat pump. Energy Convers Manag 2018;163:355–70. https://doi.org/10.1016/j.enconman.2018.02.073.

Chapter 3

THEORIES AND METHODOLOGY OF THE STUDY

CHAPTER THREE: THEORIES AND METHODOLOGY OF THE STUDY

THEORIES AND METHODOLOGY OF THE STUDY *3-1*

3.1 Motivation 3-1

3.2 Model establishment 3-2

3.2.1 Devices and distributed energy systems model 3-2

3.2.2 Performance analysis 3-15

3.2.3 Simulation model and algorithm 3-20

Reference 3-24

3.1 Motivation

Studies have shown that the DES have the ability to reduce the energy crisis and the greenhouse gases emitted by the conventional power plants, which will contribute substantially to future energy generation. At the same time, it has lots of features: variable capacity, flexible operation pattern, improvement of security in running grid system and promotion to the diversification of grid-connection patterns for renewable energy. The development of the DES promotes the transformation of the traditional power grid with a single power supply plant to a smart grid with multi-source power supply and integrated with the demand side.

The DES contains various equipment, which can meet the electricity, cooling and heating load at the same time. It increases the complexity of the energy supply mode of DESs. The same load demand can have a variety of energy supply combination mode and operation strategy. In order to realize the high economic and energy-saving potential of DESs, it is necessary to determine the quantity and capacity of each selected equipment and the system operation strategy to meet the energy demand of target users. An important factor affecting the optimal configuration and operation strategy selection of DESs is an effective evaluation method. Different evaluation criteria reflect diverse aspects of the DES. Usually, when designing a DES, its evaluation is only considering the economic benefit of system operation or primary energy utilization rate. However, only one evaluation index is not comprehensive enough to evaluate the advantages and disadvantages of DESs reasonably and accurately. For example, energy costs and carbon emissions are evaluation indicators from two different perspectives and often conflict with each other. It is necessary to optimize these objectives in a comprehensive way [1]. Trade-offs between different performances can be addressed by the multi-criteria evaluation analysis.

The main advantages of the DES are to save energy cost, reduce environmental impact and improve reliability of the power grid. Therefore, this paper explores the application potentials in the economic, environmental, and reliability performance of the DES in different scenarios from the cost-saving, grid stabilization and carbon emission reduction. Based on the above three aspects, the multi-criteria evaluation method is established to optimize the design of the DES. It is hoped that it can improve the utilization competitiveness of the DES and provide theoretical reference for the application research of the DES.

3.2 Model establishment

3.2.1 Devices and distributed energy systems model

3.2.1.1 Power generation devices

1) Diesel generator (DG)

The diesel generator uses the principle of internal combustion for power generation. It can be used for prime, continuous applications in the rural areas or backup systems in case of power outage that have no access to the main grid supply system. Quick start up, mobility, fuel flexibility, high reliability and high efficiency is the features of the diesel generator [2]. The diesel generator can operate at the 30%–90% of its nominal rating according to the equipment manufacturer. It utilizes the electronic control module to regulate the fuel consumption based on the load demand as well as to increase the efficiency of the system. The power generation cost function of the diesel generator can be determined by using polynomial fits of the diesel generator operating characteristics that are made available by the manufacturer. The fuel consumption of the diesel generator depends on the power output, type of the diesel generator, the quality of the fuel, humidity and the ambient temperature [3]. Diesel generators consist of two basic parts: a diesel engine and a synchronous generator. Fig. 3-2 [4] shows a block diagram design of a diesel generator:

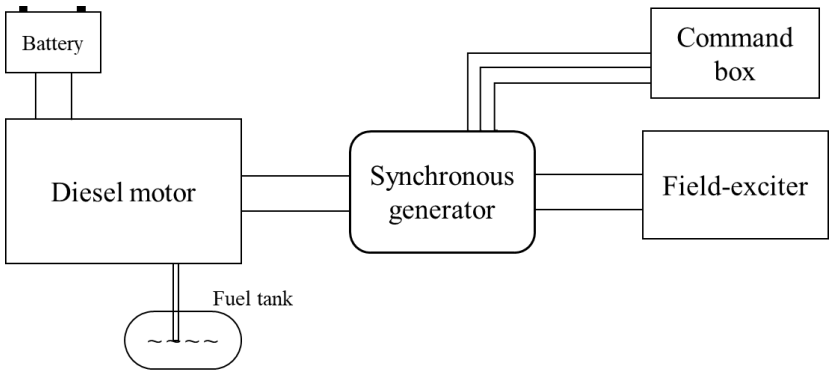

Fig.3-2 Block diagram of a diesel generator [4]

The fuel cost of the diesel generator with its output power at t-time can be expressed as:

$$F_{DG} = a_1 \cdot (E_{DG}^t)^2 + a_2 \cdot E_{DG}^t + a_3 \quad (3\text{-}1)$$

where F_{DG} is the fuel cost of the diesel generator, L/h. E_{DG}^t is the electricity generated by the diesel generator at t-time, kW. And a_1, a_2 and a_3 are the cost coefficient of the diesel generator.

The electricity generated by the diesel generator can be estimated by using Equation (3-2):

$$E_{DG}^t = Cp_{DG} \cdot \eta_{DG}^t \quad (3\text{-}2)$$

where Cp_{DG} is the power capacity of diesel generator, kW. η_{DG}^t is the is the efficiency of the diesel generator at t-time, %.

However, the operation and maintenance costs of the diesel generator are highly expensive when compared with other distributed energy resources, and due to its high emissions, more and more

systems choose to use other cleaner distributed energy sources as alternative.

2) Gas internal-combustion engine (ICE)

The gas internal combustion engine is working as following: As the Fig.3-3 shows, first, the natural gas is mixed with air in the engine and then pressurizes it through a turbocharger and enters the cylinder block to burn. The crankshaft converts the reciprocating motion of the piston into rotary motion through the connection rod. In this process, the engine undergoes four strokes of intake, compression, combustion, and exhaust to convert chemical energy into mechanical energy. Secondly, the engine drives the camshaft of the generator through elastic couplings and generates electrical energy. After the four strokes, the exhaust gas of the gas internal combustion engine and the cylinder liner water are at high temperature, which can be used to provide cooling and heating load through the waste heat utilization equipment. Thus, the primary energy utilization of the ICE can be improved.

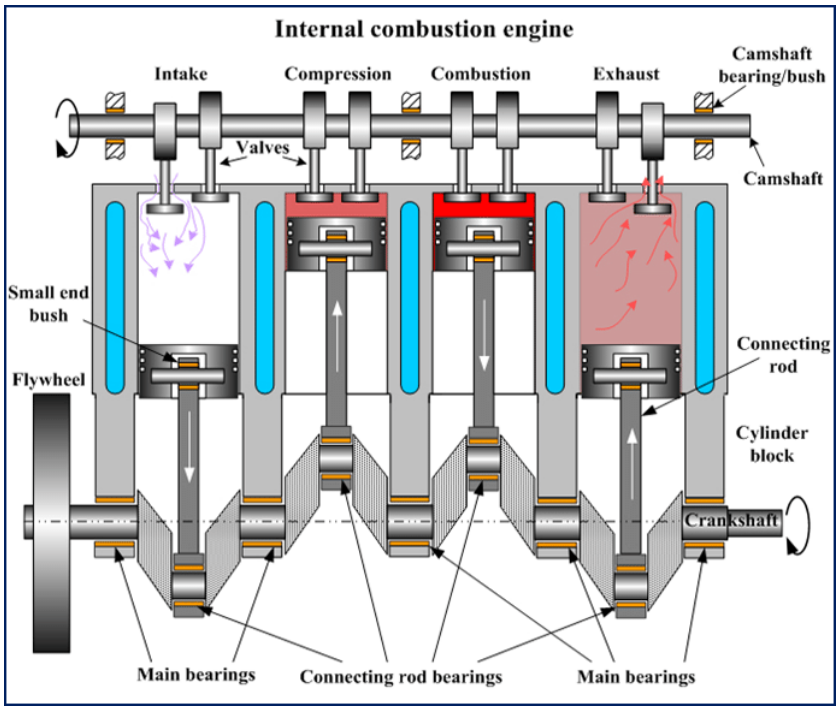

Fig.3-3 Schematic of an internal combustion engine [5]

The technology of gas-fired internal combustion generators is very mature, and there are many famous manufacturers in the world. Such as American Cummins, American Caterpillar, American Waukesha, German MWM, Finnish Wärtsilä, and American GE (Yanbach). In this paper, we select the Yanbach as an example to study the performance of the ICE.

The power generation model of the internal combustion engine can be expressed as:

$$E_{ICE}^{t} = F_{ICE} \cdot L_g \cdot \eta_{ICE,e}^{t} \tag{3-3}$$

where, E_{ICE}^{t} is the power generation power of the internal combustion engine at t-time, kW. F_{ICE} is the natural gas consumption of the internal combustion engine, kWh. L_g is the low calorific value of natural gas, MJ/Nm^3. $\eta_{ICE,e}^{t}$ is the electrical efficiency of the internal combustion engine at t-

time, %.

The output thermal power model of the internal combustion engine can be expressed as:

$$Q_{ICE}^{t} = F_{ICE}^{t} \times \eta_{ICE,heat}^{t} \quad (3\text{-}4)$$

where, Q_{ICE} is the output thermal power of the internal combustion engine, kW. $\eta_{ICE,heat}$ is the thermal efficiency of the internal combustion engine, %.

When the equipment is running under partial load, the electrical and thermal efficiency changes with the different partial load ratio [6], as shown in Fig.3-4.

It can be estimated with the polynomial fits' formulas, which are as following:

$$\eta_{ICE,e}^{t} = b_1 \cdot (PL_{ICE}^{t})^2 + b_2 \cdot PL_{ICE}^{t} + b_3 \quad (3\text{-}5)$$

$$\eta_{ICE,heat}^{t} = c_1 \cdot (PL_{ICE}^{t})^2 + c_2 \cdot PL_{ICE}^{t} + c_3 \quad (3\text{-}6)$$

where PL_{ICE}^{t} is the partial load ratio percentage of the ICE at t-time, %. And b_1, b_2, b_3, c_1, c_2, and c_3 are the efficiency coefficient of the ICE.

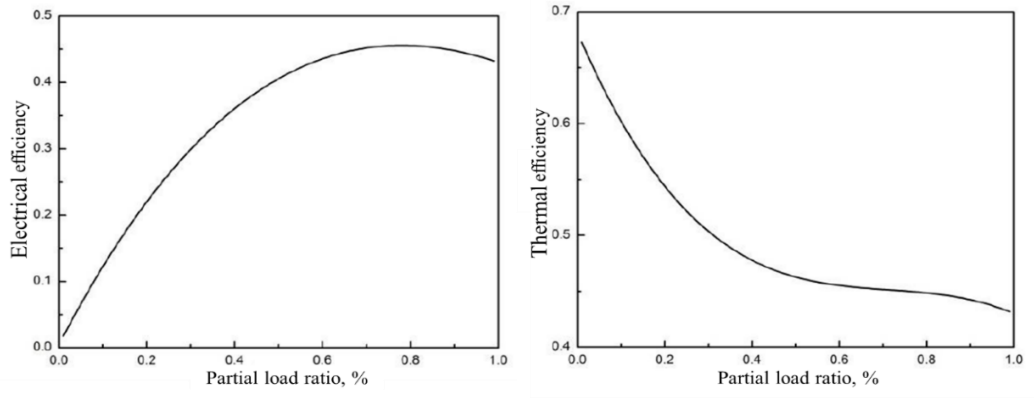

a) b)

Fig.3-4 Electrical and thermal efficiency changes with the different partial load ratio: a) Electrical efficiency; b) Thermal efficiency [6].

3) Photovoltaic system (PV)

PV is a system that generated the energy by the radiation of sun, which is harnessed by tapping light photons to generate electrons. Its implementation is mainly using semiconductor materials (such as silicon) made of solar panels, and the use of light to generate direct current. Photovoltaic cell is an important part of photovoltaic power generation system, and its probability density function is as follows. Its output power is closely related to the temperature and light intensity of the equipment.

The power outputs from PV at t-time can be estimated using the following equations [7,8]:

$$V_{pv}^{t} = V_{oc} + \eta_{v} \times T_{cell}^{t} \quad (3\text{-}7)$$

$$I_{pv}^{t} = RI(t) \times \left(I_{sc} + \eta_i \times (T_{cell}^{t} - 25)\right) \quad (3\text{-}8)$$

where V_{pv}^{t} is the circuit voltage of single cell, V. V_{oc} is the open circuit voltage, V. η_v is the voltage temperature coefficient, mV/℃. I_{pv}^{t} is the circuit current of single cell, A. $RI(t)$ is the random irradiance, W/m^2. I_{sc} is the short circuit current, A. η_i is the current temperature coefficient, mA/℃. T_{cell}^{t} is the cell temperature, ℃, which can be calculated using the following expression:

$$T_{cell}^{t} = T_{ao} + RI(t) \times \left(\frac{T_{nominal} - 20}{0.8}\right) \quad (3\text{-}9)$$

where T_{ao} is ambient operating temperature, ℃, $T_{nominal}$ is the nominal operating cell temperature, which is approximately 48 ℃ [9].

Therefore, the output power of the PV system is given as

$$E_{PV}^{t} = N_{cell} \times V_{pv}^{t} \times I_{pv}^{t} \times FF \quad (3\text{-}10)$$

where E_{PV} is the electricity generated by the PV system at t-time, W. N_{cell} is the number of solar cells, FF is fill factor, which can be obtained as follow:

$$FF = \frac{V_{\mathrm{pvmax}} \times I_{pvmax}}{V_{oc} \times I_{sc}} \quad (3\text{-}11)$$

where $V_{\max}$ is the voltage at maximum power, V. I_{max} is the current at maximum power, A.

The output power of the PV system depends on the operating temperature and solar irradiance, which may vary naturally through the day.

3.2.1.2 Thermal generation devices

1) Absorption chiller (AC)

There are many different types of absorption chillers, but they all work on a similar principle. In a low-pressure system, an absorption fluid is evaporated, removing heat from the chilled water. A heat source such as steam, exhaust gas or hot water is used to regenerate the absorption solution. In this paper, we introduce the double effect exhaust gas driven absorption chiller, which can be operated under cooling mode or heating mode. Its schematic diagram is displayed in Fig.3-5 [10].

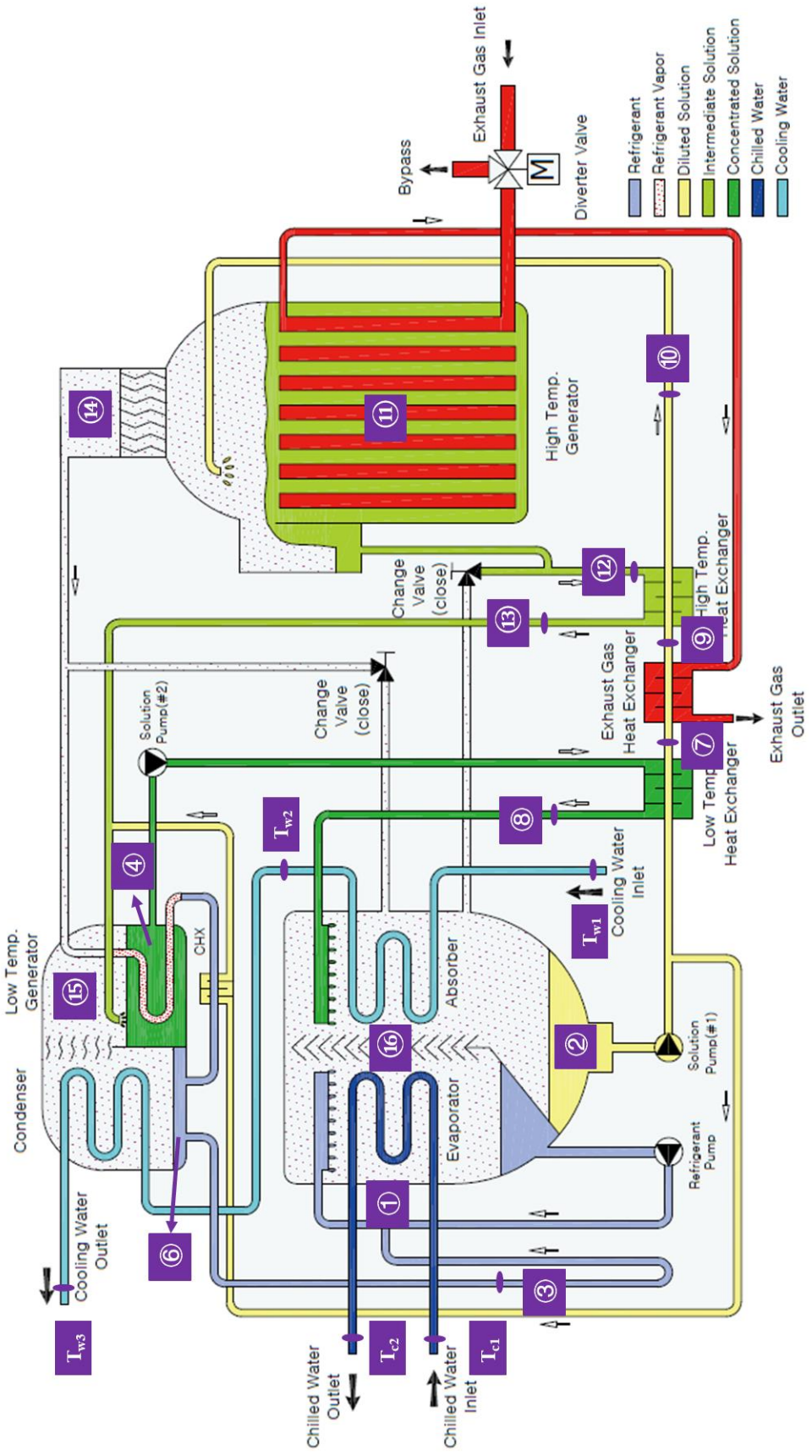

Fig.3-5 Schematic diagram of the double effect exhaust gas driven absorption chiller [10]**.**

The double-effect, exhaust-gas driven absorption chiller consists of eight parts: high temperature generator, high temperature heat exchanger, condensate heat exchanger, low temperature generator, low temperature heat exchanger, absorber, condenser, evaporator, controls and accessories. During the cooling mode, the machine operates at the condition that under vacuum, water boils at a low temperature and usually use the lithium bromide solution as absorbent and water as refrigerant. The workflow is as follows [11]: The diluted solution 2 (lithium bromide solution) from absorber is heated in two stages 7 and 10 by low temperature heat exchanger and by high-temperature heat exchanger, and then enters into high-temperature generator. It is concentrated by exhaust gas from the ICE to produce an intermediate solution 12 and a refrigerant steam 14. Then, the intermediate solution 12 is cooled down by the diluted solution in the low-temperature heat exchanger to 13. After that, it enters the low-temperature generator where it is heated and concentrated by the refrigerant steam 14 from the high-temperature generator to produce a concentrated solution 4 and refrigerant steam 15. And the refrigerant steam becomes saturated refrigerant water 6 after heat release. The concentrated solution 4 is cooled down by the low-temperature heat exchanger to 8 and enters the absorber. At the same time, the refrigerant steam 15 and saturated refrigerant water 6 generated by the low-temperature generator enter the condenser. After cooled by the cooling water, it condenses into saturated refrigerant water 3. Then, it changes into low pressure refrigerant water 1 through the throttling device and enters the evaporator. By absorbing the instantaneous evaporation of chilled water, the low-pressure refrigerant water 1 was vapored and changes to the refrigerant steam 16. After that, it enters the absorber and is absorbed by the concentrated solution 8 from the low temperature heat exchanger and becomes diluted solution 2 again.

The energy balance in the eight parts is as following:

Evaporator:

$$Q_{0,1} = D(h_{16} - h_3) \tag{3-12}$$

$$Q_{0,2} = c_p q_{V,0} \rho (t_{c1} - t_{c2}) \tag{3-13}$$

$$Q_{0,3} = (UF)_0 \frac{t_{c1} - t_{c2}}{ln \frac{t_{c1} - t_0}{t_{c2} - t_0}} \tag{3-14}$$

Condenser:

$$Q_{k,1} = q_{m,s}(h_{15} + h_6 - h_3) \tag{3-15}$$

$$Q_{k,2} = c_p q_{V,w} \rho (t_{w3} - t_{w2}) \tag{3-16}$$

$$Q_{k,3} = (UF)_k \frac{t_{w2} - t_{w3}}{ln \frac{t_k - t_{w2}}{t_k - t_{w3}}} \tag{3-17}$$

Absorber:

$$Q_{A,1} = q_{m,s}((A-1)h_8 + h_{16} - Ah_2) \tag{3-18}$$

$$Q_{A,2} = c_p q_{V,w} \rho (t_{w2} - t_{w1}) \tag{3-19}$$

$$Q_{A,3} = (UF)_A \frac{(t_8 - t_{w2}) - (t_2 - t_{w1})}{ln\frac{t_8 - t_{w2}}{t_2 - t_{w1}}} \tag{3-20}$$

$$A\xi_L = (A-1)\,\xi_H \tag{3-21}$$

Low temperature heat exchanger:

$$Q_{lex,1} = Aq_{m,s}(h_7 - h_2) \tag{3-22}$$

$$Q_{lex,2} = (A-1)q_{m,s}(h_4 - h_8) \tag{3-23}$$

$$Q_{lex,3} = (UF)_{lex} \frac{(t_4 - t_7) - (t_8 - t_2)}{ln\frac{t_4 - t_7}{t_8 - t_3}} \tag{3-24}$$

Condensate heat exchanger:

$$Q_{sc,1} = Aq_{m,s}(h_9 - h_7) \tag{3-25}$$

$$Q_{sc,2} = q_{m,s}(h_{sc1} - h_{sc2}) \tag{3-26}$$

$$Q_{sc,3} = (UF)_{sc} \frac{(t_{sc1} - t_9) - (t_{sc2} - t_7)}{ln\frac{t_{sc1} - t_9}{t_{sc2} - t_7}} \tag{3-27}$$

Low-temperature generator:

$$Q_{lg,1} = q_{m,s}((A-1)h_4 + (1-Y)h_{15} - (A-Y)h_{13}) \tag{3-28}$$

$$Q_{lg,2} = Yq_{m,s}(h_{14} - h_6) \tag{3-29}$$

$$Q_{lg,3} = (UF)_{lg} \frac{(t_{14} - t_4) - (t_6 - t_5)}{ln\frac{t_{14} - t_4}{t_6 - t_5}} \tag{3-30}$$

High-temperature heat exchanger:

$$Q_{hex,1} = Aq_{m,s}(h_{10} - h_9) \tag{3-31}$$

$$Q_{hex,2} = (A - Y)q_{m,s}(h_{12} - h_{13}) \tag{3-32}$$

$$Q_{hex,3} = (UF)_{hex} \frac{(t_{12} - t_{10}) - (t_{13} - t_9)}{ln\frac{t_{12} - t_{10}}{t_{13} - t_9}} \tag{3-33}$$

High-temperature generator:

$$Q_{hg,1} = q_{V,m}((A - Y)h_{12} + Yh_{14} - Ah_{10}) \tag{3-34}$$

$$Q_{hg,2} = q_{m,sc}(h_{sc0} - h_{sc2}) \tag{3-35}$$

$$Q_{hg,3} = (UF)_{hg} \frac{t_{12} - t_{11}}{ln\frac{t_{sc0} - t_{11}}{t_{sc0} - t_{12}}} \tag{3-36}$$

$$Aw_L = (A - Y)\, w_M \tag{3-37}$$

The coefficient of performance (COP) of the absorption chiller is calculated as following:

$$COP = \frac{Q_{0,1}}{Q_{hg,2}} \tag{3-38}$$

where, A is solution circulation rate. c_p is specific heat capacity of water at constant pressure, kJ/(kg·K). UF is unit transfer heat, kW/℃. Y is the steam generation ratio of high temperature generator, %. h is enthalpy, kJ/kg. q_m is mass flow, kg/s. q_V is volume flow, m^3/s. t is temperature, ℃. w is mass fraction of solution, %. ρ is the density of water, kg/m^3.

In the actual operation process, the absorption chiller usually operates under partial load. The partial load rate of the absorption chiller can be defined as

$$PL_a = \frac{Q_0}{Q_0^N} \times 100\% \tag{3-39}$$

The COP of the absorption chiller will change with the partial load rate, as Fig.3-5 shows. It can be estimated as [12]

$$COP_a^t = d_1 \cdot (PL_a^t)^2 + d_2 \cdot PL_a^t + d_3 \tag{3-40}$$

Equation (3-40) includes the quadratic fitting formulas, which can be estimated by the parameters of the actual devices.

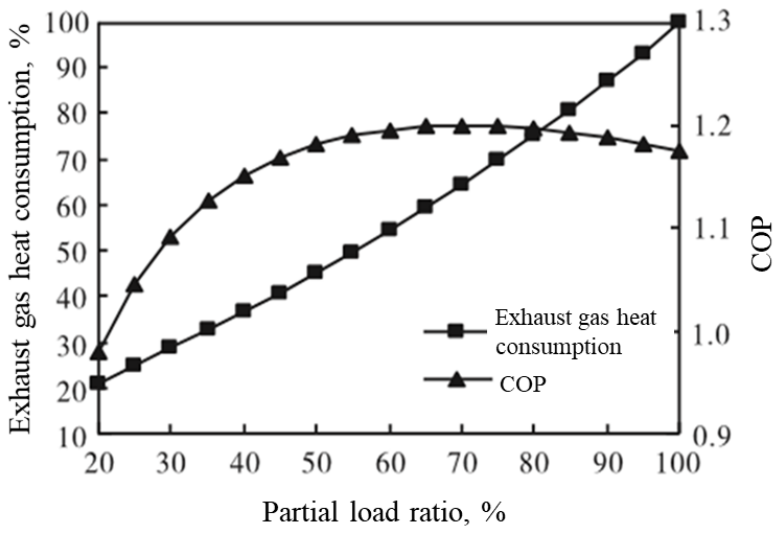

Fig.3-6 Exhaust gas heat consumption ratio and COP changes with the different partial load ratio [11].

2) Electric chiller (EC)

Electric chiller is the most widely used refrigeration equipment in various facilities currently. It is a machine that transfers heat from a cooling object with a lower temperature to the environment to obtain cooling. Fig.3-7 shows the Schematic diagram of electric chiller [13].

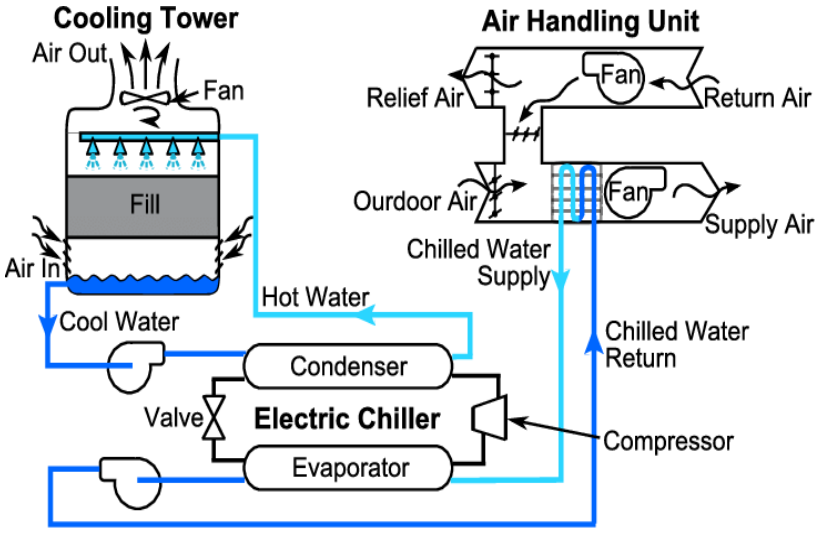

Fig.3-7 Schematic of a typical electric chiller [13]

A chiller works on the principle of vapor compression or vapor absorption. Chillers provide a continuous flow of coolant to the cold side of a process water system at a desired temperature of about 50°F (10°C). The coolant is then pumped through the process, extracting heat out of one area of a facility (e.g., machinery, process equipment, etc.) as it flows back to the return side of the process water system. A chiller uses a vapor compression mechanical refrigeration system that connects to the process water system through a device called an evaporator. Refrigerant circulates

through an evaporator, compressor, condenser and expansion device of a chiller. A thermodynamic process occurs in each of above components of a chiller. The evaporator functions as a heat exchanger such that heat captured by the process coolant flow transfers to the refrigerant. As the heat-transfer takes place, the refrigerant evaporates, changing from a low-pressure liquid into vapor, while the temperature of the process coolant reduces. The refrigerant then flows to a compressor, which performs multiple functions. First, it removes refrigerant from the evaporator and ensures that the pressure in the evaporator remains low enough to absorb heat at the correct rate. Second, it raises the pressure in outgoing refrigerant vapor to ensure that its temperature remains high enough to release heat when it reaches the condenser. The refrigerant returns to a liquid state at the condenser. The latent heat given up as the refrigerant changes from vapor to liquid is carried away from the environment by a cooling medium (air or water).

The electricity consumed by the electric chiller is calculated as following:

$$E_{ec}^{t} = \frac{Q_{ec}^{t}}{COP_{ec}^{t}} \tag{3-41}$$

where COP_{ec} is the electric chiller's COP.

3) Gas boiler

Gas-fired Boiler (GB) is usually equipped as backup heat source of the cogeneration system, which can efficiently convert the chemical energy of natural gas into heat energy. If the heat energy of the cogeneration system is lower than the heating load demand, it can be supplemented by the gas boiler.

The natural gas consumed by the gas-fired boiler is as follows:

$$F_{b}^{t} = \frac{Q_{b}^{t}}{\eta_{b}} \tag{3-42}$$

where η_b is the boiler efficiency percentage.

3.2.1.3 Battery energy storage system (BESS)

In order to achieve the purpose of peak shaving or load balancing, the BESS should be charged with the energy imported from the utility grid during off peak demand, and discharged to inject energy into the grid during peak power demand. It can be contributed to smoothing the fluctuation of the grid with typical mountain and valley shape. For the power grid, the application of the BESS to shave peak and level load can improve the utilization of power facilities, put off the upgrade of facilities, and save renewal expenses [14]. At the same time, it significantly reduces the electricity bills of users. Peak shaving is defined as a technique used to reduce electrical power consumption during periods of maximum demand on the power utility [15]. While load leveling is known as a method for reducing large fluctuations that can occur in electricity demands, by storing excess power during low demand for use during high demand time [16].

Moreover, in applications of DES integrated with the renewable energy, the BESS is utilized to address the intermittent and unstable issue of the renewable energy sources and to provide a continuous supply as current conventional systems. As we all known, renewable energy sources which are obtained from continually replenished nature, have unpredictable random behavior and dependence on the weather. Thus, it is difficult to fulfill the load demand with a steady and continuous supply of electricity from renewable energy resources. By integrating BESS with renewable energy resources, these drawbacks can be overcome, besides producing electricity from clean energy resources that have no environmental effect and enhancing the reliability of the local distribution system.

The performance of the BESS depends on the following parameters: state of charge, charge rate, discharge rate, voltage effect and ambient temperature. The factors listed also determine the battery life. For a battery to be durable, it must not be over charged which will affect the battery overall life. Over discharge will also damage the battery because it produces very high internal heat. Generally, we set the maximum state of charge of the battery to its nominal capacity. In addition, the battery has a minimum state of charge (SOC) limit. In this paper, it should not be less than 20% [6]. During the operation of BESS, SOC is expressed as following:

$$SOC^{min} \leq SOC^{t} = SOC^{t-1} + \eta_{ch} \sum_{t=1}^{t} E_{ch}^{t} - \eta_{dch} \sum_{t=1}^{t} E_{dch}^{t} \leq SOC^{max} \quad (3\text{-}43)$$

where, η_{ch} is the charge efficiency of the BESS, %. η_{dch} is the discharge efficiency of the BESS, %. E_{ch}^{t} is the charging electricity of the BESS at t-time, kWh/h. E_{dch}^{t} is discharging electricity of BESS at t-time, kWh/h. SOC^{min} is the minimum allowable capacity and SOC^{max} is the maximum allowable capacity, kWh.

$$SOC^{min} = (1 - D) \cdot SOC^{max} \quad (3\text{-}44)$$

where D is the depth of discharge, %.

3.2.1.4 DES model

1) Distributed electricity generation system

A DES is a small-scale power system or localized power station that has its own generation and storage resources and can operate independently or in parallel with the power grids [17]. The operation of a DES is typically supported by communication facility and distributed electricity generation technologies such as DG, PV, ICE and BESS as shown in Fig.3-8.

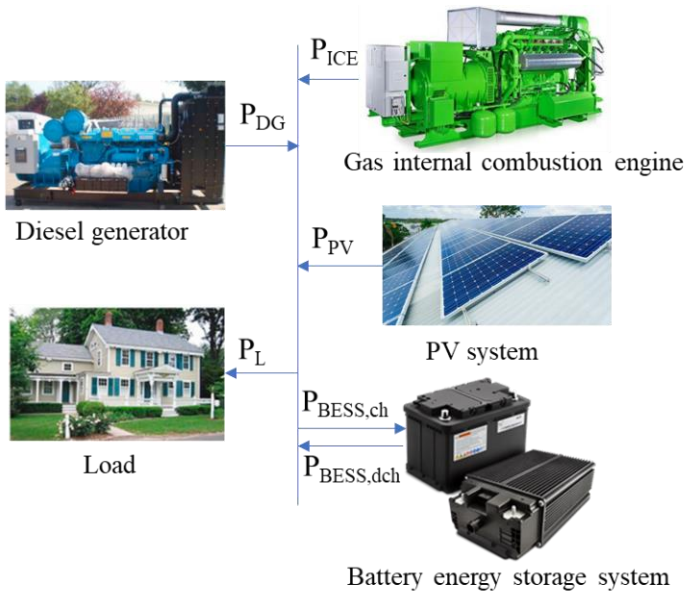

Fig.3-8 The schematic diagram of electricity generation system

The power produced from various sources such as the DG, PV, ICE and BESS units are designed to meet system load demands. This relationship is expressed as

$$\sum_{z=1}^{N_{load}} P_L^t = \sum_{i=1}^{N_{DG}} P_{DG}^t + \sum_{j=1}^{N_{PV}} P_{PV}^t + \sum_{k=1}^{N_{ICE}} P_{ICE}^t - \sum_{m=1}^{N_{BESS}} P_{BESS,ch}^t + \sum_{n=1}^{N_{BESS}} P_{BESS,dch}^t \quad (3\text{-}45)$$

where, P_{DG}^t is the power output of diesel generator during time t, P_{PV}^t is the power generated by PV at time t and P_{ICE}^t is the power generated by ICE at time t while $P_{BESS,ch}^t$ and $P_{BESS,dch}^t$ are the power charge and discharge by the electric storage system at time t. P_L^t is the total power demand at time t. In addition to this, N_{DG}, N_{PV}, N_{ICE} and N_{BESS} depict the number of DG, PV, ICE and BESS units utilized in the DES while N_{load} denotes the number of load points.

2) Combined cooling, heating and power system

(1) Energy balance

As a typical kind of DESs, the performance of the combined cooling, heating and power system (CCHP) is usually determined by the matching degree between the energy demand side and the supply side. As shown in Fig.3-9, the energy demands of users are mainly divided into three parts: 1) electric demands, E; 2) cooling demands for space cooling, Q_c; 3) heating demands for space heating and domestic hot water, Q_h. The CCHP system consists of a power generation unit (PGU), a waste recovery system, a back-up gas boiler, cooling system and heating system. In this study, the PGU is the internal combustion engine (ICE). The PGU consumes the natural gas and produces the electricity to the demand side. The system is connected with the grid, so the sufficient electricity can be imported from the grid and the excess electricity can be sent back to the grid. Then, the recovered heat from the ICE is used to provide heating and drive the absorption chiller. In addition,

the auxiliary boiler and the electric chiller are used as back-up devices to provide the additional heating and cooling load of the demand side, respectively. The energy balance in CCHP system is as following:

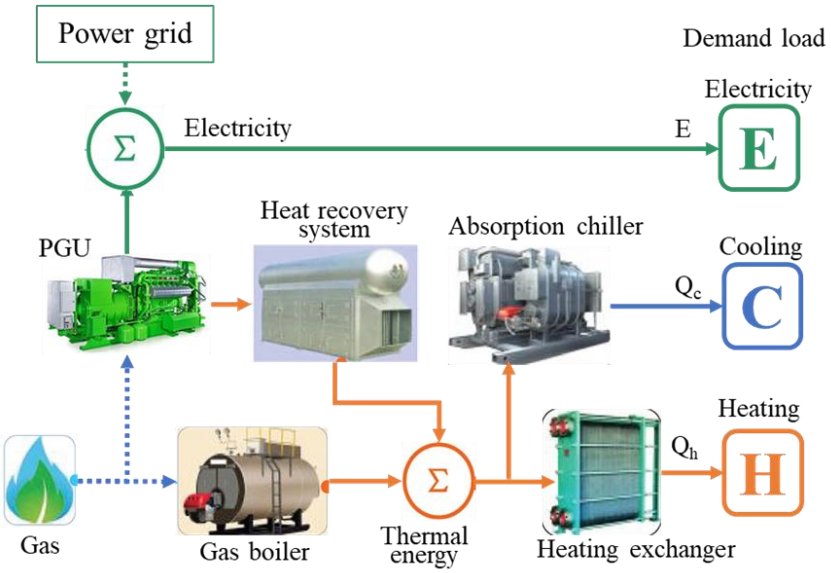

Fig.3-9 The schematic diagram of combined cooling, heating and power system

$$E_{load}^{t} = E_{ICE}^{t} - E_{ec}^{t} - E_{p}^{t} + E_{grid}^{t} \tag{3-46}$$

$$Q_{c}^{t} = Q_{ac}^{t} + Q_{ec}^{t} \tag{3-47}$$

$$Q_{h}^{t} = Q_{ah}^{t} + Q_{bh}^{t} \tag{3-48}$$

$$F_{m}^{t} = F_{ICE}^{t} + F_{b}^{t} \tag{3-49}$$

where E_{load}^{t} is the electricity load of the demand side, kW. E_{ICE}^{t} is the electricity generated by the ICE, kW. E_{p}^{t} is the parasitic electric energy consumption of CCHP system. E_{grid}^{t} is the electricity imported or sold back to the grid, kW. Q_{c}^{t} is the cooling load of the demand side, kW. Q_{ac}^{t} is the cooling produced by the absorption chiller, kW. Q_{ec}^{t} is the cooling produced by the back-up electric chiller, kW. Q_{h}^{t} is the heating load of the demand side, kW. Q_{ah}^{t} is the heating generated by the absorption chiller, kW. Q_{bh}^{t} is the supplementary heat from the back-up gas boiler. F_{m}^{t} is the total natural gas consumption at t-time, kWh. F_{ICE}^{t} is the natural gas consumption of the ICE at t-time, kWh. F_{b}^{t} is the natural gas consumption of the back-up gas boiler at t-time, kWh.

(2) Operation mode

There are two basic operation strategies of the CCHP system [5]: following the electric load (FEL) and following the thermal load (FTL). According to the definition of the above two strategies (Fig. 3-9) [18], the system operating under the FEL or FTL strategy will not generate excess electricity or thermal energy.

For FEL strategy displayed in Fig.3-10 a), electricity demand should be satisfied preferentially by the CCHP system. Therefore, the system will not generate surplus electricity. When the electricity demand cannot reach the starting condition (E_{min}) of the ICE, the electricity, heating, and cooling load of demand side will be supplied by the utility grid, the gas-fired boiler, and the electric chiller, as in the area (1) in Fig.3-10 a). In the area (2), the CCHP system operates following the electric load. When the load is at point A, the ICE will operate at A'. The excess heat cannot be used by absorption chiller, which is dissipated or stored in a thermal tank. When the load is at point B, the ICE will operate at B'. The insufficient heat will be compensated by the back-up gas boiler. The ICE operates at full load when the electricity load is high and the surplus heat (C) or insufficient heat (D) can be stored in the storage tank or imported from the boiler.

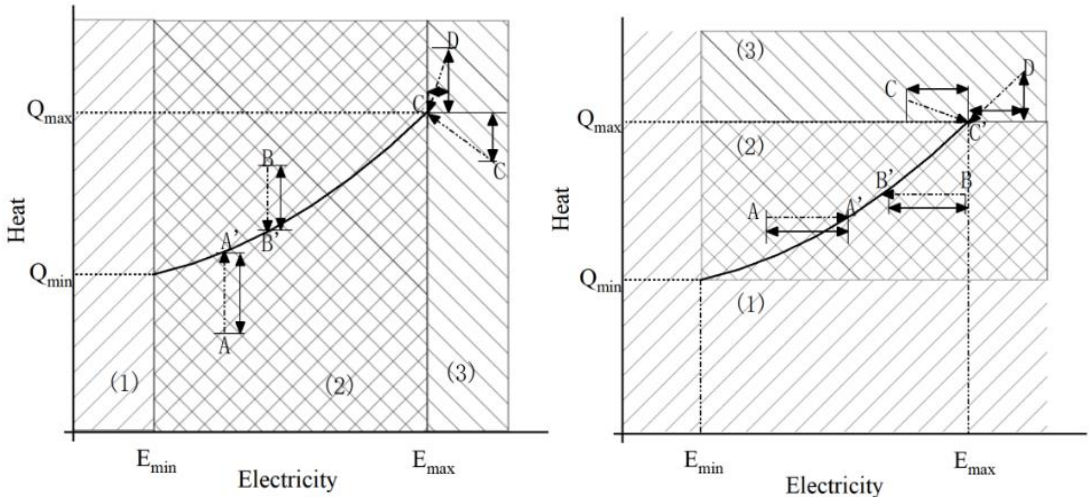

a) b)

Fig.3-10 Two basic operation strategies of the CCHP system: a) following the electric load (FEL); b) following the thermal load (FTL) [18]

For FTL strategy displayed in Fig.3-10 b), heating demand should be satisfied preferentially by the CCHP system. Therefore, the system will not generate surplus heating or cooling load. When the electricity or heating demand cannot reach the starting condition (E_{min}) of the ICE, the electricity, heating, and cooling load of demand side will be supplied by the utility grid, the gas-fired boiler, and the electric chiller, as in the area (1) in Fig.3-10 b). In the area (2), the CCHP system operates following the heating load. When the load is at point A, the ICE will operate at A'. The excess electricity can be sold to the power grid. When the load is at point B, the ICE will operate at B'. The insufficient electricity will be supplied by the power grid. The ICE operates at full load when the thermal demand is high and the surplus electricity (C) or insufficient electricity (D) can be sold to or imported from the utility grid.

3.2.2 Performance analysis

3.2.2.1 Economic performance

The economic evaluation method is divided into static evaluation analysis and dynamic evaluation analysis. Static evaluation analysis method is generally used for the evaluation and

analysis of the initial period of the system. Dynamic evaluation analysis method is to convert the inflow and outflow of current funds in different periods into the value of funds at the same time, such as the annualized total cost. The annualized total cost (ATC) includes the annualized investment cost (AIC), the annualized maintenance cost (AMC), and the annualized operation cost (AOC) of each equipment in the system, expressed as Equation (3-50). Among them, the annualized investment cost and annualized maintenance cost refer to that the total equipment investment cost and maintenance cost are evenly amortized throughout the lifetime of the system, calculated as Equation (3-51) and (3-52).

$$ATC = AIC + AMC + AOC \tag{3-50}$$

$$AIC = CRF \cdot \sum_{n=1}^{N} NC_n \cdot C_n \tag{3-51}$$

$$AMC = \beta \cdot \sum_{n=1}^{N} NC_n \cdot C_n \tag{3-52}$$

$$CRF = \frac{r(1+r)^y}{(1+r)^y - 1} \tag{3-53}$$

where NC_n is the nominal capacity of the nth equipment in the system, kW. C_n is the initial capital investment cost of the nth equipment, \$. β is the proportion of annual maintenance cost to the initial investment cost of each equipment in the system. CRF is the capital recovery factor. r is the interest rate, %. y is the lifetime of each equipment in the system, year.

The annualized operating cost of the system refers to the cost of fuel consumed by equipment of the system, such as natural gas consumed by the ICE and the purchasing electricity from the external grid, which is calculated as following:

$$AOC = \sum_{t=1}^{8760}\left(E_{grid}^{t} EC_e^t + F_m^t EC_f^t\right) \tag{3-54}$$

where EC_c^t, EC_h^t, EC_e^t and EC_f^t are the energy price of cooling, heating, electricity and natural gas at t-hour, respectively, \$/kWh.

3.2.2.2 Environmental performance

At present, the world is vigorously advocating a low-carbon economy to achieve sustainable social development. The environmental performance evaluation of the system refers to the amount of pollutants emitted by the burning of fossil energy during the operation of the system. The pollutants produced by burning fossil energy will have a variety of effects on the environment, such as soil eutrophication, greenhouse effects, and ozone layer depletion. The system burns fossil energy to produce a lot of pollutants, mainly including CO_2, NO_X, CO and particulate matter (PM). Among them, the proportion of CO_2 is as high as 99.5%, while other pollutants account for a small proportion, which can be ignored. Therefore, this research takes Carbon Dioxide Emissions (CDE) as an environmental evaluation index. It can be calculated as:

$$CDE = \sum_{i=1}^{I} \sum_{t}^{8760} E_{fuel,i}^{t} \cdot \mu_{fuel,i} \tag{3-55}$$

where i is the i[th] kind of fuel used in the DES. $E_{fuel,i}^{t}$ is the energy consumption of the fuel at t-time, kWh. $\mu_{fuel,i}$ is the emission conversion factors of the fuel. Usually, the energy fuel of the DES is natural gas and electricity. Their emission conversion factors in China and Japan are listed in Table 3-1 [23–25].

Table 3-1 Emission conversion factors of natural gas and electricity [23–25]**.**

Countries	Natural gas (t/m^3)	Electricity (g/kWh)
China	2.20	980
Japan	2.19	462

3.2.2.3 Reliability performance

1) Operating and failed status

Power system reliability can be defined as the ability to provide high quality and continuous power to demand side. For a normal power system, there are two main states: operating and failed [19]. The duration of operating state is called Time to Failure (TTF), and the duration of failed state is called Time to Repair (TTR). The life process of a repairable power system can be shown in Fig.3-11. The whole process is in continuous alternate operating state and failed state.

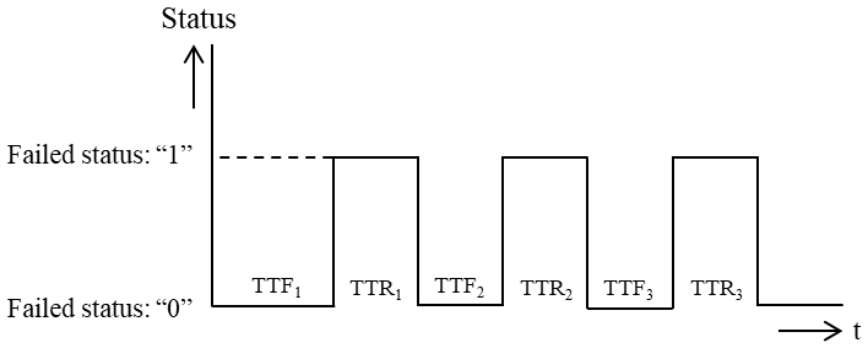

Fig.3-11 The status changes of a repairable power system.

2) Reliability indexes

Failure rate (λ), repair rate (μ), mean time to failure (MTTF), mean time to repair (MTTR), mean time between failure (MTBF) are the general reliability indices for components and system reliability engineering.

Failure rate is the frequency which a component or a system fails during a period, expressed in failures per unit of time.

Repair rate is the frequency that the failed component or system gets repaired, the unit of repair rate is same with failure rate.

Mean time to failure refers to the mean time expected until the first failure of a piece of equipment. And it is a basic measure of reliability for repairable systems. For constant failure rate systems, MTTF is the inverse of the failure rate. Thus, the failure rate can be presented as:

$$\lambda = \frac{1}{MTTF} \tag{3-56}$$

The failure rate of a component during its life is often described by the Bath-Tub Curve, see Fig.3-12. It has three periods: (1) early failure period, (2) accidental failure period, and (3) wear out period. In power system, components usually operate during the accidental failure period (so this period also called using life). Early life means the failure rate of equipment or system is decreases with time changed. Useful life means the failure rate of equipment or system is approx. constant with time changed, the failure also called occasionally failure. And the wear out life means the failure rate of equipment or system is increasing with time changed.

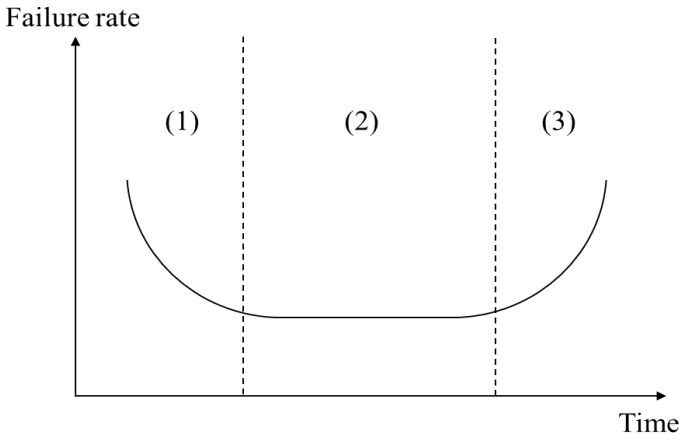

Fig.3-12 Bath-Tub Curve [20]

Mean time to repair is defined as the mean repair time of the component or system gets repaired. It is the expected span of time from a failure to the repair or maintenance completion. The term is typically only used with repairable systems. MTTR is the inverse of the failure rate, μ.

$$\mu = \frac{1}{MTTR} \tag{3-57}$$

3）Reliability and availability

Reliability

Reliability refers to the probability that the component will not fail in the time interval [0, T] under the condition that the starting time is operating status. The reliability function, R(t) = P (T > t), in practice is usually given by

$$R(t) = 1 - F(t) = \frac{N(t)}{N(0)} \tag{3-58}$$

where $N(0)$ denotes the number of the components at initial time t = 0; $N(t)$ denotes the

number of surviving components at time t; $F(t)$ stands for failure function, which is the complementary of reliability function.

Failure rate $\lambda(t)$ is defined as the frequency which a component or a system fails at t-time. Its observed value is the ration of failures that occurs in t's next per unit time to the total number of components that still survive at time t, express by

$$\lambda(t) = \lim_{\Delta t \to 0} \frac{N(t) - N(t + \Delta t)}{N(t)\Delta t} = -\frac{1}{R(t)} \frac{dR(t)}{dt} \tag{3-59}$$

Based on Equation (3-20), the reliability function R(t) can be written as a function of the failure rate $\lambda(t)$, which is expressed as:

$$R(t) = e^{-\int_0^t \lambda(t) d\tau} \tag{3-60}$$

where the failure rate $\lambda(t)$ is a constant value and Equation (3-21) is equivalent to

$$R(t) = e^{-\lambda t} \tag{3-61}$$

Availability

Availability refers to the probability of normal operation at t-time under the condition of normal operation at the starting time.

$$A = \frac{MTTF}{MTTF + MTTR} = \frac{\mu}{\lambda + \mu} \tag{3-62}$$

4) Power outage loss

Power outage loss refers to the total economic loss that the society bears when the power supply is not completely reliable or expected to be not completely reliable. To assess the reliability of a power supply system, it is necessary to estimate the economic loss caused by power outage and power supply interruption to customers. The economic losses caused by interruption of power load in a region can be divided into direct economic losses and indirect economic losses. The direct outage loss is usually determined by the short-term effect of the unexpected outage, while the indirect outage loss is caused by the longer-term consideration of the expected power outage. The cost of energy not supplied (CENS) in a power system represents the average cost during the power outage. It can be estimated by modelling the power outage loss as a function of the unsupplied energy regardless of the power outage duration and frequency [21]. The CENS consists of all financial damage that consumers experience during the power outage or load shedding. In order to estimate the CENS in the distribution system, the following details must be supplied: i. direct economic loss; ii. indirect economic loss; and iii. information on the non-supplied energy during the time period of the analysis, etc. [22]. The expression is as following:

$$CENS = \frac{\sum_{i=0}^{n} F_i D_i + \sum_{j=0}^{n} I_j}{\sum_{t=0}^{T} EENS} = \frac{\left(F_{res}D_{res} + F_{ind}D_{ind} + F_{com}D_{com} + F_{g\&i}D_{g\&i} + F_{other}D_{other}\right) + \left(\sum_j I_{jx} - \sum_j I_{jy}\right)}{\sum_{t=0}^{T} EENS} \quad (3\text{-}63)$$

where, $CENS$ is value or cost of energy not supplied for the case study, \$/kWh. F_i is vulnerability factor of consumer at the load point, %. i is type of consumers such as residential (res), industrial (ind), commercial (com), government and institution (g&i), and other (others). D_i is the direct economic losses of consumers, \$. I_j is indirect economic losses, \$. I_{jx} is total indirect cost brought about during the time of investigation, \$. I_{jy} is the indirect costs that had no association with the investigation, \$. n is number of customers in the system. $EENS$ is the non-supplied energy during the period of analysis, kWh.

The EENS is the expected unsupplied energy in a year owing to generation unavailability or inadequacy or lack of primary energy, which calculated as

$$EENS = \sum_{k=1}^{n} P_k \times E_k \quad (3\text{-}64)$$

where, P_k is the power outage with a probability (usually using the failure rate). E_k is the average load of the load point, kWh.

3.2.3 Simulation model and algorithm

3.2.3.1 Power outage model based on Monte Carlo

Monte Carlo simulation method is a kind of probability simulation method which samples the states of components by random numbers generated by computer and calculates the statistical characteristics of parameters through a large number of simulation experiments. Compared with the traditional analytical method, Monte Carlo simulation method has many advantages and is widely used in the reliability evaluation of distribution system: firstly, the use of Monte Carlo simulation method can accurately simulate the random characteristics of system components, such as random load fluctuations, distributed generation fluctuations, component random failures, climate random changes and other random factors and system control strategies. Secondly, when the setting accuracy is fixed, the sampling times of Monte Carlo simulation method is independent of the scale of the system, which is especially suitable for the reliability evaluation of large and complex distribution networks with branches. Thirdly, the simulation process of Monte Carlo simulation method is simple, intuitive, and easy to be used in practical operation.

Because the simulation adopts the method of random generation, the result is fluctuating. However, the error can be reduced by increasing the number of simulations. In order to increase the accuracy and reduce the simulation time, the error precision is set. When the simulation result reaches the accuracy, the result is credible. The expected value and variance represent the fluctuation degree of each group of simulation results, which are expressed by Equations (3-65) and (3-66), respectively

$$\overline{EENS} = \frac{1}{N}\sum_{i=1}^{n} EENS_i \tag{3-65}$$

$$V(EENS) = \frac{1}{N-1}\sum_{i=1}^{N}(EENS_i - \overline{EENS})^2 \tag{3-66}$$

where $EENS_i$ is the test value of the simulation i, and N is the total simulation times.

It is important to note that Equation (3-66) only estimates the expected value of EENS. However, the uncertainty around the indicator is measured by the variance (3-67) and standard deviation (3-68) of the expected value.

$$V(\overline{EENS}) = \frac{V(EENS)}{N} \tag{3-67}$$

$$\sigma(\overline{EENS}) = \sqrt{V(\overline{EENS})} = \sqrt{\frac{V(EENS)}{N}} \tag{3-68}$$

We define that the precision of the simulation level as ρ, which is calculated as Equation (3-69)

$$\rho = \frac{\sigma(\overline{EENS})}{\overline{EENS}} = \frac{1}{\overline{EENS}}\sqrt{\frac{V(EENS)}{N}} \leq \varepsilon \tag{3-69}$$

According to Equation (3-69), when the times of simulation increases, the value of ρ decreases. Therefore, if we can select an error tolerance (ε) to stop the simulation when ρ is less then ε. The error tolerance is the maximum error of the estimate, which is usually to use 5%.

3.2.3.2 Optimization model based on Genetic algorithm

Genetic algorithm (GA) is a search technique used in computing to find exact or approximate solutions to optimization and search problems. It is a computational model of biological evolution process simulating natural selection and genetic mechanism of Darwin's theory of biological evolution, which is a method to search the optimal solution by simulating the natural evolution process. First pioneered by John Holland in the 1960s, GA has been widely applied in bioinformatics, phylogenetics, computational science, engineering, economics, chemistry, manufacturing, mathematics, physics and other fields [26–28]. GA simulates the evolution process of an artificial population. Through selection, crossover and mutation mechanisms, a group of candidate individuals are retained in each iteration. The process is repeated. After several generations of evolution, the fitness of the population reaches the state of "approximate optimal".

Simple generational genetic algorithm procedure is to:

(1) Initialization: set the evolutionary algebra counter t = 0, set the maximum evolution algebra T, and randomly generate m individuals as the initial population P (0).

(2) Individual evaluation: the fitness of each individual in the population P (T) was calculated.

(3) Selection operation: the selection operator is applied to the population. The purpose of selection is to directly inherit the optimized individuals to the next generation or to produce new individuals through pairing and crossover, and then pass on to the next generation. The selection operation is based on the fitness evaluation of individuals in the population.

(4) Crossover operation: the crossover operator is applied to the population. Crossover operator plays a key role in genetic algorithm.

(5) Mutation operation: apply mutation operator to population. It is to change the gene value of some loci in the individual string of a population. After selection, crossover and mutation, the next generation population P (T + 1) was obtained.

(6) Termination condition judgment: if t = T, the individual with the maximum fitness obtained in the evolution process is taken as the output of the optimal solution, and the calculation is terminated.

The algorithm simulation flowchart is demonstrated in Fig.3-13 [29].

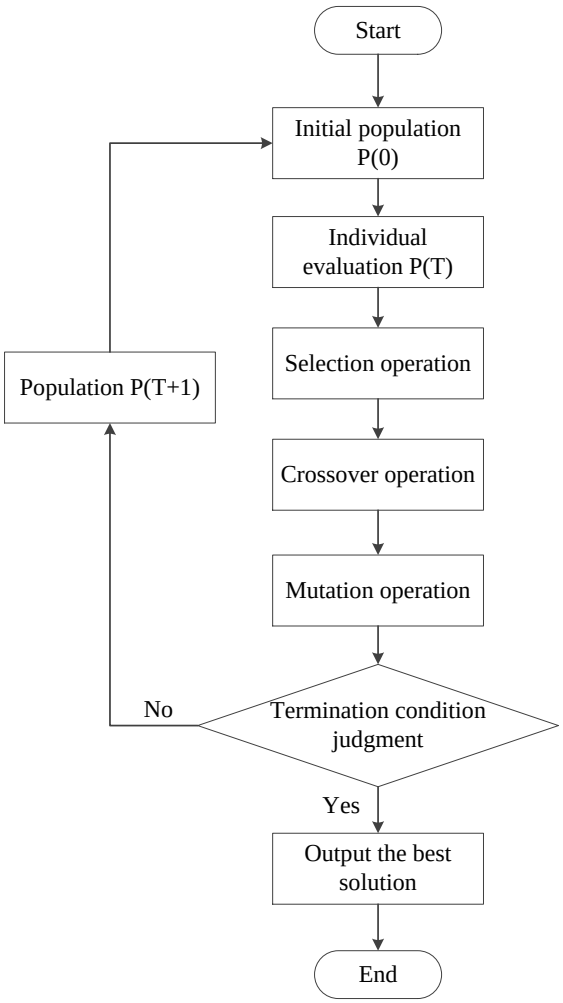

Fig.3-13 GA algorithm simulation flowchart

3.2.3.3 Operation model based on TRNSYS

TRNSYS (transient system simulation program) was first developed by solar energy laboratory (SEL) of Wisconsin Madison University in the United States, and gradually improved with the joint efforts of some European research institutes. Thermal energy systems specialists (TESS) in the United States has developed various modules for HVAC systems. The TRNSYS software is powerful and covers a wide range of functions. It can dynamically simulate the operating conditions of various systems, including solar energy applications, buildings thermal analysis, electrical systems, HVAC etc. [30].

TRNSYS software is a modular dynamic simulation software. The so-called modularization means that all systems are composed of several small systems (i.e. modules), and one module realizes a specific function. Therefore, when the system is simulated and analyzed, as long as the modules that realize these specific functions are called and the input conditions are given, the system can be simulated and analyzed. Some modules are also used in the simulation analysis of other systems. At this time, it is not necessary to program these functions separately, but to call these modules and give them specific input conditions. The modules of component consist the details of inputs, outputs and parameters. Black box model of TRNSYS is shown in Fig.3-14.

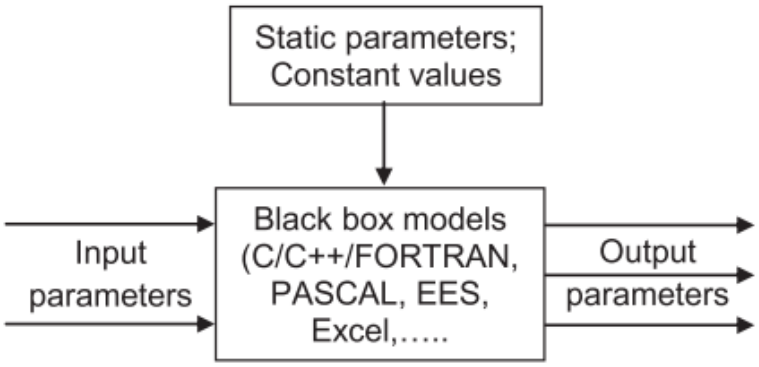

Fig.3-14 Black box model of TRNSYS

TRNSYS is a mature simulation tool, which can predict and simulate the transient performance of various energy systems based on the established analysis and differential correlation. It is suitable for complex thermal and power systems.

Reference

[1] Wu JY, Wang JL, Li S. Multi-objective optimal operation strategy study of micro-CCHP system. Energy 2012;48:472–83. https://doi.org/10.1016/j.energy.2012.10.013.

[2] Bansal R. Handbook of distributed generation: Electric power technologies, economics and environmental impacts. 2017. https://doi.org/10.1007/978-3-319-51343-0.

[3] Das BK, Al-Abdeli YM, Kothapalli G. Optimisation of stand-alone hybrid energy systems supplemented by combustion-based prime movers. Appl Energy 2017;196:18–33. https://doi.org/10.1016/j.apenergy.2017.03.119.

[4] Farret FA SM. Integration of alternative Sources of energy 2017:301–32.

[5] Tamatam LR. Tribological performance of different crankshaft bearings in conjunction with textured shaft surfaces. 2017.

[6] Wu Q, Ren H, Gao W, Ren J. Multi-criteria assessment of combined cooling, heating and power systems located in different regions in Japan. Appl Therm Eng 2014;73:660–70. https://doi.org/10.1016/j.applthermaleng.2014.08.020.

[7] Rocchetta R, Li YF, Zio E. Risk assessment and risk-cost optimization of distributed power generation systems considering extreme weather conditions. Reliab Eng Syst Saf 2015;136:47–61. https://doi.org/10.1016/j.ress.2014.11.013.

[8] Radhakrishnan BM, Srinivasan D. A multi-agent based distributed energy management scheme for smart grid applications. Energy 2016;103:192–204. https://doi.org/10.1016/j.energy.2016.02.117.

[9] Afzali P, Keynia F, Rashidinejad M. A new model for reliability-centered maintenance prioritisation of distribution feeders. Energy 2019;171:701–9. https://doi.org/10.1016/j.energy.2019.01.040.

[10] HOW DOES AN ABSORPTION CHILLER WORK? Goldman Energy n.d. https://goldman.com.au/energy/company-news/how-does-an-absorption-chiller-work/ (accessed October 30, 2020).

[11] Yang XJ, You SJ, Zhang H. Part load performance of double effect steam operated absorption chiller. Tianjin Daxue Xuebao (Ziran Kexue Yu Gongcheng Jishu Ban)/Journal Tianjin Univ Sci Technol 2012;45:994–1000.

[12] Hajabdollahi H, Ganjehkaviri A, Jaafar MNM. Assessment of new operational strategy in optimization of CCHP plant for different climates using evolutionary algorithms. Appl Therm Eng 2015;75:468–80. https://doi.org/10.1016/j.applthermaleng.2014.09.033.

[13] Elizabeth FQ. Li, X., Li, Y., Seem, J. E., Li, P. (2012). Extremum Seeking Control of Cooling Tower for Self-optimizing Efficient Operation of Chilled Water Systems, Proceedings of the 2012 American Control Confer 2012:3396–401.

[14] Dong X, Bao G, Lu Z, Yuan Z, Lu C. Optimal battery energy storage system charge scheduling for peak shaving application considering battery lifetime. Lect Notes Electr Eng 2011;133 LNEE:211–

8. https://doi.org/10.1007/978-3-642-25992-0_30.

[15] Ananda-Rao K, Ali R, Taniselass S, Malek F. A Review on Various Load Control Strategies for Battery Energy Storage System in Energy Applications. Appl Mech Mater 2015;793:129–33. https://doi.org/10.4028/www.scientific.net/amm.793.129.

[16] Rahimi A, Zarghami M, Vaziri M, Vadhva S. A simple and effective approach for peak load shaving using Battery Storage Systems. 45th North Am Power Symp NAPS 2013 2013:1–5. https://doi.org/10.1109/NAPS.2013.6666824.

[17] Adefarati T, Bansal RC. Reliability and economic assessment of a microgrid power system with the integration of renewable energy resources. Appl Energy 2017;206:911–33. https://doi.org/10.1016/j.apenergy.2017.08.228.

[18] Li L, Yu S, Mu H, Li H. Optimization and evaluation of CCHP systems considering incentive policies under different operation strategies. Energy 2018;162:825–40. https://doi.org/10.1016/j.energy.2018.08.083.

[19] Wang JJ, Fu C, Yang K, Zhang XT, Shi G hua, Zhai J. Reliability and availability analysis of redundant BCHP (building cooling, heating and power) system. Energy 2013;61:531–40. https://doi.org/10.1016/j.energy.2013.09.018.

[20] Wang Y, Gao X, Cai Y, Yang M, Li S, Li Y. Reliability evaluation for aviation electric power system in consideration of uncertainty. Energies 2020;13. https://doi.org/10.3390/en13051175.

[21] Raesaar P, Tiigimägi E, Valtin J. Assessment of electricity supply interruption costs under restricted time and information resources. Proc 2006 IASME/WSEAS Int Conf Energy Environ Syst Chalkida, Greece, May 8-10 2006;2006:409–15.

[22] Vásquez P, Vaca Á. Methodology for Estimating the Cost of Energy not Supplied -Ecuadorian Case-. Proc 2012 6th IEEE/PES Transm Distrib Lat Am Conf Expo T D-LA 2012 2012. https://doi.org/10.1109/TDC-LA.2012.6319047.

[23] Wang JJ, Jing YY, Zhang CF. Optimization of capacity and operation for CCHP system by genetic algorithm. Appl Energy 2010;87:1325–35. https://doi.org/10.1016/j.apenergy.2009.08.005.

[24] CO2 Emission coefficient by electric utility n.d. https://ghg-santeikohyo.env.go.jp/files/calc/r02_coefficient.pdf (accessed September 16, 2020).

[25] Carbon dioxide emission coefficient of urban gas n.d. http://www.saibugas.co.jp/business/others/co2_emission_factor.htm (accessed September 16, 2020).

[26] Dai Y, Wang J, Gao L. Exergy analysis , parametric analysis and optimization for a novel combined power and ejector refrigeration cycle. Appl Therm Eng 2009;29:1983–90. https://doi.org/10.1016/j.applthermaleng.2008.09.016.

[27] Almeida FS, Awruch AM. Design optimization of composite laminated structures using genetic algorithms and finite element analysis. Compos Struct 2009;88:443–54. https://doi.org/10.1016/j.compstruct.2008.05.004.

[28] Guo J, Xu M, Cheng L. The application of field synergy number in shell-and-tube heat exchanger optimization design. Appl Energy 2009;86:2079–87. https://doi.org/10.1016/j.apenergy.2009.01.013.

[29] Chen RC, Chen J, Chen TS, Huang CC, Chen LC. Synergy of genetic algorithm with extensive neighborhood search for the permutation flowshop scheduling problem. Math Probl Eng 2017;2017. https://doi.org/10.1155/2017/3630869.

[30] Shrivastava RL, Kumar V, Untawale SP. Modeling and simulation of solar water heater: A TRNSYS perspective. Renew Sustain Energy Rev 2017;67:126–43. https://doi.org/10.1016/j.rser.2016.09.005.

Chapter 4

ECONOMIC AND ENVIRONMENTAL ANALYSIS OF THE DISTRIBUTED ENERGY SYSTEM FOCUSING ON GRID STABILIZATION

CHAPTER FOUR: ECONOMIC AND ENVIRONMENTAL ANALYSIS OF THE DISTRIBUTED ENERGY SYSTEM FOCUSING ON GRID STABILIZATION

ECONOMIC AND ENVIRONMENTAL ANALYSIS OF THE DISTRIBUTED ENERGY SYSTEM FOCUSING ON GRID STABILIZATION *4-1*

4.1 Content 4-1

4.2 Methodology 4-2

4.2.1 Distributed energy system model 4-2

4.2.2 The independence and peak shaving performance of distributed energy systems 4-4

4.2.3 The economic and environmental analysis of the distributed energy systems 4-5

4.3 Research object introduction and basic data 4-7

4.3.1 Research object 4-7

4.3.2 PV production 4-9

4.3.3 Study cases 4-10

4.4 Comparison results of the case studies 4-12

4.5 Economic and environmental analysis focusing on grid stabilization 4-14

4.5.1 Distributed energy system with PV and ICE 4-14

4.5.2 Distributed energy system with PV, ICE and BESS 4-16

4.6 Summary 4-21

Appendix: 4-22

Reference 4-24

4.1 Content

In recent years, with a rapid increase in popularity and economic development, the pressure of power supply, as well as concerns of climate change, led to the use of clean and efficient energy resources in the power system. DES integrated renewable energy resources, high-efficiency generators and energy storage devices can be an effective solution for generating reliable and environmental-friendly electricity at low cost. Through the energy utilization around the demand side, the generated power from the DES can be directly supplied to users, which can achieve the power supply by themself for users. It significantly reduces the amount of power import from the utility grid, lessening the dependence on the grid which is helpful to the grid stability. At the same time, the DES can stable the fluctuation of the grid load by flexibly operating the distributed generators to shave the peak load. To explore the impact of the DES on the grid, this chapter established a DES model composed of photovoltaic, gas internal combustion engine and battery energy storage systems. And in order to reflect the grid stabilization of the DES, two novel indexes of the DES were proposed called “independence ratio” and “peak shaving ratio” to analyze the ability of self-supply and the effect of peak load reduction. Firstly, taking the Smart Community in Higashida, Japan as an example, five different types of buildings were selected to analyze the change of the regional load characteristics based on the actual load data. Secondly, six cases were used to compare the impact of the DES with different combinations on the grid stabilization effect. After that, under the objective function of the minimum annualized total cost of users, the optimal combination of the DES with different independence ratios and peak shaving ratios were obtained. The investment cost annualized total cost and carbon emission reduction of the DES with the optimal combination were calculated. By comparing the variation of annualized total cost and carbon emission reduction, the economic and environmental performance were analyzed under different independence ratios and peak shaving ratios. In addition, according to the changes of optimal configurations of the equipment in the DES with independence ratio and peak shaving ratio, the impact of different types of units on independence ratio and peak shaving ratio was discussed. The application potential of the grid stabilization was analyzed in this part.

4.2 Methodology

4.2.1 Distributed energy system model

The structure of the proposed regional DES is depicted in Fig.4-1. The distributed generators including photovoltaic (PV) system, battery energy storage system (BESS) and internal-combustion engine (ICE) is designed to meet the load requirements.

The energy balance of the proposed power system is presented in Eq. (4-1) as:

$$E_L^t = E_{PV}^t + E_{ICE}^t + E_{BESS,dch}^t - E_{BESS,ch}^t + E_{grid}^t \quad (4\text{-}1)$$

where E_L^t is the demand load at t-time, kW. E_{PV}^t is the electricity generated by the PV system at t-time, kW. E_{ICE}^t is the electricity generated by the ICE at t-time, kW. $E_{BESS,dch}^t$, $E_{BESS,ch}^t$ are the electricity discharged and charged by the BESS at t-time, kW. E_{grid}^t is the electricity imported from the utility grid.

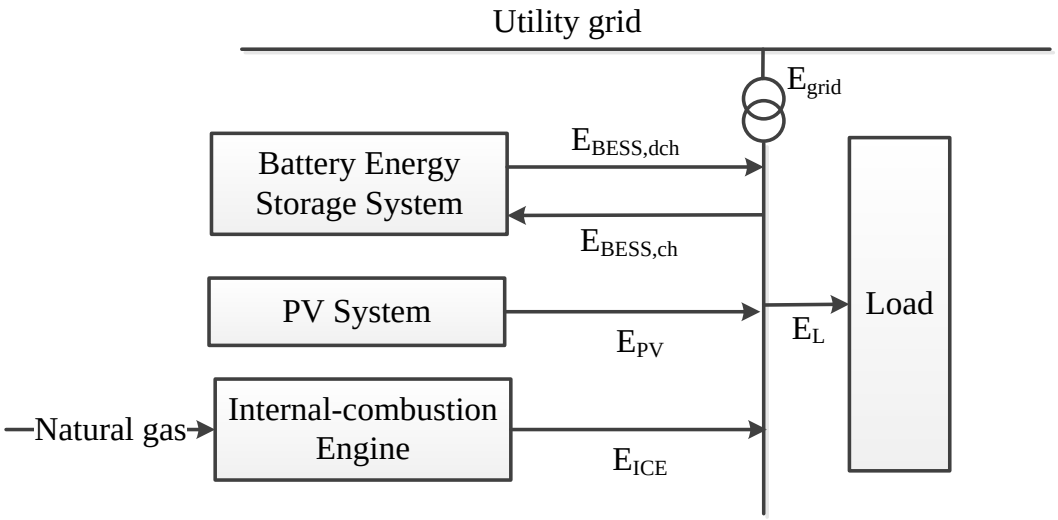

Fig.4-1 The proposed distributed energy system

4.2.1.1 PV system model

PV is a system that generated the energy by the radiation of sun, which is harnessed by tapping light photons to generate electrons. Due to the advantage of low operating and maintenance costs, no greenhouse gas emissions, environmentally friendly, no noise emission [1], PV system is now generated on a large scale around the world. The power outputs from PV at t-time can be estimated using the following equations [1,2]:

$$E_{PV}^t = \eta_{PV} \times A_\alpha \times I_\alpha \times \left(1 - 0.005(T_{am} - 25)\right) \quad (4\text{-}2)$$

where η_{PV} is the conversion efficiency of solar cell array (%), A_α is the array area (m^2), I_α is the solar random irradiation (kW/m^2), T_{am} is the ambient operation temperature (°C).

The output power of the PV system depends on the operating temperature and solar irradiance, which may vary naturally through the day.

4.2.1.2 Battery energy storage system (BESS)

The normal operation mode of the BESS is to be charged at low electricity prices and the stored energy can be utilized to cover the power at peak electricity prices, which can reduce the electricity cost in demand side. In addition, the BESS can store the electricity from PV system when the power generation from PV is excess at high penetration, which can reduce the imported power from the public grid. The state of charge (SOC) is always used to determine the behavior of the BESS at t-time, which calculated by using the following equations:

$$SOC^t = SOC^{t-1} + (E^t_{BESS,ch} - E^t_{BESS,dch}) \quad (4\text{-}3)$$

$$SOC_{min} \leq SOC^t \leq SOC_{max} \quad (4\text{-}4)$$

$$SOC_{min} = (1 - d) \times SOC_{max} \quad (4\text{-}5)$$

where $E^t_{BESS,ch}$ is charging power of BESS at t-time, kWh/h. $E^t_{BESS,dch}$ is the discharging power of the BESS at t-time, kWh/h. d is the depth of the discharge, %.

4.2.1.3 Internal-combustion engine (ICE)

Internal-combustion engine is driven by natural gas, which converts the calorific value of natural gas into electric energy. As the electrical efficiency of the internal-combustion engine can reach about 40-48%, and the waste heat can be used for cold and hot energy output, so it is widely utilized in the DES. The output power of the ICE at t-time is expressed as follows:

$$F^t_{ICE} = E^t_{ICE} \times \eta^t_{ICE,e} \quad (4\text{-}6)$$

where E^t_{ICE} is the electric power generated by the ICE at t-time, kW. F_{ICE} is the fuel energy consumption, kWh. $\eta^t_{ICE,e}$ is the electric efficiency of the ICE, %.

4.2.1.4 Operation strategy model

1) Power generation from PV system has priority in meeting the local electricity demand P_{PV}.

2) Usually the night load is low and the electricity price is cheaper, while the daytime load is higher and the electricity price is more expensive. Therefore, the BESS is charged from the utility grid during the valley period and discharged at the peak period to achieve the effect of peak shaving as well as to reduce electricity cost. The operation strategy of the BESS is simulated as:

$$E^t_{BESS,ch} = \begin{cases} E^t_{ch}, & t \in [\text{Valley period}] \\ 0, & t \in [\text{Peak period}] \end{cases} \quad (4\text{-}7)$$

$$E^t_{BESS,dch} = \begin{cases} E^t_{dch}, & t \in [\text{Peak period}] \; and \; E^t_{dch} \leq E^t_L \\ E^t_L, & t \in [\text{Peak period}] \; and \; E^t_{dch} \geq E^t_L \\ 0, & t \in [\text{Valley period}] \end{cases} \quad (4\text{-}8)$$

where E^t_{ch} is the charging capacity at t-time, kWh/h, E^t_{dch} is discharging capacity at t-time, kW/h. The charging and discharging capacity should be limited by the maximum output:

$$E^t_{ch} \leq \eta_{ch} \times E_{BESS,max} \quad (4\text{-}9)$$

$$E_{dch}^{t} \leq \eta_{dch} \times E_{BESS,max} \tag{4-10}$$

$$E_{BESS,max} = Cap_{BESS}/h_{min} \tag{4-11}$$

where, η_{ch} is the charging efficiency of the BESS, %. η_{dch} is the discharging efficiency of the BESS, %. $P_{BESS,max}$ is the maximum output, which determined by the characteristic of the BESS, kWh/h. Cap_{BESS} is the capacity of the BESS, kWh. h_{min} is the minimum time required for the BESS to be fully charged, which is 6 hours in this research.

3) Because the electricity price of valley period at night is cheap, it is more economical to consume the electricity import from the utility grid than the electricity generated by the ICE. Therefore, the ICE only turns on at peak period during the daytime, and its operating strategy is as follows:

$$E_{GE}^{t} = \begin{cases} 0 \ , \ t \in [valley\ period] \\ Cap_{ICE}, \ t \in [peak\ period]\ and\ E_{L}^{t} \geq Cap_{ICE} \\ E_{L}^{t} \ , \ t \in [peak\ period]\ and\ E_{L}^{t} < Cap_{ICE} \end{cases} \tag{4-12}$$

where Cap_{ICE} is the capacity of the ICE, kW.

4.2.2 The independence and peak shaving performance of distributed energy systems

As presented in Fig.4-2, the power produced by localized power generation systems can be self-consumed directly by the demand side in the DES, which can reduce the electricity demand of the utility grid. The dependence on the grid can be significantly fell down for the user. Peak shaving by operating the power generation systems can further help to reduce the peak load pressure of the power grid and stabilize power grid fluctuation. These two performances can achieve the grid stabilization, which contributes to the reliability of the power supply in the service region.

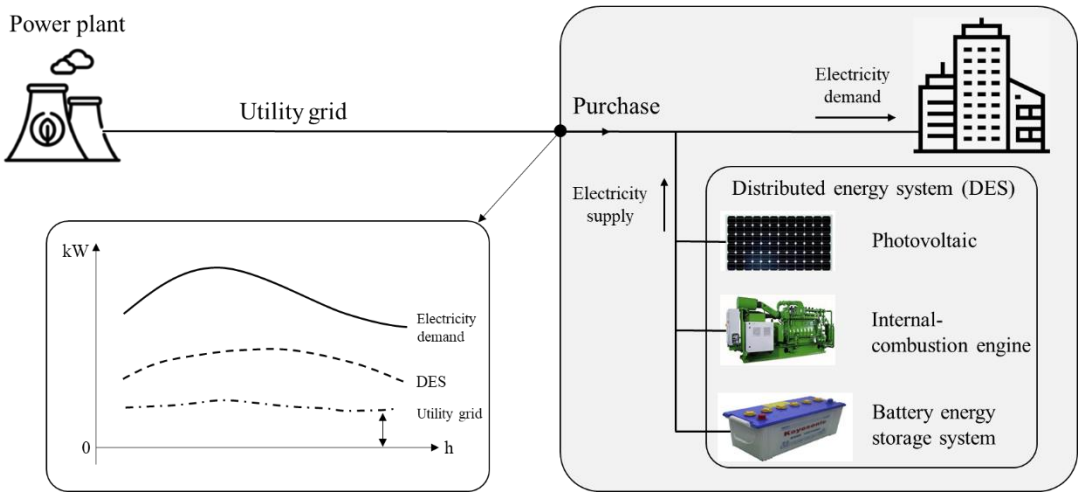

Fig. 4-2 Application of DES for grid stabilization.

Therefore, we propose two indices of "independence ratio" and "peak shaving ratio" for the grid stabilization of the DES, which are represented the power self-supply ability of users and the effect of shaving peak load by the DES. The impact of the demand load fluctuation on the utility grid is less with the improvement of the independence ratio of the DES. And the peak load pressure of the

grid reduces with the growth of the peak shaving ratio.

The expression for the independence ratio is as follows:

$$Independence\ ratio = 1 - \sum_{t=1}^{8760} E_{grid}(t) \Big/ \sum_{t=1}^{8760} E_{Load}(t) \tag{4-13}$$

where, $E_{grid}(t)$ is the electricity imported from utility grid, kWh. $E_{Load}(t)$ is the electricity load of users, kWh.

The peak shaving ratio is expressed as follow:

$$Peak\ shaving\ ratio = \left(\sum_{m=1}^{12} E_{original,max}(m) - \sum_{m=1}^{12} E_{grid,max}(m)\right) \Big/ \sum_{m=1}^{12} E_{original,max}(m) \tag{4-14}$$

where, $E_{original,max}(m)$ is the monthly maximum electricity imported from utility grid before employing the DES, which is equal to monthly maximum demand load, kWh. $E_{grid,max}(m)$ is the monthly maximum electricity imported from utility grid after application of the DES.

4.2.3 The economic and environmental analysis of the distributed energy systems

4.2.3.1 Economic analysis

Economic efficiency is usually the most important factor for the final decision-making while constructing the components of the DES. In this research, we use annualized total cost (ATC) to evaluate the economy of system.

1) Annualized total cost (ATC)

$$ATC = CRF \times IN_{init} + C_{o\&m} + C_{en} \tag{4-15}$$

2) Investment cost

The investment cost is the cost of purchasing the main components that consist of the DES as shown in Fig. 4-1. The investment cost for the entire system is the sum of the procurement costs estimated for each component of the system, and it can be expressed as:

$$IN_{init} = C_{PV} \times NC_{PV} + C_{ICE} \times NC_{ICE} + C_{BESS} \times NC_{BESS} \tag{4-16}$$

3) Annualized Operation and maintenance cost

$$C_{o\&m} = C_{O\&m,PV} + C_{O\&m,ICE} + C_{O\&m,BESS} \tag{4-17}$$

4) Annualized energy cost

$$C_{en} = \sum_{d=1}^{365} \sum_{t=1}^{24} (E_{dt,grid} C_{dt,e} + F_{dt} C_{dt,f}) \quad (4\text{-}18)$$

4.2.3.2 Environmental analysis

The amount of carbon dioxide emissions (CDEs) from the CCHP system can be determined using the emission conversion factors as follows [3,4]:

$$CDE = \sum_{t}^{8760} E_{grid}^{t} \times \mu_{CO_2,e} + \sum_{t}^{8760} F_{m}^{t} \times \mu_{CO_2,gas} \quad (4\text{-}19)$$

where $\mu_{CO_2,e}$ and $\mu_{CO_2,gas}$ are the emission conversion factors for electricity from the grid and natural gas, respectively, g/kWh. According to the investigation, the CO_2 emission conversion factors of electricity is 0.000462 t/kWh [5] and the CO_2 emission conversion factors of gas is 2.19 t/m^3 [6] in Japan.

4.3 Research object introduction and basic data

4.3.1 Research object

In 2011, Kitakyushu Smart Community Creation Project was launched in Higashida District, Yahata, Kitakyushu, the birthplace of modern industry in Japan, as shown in Fig.4-3 [7]. The project includes around 200 houses, 900 residents, 70 companies, and other public facilities, covering with 120 hectares, features with 60 0 0 employees, 10 million visitors per year, the demonstration project was co-developed by the Fuji Electric system, GE, IBM and Nippon Steel corporations from 2011 to 2014. From the birthplace of modern industry to the origin of the green revolution, The DES with renewable energy sources such as solar and wind is the focal point for this project and the main objective is to save 20% energy consumption and achieve CO_2 emission reduction over 50%. The backbone power of Higashida is using a natural gas cogeneration power with an installed capacity of 33,000kW and the introduction of new energy was reached 10% in 2015 [8]. The Smart Community is committed to the development of distributed energy and microgrid to prevent global warming, create recycling-oriented, low-carbon society, and an eco-city.

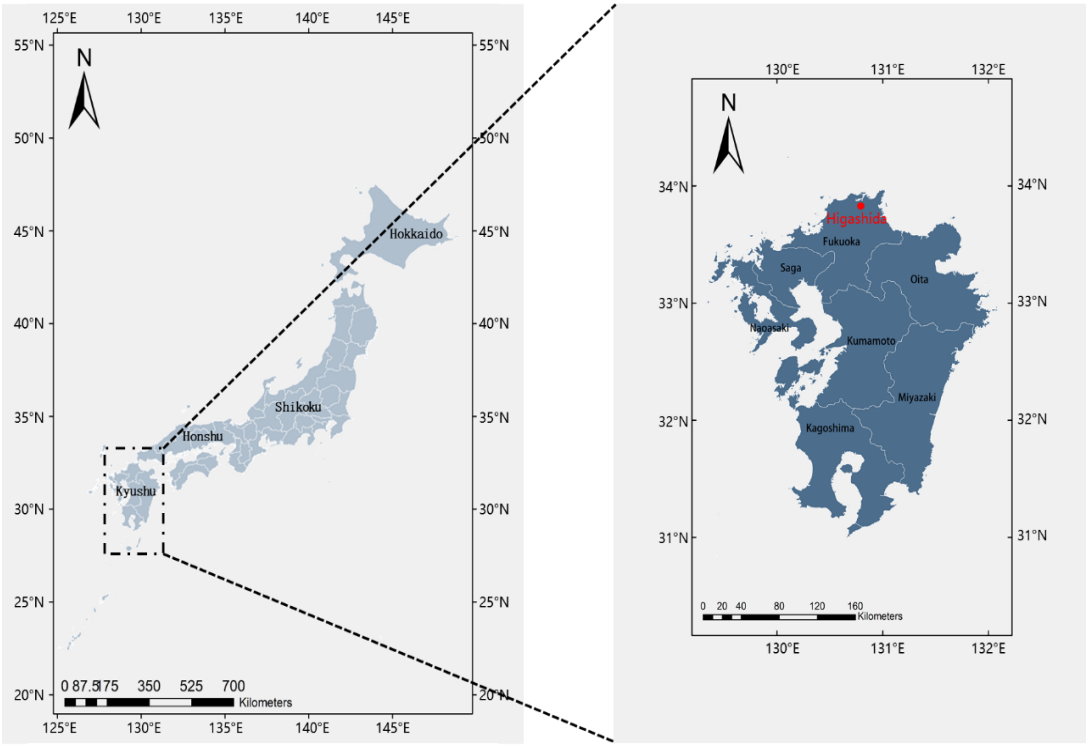

Fig. 4-3 Location of Higashida region in Japan

This research selects five types of buildings in Higashida area (included two offices, two residentials, two hospitals, two museums, and two shopping malls) as shown in Fig.4-4. The electricity load of these 10 buildings was investigated from 2013.04 to 2014.03 at hourly interval.

Fig.4-5 presents the monthly grid load of five types of buildings. It can be seen that the peak value of electricity consumption is in summer and it is considerably reduced in mid-season. As the hourly load curves in a typical day of summer demonstrated in Fig.4-6, the load curves of various building-types are significantly different. The peak residential power consumption occurred at 8:00~9:00 and

18:00~24:00 respectively. Conversely, the peak period of shopping mall's power load is from 11:00 to 20:00. And the office electricity peak also appears in the daytime. As for other types of buildings load are relatively stable. Therefore, the grid demand load combined by multi-type buildings has the characteristics of peak during daytime, and valley during night.

Fig. 4-4 The Higashida District, Yahata, Kitakyushu City.

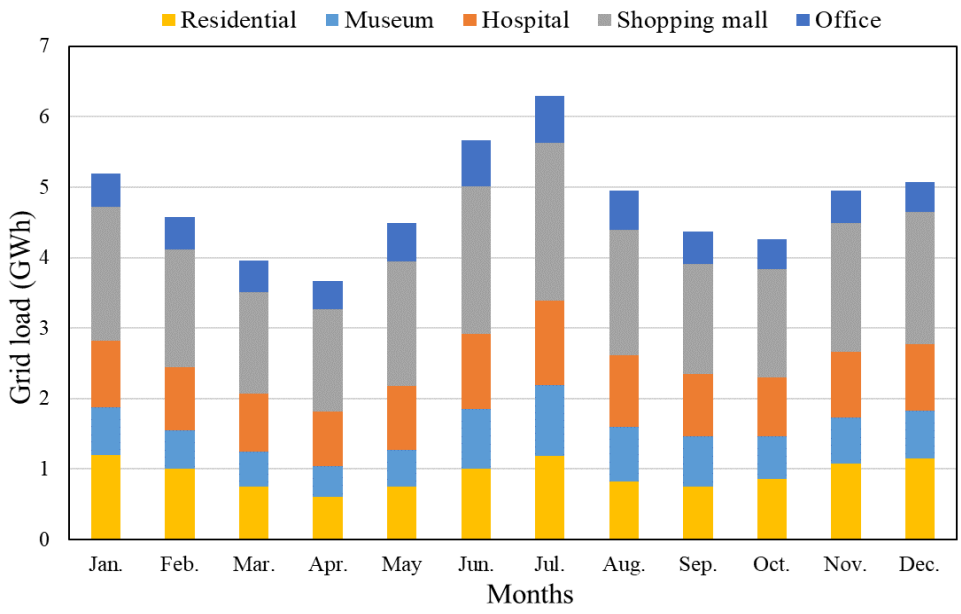

Fig. 4-5 Variations of monthly grid load.

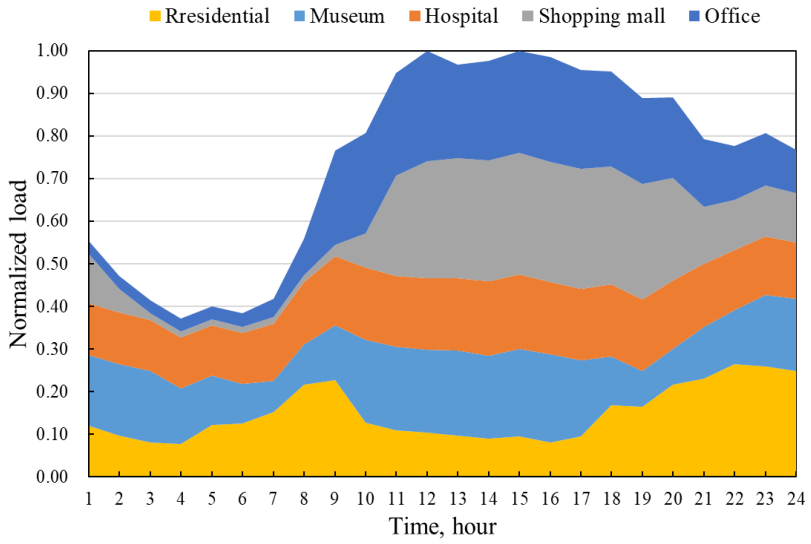

Fig. 4-6 Hourly load curves in a typical day of summer.

Fig.4-7 shows the variations of daily grid load in one year. Compared with other seasons, the fluctuation of summer load is more severe. The peak load shown in red reaches about 14 MWh, which can be 3 times of the minimum load.

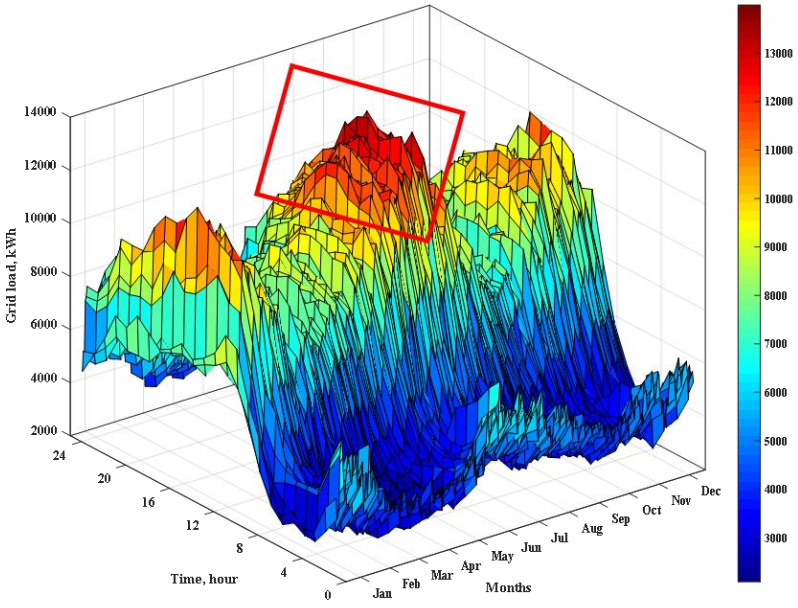

Fig. 4-7 Variations of daily grid load in one year.

4.3.2 PV production

Due to the limitation of the rooftop area of the region, the maximum power generation of PV system can be determined by Eq. (4-2) based on the local solar irradiance and temperature data. The rooftop area of each building is shown in Table A4-1. After calculation, the maximum installed capacity of PV system is 3MW. And the daily average curves of PV generation in each month are

shown in Fig. 4-8. As we can see, though the maximum capacity of PV system can be reached 3MW, the power generation is only half of the capacity due to the instability of solar radiation and ambient temperature.

Because of the low cost and zero carbon emission of PV system, we assume that the total installed capacity of PV system is 3MW and the power generation from PV system has priority in meeting the demand load in the proposed DES.

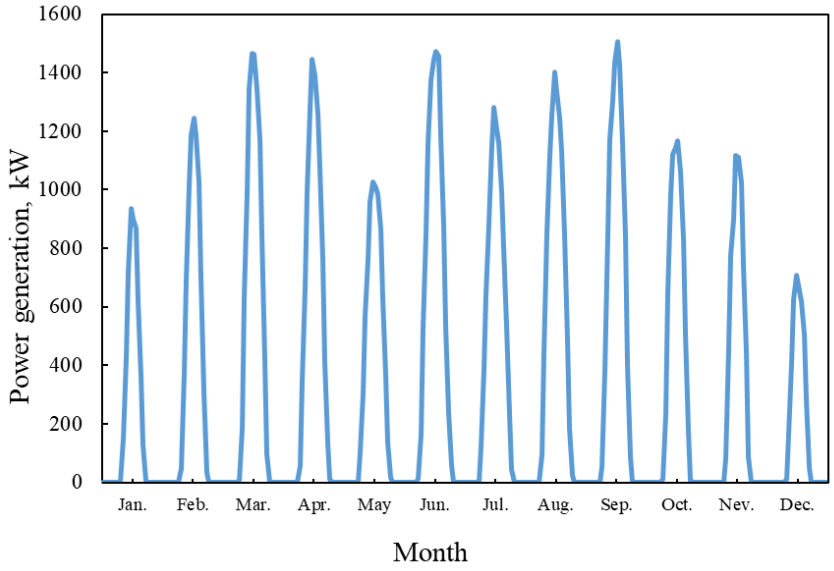

Fig. 4-8 Daily average curves of PV generation in each month.

4.3.3 Study cases

In order to analyze the grid stabilization of the DES, four cases are proposed based on different combinations of the DES units, demonstrated as Table 4-1 (the basic case is that the demand load is provided by utility grid without DES):

Table 4-1 Capacity of the PV, ICE and BESS units.

Cases	Capacity of DES1-5 units			Total capacity of DES (MW)
	PV (MW)	ICE (MW)	BESS (MW)	
Case 0: Without DES	0	0	0	0
Case 1: DES_1	3	0	0	3
Case 2: DES_2	3	4	0	5
Case 3: DES_3	3	4	2	7

The technical specifications and cost data details for each units of the proposed DES systems are presented in Table 4-2 and. According to the Kyushu Electric Power Company, the electricity price is adopted the time of use (TOU) event, which is presented in Table 4-3 [9]. Other prices are listed in Table 4-3 as well.

Table 4-2 Technical parameters of the units in the distributed energy systems [10–13]**.**

System	Capital cost*	Lifetime	Other operation parameters
PV	1904.8 ($/kW)	15 years	conversion efficiency=16%
			angle of incidence=30°
ICE	2857.1($/kW)	15 years	Electricity efficiency=0.4
			Lower Heating Value=45MJ/Nm^3
BESS	1428.6 ($/kW)	9 years	d=0.8
			max SOC=95%
			max SOC=15%
			charge/discharging efficiency=100%

*(The U.S. dollar exchange rate against RMB is 1:7; The U.S. dollar exchange rate against JPY is 1:105).

Table 4-3 Energy prices [9,14]**.**

	Time			Prices*
Electricity	Summer	Peak time	13:00-16:00	0.248 ($/kWh)
		Daytime	8:00-13:00,16:00-22:00	0.213 ($/kWh)
	Other seasons	Daytime	8:00-22:00	0.203 ($/kWh)
	Night		22:00-8:00	0.0863 ($/kWh)
	Peak load price		Monthly	12.571 ($/kW)
Natural gas	0.575 $/m^3			

*(The U.S. dollar exchange rate against RMB is 1:7; The U.S. dollar exchange rate against JPY is 1:105).

4.4 Comparison results of the case studies

According to the electricity and gas prices of demand side, the electricity cost of ICE is higher than the electricity tariff during valley time. Therefore, the operation strategy of ICE is running only in the daytime, that is, from 8:00 to 22:00. The operation strategy of BESS is charging at valley value and discharging at peak value to shave peak and fill valley to smooth load fluctuation. According to the above economic operation strategy, the output of each unit in the cases can be obtained. The hourly output of each unit in the DES and hourly shift load curve on a typical day in summer are displayed in Fig.4-9. And the daily shift load curve after shaving peak by the DES in one year are demonstrated in Fig. A4-1.

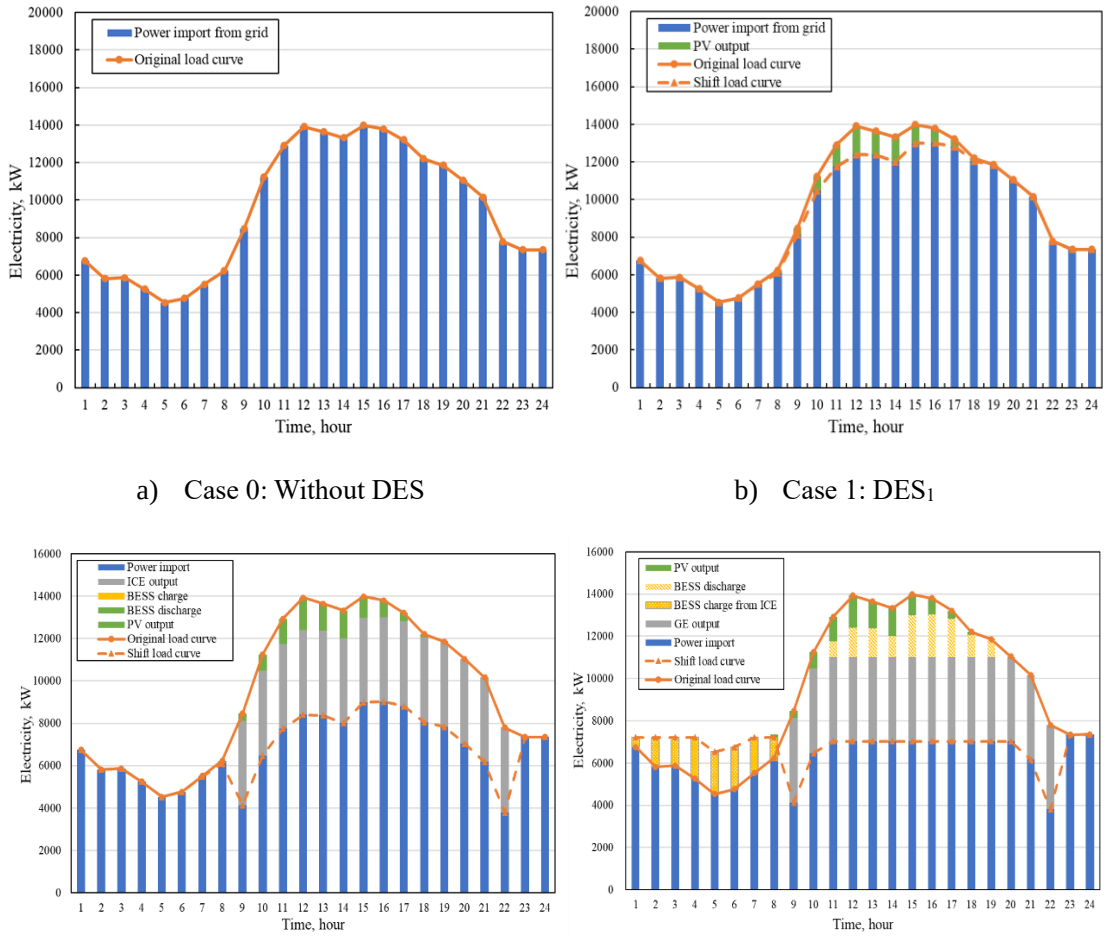

a) Case 0: Without DES

b) Case 1: DES_1

c) Case 2: DES_2

d) Case 3: DES_3

Fig. 4-9 The hourly output of each unit in the distributed energy systems and hourly shift load curve on a typical day in summer.

The changing trend of the photovoltaic power generation curve is consistent with the change in the demand load curve. After the introduction of the PV system, the peak load of the grid decreases. However, due to intermittence and volatility, its output is far less than the installed capacity, which led to less effect on peak shaving, shown as Fig 4-9b). The ICE is a controllable and stable power generation equipment, it can greatly reduce the peak load without change the trend of the load curve,

shown as Fig 4-9c). The BESS can move the load of the daytime to the night, so that the load of the power grid will be kept in a small fluctuation range, and the power grid will be leveled. However, when the capacity of the BESS is large, the peak load will appear at night, which will have an impact on the peak shaving effect, shown as Fig 4-9d). After calculation, the independence ratio, peak shaving ratio, economic and environmental analysis of each case are shown in table 4-4.

Table 4-4 The results comparison of six distributed energy systems

Cases	Case 0: Without DES	Case 1: DES_1	Case 2: DES_2	Case 3: DES_3
Independence ratio	0	5.34%	40.95%	40.95%
Peak shaving ratio	0	5.76%	30.34%	35.64%
Investment cost (million $)	0.0	5.7	17.1	20.0
ATC (million $)	11.8	11.6	10.2	10.1
Carbon emission (10^4 t)	2.65	2.51	2.46	2.46

*(The U.S. dollar exchange rate against RMB is 1:7; The U.S. dollar exchange rate against JPY is 1:105).

The introduction of DES can improve the independence ratio and peak shaving ratio, and reduce the annualized total cost and carbon dioxide emissions. By comparing DES_1 and DES_2, DES_3 and DES_5, it can be seen that the increase of ICE can effectively improve the independence ratio and peak shaving ratio. Compared with DES_2, DES_3 and DES_4, the increase of BESS capacity can improve the peak shaving rate, but it has no effect on the independent ratio. This is because the BESS is only charged and discharged from the grid, which does not increase the total output of the DES, so it is unable to increase the power supply independence ratio. With the increase of independence ratio and peak shaving ratio, the investment cost of DES gradually increases, but the annualized total cost of users is effectively reduced, and carbon emission is also gradually reduced.

DESs provide users with an alternative kind of power supply mode that can replace the power grid, and is committed to reducing the impact of user load fluctuation on the grid, so as to effectively achieve grid stabilization and improve the reliability of regional power supply. At the same time, the economic and environmental benefits can be improved by reducing the power cost and carbon emission of consumers. The investment cost of DES to realize the different requirements of the power supply independence ratio and peak shaving ratio of users is different, and the economic and environmental benefits are also diverse. Therefore, the economic and environmental analysis of DES focusing on grid stabilization is worth studying.

4.5 Economic and environmental analysis focusing on grid stabilization

As analyzed in Section 4.4, due to environmental constraints, photovoltaic output is low and there is no overproduction of PV system. In addition, because the electricity price from utility grid during valley period is cheaper than the energy cost of the ICE, the ICE only operates during the daytime. Considering the economical operation mode of the BESS, the BESS is discharged during the peak period for users and charged during the valley period from the utility grid, which dispatches the peak-valley power demand without increasing the output of the DES. Therefore, the increase of installed capacity in the BESS does not contribute to independence ratio. It can be concluded that the independence ratio is determined by the power generation of the PV and ICE. Therefore, firstly we analyze the economic and environmental performance of the DES consisted of PV and ICE based on the independence ratio and peak shaving ratio. Subsequently, the impact of the BESS on the peak shaving ratio was explored. And the optimal combinations of the DES under different grid stabilization indices can be obtained by minimizing the annualized total cost after introducing the BESS.

4.5.1 Distributed energy system with PV and ICE

The output of PV and ICE system reduces the peak load in the daytime and improves the independence ratio and peak shaving ratio. Fig. 4-10 displays the change of peak shaving ratio with the increase of independence ratio. It can be seen that the peak shaving ratio of PV system is 5.76%. The peak shaving ratio increases linearly with the increase of independence ratio. Because the ICE only operates in the daytime and cannot cover the night load, the maximum independence ratio can reach 73.6%. When the peak value appears at night, the increase of ICE output cannot improve the peak shaving ratio. Therefore, when the independence ratio is above 50%, the peak shaving ratio of the DES reaches the maximum value of 39.4%.

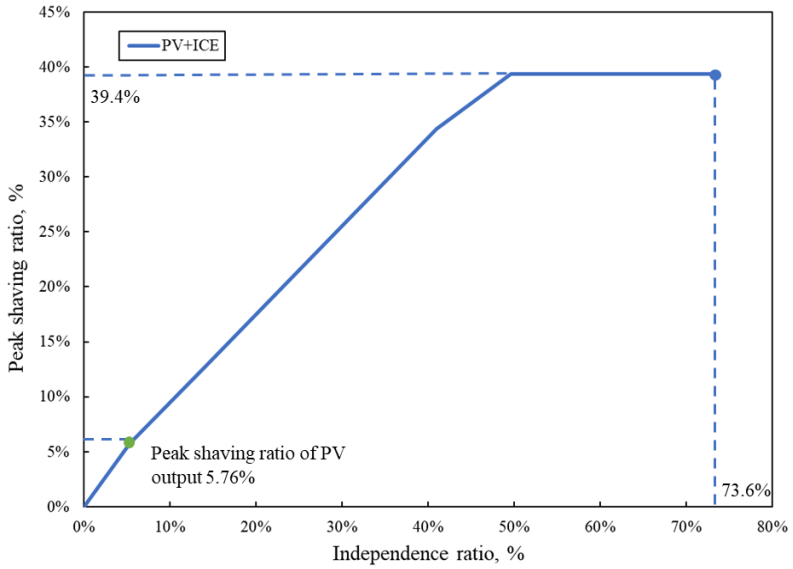

Fig. 4-10 Peak shaving ratio changes of PV and ICE with increase of independence ratio.

The investment cost change of PV and ICE under different independence ratios is shown in Fig. 4-11. It can be seen from the figure that the investment cost growth rate of the DES is accelerating

with the increase of independence ratio.

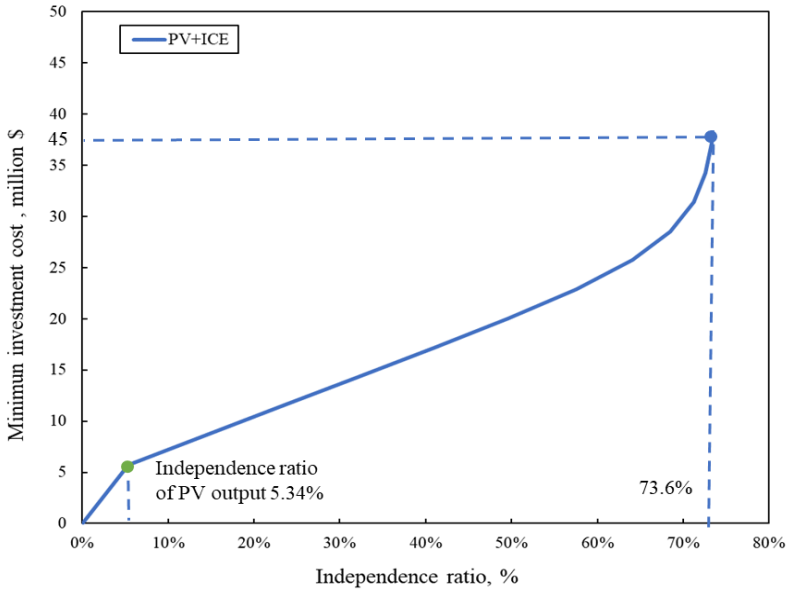

Fig.4-11 Investment cost change of PV and ICE under different independence ratios.

When the independence ratio is low, the investment cost of the DES rises linearly with the increase in the independence ratio. When the independence ratio reaches more than 60%, the decrease in the proportion of regional peak load will reduce the effective utilization hours of the ICE. Therefore, the improvement of the independence ratio per unit capacity of the ICE achieving will decrease. The investment cost needs to increase exponentially to continue improving the independence ratio. And the required investment cost of the maximum independence ratio is 42.86 million $.

The application of DES improves the independence ratio of regional power supply and reduces the peak load of power grid. As a result, it can reduce the energy cost of users. Considering both annual energy cost and annualized system cost, the ATC (annualized total cost) changes with the independence ratio is shown in Fig.4-12. The increase of independence ratio can reduce the annual energy cost. The higher the independence ratio is, the higher the investment cost of DES is. Therefore, when considering the changes of investment and energy costs, the annualized total cost shows a "first decrease and then increase" change. When the independence ratio reaches 64%, the annualized total cost is the least which represents that the economic performance of the DES is the best. At this time, the investment cost of DES is 25.71 million $ according to Fig.4-11.

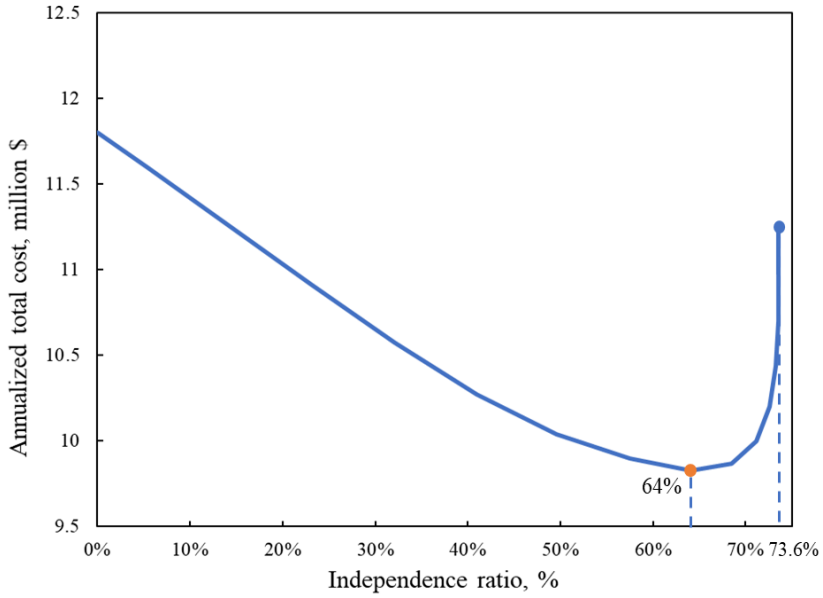

Fig. 4-12 ATC changes with the increase of independence ratio.

Fig.4-13 demonstrates the change of emission reduction rate with different independent ratio. It can be seen that the emission reduction rate of PV system output is 5.3%. After that, with the increase of independence ratio, the emission reduction rate increased linearly. The higher the independence ratio, the more grid power will be replaced by DES. Therefore, the carbon emission will be less. When the independence ratio reaches the maximum of 73%, the emission reduction rate reaches the maximum of 8.9%.

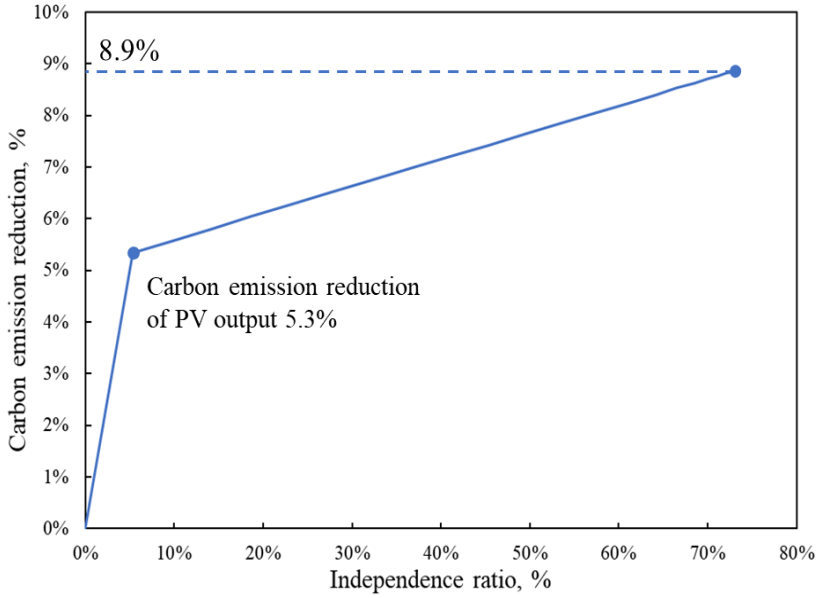

Fig. 4-13 Carbon emission reduction changes with the increase of independence ratio.

4.5.2 Distributed energy system with PV, ICE and BESS

Due to the peak shaving and valley filling operation strategy of the BESS, the more expensive

power in the daytime can be replaced by the cheaper power at night, which reduces the electricity cost of users. Therefore, the advantage of the BESS may improve the economic performance of the DES. To assess the economic benefits of the BESS, the annualized total cost of users is calculated and compared. Under different independence ratios, the change of annualized total cost with the increase of the BESS capacity is shown in Fig.4-14. It can be seen that when the installed capacity of the BESS increases, the annualized total cost of users first decreases and then increases. And there is the best installed capacity of the BESS, which realizes the minimum annualized total cost.

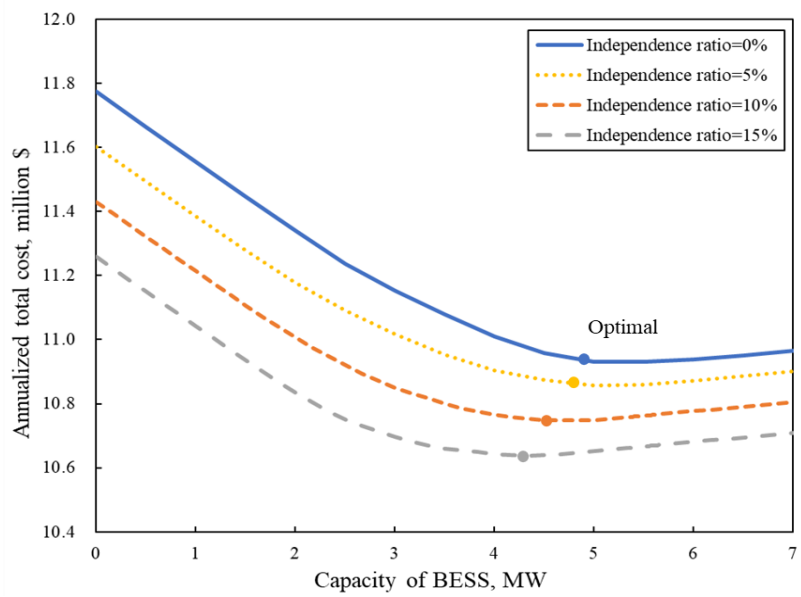

Fig.4-14 ATC changes with the increase of BESS capacity under different independence ratios.

Therefore, the optimal installed capacity of BESS under different independence ratios is obtained by taking the minimum annualized total cost as the objective function, as shown in Fig. 4-15. The blue dotted line shows the change of the ICE installed capacity with the increase of independence ratio, and the orange solid line shows the change of the BESS installed capacity with the increase of independence ratio. With the increase of independence ratio, the installed capacity of the BESS gradually decreases. When the independence ratio is low, the output of PV and ICE system is low, and the peak load in the daytime is still large. The BESS still has the profit space through peak shaving and valley filling operation. However, with the increase of the independence ratio, the peak load of the grid load in the daytime is gradually reduced, which suppresses the economic benefit of the BESS. When the independence ratio reaches 35%, the optimal installed capacity of the BESS drops suddenly. This is because the peak shaving and valley filling operation of the BESS will reduce the daytime load, which leads to the reduction of the DES output. It will affect the independence ratio of the system. Therefore, the installed capacity of the BESS is limited by the independence ratio. When the independence ratio reaches more than 45%, the output of PV and the ICE system is larger, and the peak load occurs at night. Therefore, the economic benefit from peak shaving and valley filling operation of the BESS significantly declines, and the increase of the BESS capacity cannot bring the reduction of energy cost. Therefore, when the independence ratio is more than 45%, the installed capacity of the BESS gradually falls to 0.

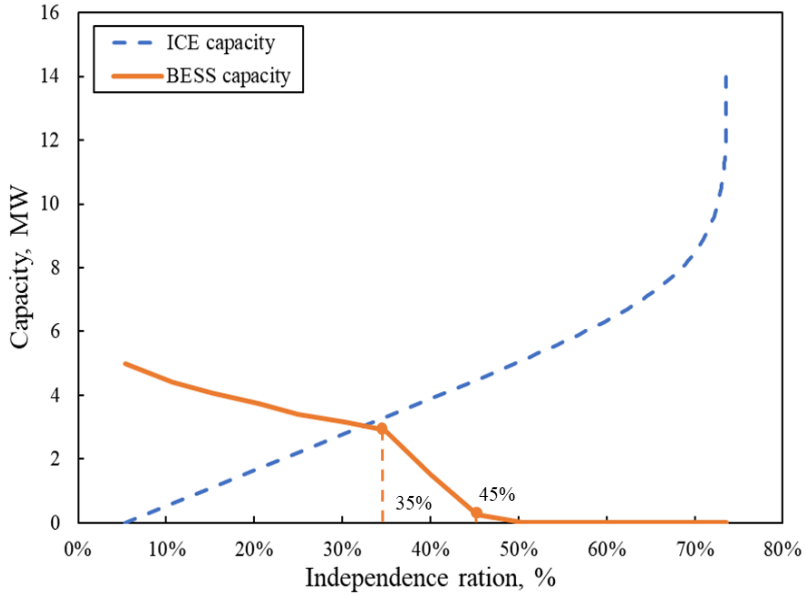

Fig.4-15 ICE and BESS optimal capacity changes with the increase of independence ratio.

After introducing the BESS, the peak shaving ratio is improved, as displayed in Fig.4-16. When the independence ratio is low, the peak shaving effect of the PV and ICE is not obvious. Therefore, the BESS can help to improve peak shaving ratio. As the independence ratio increasing, the output of the PV and ICE is becoming high, the benefit of peak shaving for the BESS is decreased. When it comes to the maximum peak shaving ratio, increasing the capacity of the BESS is not economical.

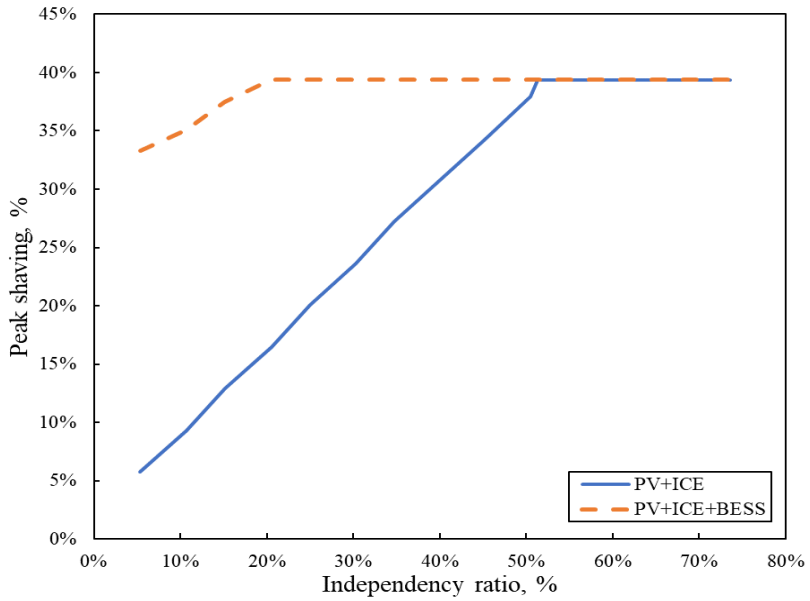

Fig.4-16 Peak shaving ratio changes after introducing the BESS.

Fig. 4-17 displays the change of annualized total cost with the increase of independence ratio. The blue dotted line indicates the change of the annualized total cost with the increase of the independence ratio when the DES do not introduce the BESS; the orange solid line indicates the change of annualized total cost with the increase of the independent ratio after the DES adopt the

BESS. Comparing the minimum annualized total cost of the DES under different independence ratios, we can see that the economy of DES after introducing the BESS also shows the change of " decrease first and then increase" with the increase of independence ratio. Obviously, increasing the capacity of the BESS can reduce the annualized total cost at lower independence ratios by comparing the annualized total cost of the DES before and after introducing the BESS. But due to the limitation of the BESS capacity at high independence ratios, the annualized total cost cannot be reduced by the BESS when the independence ratio is increased above 45%. When the independence ratio reaches 64%, the minimum annualized total cost is 9.81 million $, which means that the DES has the best economy when the independence ratio is 64%.

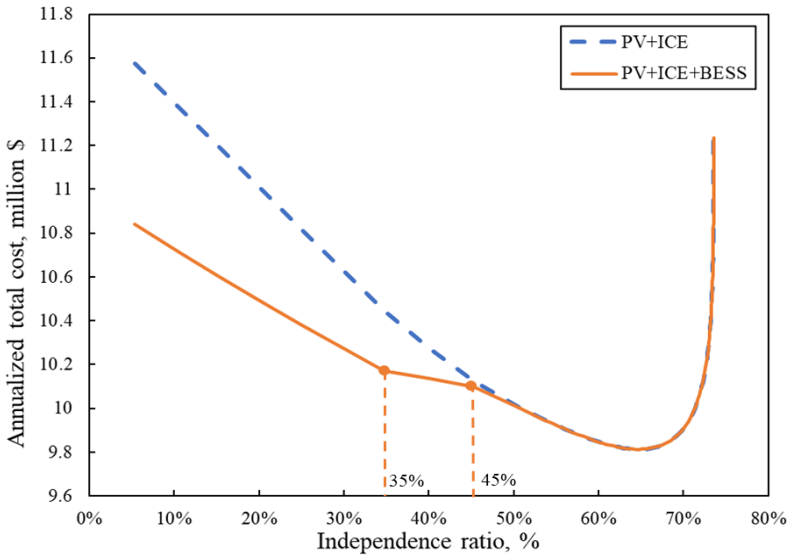

Fig.4-17 ATC changes before and after introducing BESS.

The change of total investment cost of DES with the increase of independence ratio is shown in Fig.4-18.

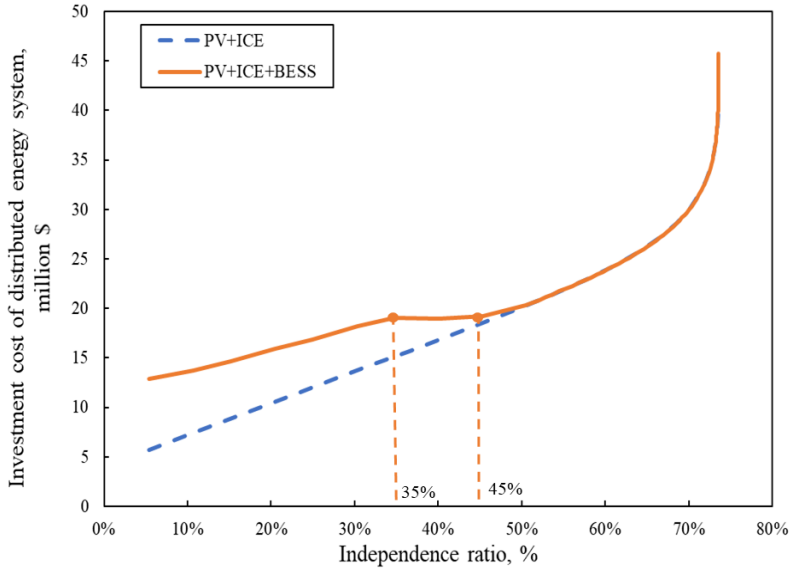

Fig.4-18 Investment cost changes of distributed energy system with different independence ratios.

When the independence ratio is less than 45%, the total investment cost increases due to the increase of the BESS capacity. Because the installed capacity of the BESS decreases with the increase of independence ratio, the growth rate of total investment cost decreases. When the independence ratios are among 35% to 45%, the installed capacity of the BESS is limited by the independence ratio. The installed capacity of the BESS falls sharply with the higher requirement of independence ratio, while the capacity of the ICE continues to increase with the improvement of independence ratio. Therefore, the total investment cost of DES has little change. When the independence ratio is more than 45%, the installed capacity of the BESS is reduced to 0, and the change of total investment cost is only related to the installed capacity of PV and the ICE.

However, the carbon emission is not affected by adopting the BESS under certain independence ratio. Because the BESS is only charged from the power grid. When the independence ratio is determined, the total output of the grid will not be reduced by the increase of the BESS, that is, the carbon emission of the grid will not change. Therefore, the change of emission reduction rate of DES under different independence rates is still shown in Fig.4-13.

4.6 Summary

In order to address the greatly increasing power load demand and relieve the peak load pressure of the utility grid, the DES is identified as an alternative to achieve the grid stabilization by users themselves. It is committed to reducing the peak load of the power grid and abating the impact of user load fluctuation on the power grid, so as to improve the reliability of the regional power supply. At the same time, the economic and environmental benefits can be improved by reducing the energy cost and carbon emissions.

Independence ratio and peak shaving ratio were proposed as the indices of the DES on grid stabilization, to indicate the ability of users to supply power by themselves and the effect of reducing grid peak load through the DES. The DES with different combinations can realize the different independence ratio and peak shaving ratio, and the economic and environmental benefits are also diversity. In this chapter, a DES model composed of photovoltaic, gas driven internal-combustion engine and battery energy storage system was established. Taking the Smart Community in Higashida, Japan as an example, the impact of different DES on grid stabilization were carried out, and the economic and environmental performance of the DES based on different independence ratios and peak shaving ratios were analyzed and compared.

Through comparative analysis, it can be found that the DES consisted of PV and ICE can improve the user independence ratio and peak shaving ratio. The economic operation of "peak shaving and valley filling" of the BESS can effectively reduce the annualized total cost, but it has no contribution to the independent ratio, only plays the role of peak shaving. If there is no independent ratio restriction, the BESS can effectively reduce the annualized total cost by transferring the load peak from daytime to nighttime. Therefore, the economy of the BESS is better than that of ICE when the independence ratio requirement is low. However, with the improvement of the independence ratio, the output of the BESS is limited, and the economic benefits of peak shaving and valley filling decrease. Therefore, the BESS does not play a role at high independence ratios.

The growth rate of investment cost gradually accelerated with the growth of independence ratio. It presented an exponential change under high independence ratio. With the increase of independence ratio, the annualized total cost decreased first and then increased. The capacity of the ICE grew with higher independence ratio, but its effective utilization hours showed a downward trend. As for the environmental performance, the emission reduction of the DES is also improved with the increase of independence ratio and peak shaving ratio, which demonstrated that the introduction of the DES is conducive to improving environmental benefits. From the perspective of economic benefits, the introduction rate of the DES on the demand side has an economic optimal proportion. If continuing to increase the independence ratio, the gains of improving the grid stability and environment came at the expense of economic benefits. It is essential to balance both. It is essential to balance both.

Appendix:

1) Direct solar radiation:

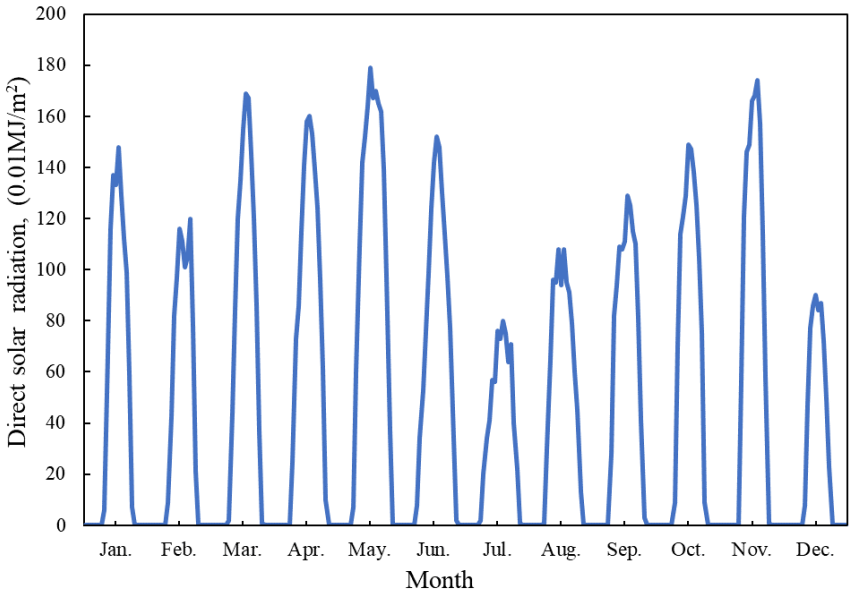

Fig.A4-1 Daily average direct solar radiation of Kitakyushu in each month

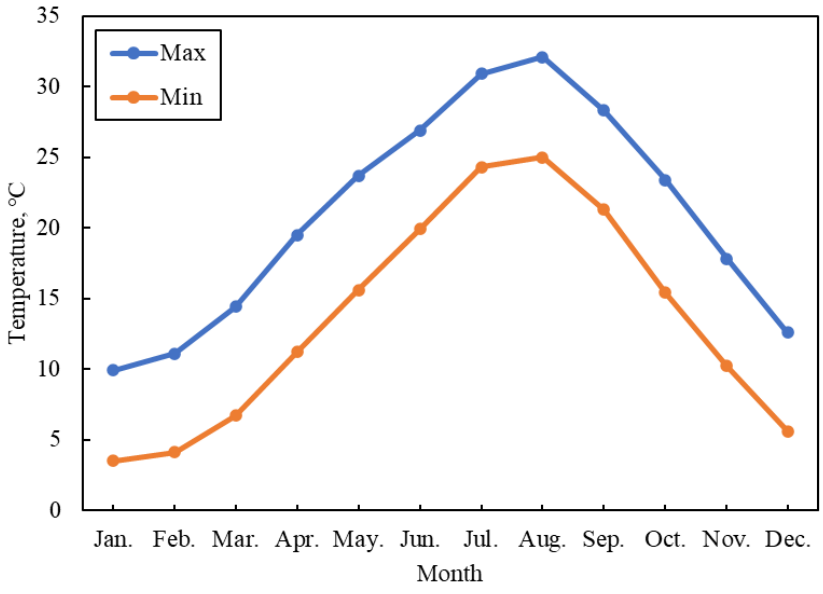

Fig.A4-2 Monthly ambient temperature of Fukuoka

2) The daily shift load curve after shaving peak by the distributed energy systems in one year:

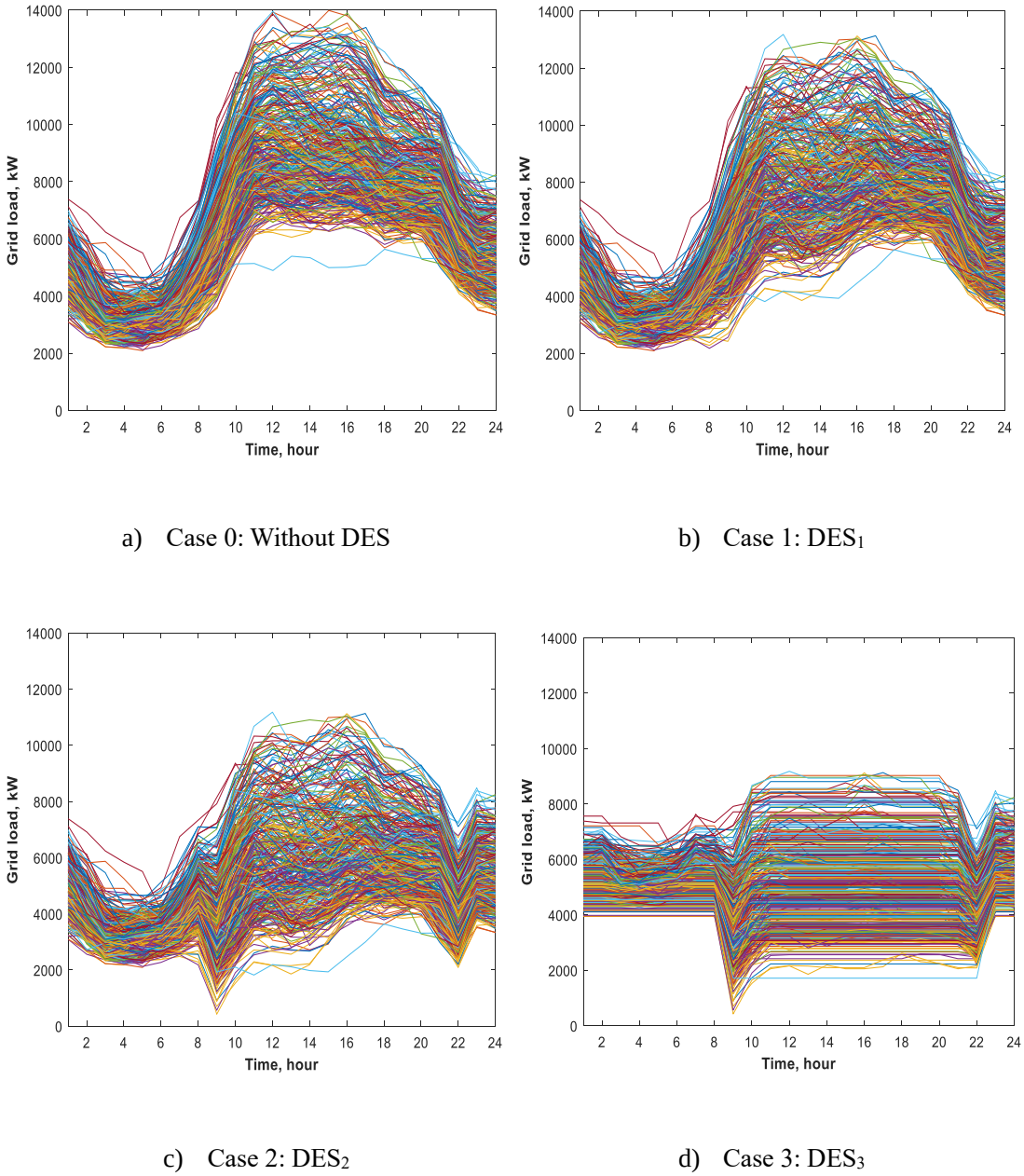

a) Case 0: Without DES

b) Case 1: DES_1

c) Case 2: DES_2

d) Case 3: DES_3

Fig.A4-3 The daily shift load curve in one year of different cases.

Reference

[1] Radhakrishnan BM, Srinivasan D. A multi-agent based distributed energy management scheme for smart grid applications. Energy 2016;103:192–204. https://doi.org/10.1016/j.energy.2016.02.117.

[2] Rocchetta R, Li YF, Zio E. Risk assessment and risk-cost optimization of distributed power generation systems considering extreme weather conditions. Reliab Eng Syst Saf 2015;136:47–61. https://doi.org/10.1016/j.ress.2014.11.013.

[3] Feng L, Dai X, Mo J, Shi L. Performance assessment of CCHP systems with different cooling supply modes and operation strategies. Energy Convers Manag 2019;192:188–201. https://doi.org/10.1016/j.enconman.2019.04.048.

[4] Jing YY, Bai H, Wang JJ. Multi-objective optimization design and operation strategy analysis of BCHP system based on life cycle assessment. Energy 2012;37:405–16. https://doi.org/10.1016/j.energy.2011.11.014.

[5] CO2 Emission coefficient by electric utility n.d. https://ghg-santeikohyo.env.go.jp/files/calc/r02_coefficient.pdf (accessed September 16, 2020).

[6] Carbon dioxide emission coefficient of urban gas n.d. http://www.saibugas.co.jp/business/others/co2_emission_factor.htm (accessed September 16, 2020).

[7] Kitakyushu Smart Community n.d. https://www.esci-ksp.org/archives/project/kitakyushu-smart-community?task_id=915 (accessed September 4, 2020).

[8] Result of the Kitakyushu Smart Community Creation Project n.d. https://www.esci-ksp.org/wp/wp-content/uploads/2016/11/100750432.pdf (accessed September 4, 2020).

[9] No Title n.d. http://www.kyuden.co.jp/agreement_rate_gyomukijia-1_h26_5.html (accessed September 16, 2020).

[10] Li Y, Gao W, Ruan Y. Performance investigation of grid-connected residential PV-battery system focusing on enhancing self-consumption and peak shaving in Kyushu, Japan. Renew Energy 2018;127:514–23. https://doi.org/10.1016/j.renene.2018.04.074.

[11] Cost of solar power generation in Japan n.d. https://www.renewable-ei.org/pdfdownload/activities/Report_SolarCost_201907.pdf (accessed September 16, 2020).

[12] New energy related technology trend survey n.d. http://www.city.takatsuki.osaka.jp/ikkrwebBrowse/material/files/group/82/newe-h14.pdf (accessed September 16, 2020).

[13] A study on expansion of stationary batteries and its application to aggregation services n.d. https://www.meti.go.jp/meti_lib/report/H28FY/000479.pdf (accessed September 18, 2020).

[14] Natural gas price of power generation industry in Kitakyushu n.d. http://www.saibugas.co.jp/business/rates/index.htm (accessed September 18, 2020).

Chapter 5

MULTI-CRITERIA ASSESSMENT FOR OPTIMIZING THE DISTRIBUTED ENERGY SYSTEM

CHAPTER FIVE. MULTI-CRITERIA ASSESSMENT FOR OPTIMIZING DISTRIBUTED ENERGY SYSTEM

MULTI-CRITERIA ASSESSMENT FOR OPTIMIZING THE DISTRIBUTED ENERGY SYSTEM *5-1*

5.1 Content 5-1

5.2 Methodology 5-3

5.2.1 Operation strategy model of the distributed energy system 5-3

5.2.2 Evaluation criteria 5-5

5.2.3 Configuration optimization model 5-6

5.3 Research object and PV penetration prediction 5-8

5.4 Optimal design and comparison 5-12

5.4.1 The results under objective function of annual basic cost 5-12

5.4.2 The results under objective function of annual basic cost and peak load cost 5-16

5.4.3 The results under objective function of annual basic cost, peak load cost and CO_2 emission cost 5-19

5.4.4 The results comparison under three objective functions 5-21

5.5 Sensitivity analysis 5-26

5.5.1 Peak load price change 5-26

5.5.2 Carbon tax change 5-27

5.6 Summary 5-30

Reference 5-31

5.1 Content

The purposes of the DES are more than energy costs saving, along with grid stabilization and carbon dioxide emissions reduction. Economic performance is recognized as the evaluation criterion of DES, which consists of the investment cost, operation and maintenance cost (O&M cost), and energy bills [1–3]. The grid stabilization effect of the DES plays an important role in the improvement of the grid reliability, which depends on the output capacity and operation of the energy equipment in the DES [4]. In most of the researches, apart from the economic benefits, the grid stabilization effect of the DES do not take into consideration when analyzing the sizing problem. Moreover, the advantage of DES is the environmental benefit, but it often conflicts with the economic performance [5]. Therefore, all of them should be used as objective functions to optimize the configuration of DES at the same time, instead of considering one of them separately. This chapter proposes a comprehensive evaluation criterion of the DES taking the economy, reliability and environment into consideration. The effect of different evaluation criteria on the configuration optimization of the DESs is analyzed as well.

Taking a Smart Community in Higashida District of Japan as an example, five different types of buildings are selected in this research. Based on the actual load data of these buildings, the characteristics of the grid load for the multi-type buildings are analyzed in detail. In order to meet the energy load of the research area, a DES model equipped with PV, battery energy storage system and gas internal-combustion engine was established. The improvement of reliability and environmental performance will weaken the economic benefits of the DES. In order to evaluate the effects of the DES comprehensively, an evaluation method with three criteria from different aspects, economic, reliability and environmental performance, was proposed. Different configurations of the equipment will profoundly affect the performance of the DES, especially the grid stabilization and CO_2 emission reduction effect. Therefore, the PV penetration is used as the variable to establish different configuration application scenarios of the DES. In order to compare three different evaluation criteria, the grid stabilization and CO_2 emission reduction effect of the DES are added to the total cost after transforming into economic benefits through peak load price and carbon tax. After that, the configuration optimization model with the goal of minimizing the total cost is established based on the Genetic Algorithm. Then, the optimal combination of the DES under different PV penetration scenarios is obtained and compared to analyze the impact of grid stabilization and emission reduction effect on the configuration optimization of equipment in the DES. The research flow is presented as follows:

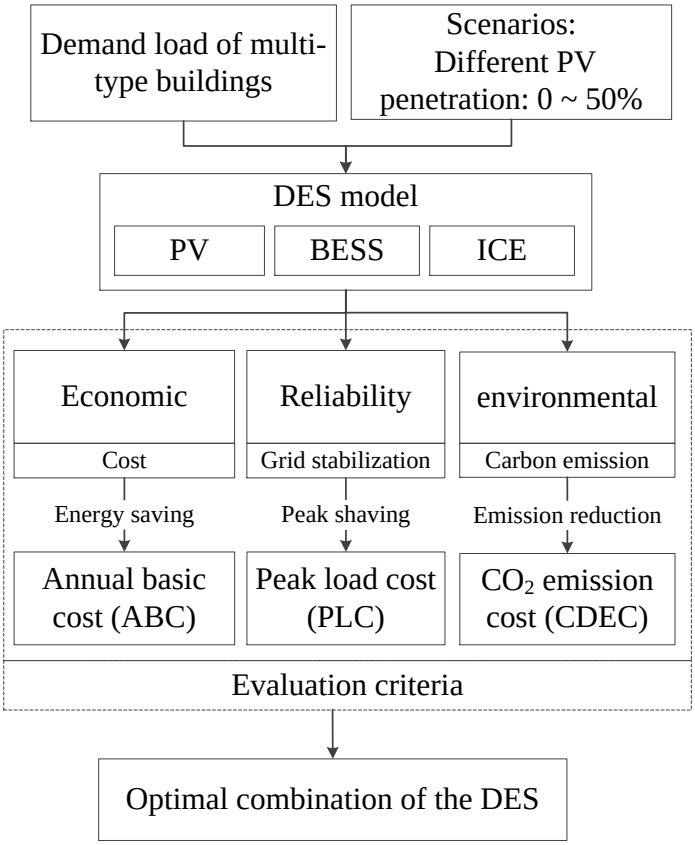

Fig.5-1 The research flow diagram

5.2 Methodology

5.2.1 Operation strategy model of the distributed energy system

1) Distributed energy system model

As described in Fig.5-2 a), a DES consisted of Photovoltaic (PV), battery energy storage system (BESS) and internal-combustion engine (ICE) is established to supply the electricity for the demand side. The aim of the proposed DES is to reduce the cost of electricity, stabilize power grid fluctuation and lower the CO_2 emissions through peak shaving and maximizing the energy efficiency of distributed energy resources [6], as shown in Fig.5-2 b).

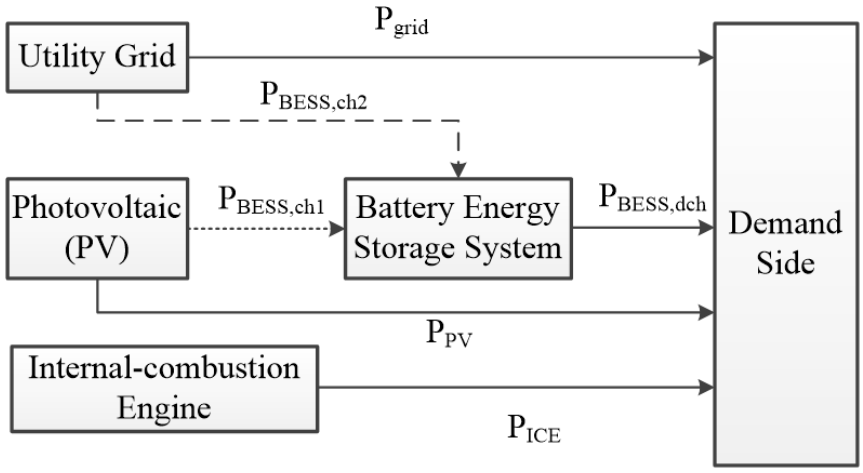

a)

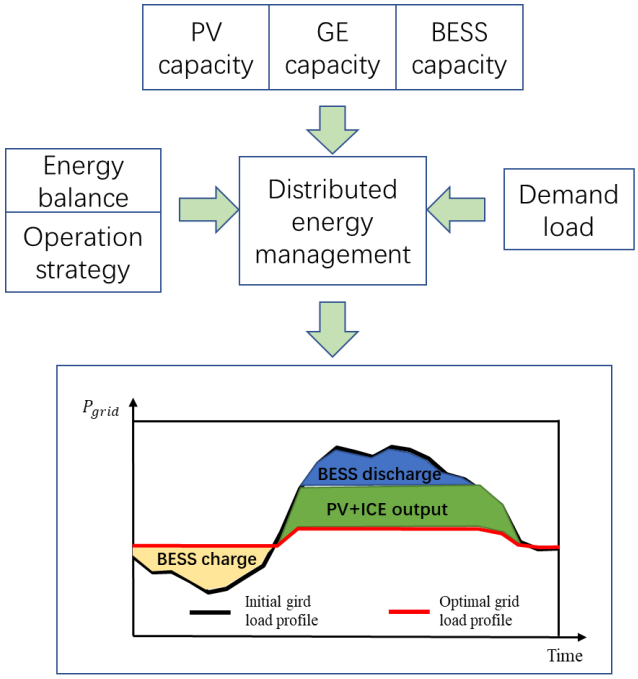

b)

Fig.5-2 a) Proposed distributed energy system; b) The purpose of the distributed energy system.

The energy balance of the proposed power system is presented in Equation (5-1) as:

$$P_L^t = P_{PV}^t + P_{ICE}^t + P_{BESS,dch}^t - P_{BESS,ch}^t + P_{grid}^t \quad (5\text{-}1)$$

where P_L^t is the demand load at t-time, kW. P_{PV}^t is the electricity generated by PV system at t-time, kW. P_{ICE}^t is the electricity generated by the ICE at t-time, kW. $P_{BESS,dch}^t$ is the electricity discharged by the BESS at t-time, kW. $P_{BESS,ch}^t$ is the electricity charged by the BESS from PV system when there is overproduction of PV system or imported from the utility grid. P_{grid}^t is the electricity supply to the demand load from utility grid.

2) Operation strategy model

- Power generation from PV system has priority in meeting the local electricity demand P_{PV}, excess generation can be stored in the BESS.
- Generally, the load at night is lower and the electricity price is cheaper. On the contrary, the load in the daytime is higher and the electricity price is more expensive. Therefore, the BESS is charged from the utility grid during the valley period and discharged during the peak period to achieve the effect of peak shaving as well as to reduce electricity cost. The operation strategy of the BESS is simulated as:

$$P_{BESS,ch}^t = \begin{cases} P_{ch}^t & , \ t \in [\text{Valley period}] \\ \max\{0, (P_{PV}^t - P_L^t)\}, & t \in [\text{Peak period}] \end{cases} \quad (5\text{-}2)$$

$$P_{BESS,dch}^t = \begin{cases} \max(P_{dch}^t, \ P_L^t), & t \in [\text{Peak period}] \\ 0 & , \ t \in [\text{Valley period}] \end{cases} \quad (5\text{-}3)$$

where P_{ch}^t is the charging capacity at t-time, kWh/h, P_{dch}^t is discharging capacity at t-time, kW/h. The charging and discharging capacity should be limited by the maximum output:

$$P_{ch}^t \leq \eta_{ch} \times P_{BESS,max} \quad (5\text{-}4)$$

$$P_{dch}^t \leq \eta_{dch} \times P_{BESS,max} \quad (5\text{-}5)$$

$$P_{BESS,max} = Cap_{BESS}/h_{min} \quad (5\text{-}6)$$

where, η_{ch} is the charging efficiency of the BESS, %. η_{dch} is the discharging efficiency of the BESS, %. $P_{BESS,max}$ is the maximum output, which determined by the characteristic of the BESS, kWh/h. Cap_{BESS} is the capacity of the BESS, kWh. h_{min} is the minimum time required for the BESS to be fully charged, which is 6 hours in this research.

- Because the electricity price of valley period at night is cheap, it is more economical to consume the electricity import from the utility grid than the electricity generated by the ICE. Therefore, the ICE only turns on at peak period during the daytime, and its operating strategy is as follows:

$$\boldsymbol{P_{GE}^t} = \begin{cases} \mathbf{0} & , \ \boldsymbol{t \in [valley\ period]} \\ \mathbf{max}\ (\boldsymbol{Cap_{ICE}}, \boldsymbol{P_L^t}) & , \ \boldsymbol{t \in [peak\ period]} \end{cases} \quad (5\text{-}7)$$

where Cap_{ICE} is the capacity of the ICE, kW.

5.2.2 Evaluation criteria

Economic performance is usually the most important factor for the final decision-making while constructing the components of the DES. From the actual power supply issue, the grid fluctuation is an urgent problem to be solved. And environmental effect should also be ignored. In order to evaluate the performance of the DES more clearly and comprehensively, this paper defines three evaluation criteria including annual basic cost, peak load cost and CO_2 emission cost. The optimal configuration of the equipment in the DES should be determined from these different perspectives. The calculation is as follows:

1) Annual basic cost (ABC)

The annual basic cost is the amount of money that users need to spend for their demand each year, which includes the annual investment cost (AIC), the annual maintenance cost (AMC), and the annual energy bills. It is calculated as:

$$ABC = CRF\sum_{k=1}^{l} IP_k C_k + AMC_k + \sum_{d=1}^{365}\sum_{t=1}^{24}(E_{dt,grid}C_{dt,e} + F_{dt}C_{dt,f}) \quad (5\text{-}8)$$

where IP_k is the installed power of equipment$_k$, C_k is the initial investment cost of each kind of equipment, l is the number of equipment, AMC_k presents the operation and maintenance costs, $C_{dt,e}$ and $C_{dt,f}$ are the hourly energy of electricity and natural gas, respectively. $E_{dt,grid}$ and F_{dt} are the hourly demands of the electricity bought from grid and the natural gas. CRF is the capital recovery factor.

2) Peak load cost (PLC)

Peak load cost refers to the fee paid by users according to the monthly maximum grid load. The peak load can be reduced through operating reasonably power generation system in DES, which can reflect the effect of the DES on grid stabilization through peak shaving.

$$PLC = \sum_{m=1}^{12} max\left(E_{m,grid}\right) \cdot Price_{ps} \quad (5\text{-}9)$$

where $E_{m,grid}$ is monthly maximum grid load (kW), $Price_{ps}$ is peak load price ($/kW).

3) CO_2 emission cost (CDEC)

The amount of carbon dioxide emissions (CDEs) from the DES can be determined using the emission conversion factors as follows [5]:

$$CDE = \sum_{t}^{8760} E_{grid}^{t} \cdot \mu_{CO_2,e} + \sum_{t}^{8760} F_{ICE}^{t} \cdot \mu_{CO_2,gas} \quad (5\text{-}10)$$

where $\mu_{CO_2,e}$ and $\mu_{CO_2,gas}$ are the emission conversion factors for electricity from the grid and natural gas, respectively. According to the investigation, the CO_2 emission conversion factors of electricity is 0.000462 t/kWh [7] and the CO_2 emission conversion factors of gas is 2.19 kg/m^3 [8] in Japan.

Carbon taxes is an effective way contributing to reduce the CO_2 emissions. Through carbon taxes, the environmental performance can be transformed into economic performance to evaluate the comprehensive performance of DES. The calculation of CDEC is as follows:

$$CDEC = CDE * Tax_{CO_2} \quad (5\text{-}11)$$

where Tax_{CO_2} is the carbon tax (\$/kg). In Japan, the carbon tax is 20.76 \$/t in 2020 [9]. (The U.S. dollar exchange rate against RMB is 1:7).

5.2.3 Configuration optimization model

1) Objective function

The economic performance of the DES with different combinations of energy supply systems will be widely divergent. Taking the minimum costs as the objective function, the optimal configuration of the ICE and the BESS can be obtained based on the PV penetration. In order to compare the effects of peak shaving and CO_2 emission reduction on configuration in DES, three different costs calculation methods are proposed as the objective function, as shown in the following formula:

The cost consists of annual basic cost only:

$$F_1 = \min(ABC) \tag{5-12}$$

The costs consist of annual basic cost and peak load cost:

$$F_2 = \min(ABC + PLC) \tag{5-13}$$

The total costs consist of annual basic cost, peak load cost, as well as CO_2 emission cost:

$$F_3 = \min(ABC + PLC + CDEC) \tag{5-14}$$

2) Constraint functions

i. Power balance constraints

The power demands of load point should be satisfied by the power output of systems in DES or the power supply of utility grid.

$$P_L^t = P_{PV}^t + P_{GE}^t + P_{ESS,dch}^t - P_{ESS,ch}^t + P_{grid}^t \tag{5-15}$$

where P_{grid}^t is the imported power from the utility grid (kWh), P_L^t is the power demands at t-time (kWh).

ii. Constraints of battery storage system

State of charge (SOC) limits:

$$SOC_{min} \leq SOC^t \leq SOC_{max} \tag{5-16}$$

$$SOC_{min} = (1 - d) \times SOC_{max} \tag{5-17}$$

where d is the depth of the discharge.

iii. Power output constraints

There are output power limits of the PV, ICE and BESS at time which should be able to operate within their specific minimum and maximum. The output power of each generation source has minimum and maximum limits as expressed in Equation (5-18).

$$\begin{cases} P_{PV}^{min} \le P_{PV}^{t} \le P_{PV}^{max} \\ P_{GE}^{min} \le P_{GE}^{t} \le P_{GE}^{max} \\ P_{BESS,ch}^{min} \le P_{BESS,ch}^{t} \le P_{BESS,ch}^{max} \\ P_{BESS,dch}^{min} \le P_{BESS,dch}^{t} \le P_{BESS,dch}^{max} \end{cases} \quad (5\text{-}18)$$

3) Optimization logic

The optimization logic diagram is shown in Fig.5-3.

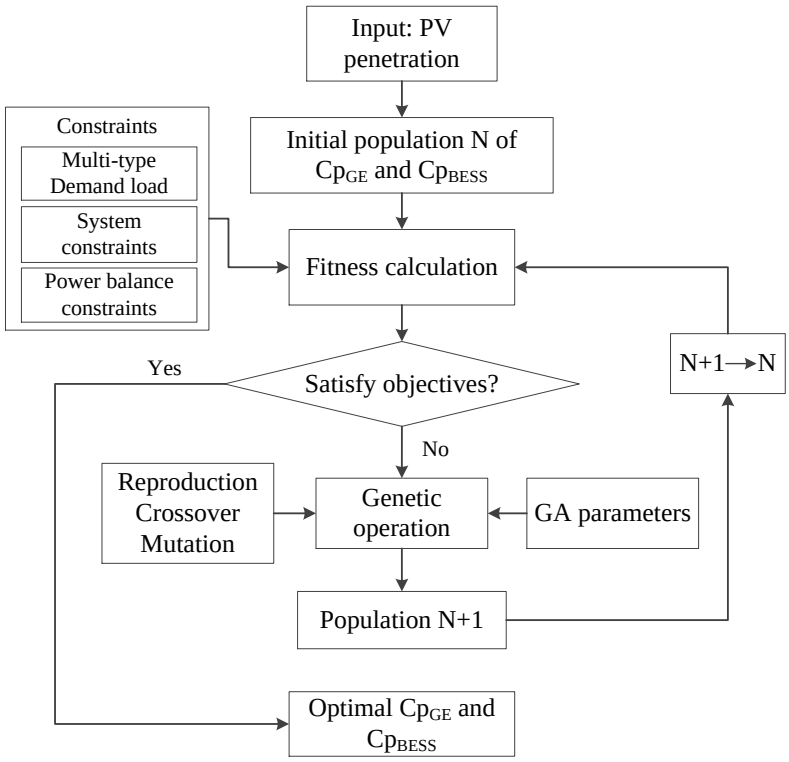

Fig.5-3 Logical scheme optimizing the configuration of the equipment in the DES

5.3 Research object and PV penetration prediction

The research object selects five types of buildings in the Smart Community in Higashida area, Japan (included two offices, two residentials, two hospitals, two museums, and two shopping malls) as shown in Fig.5-4. According to the actual electricity load data of these 10 buildings, the daily average curves of demand load in each month is shown in Fig.5-5. Due to the limitation of the rooftop area of the region, the power generation of PV system can be 3MW at present, and the daily average curves of PV generation in each month is demonstrated in Fig. 5-6. It can be calculated that the penetration of PV is 5.3% of the total demand load.

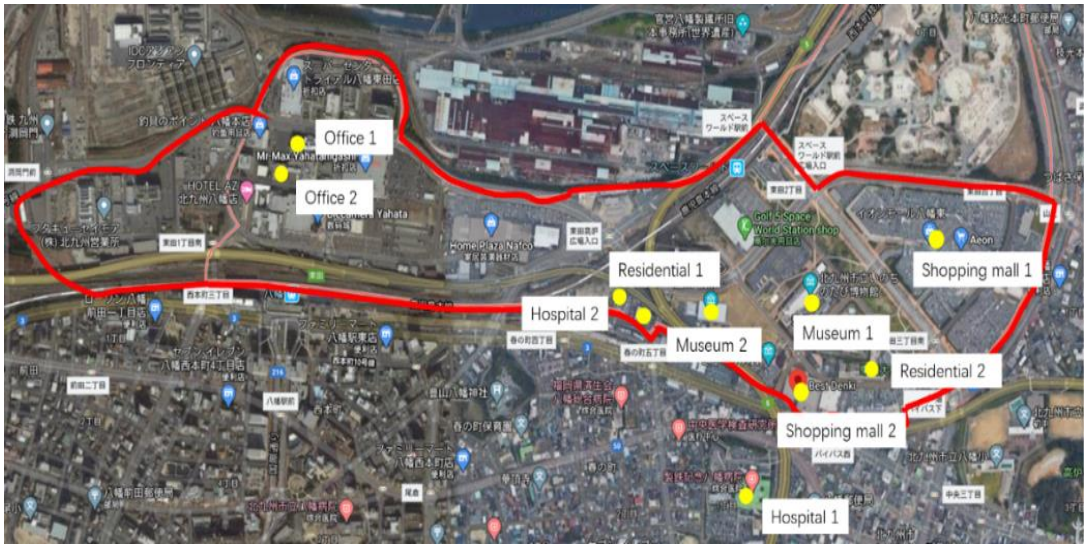

Fig.5-4 The Higashida District, Yahata, Kitakyushu City.

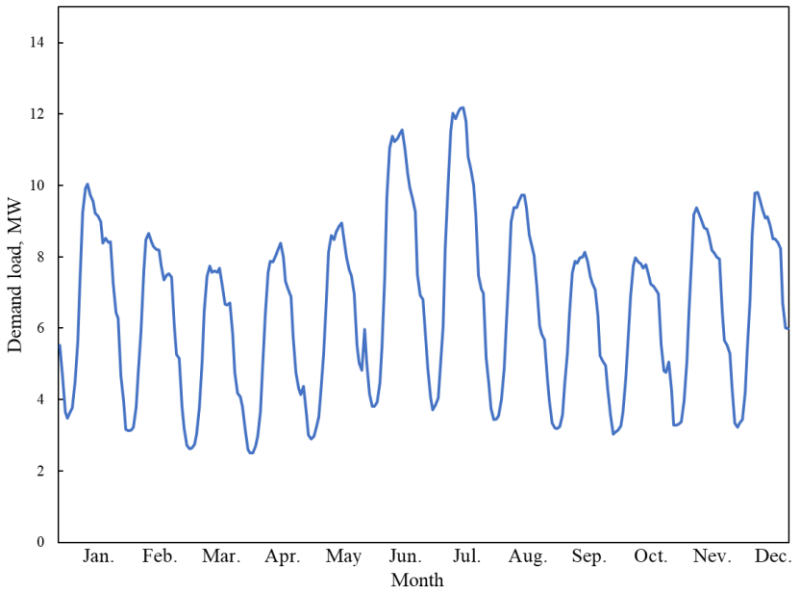

Fig.5-5 Daily average curves of demand load in each month.

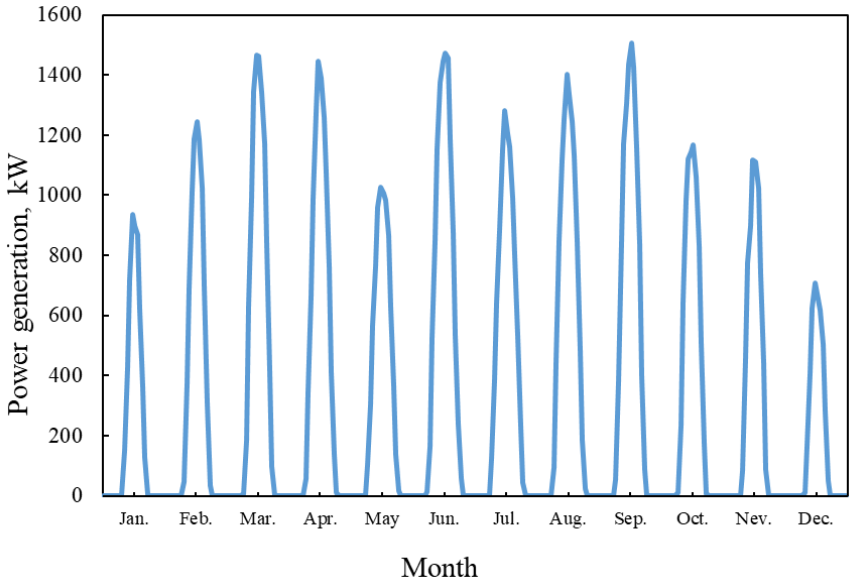

Fig.5-6 Daily average curves of PV generation in each month.

Smart Community of Higashida is committed to build an eco-city where supply clear, reliable power with low cost. The renewable energy resources are one of the contributions for establishment an independent and efficient energy system, which can improve the independence and reduce the carbon emission of the energy supply for this region. The publication of a 2050 Renewable Energy Vision indicated that Japan could supply 67% of its electricity needs from renewables by 2050 [10]. Therefore, we assume that there are more PV plant introducing to the DES of the research object in the future, the PV penetration can be increased. In this research, the PV penetration is changing from 0% to 50% to analyze optimal combinations of the DES.

By subtracting PV production with different penetration, Fig.5-7 presents the demand load duration curve for different penetration PV capacities. High PV penetration will cause the overproduction. Fig.5-8 demonstrates daily average curves of load in each month after introducing with different penetration PV capacities, respectively. PV generation will reduce the peak load at daytime and significantly reshape the load curve.

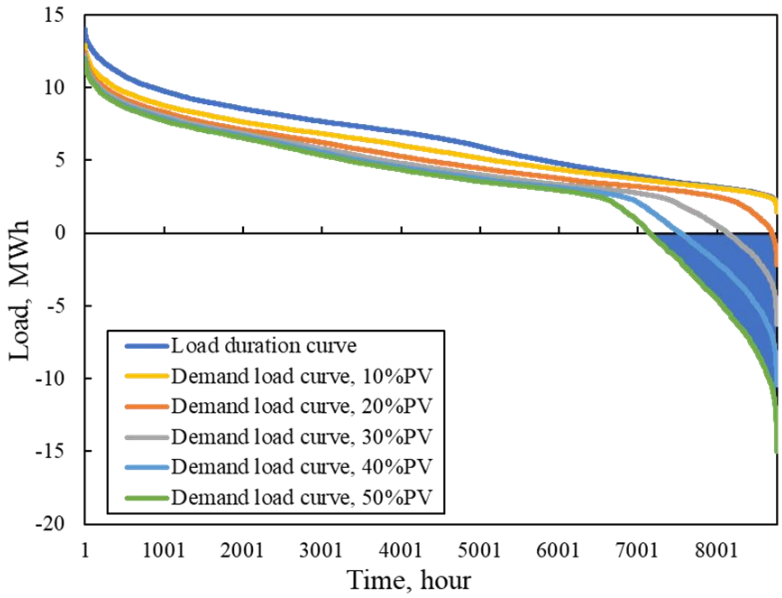

Fig. 5-7 Demand load duration curve with different penetration PV capacities.

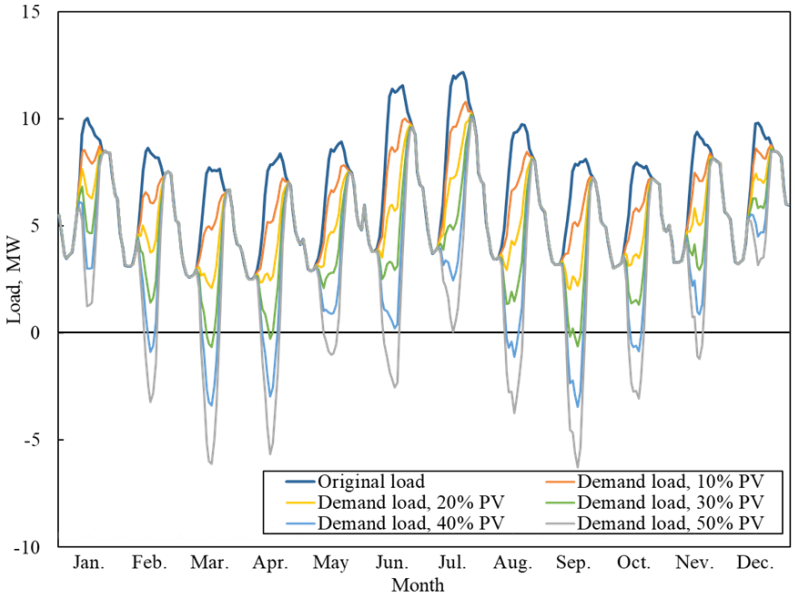

Fig.5-8 Daily average curves of load in each month with 0-50% PV generation.

Fig.5-9 demonstrated the peak shaving and CO_2 emission reduction with the increase of the PV penetration. Due to the inherent intermittent and uncertainty of the PV, the peak shaving effect is not obvious at the high share of the PV penetration. Moreover, when the PV penetration rate continues to increase (more than 20%), it may occur overproduction and aggravate the grid fluctuation which will be a challenging problem to the reliability of the public grid. Load shifting through BESS could not only improve the utilization rate of the PV systems, but also balance the fluctuation, which is essential for both supply-side and demand-side.

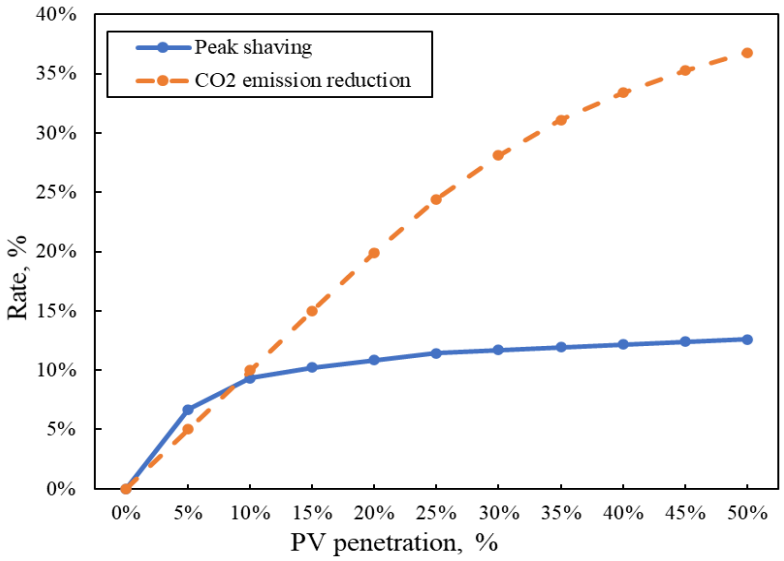

Fig.5-9 The peak shaving and CO_2 emission reduction with the increase of PV penetration.

In this paper, a DES is developed through the combination of the PV, BESS and ICE to solve the above problem. It can not only improve the self-consumption of the PV, but also play the role of peak shaving and stabilize the fluctuation of power grid.

5.4 Optimal design and comparison

In this section, we assume that the PV penetration changes from 0% to 50% and it is divided into 11 scenarios with increasing by 5%. The surplus PV production cannot be sold out to the grid in this case. The results of the different scenarios are obtained and compared. The technical specifications and cost data details for each equipment of the proposed DES systems are presented in Table 5-2 in Chapter 5.

5.4.1 The results under objective function of annual basic cost

The optimal configuration of the ICE and the BESS with increasing PV penetration and their costs under F1 (ABC only) are presented in Fig.5-10.

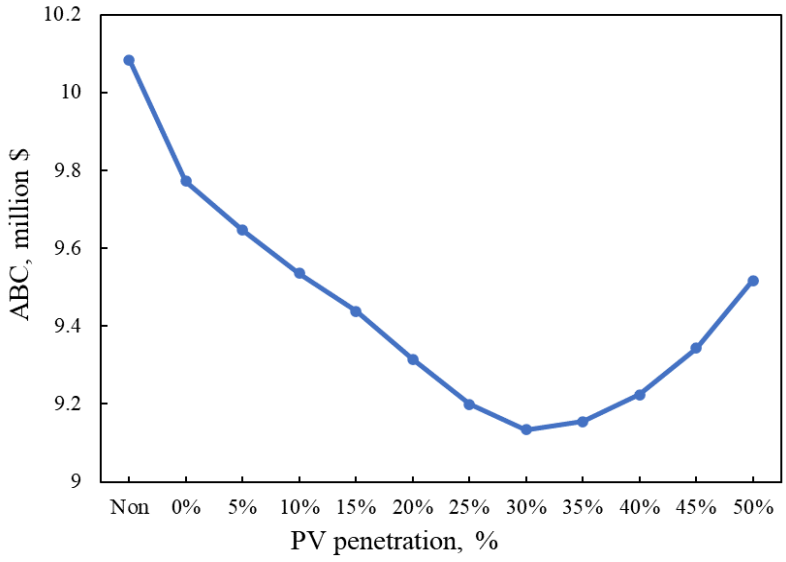

a)

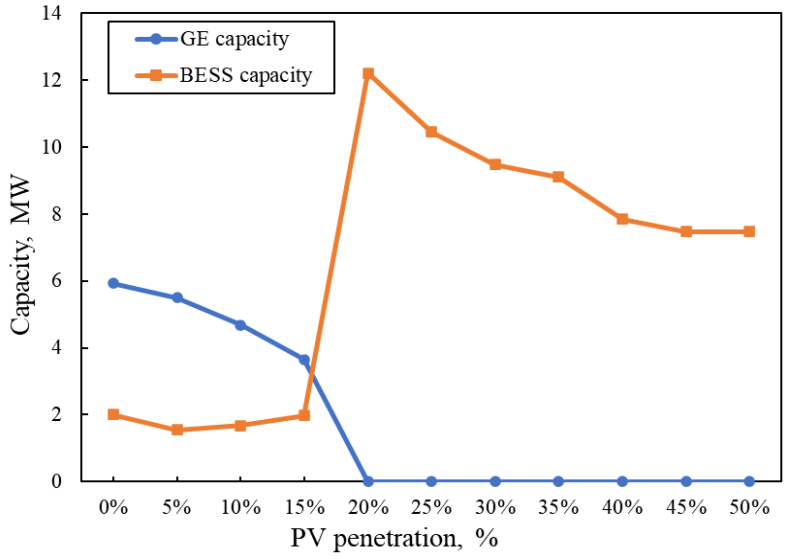

b)

Fig.5-10 The simulation results of F1: a) annual basic cost changes with increase of PV penetration; b) optimal configuration changes of the ICE and the BESS with increasing PV penetration.

(Note: The U.S. dollar exchange rate against RMB is 1:7)

With the increase of the PV penetration, the annual basic cost is decreased initially but then raised, illustrated in Fig.5-10a). Obviously, when PV penetration is 30%, the ABC is the least. Fig.5-10b) shows the optimal configuration of the ICE and the BESS under different PV penetration scenarios. Under the low share of PV penetration scenarios (0 to 20%), the optimal installed capacity of ICE gradually decreases with the rising of PV output, and then it sharply drops to 0 at PV penetration of 20%. At the same time, the optimal capacity of BESS spurts suddenly, but then diminishes with the growth of PV penetration.

From the proportion of various costs in ABC under the different PV penetration scenarios as described in Fig.5-11, we can see that at lower PV penetration, the energy consumption cost dominates overall cost, and the proportion of annualized investment cost gradually increases with the rising of the PV penetration. When PV penetration is high, the increase of the DES investment cannot bring ideal energy-saving benefits, which cause the waste due to excessive installed capacity of equipment.

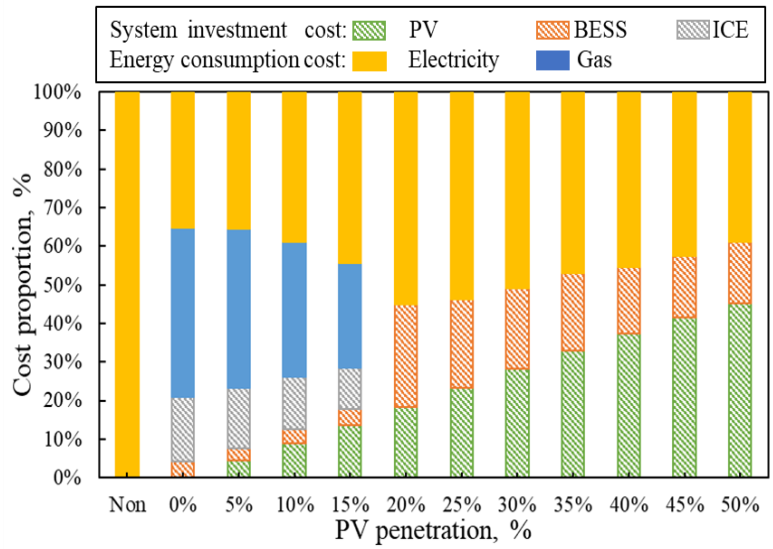

Fig.5-11 Cost proportion changes with the increase of the PV penetration under the optimal configuration results of F1.

The optimization results of the configuration are depended on the economic performance of the ICE and BESS. Fig.5-12 shows the unit capacity profit change of the ICE and BESS with the increase of the PV penetration. The economic performance of the PV is better than that of the ICE. When the PV penetration increases, the operating hours of the ICE decrease and the unit capacity profit of the ICE becomes worse. When the PV penetration reaches 20%, the ICE takes no economic advantage. Therefore, the optimal installed capacity of the ICE decreases with the increase of the PV penetration and finally becomes 0. As the installed capacity of the ICE gradually decreases, the BESS needs to replace it as the main energy supply system at peak time. At the same time, overproduction of the PV system had occurred shown as Fig.5-13. Therefore, the economic benefit of BESS improves due to recovering surplus PV production. As a result, when the PV penetration is 20%, the installed capacity of the BESS sharply increases.

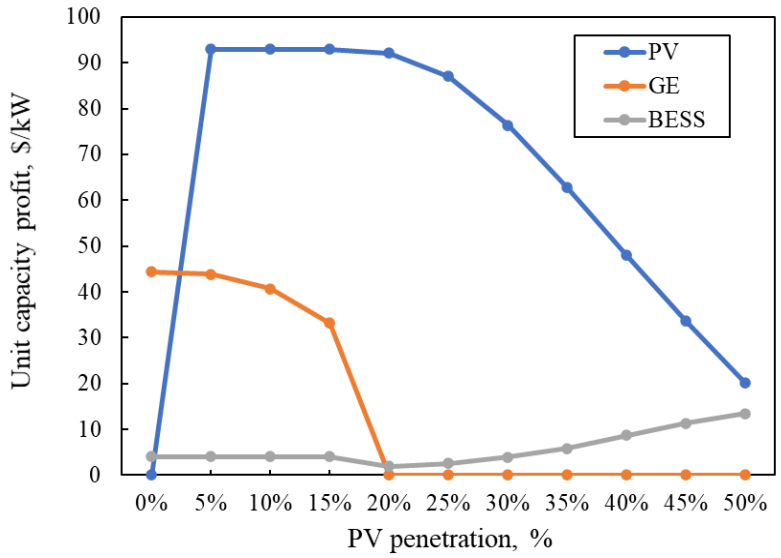

Fig.5-12 Unit capacity profit of PV, ICE and BESS under the optimal configuration results of F1.

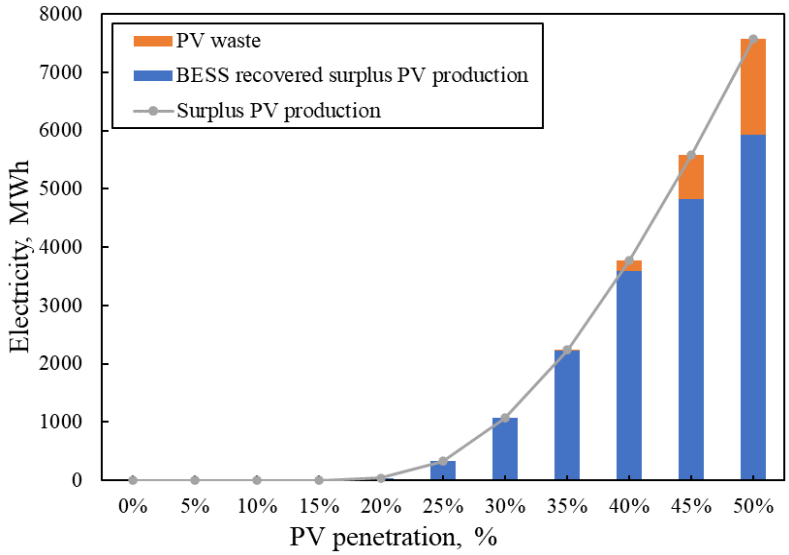

Fig.5-13 BESS recovered surplus PV production and PV waste under the optimal configuration results of F1.

However, when the penetration of PV continues to raise, the increase of surplus PV production leads to the decline of PV benefits. Although the BESS can improve its own profit by storing the surplus PV production, the amount of the increased profit cannot make up for the loss of PV benefit. Moreover, due to the increase of PV penetration, the average cost of electricity purchased from grid decreases (as presented in Fig.5-14), which reduces the profit space of BESS, resulting in the decrease of installed capacity of BESS.

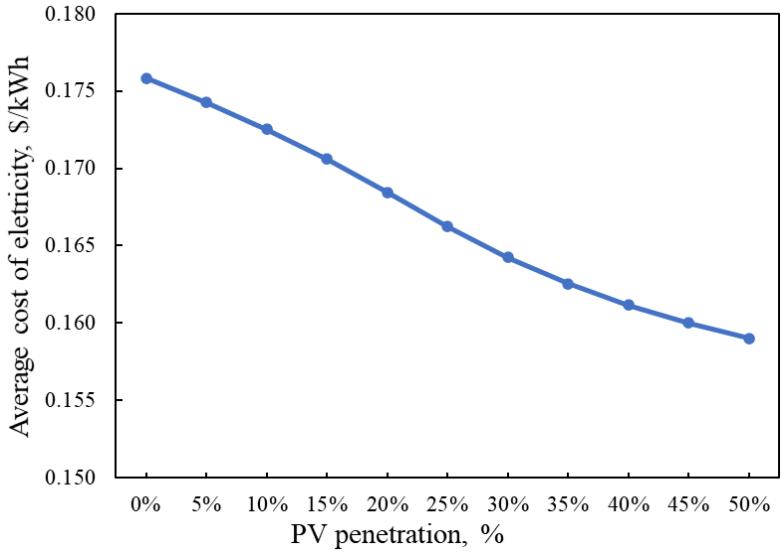

Fig.5-14 The average cost of electricity with increase of PV penetration.

Since the peak load cost and CO_2 emission cost are not included in the objective function F1, the optimal configuration results of the ICE and the BESS are only determined by their own operation benefits. The peak shaving rate and CO_2 emission reduction rate of different PV penetration scenarios are displayed in Fig.5-15.

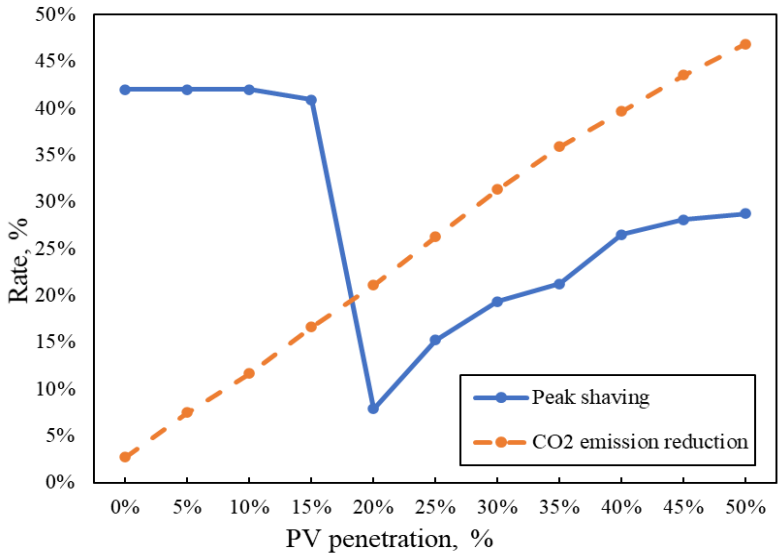

Fig.5-15 Peak shaving rate and CO2 emission reduction rate of different PV penetration scenarios under the optimal configuration results of F1.

The introduction of the DES can realize peak shaving and CO_2 emission reduction. When the PV penetration is less than 20%, the peak load is greatly reduced due to the power generation of ICE, which is above 40%. When PV penetration is more than 20%, ICE is no longer installed, and peak shaving is only carried out by PV and BESS in the daytime. However, the power load increases at night because of the 'peak discharge and low valley charging' operation mode of BESS, which led to a rapidly falling in peak shaving rate at the 20% PV penetration. Then, with the continuous

increase of PV penetration, the output of PV power increased in peak time. There is more overproduction of the PV system, which can be charged to BESS instead of importing power from the grid at night. Therefore, the peak shaving rate increased. The peak shaving and CO_2 emission is 19% and 31% respectively under the optimal combination of the DES which PV penetration is 30%.

5.4.2 The results under objective function of annual basic cost and peak load cost

The optimal configurations of each scenario and their costs under F2 (ABC+PLC) are demonstrated in Fig.5-16. It can be seen that the total cost is least at 30% of PV penetration as shown in Fig.5-16 a).

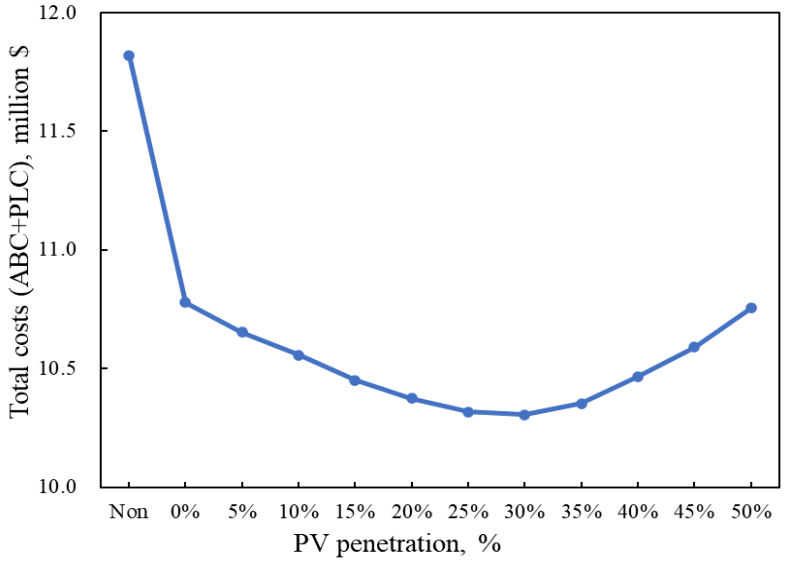

a)

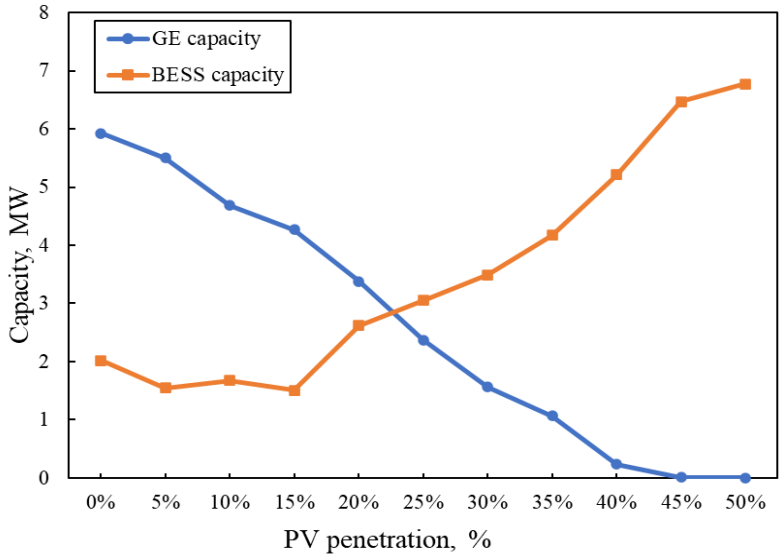

b)

Fig.5-16 The simulation results of F1: a) optimal configuration changes of the ICE and the BESS with increasing PV penetration; b) annual basic cost changes with increase of PV

penetration.

Fig.5-17 and 5-18 display the proportions of various costs with the increase of the PV penetration and the cost-saving change in ABC and PLC. It can be seen that the investment cost of the system accounts for a large proportion at higher penetration of the PV, and the energy consumption cost decreases gradually due to the expansion of the PV system. The peak power cost remains almost unchanged when the PV penetration is low, but when the PV penetration is more than 20% it slightly rises. Fig.5-16 b) shows the optimal configurations of the ICE and the BESS under different PV penetration. The optimal installed capacity of the ICE gradually decreases with the increase of the PV penetration. The optimal capacity of the BESS does not change much at the low share of the PV penetration, and then increases when the PV penetration raises more than 20%.

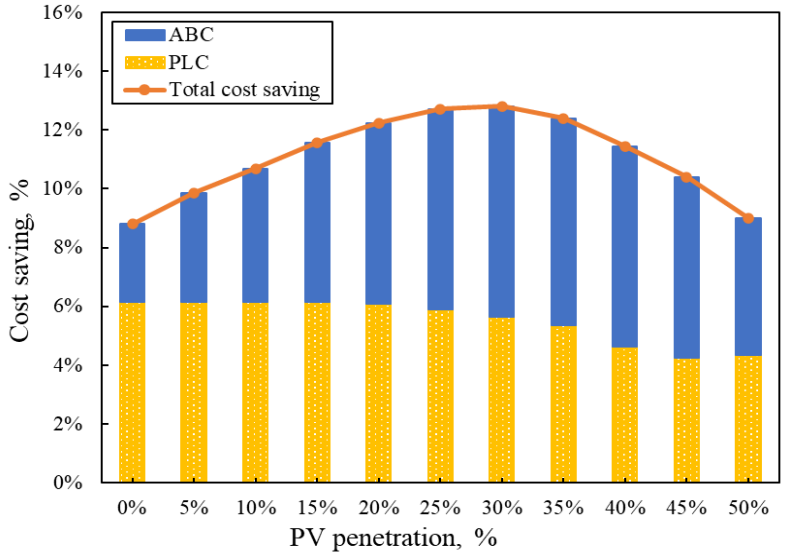

Fig.5-17 The cost saving changes with the increase of the PV penetration under the optimal configuration results of F2.

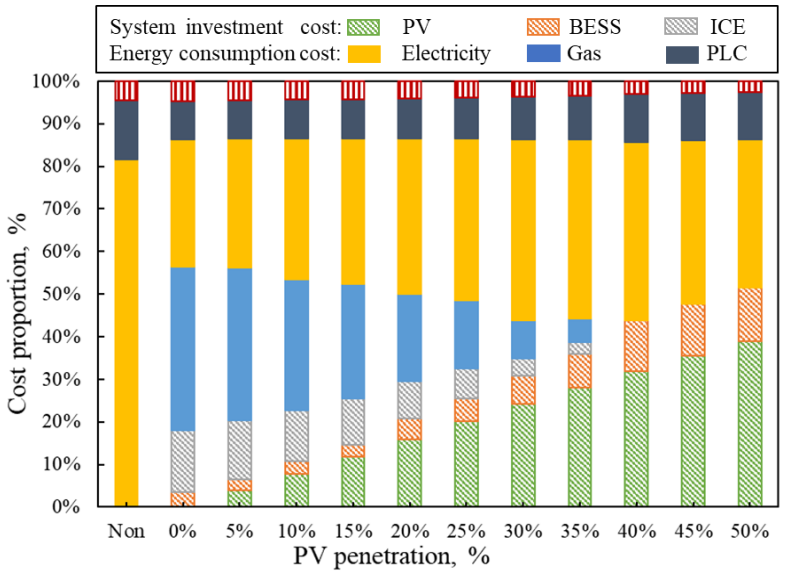

Fig.5-18 Cost proportion changes with the increase of the PV penetration under the

optimal configuration results of F2.

Because the contribution of ICE to peak shaving is greater, the economic advantage of ICE is improved when the peak load cost is added to the objective function (F2) of optimization simulation. Therefore, the optimal installed capacity of ICE does not decrease sharply to 0 at the PV penetration of 20% as the results under F1. The peak shaving rate and CO_2 emission reduction rate of different PV penetration scenarios are carried out in Fig.5-19. When the PV penetration is less than 20%, the PV, ICE and BESS cooperate to cover the demand load at the peak time. With the increase of PV output, the output of ICE decreases correspondingly, so the peak load cost is almost the same and the installed capacity of BESS changes little. However, as shown in Fig.5-20, when the penetration is greater than 20%, PV system produce surplus power. At the same time, due to characteristics of PV power generation, it is unable to cover the amount of electricity caused by the configuration decrease of the ICE. In order to provide the power output reduced by the capacity decline of the ICE and store the excess power from the PV system, the installed capacity of the BESS is increased.

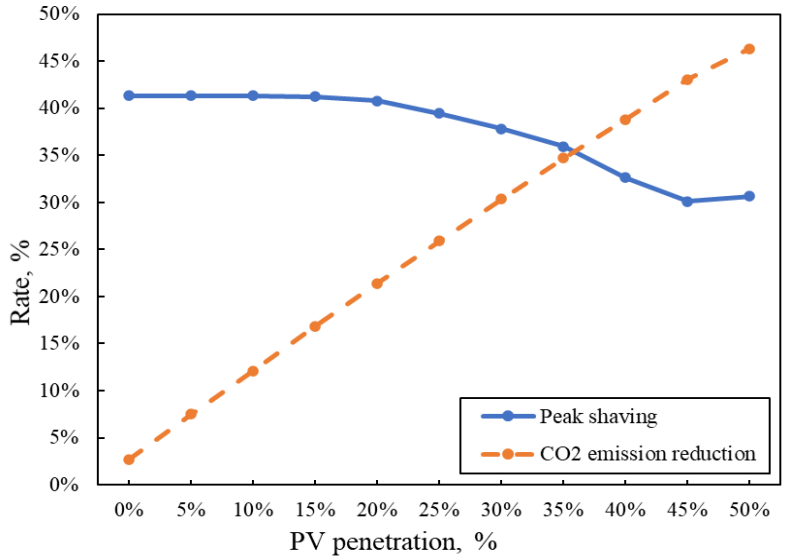

Fig.5-19 Peak shaving rate and CO2 emission reduction rate of different PV penetration scenarios under the optimal configuration results of F2.

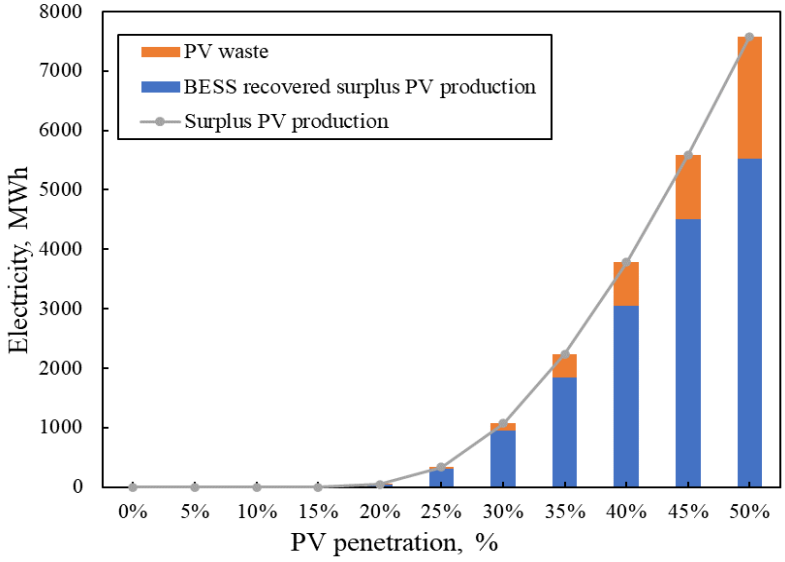

Fig.5-20 BESS recovered surplus PV production and PV waste under the optimal configuration results of F2.

5.4.3 The results under objective function of annual basic cost, peak load cost and CO_2 emission cost

The optimal configurations of each scenario and their costs under F3 (ABC+PLC+CDEC) are presented in Fig.5-21. With the increase of PV penetration, the total cost still decreases first and then increases, as shown in Fig. 5-21 a). The total cost is least when PV penetration is 30%, which is the same as the results of F1 and F2. Fig. 5-21 b) demonstrated the optimal configurations of the ICE and the BESS under different PV penetration when the objective function is F3.

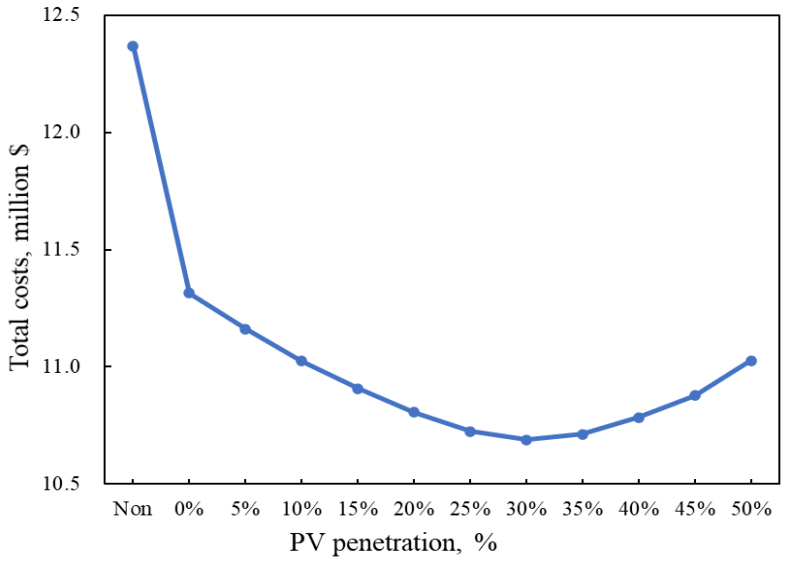

a)

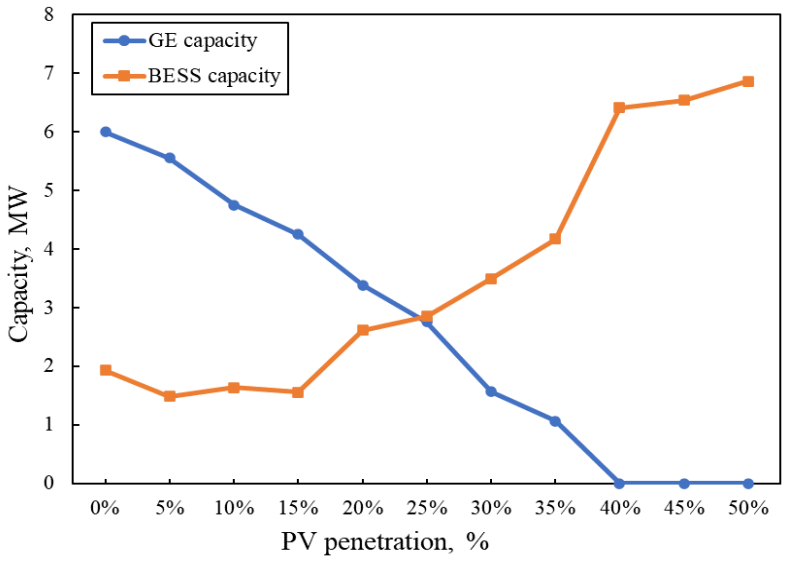

b)

Fig.5-21 The simulation results of F3: a) Change of total costs (ABC+PLC+CDEC) with increase of PV penetration. b) optimal configurations of the ICE and the BESS with

increasing PV penetration.

Fig.5-22 and 5-23 show the proportions of various costs with the increase of PV penetration and the cost-saving change in ABC, PLC and CEDC.

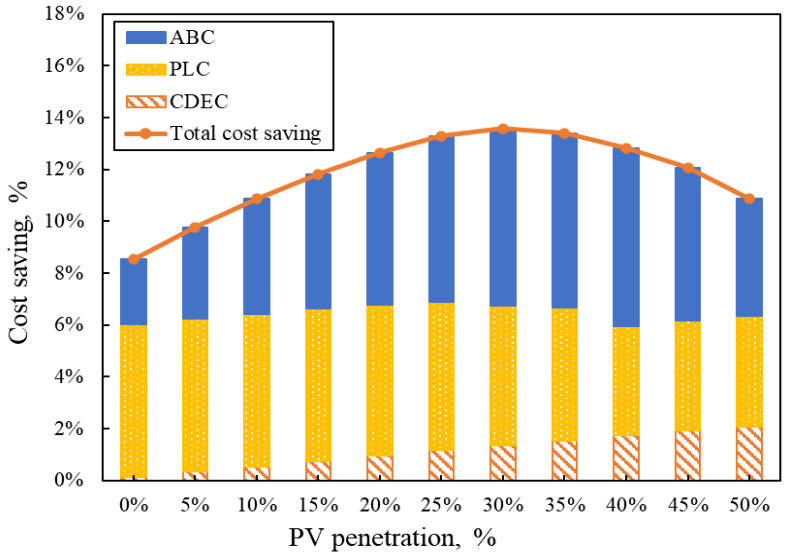

Fig.5-22 The cost saving change with the increase of PV penetration under the optimal configuration results of F3.

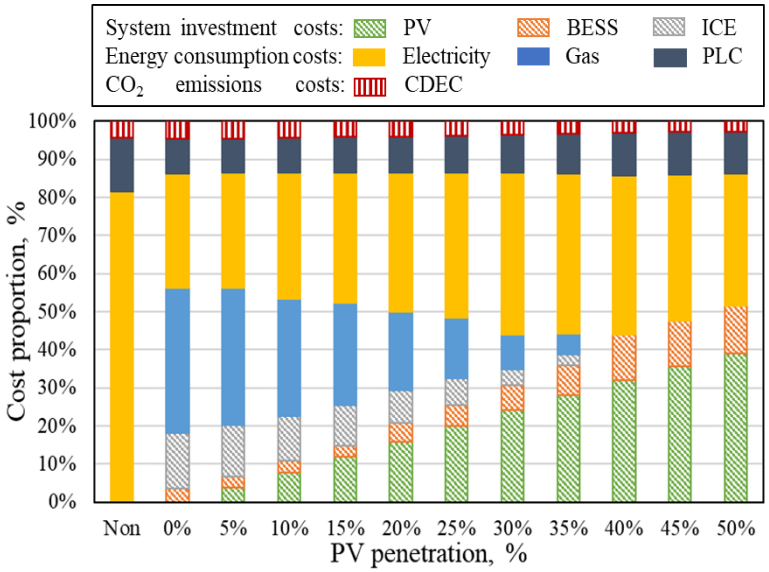

Fig.5-23 Cost proportion changes with the increase of PV penetration under the optimal configuration results of F3.

The expansion of PV plays an important role in the reduction of the CO_2 emission. However, the current carbon tax in Japan is not high enough to account large proportion of total cost. The impact of carbon tax on improving PV penetration is not obviously. The change trends of optimal configurations under F3 are basically the same as that under F2. Compared with the results of F2, the optimal installed capacity of ICE in each scenario is slightly declined. This is because the CO_2 emission of power generated by ICE is larger than the power produced by PV system, thus the output

of ICE is suppressed. And the reduction of ICE promotes the increase of BESS. In addition, BESS can achieve the purpose of reducing CO_2 emissions by storing overproduction of PV system and improve its economic advantages, so its installed capacity of BESS in each scenario is increased. Fig.5-24 shows BESS recovered surplus PV production and PV waste under the optimal configuration results of F3.

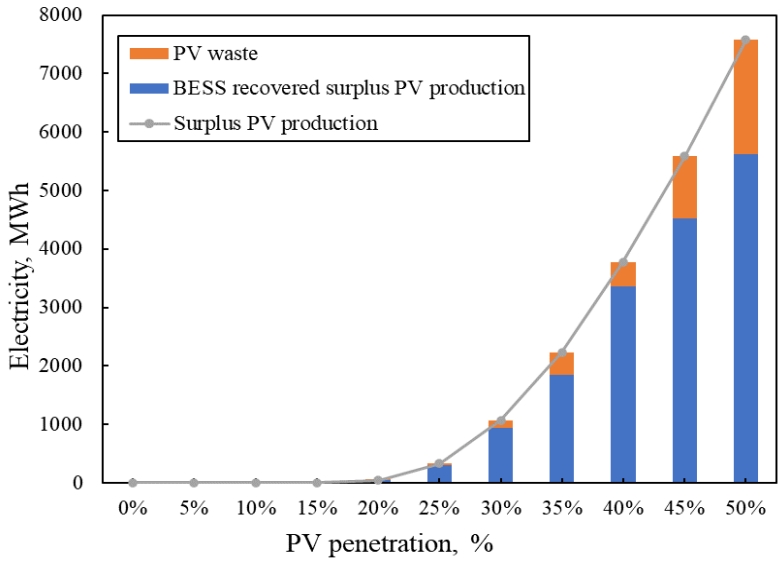

Fig.5-24 BESS recovered surplus PV production and PV waste under the optimal configuration results of F3

The peak shaving rate and CO_2 emission reduction rate of different PV penetration scenarios are calculated in Fig.5-25.

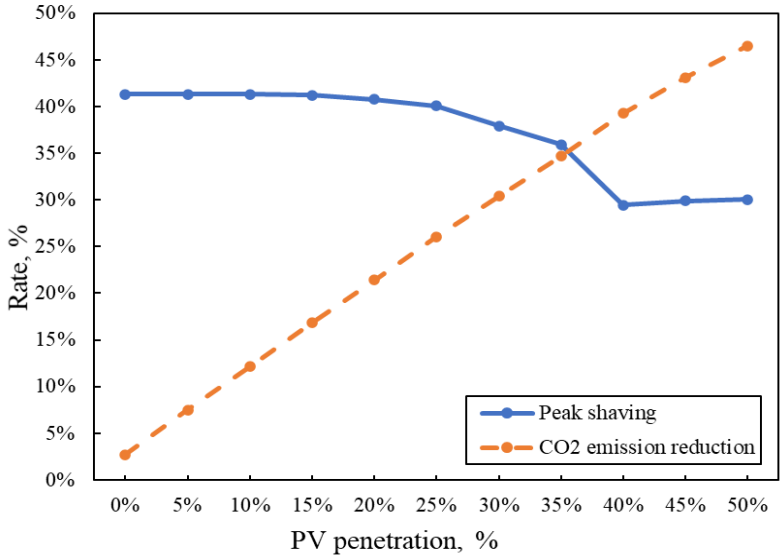

Fig.5-25 Peak shaving rate and CO_2 emission reduction rate of different PV penetration scenarios under the optimal configuration results of F3.

5.4.4 The results comparison under three objective functions

In summary, the change trend of F2 (ABC + PLC) and F3 (ABC + PLC + CDEC) is consistent with that of F1 and similarly attain the minimum when the PV penetration is 30%, as shown in

Fig.5-26. But the optimal configuration of each equipment in the DES is different under different objective functions. Fig.5-27 shows the optimal configuration of the ICE and the BESS at different PV penetration scenarios under three objective functions. It can be seen that the optimal installed capacity of ICE under F2 and F3 changes similarly, and gradually decreases with the increase of PV penetration. Because the contribution of ICE to peak shaving is greater, the economic advantage of ICE is improved when the peak load cost is added to the objective function of optimization simulation. Therefore, the optimal installed capacity of ICE does not decrease sharply to 0 at the PV penetration of 20% as the results under F1. The optimal capacity of BESS does not change much at the low share of PV penetration, but then gradually grows with the increase of PV penetration. There are two reasons for the increase of BESS capacity: 1) the decrease of ICE installed capacity leads to the reduction of peak shaving; 2) the increase of PV overproduction. In order to provide the power output reduced by the capacity decline of ICE and store the excess power from PV system, the installed capacity of BESS is increased. Compared with the results of F2, the optimal installed capacities of ICE in high PV penetration scenarios under F3 are slightly declined. This is because the CO_2 emission of power generated by ICE is larger than the power produced by PV system, thus the output of ICE is suppressed. And the reduction of ICE promotes the increase of BESS. In addition, BESS can achieve the purpose of reducing CO_2 emissions by storing overproduction of PV system and improve its economic advantages, so its installed capacity of BESS in each scenario is increased.

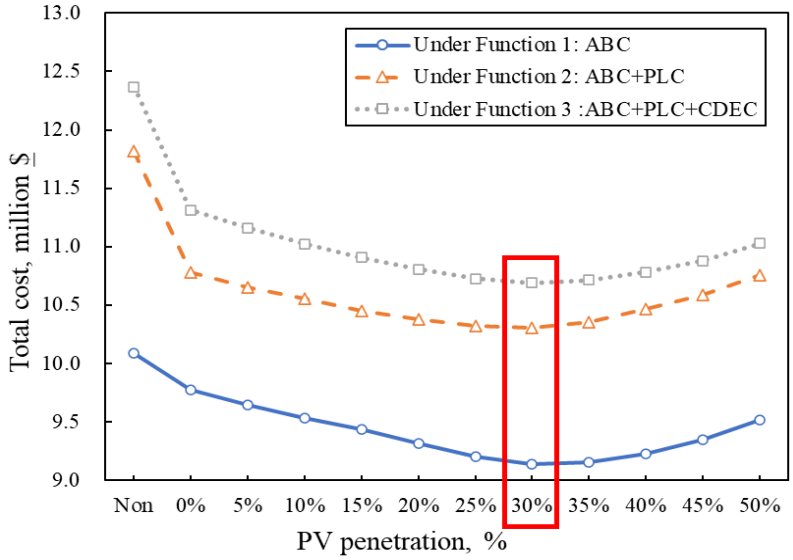

Fig.5-26 The change of three objective functions with the different PV penetration.

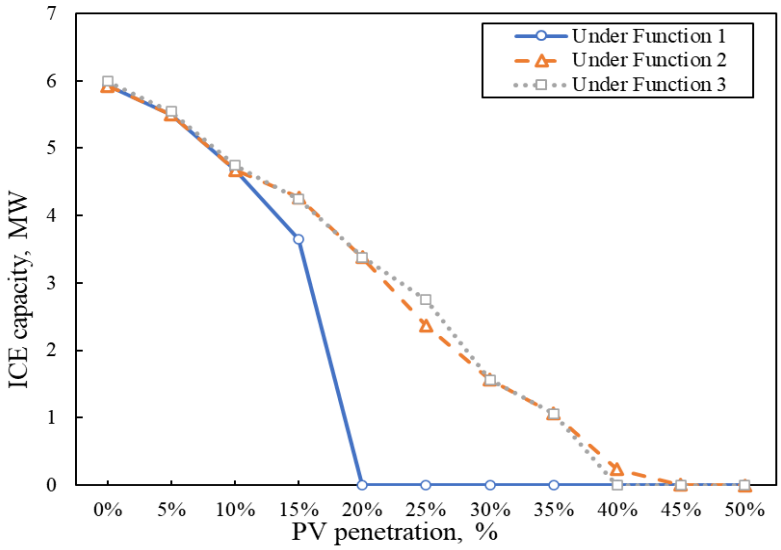

a)

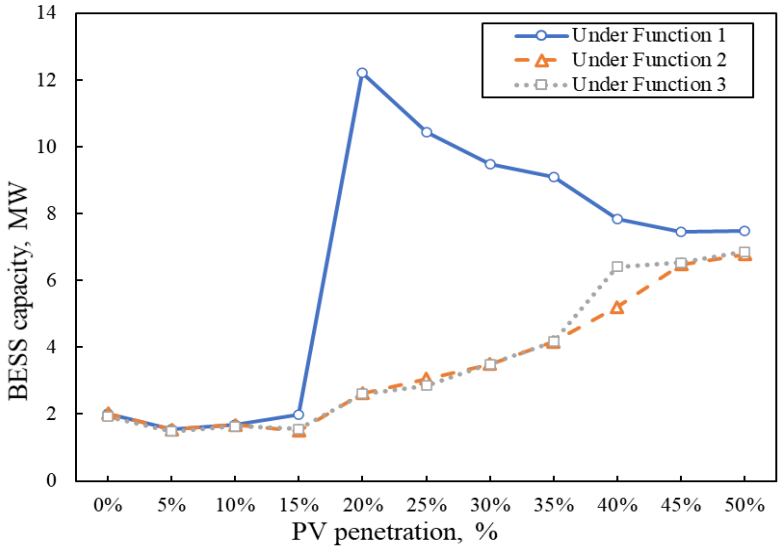

b)

Fig.5-27 The optimal configuration of the ICE and the BESS at different PV penetration scenarios under three objective functions: a) ICE capacity change; b) BESS capacity change.

Three different objective functions set in this chapter reflect the effect of three evaluation aspects of economic, grid stabilization and environment performance on the configuration of the equipment in the DES. The changes and comparisons of the evaluation criteria (ABC, PLC and CEDC) under the optimal configuration of each scenario are shown in Fig.5-28. The F1 only includes annual basic cost, so the ABC under F1 is the smallest compared with the other two objective functions, as shown in Fig. 5-28 a). The Fig.5-28 b) demonstrated that when the PV penetration is less than 20%, the PV, ICE and BESS cooperate to supply power at the peak period. The peak load cost is almost the same under three objective functions and reduces with the growth of the PV penetration. It indicates that the introduction of DES can reduce the peak load. However, the peak load cost under F1 is much higher than that under F2 and F3 when the PV penetration is higher than 20%. It is because that there is no limitation of peak load cost in F1. And the capacity of the BESS is increased sharply at high PV penetration scenarios. Therefore, the BESS can charge the power from the grid at night as much as possible to get the maximum economic benefit, which leads to the increase of peak load at

night. Thus, the peak load cost is high under F1. After considering the peak load cost, the optimal installed capacity of the ICE of each scenario increases. It proves that the effect of ICE on peak shaving is better. However, the CDEC under F2 and F3 is a little bit higher than that under F1 at high PV penetration scenarios as Fig.5-28 c) displayed. Because the CO_2 emission of the ICE is larger than that of BESS which charges power from the surplus PV generation. In addition, the current CDEC accounts for a small proportion of the total cost, so there is little difference between the simulation results of F2 and F3. In the future, the carbon tax will continue to increase to achieve the goal of emission reduction more effectively, which will greatly affect the configuration of the equipment in the DES.

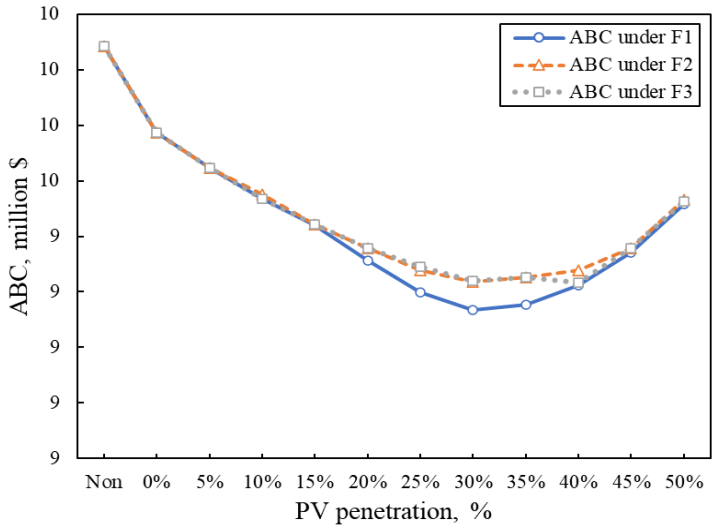

a)

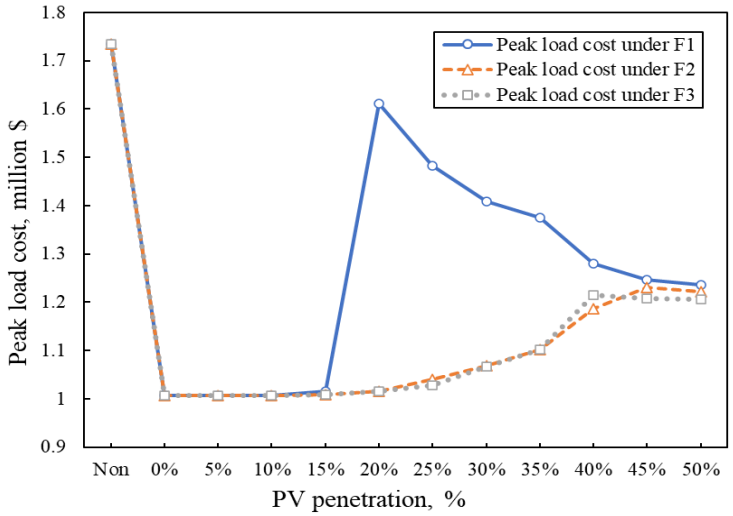

b)

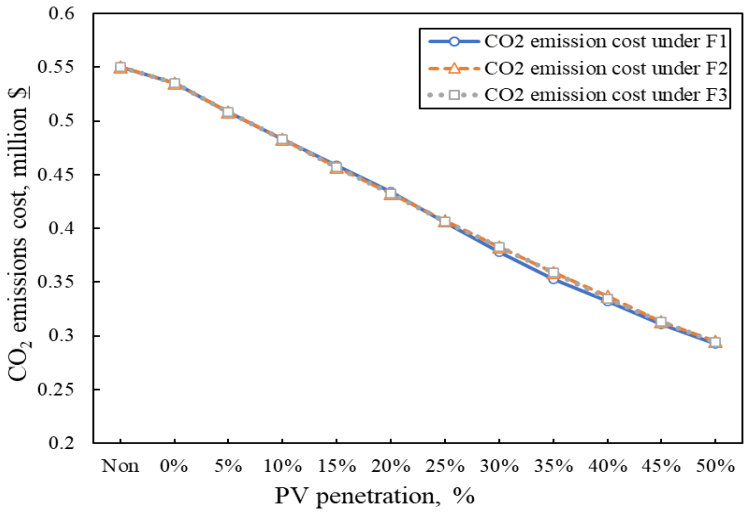

c)

Fig.5-28 The comparison of evaluation criteria with the different PV penetration scenarios under three objective functions: a) ABC; b) PLC; c) CDEC.

Table 5-1 presented the optimal configurations of the equipment in the DESs under the three objective functions and their performance comparison (Here, we define that the DESs with the optimal combinations under F1, F2, and F3 are the abbreviated to "DES_1", " DES_2", and "DES_3", respectively).

Table 5-1 The optimal configurations of units in the DESs under the three objective functions and their performance comparison.

DESs		DES_1	DES_2	DES_3
Configuration	PV penetration	30%	30%	30%
	ICE	0 MW	1.573 MW	1.565 MW
	BESS	9.479 MW	3.488 MW	3.491 MW
Cost saving	ABC saving	7.677%	6.837%	6.839%
	PLC saving	2.634%	5.392%	5.390%
	CDEC saving	1.394%	1.349%	1.350%
	Total cost saving	11.706%	13.578%	13.579%
Peak shaving		19.372%	37.848%	37.945%
CO_2 emission reduction		31.346%	30.365%	30.380%

It can be seen that the total cost saving of the DES_3 is the most, which improves 1.87% compared with the DES_1. The peak shaving performance of DES_3 is the most significant, it reduces 37.945% of the peak load. But the CO_2 emission reduction of DES_1 is most, it declines 31.346% of the carbon emission. The results demonstrated that when the peak shaving capacity and emission reduction effect are converted into economic benefits, the peak load price and carbon tax will have a greater impact. The comprehensive evaluation criteria should be taken into account when determines the configuration of DES. The competitiveness of the DES depends mainly on the ability to balance peak shaving and carbon emissions reduction with economic benefits as well as maximizing the overall performance.

5.5 Sensitivity analysis

5.5.1 Peak load price change

One of the main advantages of DES is that it can shave peak demand without affecting the energy consumption behavior of customers. The peak load cost has a great impact on the configuration optimization of DES. By changing ±20% of the peak load price, its impact on DES configuration is explored in Fig.5-29. Fig.5-29 a) shows that when the peak load price changes, the total costs of DES are always optimal at 30% of PV penetration. But the installed capacity of the ICE increase at high PV penetration with the rising of the peak load price, the BESS is on the contrary.

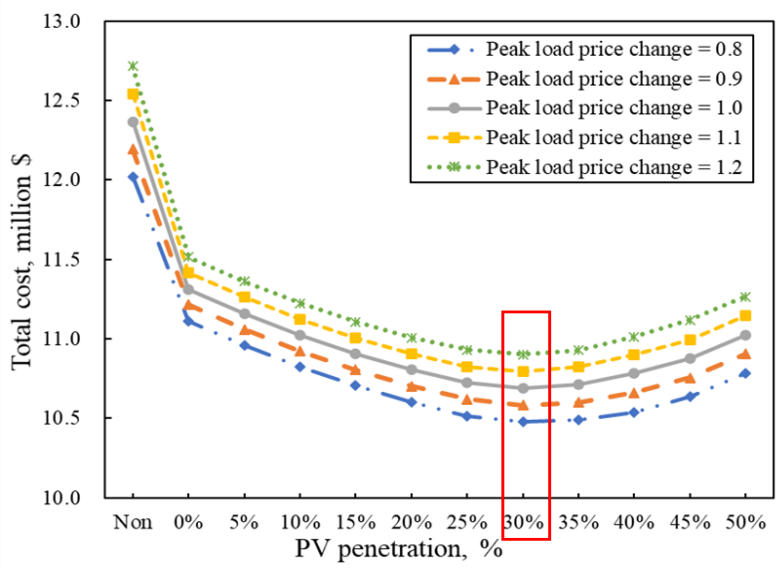

a)

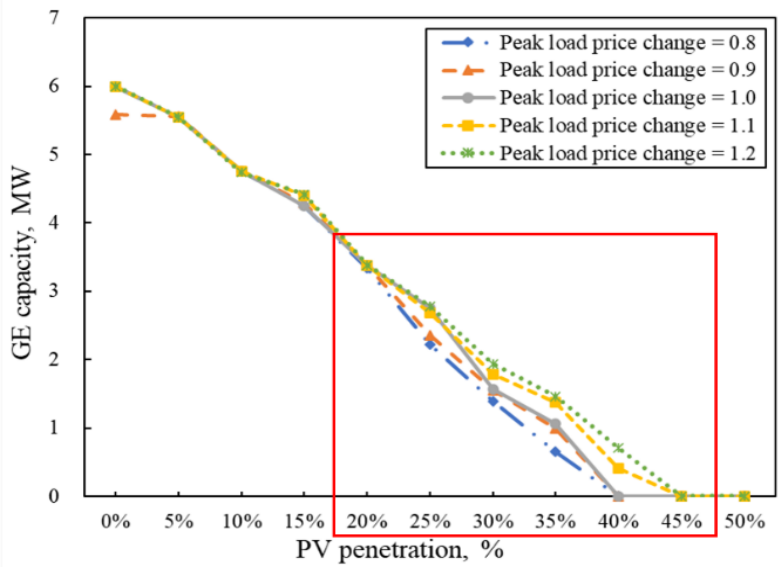

b)

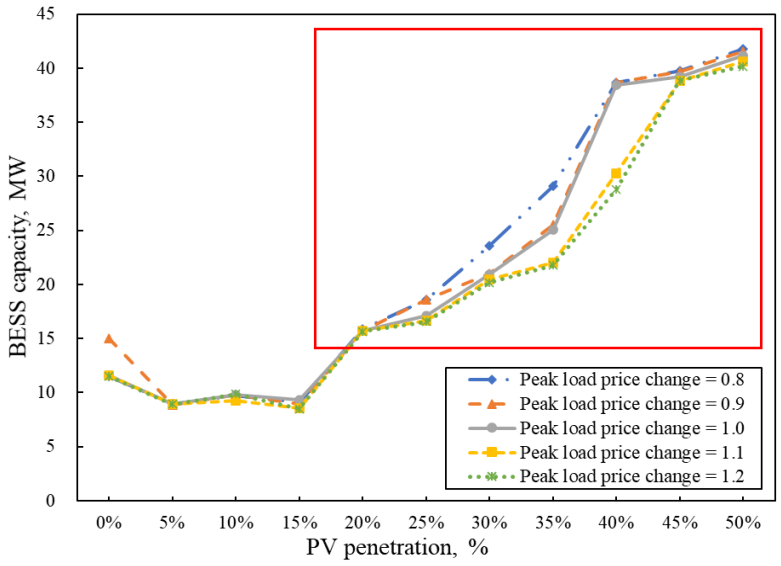

c)

Fig.5-29 Impact on the total cost, capacity of the ICE and the BESS when the peak load price changes: a) total cost; b) capacity of the ICE; c) capacity of the BESS

The peak shaving rate of the DESs under different PV penetration scenarios with the change of the peak load price is displayed in Fig.5-30. When the PV penetration is low, the peak shaving rate is almost the same. This is because the installed capacity of each equipment has little difference. However, when the PV penetration increases to more than 20%, it indicated that grid stabilization effect enhances at high PV penetration with growth of peak load price, which is contributed by the increasing of installed capacity of the ICE.

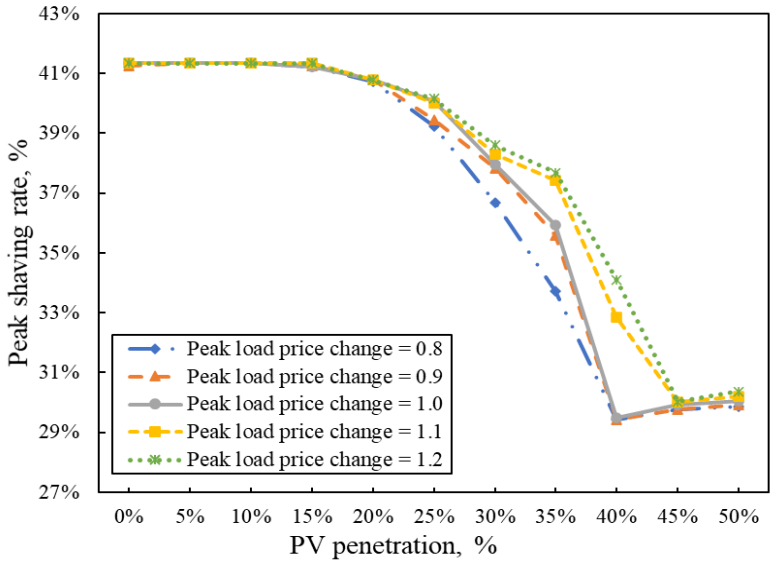

Fig.5-30 The peak shaving rate of the DES under different PV penetration scenarios with the change of the peak load price.

5.5.2 Carbon tax change

As Section 4.2 shows, the results of F2 and F3 is similar because of the low proportion CO_2

emission cost compared with other two costs. With the development of the carbon tax, CO_2 emission will occupy higher attention due to the larger payment of environment cost. It is predicted that the carbon tax of Japan reaches 104.6 $/t in 2030 [11]. Different carbon taxes are assumed to analyze the effect of environmental performance on the configuration optimization of DES. The total costs of the DES under different PV penetration scenarios with the increase of the carbon tax are demonstrated in Fig.5-31. As Fig.5-31 shows, the PV penetration is increased with the development of the carbon tax. It can be seen that the total cost is least when the PV penetration is 40% when the carbon tax reaches 104.6 $/t in 2030.

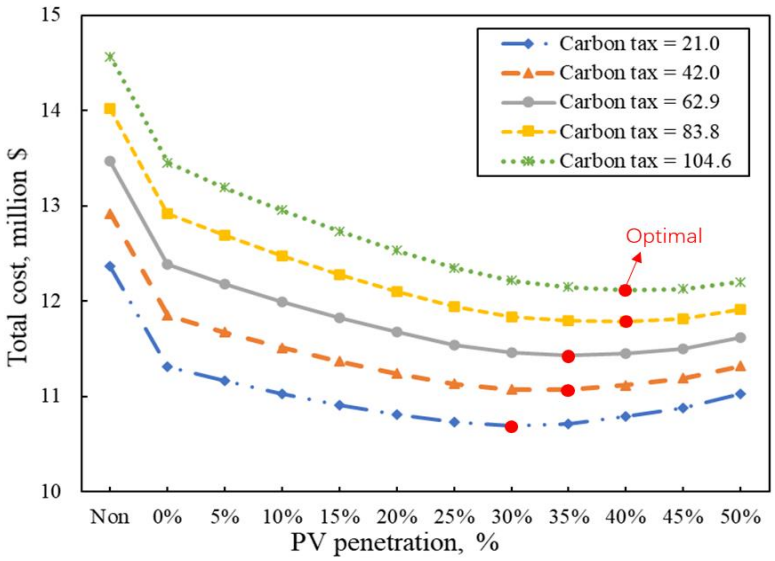

Fig.5-31 The total costs changes of the DES under different PV penetration scenarios with the increase of the carbon tax.

The total costs and optimal configurations of the DES with the different PV penetration scenarios under F3 after the increase of the carbon tax are changed, shown in Fig.5-32. It can be seen that the total cost is least when the PV penetration is 40%.

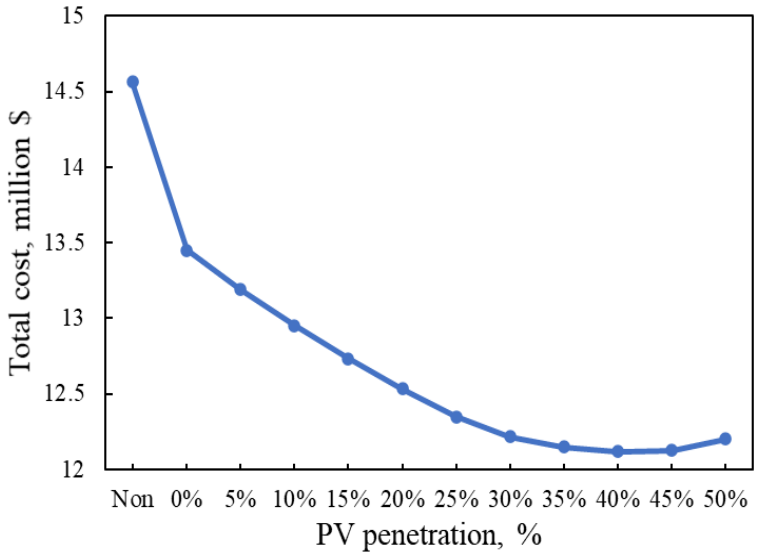

a)

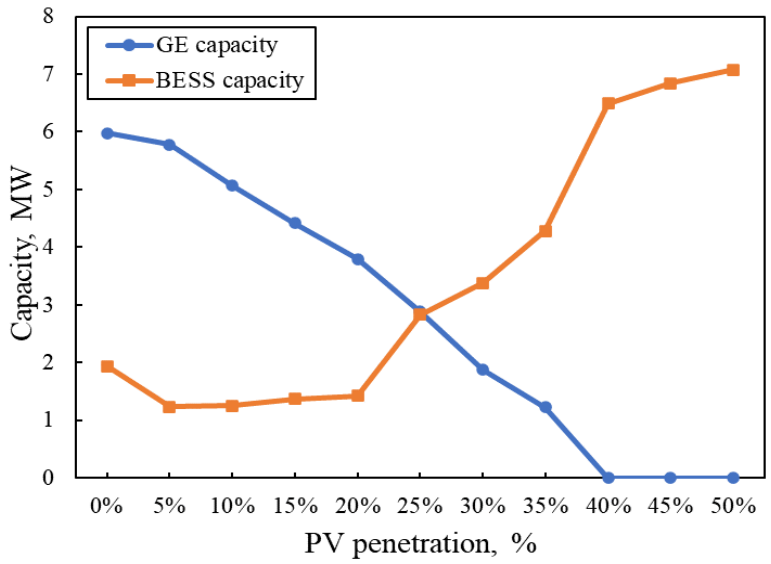

b)

Fig.5-32 The total cost and optimal configurations changes with the different PV penetration scenarios when the carbon tax is 104.6 $/t: a) The total costs; b) the optimal configurations of ICE and BESS.

Table 5-2 demonstrated the optimal configurations of the DESs under the three objective functions and their performance comparison when the carbon tax is 104.6 $/t. The results show that the total cost saving of DES_3 is improved 2.13% compared with DES_1. The peak shaving of DES_3 is less than that of DES_2, whereas the CO_2 emission reduction of DES_3 is more than DES_2. It indicated that with the increase of carbon tax, the environmental advantages are significant, which will greatly affect the overall performance of DES.

Table 5-2 The optimal configuration of the DES under the three objective functions when the carbon tax is 104.6 $/t.

DESs		DES_1	DES_2	DES_3
Configuration	PV penetration	30%	30%	40%
	ICE	0 MW	1.573 MW	0 MW
	BESS	9.479 MW	3.488 MW	6.840 MW
Cost saving	ABC saving	6.52%	5.81%	5.85%
	PLC saving	2.24%	4.58%	3.55%
	CDEC saving	5.91%	5.72%	7.40%
	Total cost saving	14.67%	16.11%	16.80%
Peak shaving		18.783%	38.426%	29.804%
CO_2 emission reduction		31.346%	30.366%	39.278%

5.6 Summary

Cost saving, grid stabilization and CO2 emission reduction are three reasons that cause increasing attention of the DES with renewable energy. In this chapter, the annual basic cost, peak load cost and carbon emission cost are put forward to assess the comprehensive performance of DES with different combinations. By introducing the peak load price and carbon tax, the peak shaving capacity and emission reduction effect of DES can be transformed into economic benefit. As a case study, the Smart Community in Higashida of Japan is used to explore the impact of different evaluation criteria on the configuration optimization of DES, after considering peak shaving ability and emission reduction effect. Compared the optimization results at different PV penetration scenarios, the following conclusions can be deduced:

1) Based on the actual grid load data of five different types of buildings in Higashida, Japan, the power of the area consisted of multi-type buildings has the characteristics of daytime peak and midnight valley. The difference of peak and valley load is significant, especially in summer. Convenient installation and environmentally friendly are the reasons that cause rapidly development of PV system in electrical networks. However, due to intermittence and instability, the increase of PV penetration has little effect on the enhancement of peak shaving. High PV penetration may not relieve the pressure of the power grid but will increase the volatility of the power grid. Therefore, the development of PV system in practical application is impeded.

2) By comparing the comprehensive benefits of DES in different PV penetration scenarios, it can be found that when PV penetration is 30%, the total cost of DES is the lowest which decreases by 13.579% of the initial energy bill. As the output of the ICE is limited by the PV generation at daytime, the optimal installed capacity of the ICE decreases with the growth of the PV penetration. Due to the economic operation strategy, the installed capacity of the BESS is affected by peak load and PV overproduction. Therefore, with the increase of the PV penetration and the decline of the ICE output, the optimal installed capacity of the BESS gradually increases.

3) When the peak load cost is added into the objective function, the peak shaving rate of the DES_3 are improved, which is 19.372% higher than that of DES_1. However, the annual basic cost saving is decreased compared with DES_1. It indicates that the improvement of the grid stabilization effect of DES came at the expense of partial system basic economic benefit. it is necessary to determine the optimization direction according to the evaluation criteria based on the urgent issues of local energy supply and power demand when optimizing the configuration of DES.

4) The power generation of the PV system can reduce the peak load, but its effect is not obvious compared with the stable output of the internal-combustion engine. According to the sensitivity analysis, the increase of peak load price can improve the configuration of the ICE, but it has little effect on the PV penetration. Carbon emission has a significant impact on the promotion of photovoltaic. The development of carbon tax has greatly increased PV penetration. By 2030, the carbon tax will reach 104.6 $/t, and the PV penetration can be increased by 10%. And the CO2 emission reduction can reach 39.28% after applying the DES with optimal combination.

Based on the above analysis, the multi-criteria evaluation method can fairly balance the different performance of the DES, which will maximize the application potential of the DES and improve its market competitiveness.

Reference

[1] Tooryan F, HassanzadehFard H, Collins ER, Jin S, Ramezani B. Optimization and energy management of distributed energy resources for a hybrid residential microgrid. J Energy Storage 2020;30:101556. https://doi.org/10.1016/j.est.2020.101556.

[2] Awad ASA, EL-Fouly THM, Salama MMA. Optimal ESS Allocation for Benefit Maximization in Distribution Networks. IEEE Trans Smart Grid 2017;8:1668–78. https://doi.org/10.1109/TSG.2015.2499264.

[3] Das CK, Bass O, Mahmoud TS, Kothapalli G, Mousavi N, Habibi D, et al. Optimal allocation of distributed energy storage systems to improve performance and power quality of distribution networks. Appl Energy 2019;252:113468. https://doi.org/10.1016/j.apenergy.2019.113468.

[4] García-Plaza M, Eloy-García Carrasco J, Alonso-Martínez J, Peña Asensio A. Peak shaving algorithm with dynamic minimum voltage tracking for battery storage systems in microgrid applications. J Energy Storage 2018;20:41–8. https://doi.org/10.1016/j.est.2018.08.021.

[5] Zhang L, Gao W, Yang Y, Qian F. Impacts of investment cost, energy prices and carbon tax on promoting the combined cooling, heating and power (CCHP) system of an amusement park resort in shanghai. Energies 2020;13. https://doi.org/10.3390/en13164252.

[6] Adefarati T, Bansal RC. Reliability, economic and environmental analysis of a microgrid system in the presence of renewable energy resources. Appl Energy 2019;236:1089–114. https://doi.org/10.1016/j.apenergy.2018.12.050.

[7] CO2 Emission coefficient by electric utility n.d. https://ghg-santeikohyo.env.go.jp/files/calc/r02_coefficient.pdf (accessed September 16, 2020).

[8] Carbon dioxide emission coefficient of urban gas n.d. http://www.saibugas.co.jp/business/others/co2_emission_factor.htm (accessed September 16, 2020).

[9] Zhao X, Gao W, Qian F, Li Y, Ushifusa Y, Yang Z, et al. Economic performance of multi-energy supply system in a zero-carbon house. Energy Build 2020;226:110363. https://doi.org/10.1016/j.enbuild.2020.110363.

[10] Brendan F.D. Barrett. Can Japan Go 100% Renewable by 2050? Sci Technol 2011. https://ourworld.unu.edu/en/can-japan-go-100-renewable-by-2050 (accessed October 26, 2020).

[11] Japan. Ministry of the Environment. Introduction of tax for measures against global warming. Compr Environ Policy 2018. https://www.env.go.jp/policy/tax/about.html (accessed November 15, 2020).

Chapter 6

PROMOTION AND UTILIZATION OF THE DISTRIBUTED ENERGY SYSTEM: A CASE STUDY OF COMBINED COOLING, HEATING AND POWER SYSTEM

CHAPTER SIX: PROMOTION AND UTILIZATION OF THE DISTRIBUTED ENERGY SYSTEM: A CASE STUDY OF COMBINED COOLING, HEATING AND POWER SYSTEM

PROMOTION AND UTILIZATION OF THE DISTRIBUTED ENERGY SYSTEM: A CASE STUDY OF COMBINED COOLING, HEATING AND POWER SYSTEM 6-1

6.1 Content 6-1

6.2 Methodology 6-1

6.2.1 Establishment of the CCHP system model 6-1

6.2.2 Evaluation criteria 6-4

6.3 Case study 6-6

6.3.1 Introduction of the research case 6-6

6.3.2 Simulation model 6-9

6.4 Results and discussion 6-12

6.4.1 Simulation results of the energy consumption and generation 6-12

6.4.2 Comparison of economic and environment performance in three systems 6-16

6.4.3 Impact of different factors on the economic performance of CCHP system 6-18

6.4.4 Sensitivity analysis 6-23

6.5 Summary 6-24

Appendix 6-26

References 6-30

6.1 Content

According to the analysis of the previous chapters, the gas internal combustion engine is one of the most important components of distributed energy systems. It can provide a stable and safe power, which increases the independent ratio of the regional power supply. Peak shaving can be realized by flexibly controlling the output of the ICE. In addition, because the waste heat produced by the ICE while generating electricity can be recovery used, the combined cooling, heating and power (CCHP) system as a typical DES which consisted of the ICE and heat recovery device is identified as an alternative to solve energy problems on account of the high comprehensive utilization efficiency. However, poor economic performance has limited the diffusion of the CCHP system. Various factors influence the economic performance of the CCHP system. In order to analyze the impacts of these different factors on the promotion of the CCHP system, this chapter evaluated the comprehensive performance of the CCHP system through a multi-criteria method, using an amusement park resort in Shanghai as a research case. First, three CCHP systems with different penetration were presented and simulated in a transient simulation model for comparison. The economic and environmental performance of these different penetration CCHP systems were evaluated based on the dynamic payback period and carbon dioxide emissions. The impacts of investment cost, energy prices, investment subsidy, and a carbon tax on the economic performance of the three systems were discussed. Through sensitivity analysis, the impact significance of different factors on the economy of the CCHP system was compared, and the correlation with the promotion effect of the CCHP system was analyzed. The research flow is shown in Fig.6-1.

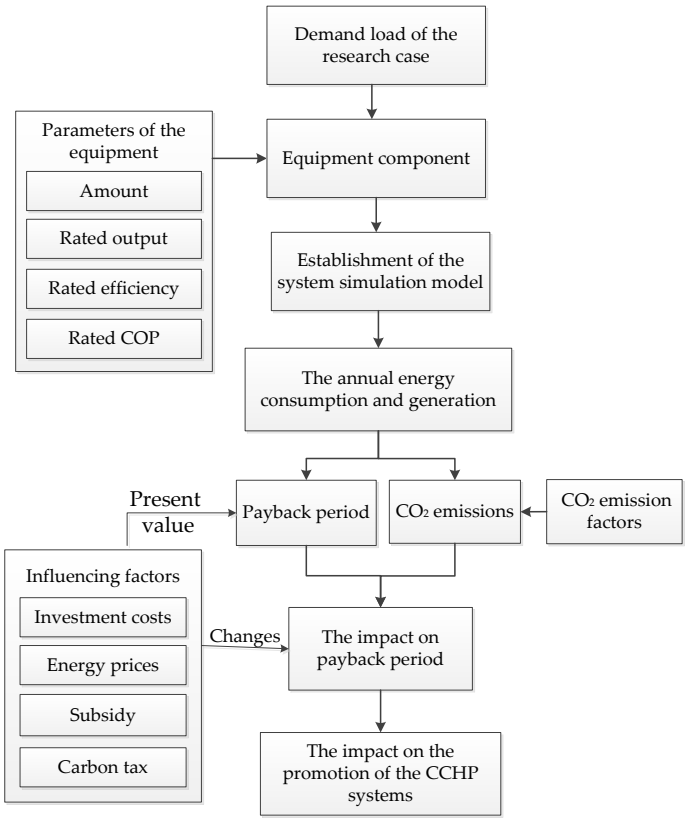

Fig.6-1 Diagram of the research flow.

6.2 Methodology

To analyze the economic performance of the CCHP system, assessment of the energy flow of the CCHP system was carried out to calculate the energy consumption and generation. After that, the economic and environmental performance of the CCHP system could be obtained.

According to the literature [1–3], the payback period is one of the main indicators to evaluate the economics of a project. The carbon dioxide emissions are usually used to represent the environmental performance of the system [4–6]. In order to compare the comprehensive performance of different systems, this chapter uses the payback period and carbon emissions in a multi-criteria evaluation. Through the carbon tax, the environmental indicator of carbon emissions is integrated into the economic performance of the system. Therefore, the impacts of the changes in different factors on the promotion of the CCHP system can be analyzed by comparison of the payback period.

6.2.1 Establishment of the CCHP system model

1) Energy flow of CCHP system

In the CCHP system, the power generation unit (PGU) is driven by natural gas and produces electricity. The high-temperature exhaust gas of the PGU is recovered to accommodate the thermal load for cooling and heating for the demand side. In applications, due to large fluctuations in the load on the demand side, electric chillers and gas boilers are usually used in combination with waste recovery equipment, to satisfy the cooling or heating demand load.

The CCHP system consists of PGUs and absorption units, electric chillers and boilers, and its energy flow is shown in Fig. 6-2.

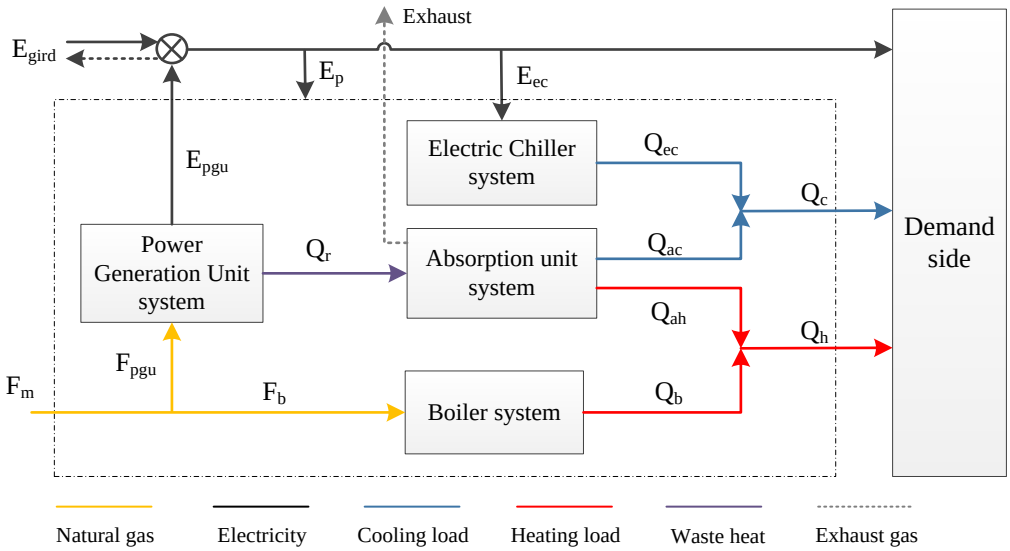

Fig.6-2 Energy flow diagram of the CCHP system

The balances of electricity load in the CCHP system at t-hour are expressed as [6]:

$$E_{grid}^{t} + E_{pgu}^{t} = E_{p}^{t} + E_{ec}^{t} + E^{t} \quad (6\text{-}1)$$

where E_{grid}^{t} is the electricity from the grid at t-hour in the CCHP system (when the PGU generates excess electricity, E_{grid}^{t} is negative and its value is equal to the excess electricity in kWh, and the electricity is sold back to the grid). E_{pgu}^{t} is the electricity generated by the PGU in kWh. E_{p}^{t} is the parasitic electric energy consumption of the CCHP system (considering the auxiliary equipment required for the energy supply and the daily power needs of the system) in kWh. E_{ec}^{t} is the electric energy consumption for electric chillers providing cooling to the demand side in kWh. E^{t} is the electric energy load of the demand side in kWh.

The fuel energy consumption (F_{pgu}^{t}) and the waste heat (Q_{r}^{t}) generation of the PGU at t-time can be calculated as Equation (2) and Equation (3), respectively.

$$F_{pgu}^{t} = E_{pgu}^{t} / \eta_{e}^{t} \quad (6\text{-}2)$$

$$Q_{r}^{t} = F_{pgu}^{t} \cdot \eta_{rec}^{t} \cdot (1 - \eta_{e}^{t}) \quad (6\text{-}3)$$

$$\eta_{e}^{t} = a_0 + a_1 \cdot PL_{pgu} + a_2 \cdot PL_{pgu}^{2} \quad (6\text{-}4)$$

$$\eta_{rec}^{t} = b_0 + b_1 \cdot PL_{pgu} + b_2 \cdot PL_{pgu}^{2} \quad (6\text{-}5)$$

where E_{pgu}^{t} is the electricity generated by the PGU at t-time in kWh. η_{e}^{t} is the electric efficiency percentage of the PGU at t-time. η_{rec}^{t} is the heat recovery system efficiency percentage. PL_{pgu} is the part load ratio percentage of the PGU. Equation (4) and (5) are quadratic fitting formulas which can be estimated by the parameters of the actual devices [7].

The waste heat generated by the PGU can be used for cooling or heating. Therefore, the cooling load or heating load produced by the absorption units are estimated, respectively as

For cooling, $Q_{ac}^{t} = Q_{r}^{t} \cdot COP_{ac}^{t}$ (6-6)

For heating, $Q_{ah}^{t} = Q_{r}^{t} \cdot COP_{ah}^{t}$ (6-7)

$$COP_{a}^{t} = c_0 + c_1 \cdot PL_{a} + c_2 \cdot PL_{a}^{2} \quad (6\text{-}8)$$

where, Q_{r}^{t} is the waste heat generated by the PGU in kWh. Q_{ac}^{t}, Q_{ah}^{t} are the cooling load or heating load produced by the absorption units, respectively, in kWh. COP_{ac}^{t} is the coefficient of performance (COP) of the absorption units for cooling, and COP_{ah}^{t} is the coefficient of performance (COP) of the absorption units for heating. PL_{a} is the part load ratio percentage of the absorption unit. Equation (8) includes the quadratic fitting formulas, which can be estimated by the parameters of the actual devices [7].

The balance of the cooling and heating load is expressed as:

$$Q_{ac}^{t} + Q_{ec}^{t} = Q_{c}^{t} \tag{6-9}$$

$$Q_{ah}^{t} + Q_{b}^{t} = Q_{h}^{t} \tag{6-10}$$

where Q_{ac}^{t} is the cooling produced by the absorption units in kWh. Q_{ec}^{t} is the cooling produced by the electric chillers in kWh. Q_{c}^{t} is the cooling load of the demand side in kWh. Q_{ah}^{t} is the heating produced by the absorption units in kWh. Q_{b}^{t} is the heating produced by the boilers in kWh. Q_{h}^{t} is the heating load of the demand side in kWh.

The electricity used by the electric chiller is calculated as:

$$E_{ec}^{t} = \frac{Q_{ec}^{t}}{COP_{ec}^{t}} \tag{6-11}$$

where COP_{ec} is the electric chiller's COP.

The supplementary fuel energy consumption to the boiler, F_b, can be estimated as:

$$F_{b}^{t} = \frac{Q_{b}^{t}}{\eta_{b}} = \frac{Q_{h}^{t} - Q_{ah}^{t}}{\eta_{b}} \tag{6-12}$$

where η_b is the boiler efficiency percentage.

The purpose of this research was to analyze the impacts of the investment cost, energy prices, subsidy, and the carbon tax on the economic performance of the CCHP system, which could significantly improve its promotion. Therefore, the hypotheses were: (1) There is no transmission consumption; the cold, heat, and electricity obtained by the simulation can be 100% used; (2) Ignore the thermal inertia in the process of cold and heat supply, and consider that the start and stop of the equipment is consistent with the change in demand load; (3) The parasitic electric energy consumption of the CCHP system (considering the auxiliary equipment required for energy supply and the daily power needs of the system) is estimated to be 10% of the electricity generation of the CCHP system [8].

2) Operational mode

The CCHP system is operated following thermal load. In this mode, the heat (cold capacity) to be provided by the supply system will have priority to meet the demand cooling and heating load requirements, and the power generation may be redundant or insufficient. At a certain moment, when the generated power is higher than the demand electrical load demand, the excess power can be used to drive the electric refrigeration, air conditioning, refrigeration or sold to the grid; when the generated power is lower than the demand electrical load demand, the insufficient power is replenished from the grid. This mode is suitable for the bidirectional grid-connected heat, power and cooling combined supply system, which is the most widely used.

6.2.2 Evaluation criteria

6.2.2.1 Economic analysis

1) Annual total profit (ATP)

The annual total profit (ATP), which is the energy income minus the annual energy cost and operation and maintenance cost, is calculated as follows:

$$ATP = \sum_{t=1}^{8760} [Q_c^t \cdot EC_c^t + Q_h^t \cdot EC_h^t] + \sum_{t=1}^{8760} [E^t \cdot EC_e^t] - \sum_{t=1}^{8760} \left(E_{grid}^t EC_e^t + F_m^t EC_f^t\right) \quad (6\text{-}13)$$

where EC_c^t, EC_h^t, EC_e^t and EC_f^t are the energy price of cooling, heating, electricity and natural gas at t-hour, respectively in \$/kWh.

2) Investment cost

The investment cost is spent at the beginning when purchasing the equipment in the construction of the system, calculated as follows:

$$IN = \sum_{n=1}^{N} (C_{pgu} \times NC_n) + \sum_{n=1}^{N} (C_{ab} \times NC_n) + \sum_{m=1}^{M} (C_{ec} \times NC_m) + \sum_{i=1}^{I} (C_b \times NC_i) \quad (6\text{-}14)$$

where, C_{pgu}, C_{ab}, C_{ec}, and C_b are the equipment unit cost of the PGU, absorption unit, electric chiller, and boiler, respectively, in \$/kW. NC_n, NC_m, and NC_i are the nominal capacity of the PGU, electric chiller, and boiler, respectively, in kW. N, M and I are the number of PGUs, electric chillers and boilers. The absorption unit should be matched with the PGU, so the number is the same as for the PGU.

3) Dynamic payback period (PB)

The payback period, an index of economic performance, is the time required for the project to recover the initial investment cost. By calculating payback period, the economic performance of the projects can be compared. A short payback period means that the economic benefits of the system are high. The dynamic payback period is calculated when the cumulative net present value (NPV) is zero, as shown by Equation (6-15).

$$NPV(n) = 0 \quad \rightarrow \quad PB = n \quad (6\text{-}15)$$

The payback period cannot be longer than the lifetime of the system, which is 25 years in China.

The net present value (NPV) is the difference between the present value of cash inflows and the present value of cash outflows during a period, which mainly represents the balance between the present value of total profit and the initial investment. It can be expressed as [2]:

$$NPV = \sum_{n=1}^{PB} \frac{ATP_n}{(1+i)^n} - IN \tag{6-16}$$

where ATP_n is the annual total profit in \$. i is the discount rate percentage. IN is the total investment cost in \$.

6.2.2.2 Environment Analysis

The amount of carbon dioxide emissions (CDEs) from the CCHP system can be determined using the emission conversion factors as follows [5,6]:

$$CDE = \sum_{t}^{8760} E_{grid}^{t} \cdot \mu_{CO_2,e} + \sum_{t}^{8760} F_{m}^{t} \cdot \mu_{CO_2,gas} \tag{6-17}$$

where $\mu_{CO_2,e}$ and $\mu_{CO_2,gas}$ are the emission conversion factors for electricity from the grid and natural gas, respectively, in g/kWh.

A carbon tax is one of the effective means to reduce carbon emissions. At present, at least 20 countries in the world have imposed carbon taxes [9]. The carbon tax can be calculated into the total annual profit, as follows:

$$ATP' = ATP - \Delta CDE * Tax_{co_2} \tag{6-18}$$

where ATP' is the total annual profit considering the carbon tax. ΔCDE is the difference in carbon dioxide emissions before and after utilization of the energy supply system. Tax_{co_2} is the carbon tax.

6.3 Case study

This chapter takes a typical CCHP system in an amusement park resort in Shanghai, China, as a research case, and its economic performance was analyzed. As the first CCHP system under stable operation in China, its equipment selection, system design, and operation strategy are highly representative and universal. At the same time, it provides electricity, cooling, and heating for the demand side with different load characteristics. Based on this research case, the study of the impacts of different factors on the promotion of CCHP system in China is valuable.

Generally, centralized energy supply systems with electric chillers and gas boilers are commonly used in amusement parks to provide cooling and heating [32]. Nowadays, a few major theme park companies are embracing a more energy-saving and environmentally friendly way to solve energy problems. The CCHP system is an alternative to conventional systems. The research case of this chapter is a hybrid CCHP system with penetration of 50% (the cooling and heating load provided by waste heat from PGUs account for 50% of the total demand). In order to study the promotion of CCHP systems, this chapter proposed three CCHP systems with different penetration, using the current system for comparison:

- **System 1:** conventional system without CCHP (only adopting electric chillers and boilers to supply cooling and heating load, the electricity is from the utility grid);
- **System 2:** CCHP with 50% penetration (adopting PGUs, absorption units, electric chillers and boilers to cooperate to supply electricity, cooling and heating);
- **System 3:** CCHP with 100% penetration (only adopting PGUs and absorption units to supply energy).

In this chapter, by comparing the above three CCHP systems with different penetration, the economics and environmental performance of the CCHP system were analyzed, and the impacts of different factors could be discussed.

6.3.1 Introduction of the research case

6.3.1.1 System configuration

Due to the large electricity load of the resort, the CCHP system is operated following thermal demand, and the excess electricity can be sold back to the grid. The system makes full use of waste heat from PGU to provide cooling and heating load for the resort.

In the CCHP system, the PGU adopts a gas internal combustion engine (ICE). The waste recovery equipment adopts a flue gas hot water-type lithium bromide absorption heat transformer unit (absorption unit), which can produce cooling or heating. Electric chillers and Gas-fired boilers are employed to operate with the absorption unit to meet the cooling and heating needs of the tourism resort. The penetration of this CCHP system is 50%. The configuration of the CCHP system with 50% penetration is shown in Table 6-1. After investigating and consulting the equipment manufacturers, the characteristic parameters of these equipment of this CCHP system are listed in Table 6-2.

Table 6-1 The configuration of the CCHP system with 50% penetration.

Equipment	Type	Amount	Rated output(kW)
ICE	JMS624GS	5	4401
Absorption unit	YRXII368	5	3931
Electric chiller 1	YKR2R2K45DGG	4	6330
Electric chiller 2	YKK8K4H95CWG	2	3165
Boiler	FBD-7.0-1.0/90/65.5	2	7000

Table 6-2 The characteristic parameters of the CCHP system with 50% penetration.

Equipment	Variable	Symbol	Rated value
ICE	Efficiency	η_e	0.45
Electric chiller	COP	COP_e^t	5.353
Absorption unit	COP	COP_a^t	1
Boiler	Efficiency	η_b	0.98

To compare the economic and environmental performance of the three different systems, we adopted the same equipment for the conventional system (without CCHP) and CCHP system with 100% penetration. The energy generated by these three systems can meet the same cooling and heating load. Other characteristic parameters of the equipment are the same as in the CCHP system with 50% penetration. The configurations of the three systems are listed in Table 6-3.

Table 6-3 The configurations of the conventional system without CCHP and the CCHP system with 100% penetration.

System	Equipment	Type	Amount	Rated output(kW)
Conventional system (without CCHP)	Electric chiller 1	YKR2R2K45DGG	6	6330
	Electric chiller 2	YKK8K4H95CWG	4	3165
	Boiler	FBD-7.0-1.0/90/65.5	4	7000
The CCHP system with 100% penetration	ICE	JMS624GS	15	4401
	Absorption unit	YRXII368	15	3931

6.3.1.2 Load curve

The total area of the amusement park resort in Shanghai is 116 km^2 (Fig.6-3). There are two themed hotels, many amusement facilities, and lots of restaurants and shopping stores in the resort. The total construction area of these two themed hotels is 161,000 m^2. Through the pipe network system and cables, the CCHP system provides cold, heat, and electricity to the resort. Because the CCHP system is operated following the thermal demand and the excess electricity can be sold back to the grid, the cooling and heating load should be satisfied preferentially. The hourly cooling and heating load demand from January 2016 to December 2016 of the resort is shown in Fig. 6-4, and the following characteristics can be derived:

1. Both cooling load and heating load are required throughout the year;
2. The cooling load peak is greater than the heating load peak because of the hot climate of Shanghai;

3. The cooling load is high, and the heating load is low in summer. The heating load is high, and the cooling load is low in winter;
4. Mid-season, the energy demands for cooling and heating are similar.

Fig.6-3 Research area

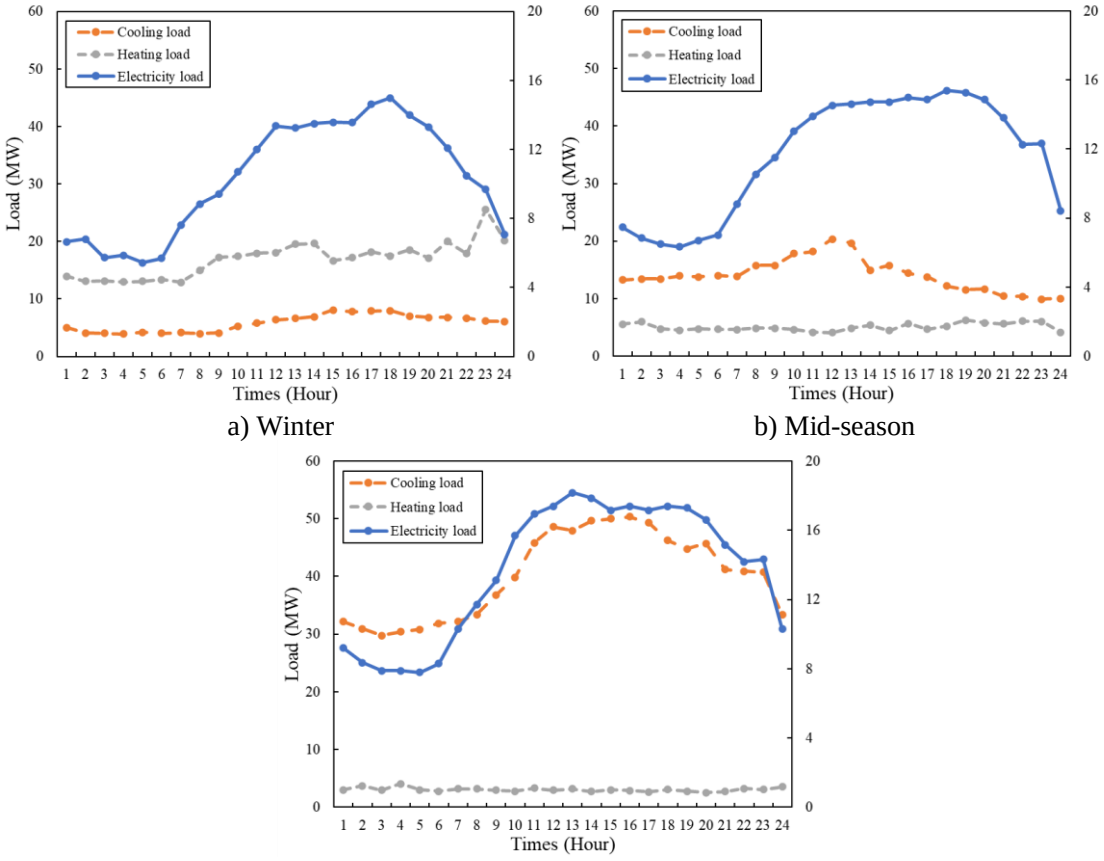

Fig.6-4 Hourly loads on typical day of three seasons.

6.3.2 Simulation model

6.3.2.1 Establishment of simulation model

We used TRNSYS [33, 34] to establish the operation simulation model of the CCHP systems. The key step for TRNSYS to build a system simulation model is to generate and access subroutines of each component model in the simulation system. TRNSYS software contains all the equipment model components in the CCHP system, which can be basically matched with actual equipment by modifying the model subroutine. And it is available to simulate the instantaneous changes of the simulation conditions, such as weather temperature, demand load or start and stop of equipment. Therefore, the system components, including ICEs, absorption units, electrical chillers, gas boilers and other auxiliary equipment should be adjusted according to the actual parameters and characteristics of the components. Based on the components modules, the operation model of the CCHP system was established to simulate instantaneous energy consumption and generation, as shown in Fig.6-5. N is the number of ICEs/absorption units, M is the number of electric chillers and I is the number of boilers in the diagram, which are listed in Table 6-4. Other parameters in detail of the equipment and other auxiliary equipment are demonstrated in the Appendix.

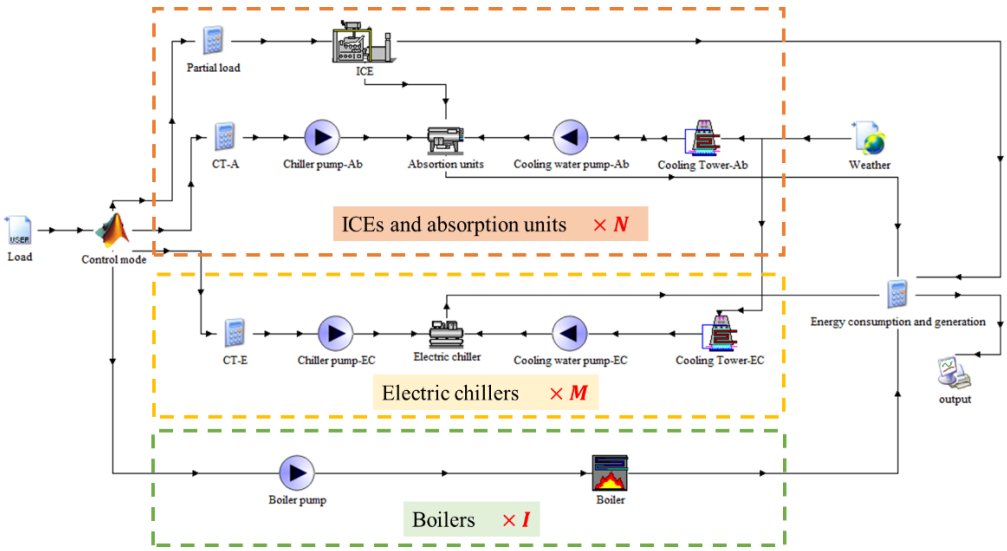

Fig.6-5 The simulation diagram of proposed systems.

Table 6-4 The numbers of various types of equipment in the three systems.

System	N	M	I
Conventional system (without CCHP)	0	10	4
The CCHP system with 50% penetration	5	5	2
The CCHP system with 100% penetration	15	0	0

6.3.2.2 Setting of partial load performance and validation of the simulation model

The number of units started is determined based on the load change at the previous moment. Therefore, the start and stop sequence of each piece equipment was simulated in MATLAB. The part load ratio ε of units is：

$$\varepsilon \in [0\ 1] \tag{6-19}$$

Each module was set according to the actual performance of the equipment. The partial load performance of the ICE, absorption unit and electric chiller were set by an external file according to the specifications provided by the manufacturer, as shown in Table 6-5 and Fig.6-5. The weather conditions of Shanghai are obtained through the typical meteorological year (TMY2) module, which can make the simulated environment consistent with the actual operating environment.

Table 6-5 The partial load data of the ICE (external file).

Partial load output rate	37%	50%	75%	100%
Mechanical efficiency	0.408	0.421	0.443	0.45
Electrical efficiency	0.965	0.97	0.977	0.978
Cylinder water waste heat ratio	0.23	0.266	0.324	0.339
Total oil excess heat	0.11	0.105	0.084	0.071
Emissions waste heat ratio	0.49	0.468	0.449	0.425
Medium cooler waste heat ratio	0.09	0.09	0.09	0.12
Environmental waste heat ratio	0.08	0.071	0.053	0.045
Exhaust capacity rated	0.48	0.57	0.77	1

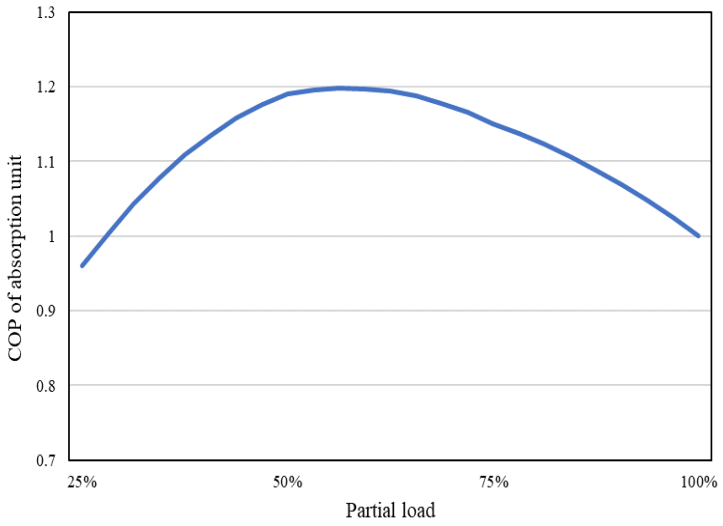

(a)

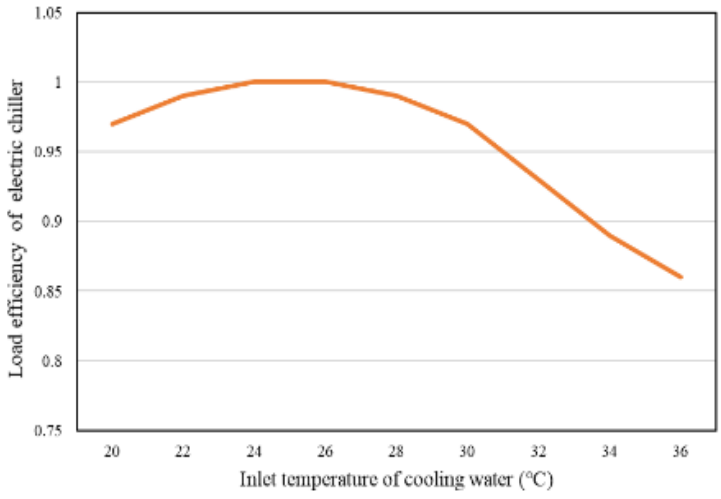

(b)

Fig.6-6 The performance of the absorption unit and electric chiller under partial load: (a) The part load performance of the absorption unit; (b) the load efficiency of the electric chiller.

For accuracy of the simulation, the performance of the model was compared with the actual operation data at full load of system 2, as shown in Table 6-6. From Table 6-6, we can see that the relative errors are within 3% after comparing the simulation results with actual data. This demonstrates that the results simulated by the model are in good agreement with the actual operational data. And the output of the ICE, absorption unit, electric chiller and boiler simulated in the TRNSYS model in detail are shown in Fig. A6-4.

Table 6-6 Validation of simulation results performance with operating parameters at full load of the CCHP system with 50% penetration.

Equipment	Parameter	Rated value	Simulation results	Error ratio (%)
ICE	Power generation efficiency (%)	45.4	44.41	2.18%
	Power output(kW)	4401	4400	0.02%
	Exhaust temperature (°C)	368	359.6	2.28%
Absorption Unit	Cylinder water outlet temperature (°C)	95	94.88	0.13%
	Chilled water outlet temperature (°C)	6	6	0.00%
	Cooling capacity (kW)	3931	3922	0.22%
	Heating capacity (kW)	3931	3922	0.22%
	Cooling water outlet temperature (°C)	38	38.2	-0.53%
Electric chiller	Cooling capacity (kW)	6330	6315	0.23%
	Chilled water outlet temperature (°C)	6	6	0.00%
Boiler	Efficiency (%)	0.95	0.95	0.00%

6.4 Results and discussion

6.4.1 Simulation results of the energy consumption and generation

After simulating with the TRNSYS model, the hourly energy consumption and generation of the three systems was obtained. In order to comprehensively explain the operation situation of all the equipment, the CCHP system with 50% penetration was taken as an example for analysis and description.

In the CCHP system with 50% penetration, the absorption units and electric chillers are operated cooperatively to meet the cooling load of demand side. The simulation model of the CCHP system with 50% penetration was established according to Section 3.2, with the parameters outlined in Tables 1, 2, and 4. The hourly cooling supply and demand balance of the system in summer was illustrated in Fig.6-7.

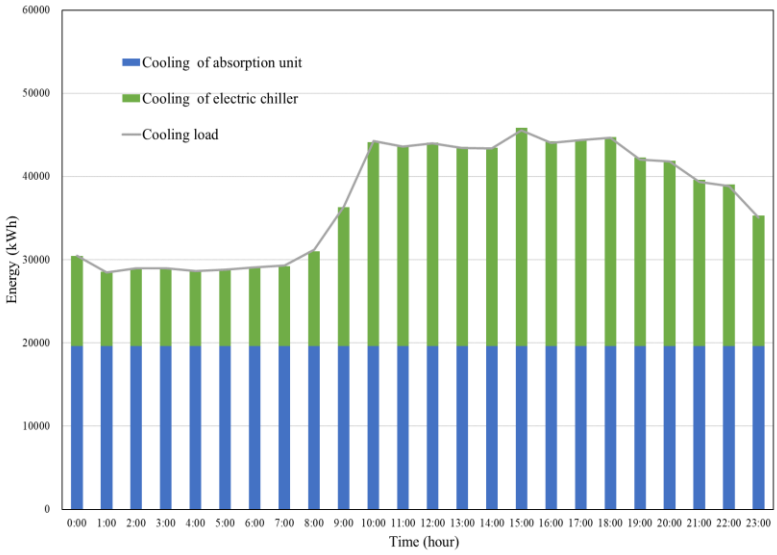

Fig.6-7 Hourly cooling supply and demand balance in summer.

We obtained the hourly energy consumption and generation from the output of the TRNSYS model, shown in Fig.6-8. A positive value indicates energy generation, and a negative value indicates energy consumption. Because the cooling load is high in summer, all the ICEs and absorption units are turned on at full load to supply the cooling load. An insufficient cooling load is supplemented by the electric chillers. Therefore, electricity is consumed by the electric chillers and other auxiliary equipment. The excess electricity is sold back to the grid.

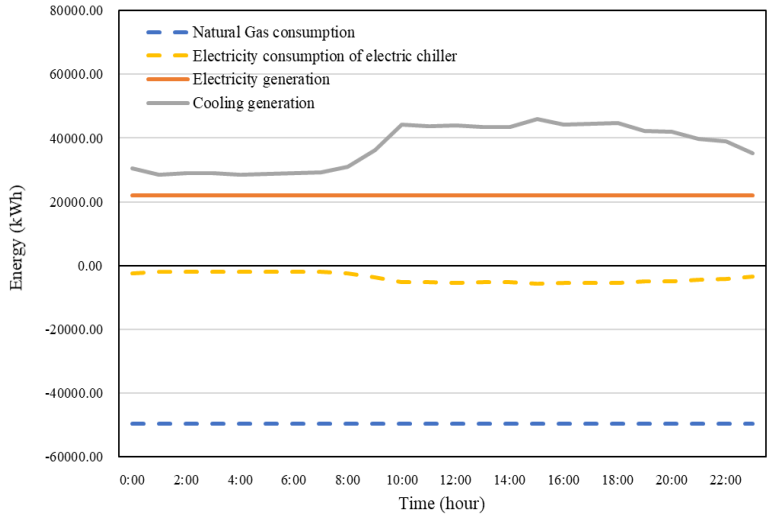

Fig.6-8 Hourly energy consumption and generation in summer of the CCHP system with 50% penetration.

The monthly energy consumption and generation over one year is shown in Fig.6-9. The solid line represents energy generation; the dashed line represents energy consumption. In the CCHP system with 50% penetration, the absorption units are used to supply cooling load for the demand side cooperating with electric chillers and heating load for the demand side with gas boilers.

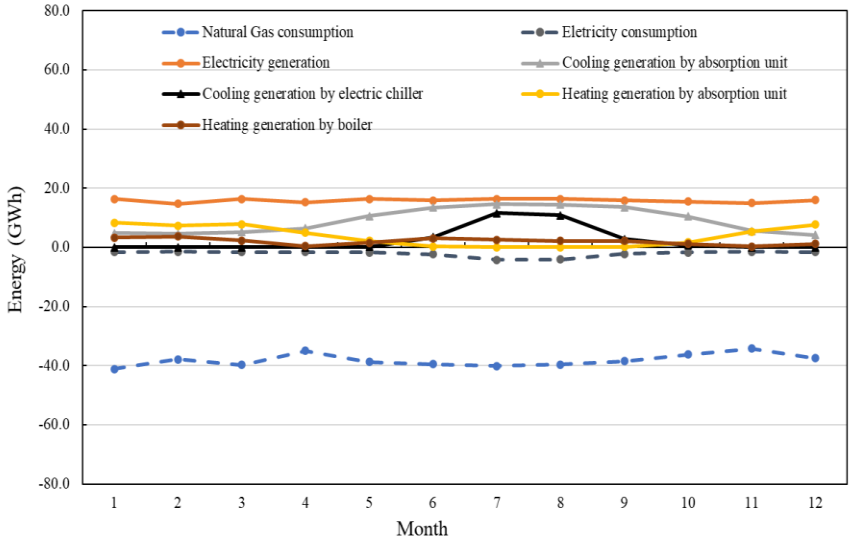

Fig.6-9 The monthly energy consumption and generation of the CCHP system with 50% penetration.

In summer, the absorption units preferentially meet the demand cooling load, and the insufficient is provided by the electric chillers. During this period, if there is heating load demand, the boiler heating will be handled. In winter, the absorption units take priority to meet the heating load for the demand side, and the insufficient is provided by the gas boilers. During this period, if there is cooling load demand, it is met by electric chillers. Since the CCHP system operates following thermal load,

the electricity produced by the ICE is directly supplied to the demand side, and the insufficient supplement is purchased from the grid.

Similarly, according to the parameters of Tables 6-2 and 6-3, the energy consumption and generation can be obtained through the simulation models of the conventional system (without CCHP) and the CCHP system with 100% penetration as well. The monthly energy consumption and generation of the conventional system (without CCHP) and the CCHP system with 100% penetration are displayed in Fig.6-10 and Fig.6-11.

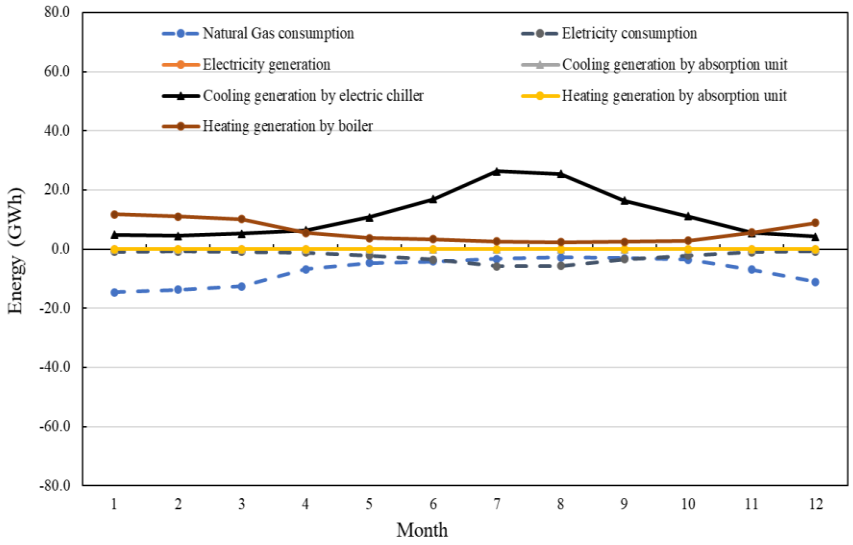

Fig.6-10 The monthly energy consumption and generation of the conventional system (without CCHP).

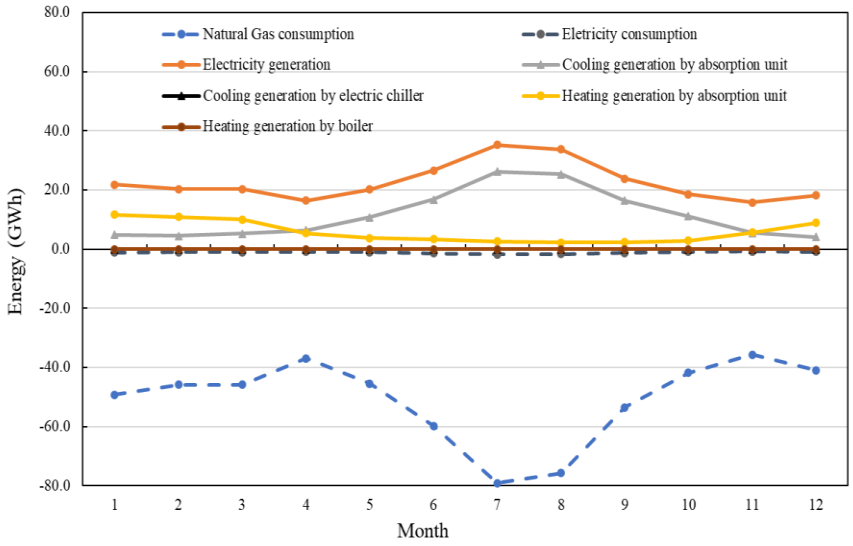

Fig.6-11 The monthly energy consumption and generation of the CCHP system with 100% penetration.

The conventional system (without CCHP) only uses electric chillers and boilers to produce cooling and heating load for the demand side, so the main energy consumption is electricity and

natural gas. In addition, there is no electricity production, and the electricity demand is all imported from the grid.

The CCHP system with 100% penetration is only consisted of the internal combustion engines and absorption units. The main energy consumption is natural gas, and electricity produced by the ICE can reduce the amount of electricity demand imported from the grid.

From the simulation results, we compared the energy consumption and generation of the three systems. Fig.6-12 shows the seasonal natural gas consumption of the three systems.

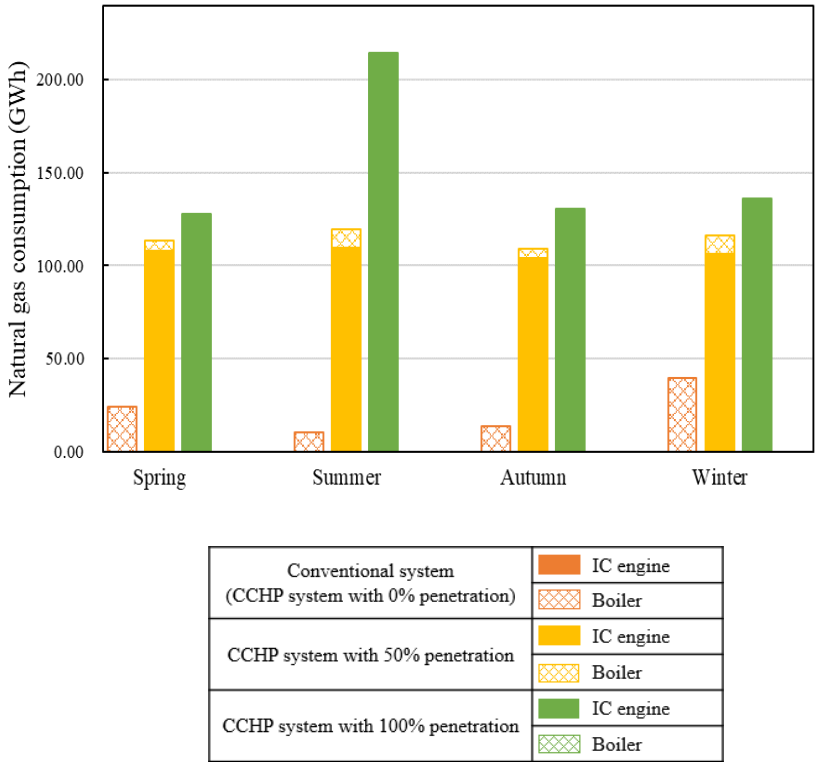

Fig.6-12 The seasonal natural gas consumption of the three systems obtained from simulation.

Natural gas consumption of the conventional system (without CCHP) is most in winter and least in summer. This is because the system only adopts the boilers to supply the heating load, and the heating load of demand side is larger in winter and less in summer. Natural gas consumption of the CCHP system with 50% penetration is almost the same in one year. The natural gas consumed by the ICEs accounts for a large proportion. Since both cooling load and heating load are required through the year, and the absorption units have priority to meet the cooling and heating of demand side, the utilization hours of the absorption units do not change much in a year. The ICEs need to provide waste heat for cooling and heating of absorption units stably, so its natural gas consumption and electricity generation change little. The natural gas consumption of the boilers is related to the heating load of the demand side and the output the absorption units. In summer, the cooling load is high, and the absorption units only provide cooling load. The heating load is all provided by the boilers, so the natural gas consumption of the boilers is the same as that of the conventional system (without CCHP). With the gradual increase of heating load, the absorption units handle a part of the

heating load, which reduces the output of the boilers. Therefore, the natural gas consumption of the boilers is significantly reduced compared with the conventional system (without CCHP). Natural gas consumption of the CCHP system with 100% penetration is sharply increase in summer. The cooling load and heating load of demand side are only provided by the absorption units in this system. In summer, the cooling load increases sharply, as a result, the natural gas consumption of the ICE increases.

Fig.6-13 demonstrates the seasonal electricity consumption and generation. It can be seen from the above figures that there is excess electricity sold back to the grid in the CCHP system with 50% and 100% penetration because the electricity from the grid is negative. The electricity from the grid consumption of the conventional system (without CCHP) is the highest, because it only uses electric chillers to supply cooling.

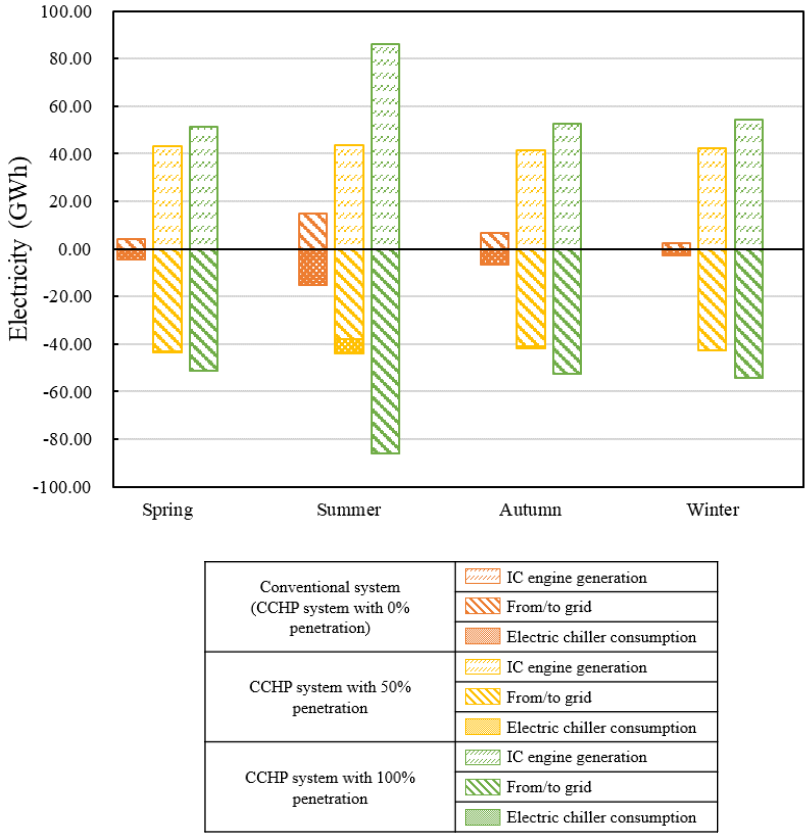

Fig.6-13 The seasonal electricity consumption and generation of the three systems obtained from simulation.

6.4.2 Comparison of economic and environment performance in three systems

According to the investigation, the equipment, energy prices and other parameters of the Shanghai CCHP system are shown in Table 6-7.

Table 6-7 The facility price, energy price, and other parameters of the CCHP system.

Parameter			Symbol	Unit	Value
Facility price [1] [28]		IC engine	C_{pgu}	$/kW	971
		Absorption unit	C_{ab}		172
		Electric chiller	C_{ec}		139
		Boiler	C_b		43
Energy prices [2] [35]	Natural gas		EC_f^t	$/kWh	0.039
	Cooling/Heating		EC_c^t/EC_h^t,	$/kWh	0.04
	Electricity	22:00–6:00	EC_e^t	$/kWh	0.044
		6:00–8:00, 11:00–18:00, 21:00–22:00			0.089
		8:00–11:00, 18:00–21:00			0.151
The CO_2 emission conversion factors [3] [36]		Natural gas	$\mu_{CO_2,gas}$	g/kWh	220
		Electricity from grid	$\mu_{CO_2,e}$		968
The discount rate [4] [37]			i	%	4.9

[1] The facility prices were determined according to the Li. [28] in 2020.

[2] Energy prices were determined according to the present energy prices in Shanghai in 2020.

[3] The CO2 emission conversion factors were determined according to the Khodaei. [36] in 2018.

[4] The discount rate was determined by the benchmark lending rate set by the People's Bank of China in 2017.

Based on the simulation results, the economic and environmental performance are shown in Table 6-8 and 6-9. The comparison of the payback period and CO_2 emissions of the three different systems are shown Fig.6-14.

Table 6-8 The economic performance of the three systems

Systems	ATP ($)	IN ($)	Payback period (year)
Conventional system (without CCHP)	2.28	8.3	4.01
CCHP with 50% penetration	5.35	29.8	6.5
CCHP with 100% penetration	7.09	74.2	14.67

Table 6-9 The environmental performance of the three systems

Systems	Natural consumption (GWh)	Electricity consumption (GWh)	Electricity generation (GWh)	CO_2 emissions (ton)
Conventional system (without CCHP)	87.42	135.49	0.00	150390
CCHP with 50% penetration	457.91	132.50	190.00	45080
CCHP with 100% penetration	609.33	134.05	271.46	1030

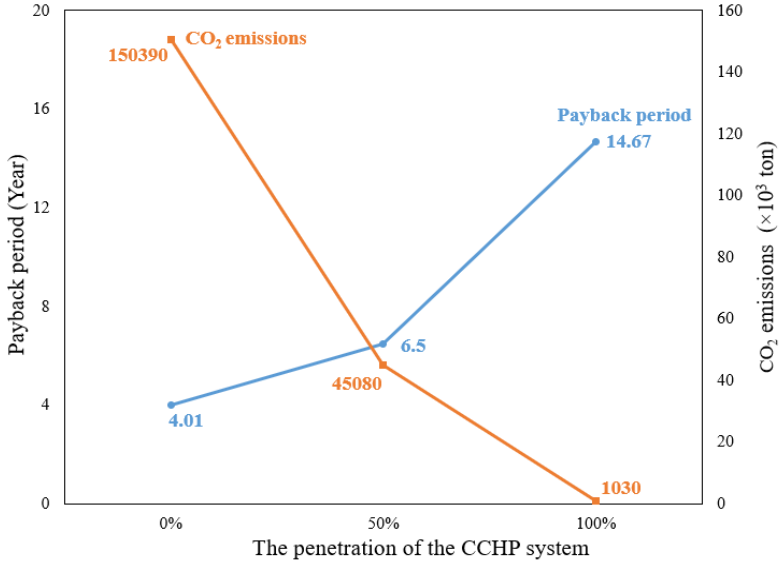

Fig.6-14 The economic and environmental performance of the CCHP system with different penetrations.

As Table 6-8 and Fig.6-14 show, although the annual total profit is better after adopting the CCHP system, the economic performance is worse as the penetration of the CCHP system increases. This is because the payback period is postponed as the increase of investment in the CCHP system. From Table 6-9 and Fig.6-14, we can see that the amount of carbon emissions is significantly reduced with higher penetration of the CCHP system. This is because the CCHP system uses natural gas as fuel, and the excess electricity generated by ICEs could be sold back to the grid and completely consumed by users. The power generated by clean energy, with high power generation efficiency, replaces the same amount of electricity from the grid which is produced by coal power plants. Therefore, to comprehensively consider the performance gap between systems with different penetration, the carbon tax was introduced to convert the environmental advantages of the CCHP system into economic advantages for comparison in the follow-up research.

6.4.3 Impact of different factors on the economic performance of CCHP system

In this section, we analyzed the economic influence factors of the CCHP system and compared the economic performance of the three CCHP systems with different penetrations with various changes in these factors.

Investment cost is one of the main factors affecting the economics of the CCHP system. In the future, as the cost of the ICE decreases, its economy will gradually improve.

Energy prices determine the operation cost and profit of the CCHP system, which directly reflect the economic performance of the CCHP system.

Supportive policy is one of the most effective measures that can contribute to the economics of the CCHP system. At present, an investment subsidy is available in Shanghai [13]. This investment subsidy is a direct grant provided by the government according to the installed capacity of the CCHP system during construction. With reasonable subsidies, the attraction of the investment into and installed capacity of the CCHP system can be improved.

With an emphasis on energy saving and emissions reduction, the implementation of a carbon tax can increase the operation cost of an energy system, because the energy becomes more expensive when imposing taxes on fossil energy consumption. Compared with the conventional system, the advantage of the CCHP system would be more obvious after employing a carbon tax due to the low emission character.

Therefore, how the above factors affect the economics of the CCHP system are discussed below.

The influencing factors and values were shown in Table 10.

Table 6-10 The changes in factors on the economic performance of CCHP system.

Factors		Changes
Penetration of CCHP system		0%, 50%, 100%
Investment cost of ICE decrease		0% to 50%
Energy prices	Electricity price	-50% to 50%
	Natural gas price	-50% to 50%
Investment subsidy		0 to 2 times the current subsidy[1]
Carbon tax		0 to 50 $/ton [38]

[1] According to the current subsidy policy of the CCHP system in China, the total subsidy is 430 $/kW at present (the U.S. dollar exchange rate against RMB is 1:7) [10, 39].

1) Impact of the investment cost of ICE on the economic performance of the CCHP system

Because the investment cost of the ICE is much larger than that of equipment in conventional system (electric chiller and gas boiler), the payback period is lengthened as the CCHP penetration improved. The impacts of changes in the investment cost of ICE on the payback periods of the considered CCHP systems are shown in Fig.6-15.

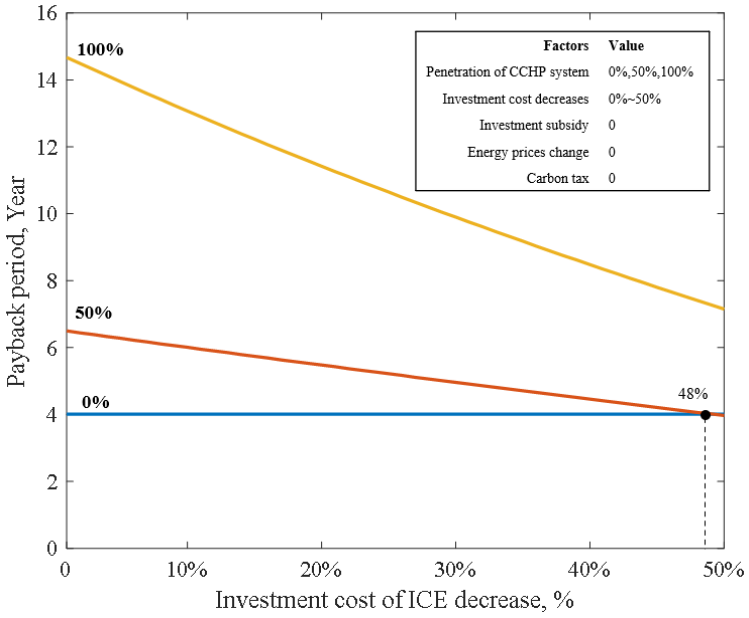

Fig.6-15 Impacts of investment cost.

As can be seen from Fig.6-15, the investment of the CCHP system needs to be reduced by 48% to achieve a shorter payback period for the CCHP system with 50% penetration, when compared to the conventional system (without CCHP). But the 100% penetration CCHP system is still unable to reach the same payback period as the conventional system (without CCHP), even the investment cost of ICE is reduced by 50%.

2) Impact of energy prices on the economic performance of the CCHP system

Energy prices determine the operating costs and profits of the system. With an increase of energy price subsidies, the operating profits of the CCHP system can be increased, thereby shortening the payback period. Fig.6-16 presents changes in the payback periods of CCHP systems with different energy prices. The electricity price and natural gas price increase or decrease by 10%, 20%, 30%, 40%, and 50%, respectively.

As can be seen from Fig.6-16a), the operating cost of the conventional system (without CCHP) increases with the electricity price, which leads to a longer payback period. On the contrary, the increase in electricity prices brings greater benefits for the CCHP systems with 50% and 100% penetration. Therefore, the payback periods of these two CCHP systems decrease as the electricity price increases. When the electricity price increases by more than 11.5%, the payback period of the CCHP system with 50% penetration can be shorter than that of the conventional system (without CCHP). For the CCHP system with 100% penetration, the electricity price needs to rise by 30%.

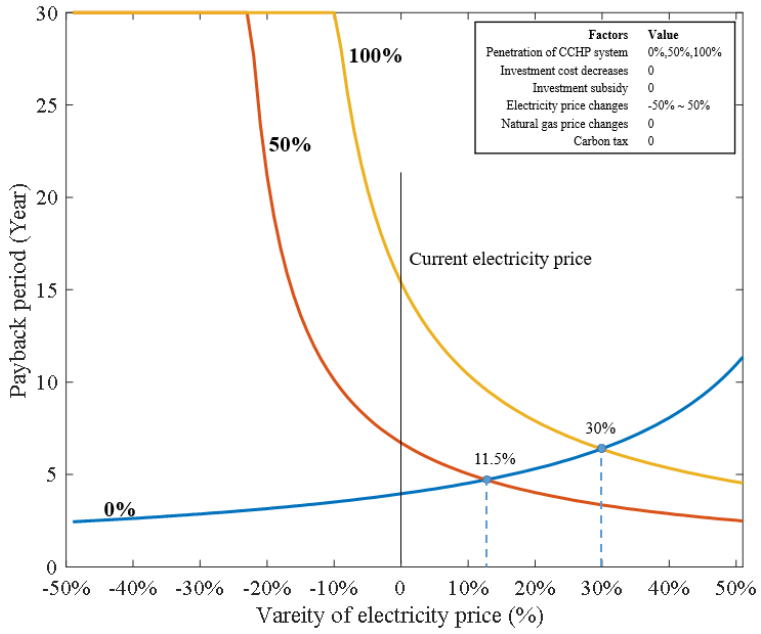

a)

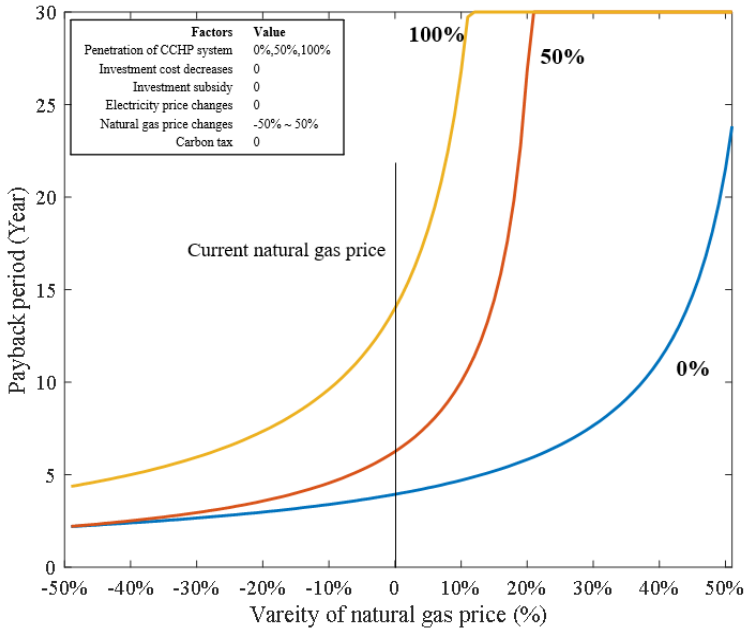

b)

Fig.6-16 The impacts of energy prices: a) Electricity price; b) natural gas price.

It can be seen from Fig.6-16b) that with the changes of natural gas price, the change trends of the payback period of the three systems are the same. As the three systems are all driven by natural gas, the operating costs increase with the increase in natural gas prices, which caused the extent of the payback period. The economic gap between the three systems decreases as the natural gas price reduces. But even with a 50% reduction, the payback period of the conventional system (without CCHP) is still optimal.

3) Impact of the investment subsidy on the economic performance of the CCHP system

Herein, we considered the current investment subsidy (430 $/kW) and increased it by 0 to 2 times to analyze the impacts on the payback period of the CCHP systems, as Fig.6-17 shows. According to figure, with the investment subsidy increases, the improvement of the economic performance of the CCHP system is significant. Under the current investment subsidy, the payback period of the CCHP system with 50% penetration is almost the same as that of the conventional system (without CCHP), which indicates that the current subsidy policy can bring economic advantages to the CCHP system. With the increase of investment subsidies, the penetration of the CCHP system can be increased. When the investment subsidy reaches more than 733$/kW (that is, 1.71 times the current subsidy), the 100% CCHP system will achieve better economic performance than the conventional system (without CCHP).

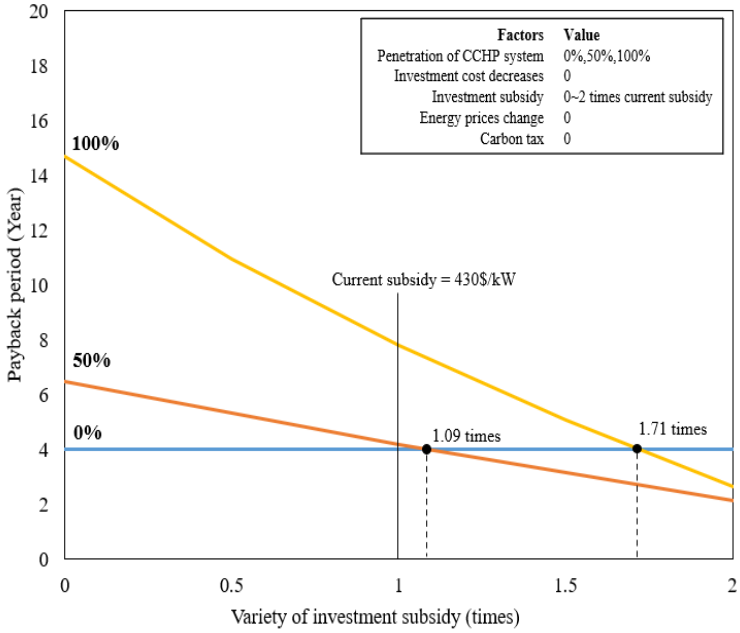

Fig.6-17 The impacts of the investment subsidy.

4) Impact of a carbon tax on the economic performance of the CCHP system

The purpose of a carbon tax is to create economic value from defined environmental benefits such as the reduction of carbon dioxide emissions. Fig.6-18 shows the changes of the payback period in the three systems when the carbon tax is increased.

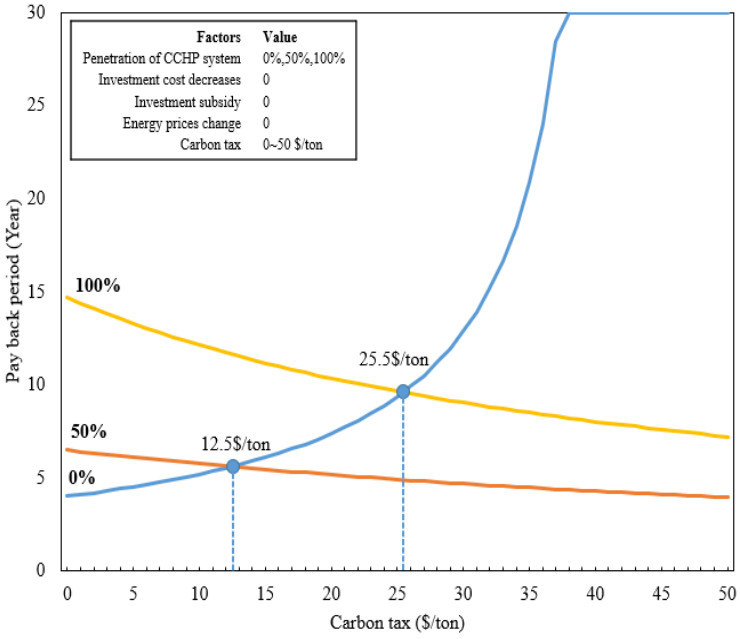

Fig.6-18 The impacts of the carbon tax.

The carbon tax has a positive effect on the economic performance of the CCHP system. With the increase of the carbon tax, the economy of the conventional system (without CCHP) decreases rapidly. When the carbon tax is more than 12.5 $/ton, it gives an economic advantage to the 50%

CCHP system even without other incentive policies. The more the carbon tax increases, the environmental advantage is more prominent with the penetration of CCHP system. When the carbon tax reaches 25.5 $/ton, the economic performance of the 100% CCHP system is superior to that of the conventional system (without CCHP).

6.4.4 Sensitivity analysis

In this section, an optimistic sensitivity analysis of the factors was conducted to obtain the effect of promoting the development of the CCHP system. The average degree of adjustment of natural gas and electricity price has been about 10% in the past [13], so 10% was selected as the sensitivity index. Since the carbon tax has not yet been implemented; according to IEA's World Energy Outlook 2014 forecast, the carbon tax of China's power generation sector will be positioned at 10$/ton in 2020. Therefore, the carbon tax will be analyzed with a sensitivity index of 10. The analysis results are shown in Table 6-11.

Table 6-11 Sensitivity analysis of economic factors affecting the CCHP system.

Factors		Variety	Interval	Mean sensitivity value
Investment cost of ICE		Decrease 0~50%	10%	16.43
Energy price	Electricity price	Increase 0~50%	10%	27.60
	Natural gas price	Decrease 0~50%	10%	28.75
Investment subsidy		Increase 0~50%	10%	7.45
Carbon tax		Increase 0~50	10	14.89

It can be seen from Table 6-11 that the adjustment of energy prices has the greatest impact on the economic performance of the CCHP system. From the results obtained in Fig.6-15, the increase in electricity prices can give economic advantages to the CCHP system. However, the economic performance of the conventional system (without CCHP) also improves with the decrease in gas prices. Although the economic gap between the conventional system and the CCHP system is decreasing, it is still too large for promotion of the CCHP system. Therefore, an increase in electricity price will be beneficial to the promotion of the CCHP system. Compared with other factors, the carbon tax has less effect on the economics of the CCHP system, but the introduction of a carbon tax will lead to an increase in the environmental costs of conventional systems, which could improve the economic competitiveness of the CCHP system. The levy of the carbon tax can significantly promote the development of the CCHP system.

6.5 Summary

This chapter evaluated the economic and environmental performance of the CCHP system based on its dynamic payback period and carbon dioxide emissions, and analyzed the impacts of different factors on the promotion of the CCHP system.

Taking a typical CCHP system of an amusement park resort in Shanghai, China, as a research case, the simulation of three CCHP systems with different penetrations was carried out. Based on the comparison of the different penetration, four factors (investment cost, energy prices, subsidies, and a carbon tax) affecting the economic performance of the CCHP system were discussed and compared through a sensitivity analysis.

Some conclusions from the results and analyses above include:

1. As the penetration of the CCHP system increase, carbon dioxide emission is reduced, but the economic performance worsens because of the large investment cost.

2. The impacts of prices: The economic performance of the CCHP system with 50% penetration can be better than that of the conventional system if the investment cost of ICE is reduced by 48%, or the electricity price is increased by 11.5%. To promote the CCHP system with 100% penetration, investment costs of ICE must be reduced by 76% or electricity prices increased by 30%.

3. The impacts of policies: The current investment cost and energy prices cannot be changed significantly in the short term. Therefore, incentive policies are an effective way to contribute to the economics of the CCHP system. The current subsidy can basically achieve the promotion of the CCHP system with 50% penetration. With an increase of penetration to 100%, the subsidy should increase to 1.71 times. Furthermore, the introduction of a carbon tax can highlight the superiority of the low-emission characteristics of the CCHP system. The CCHP system with 50% and 100% penetration will achieve economic competitiveness when the carbon tax reaches 12.5$/ton and 25.5$/ton, respectively.

4. According to the sensitivity analysis, electricity and gas prices have the greatest impact on the economics of the CCHP system. However, changes in gas prices cannot effectively reduce the economic gap between the CCHP system and conventional systems. Although the impact of a carbon tax on the economics of the CCHP system is not the largest, the environmental costs of the conventional system increase greatly with the development of carbon tax. Even if price concessions and subsidies were eliminated, the market competitiveness of the CCHP system will gradually increase. Therefore, it is necessary and significant to focus on the carbon tax for promoting the development of the CCHP system.

This chapter takes the CCHP system in an amusement park resort in Shanghai as an example to analyze the influence of different factors on the promotion of the DES. The results can provide guidance for improving the economics of the DES. In the future, with the increase of the carbon tax, the DES will become a better choice for investors.

There is fewer research on the energy supply systems of amusement parks which have high energy consumption. This paper can provide a reference for amusement parks to establish a CCHP

system to improve energy efficiency and reduce costs. However, the demand load, price mechanism and subsidies in different regions will be different. Therefore, the results will be different according to the specific research case. Nevertheless, the research method used in this paper has strong adaptability and practical application significance.

Appendix

Simulation model of three systems in detail:

System 1 (conventional system):

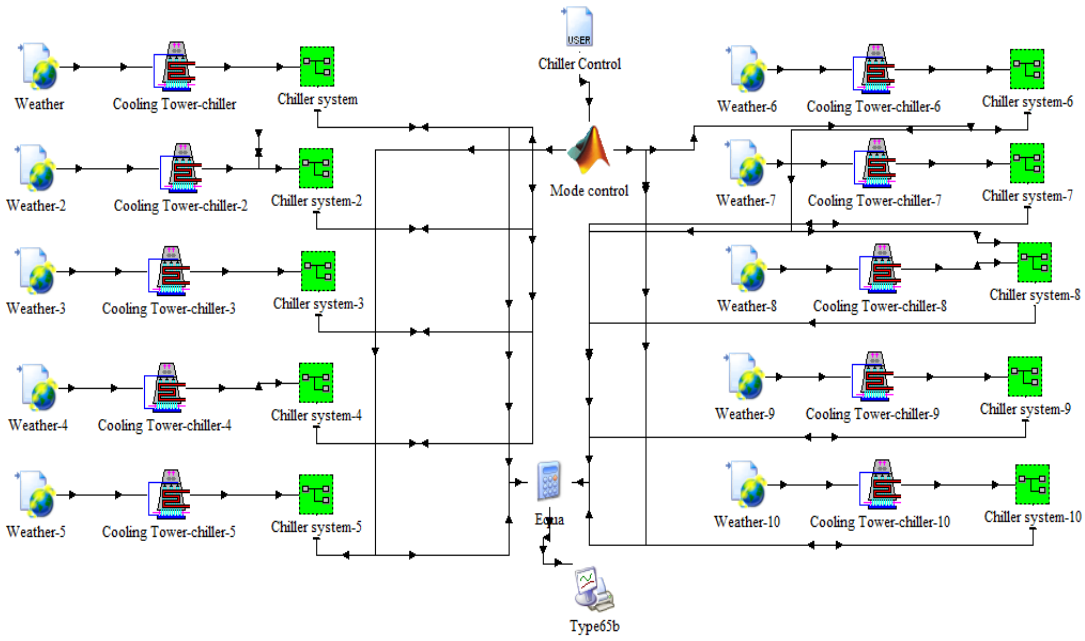

Fig.A6-1 The simulation diagram of System1

System 2 (current system): CCHP with 50% penetration:

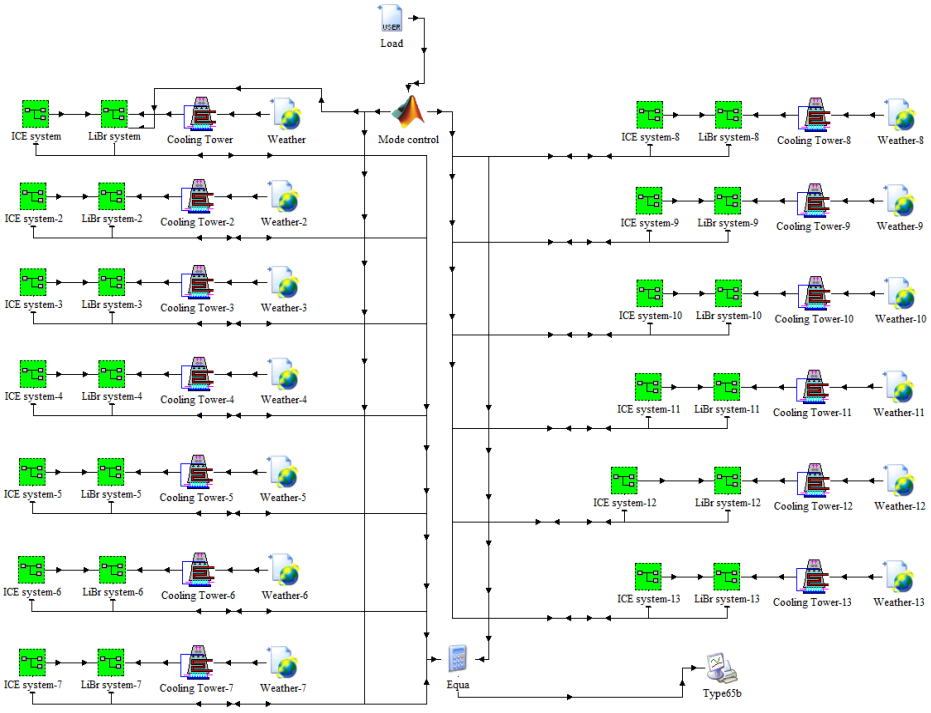

Fig.A6-2 The simulation diagram of System2

System 3 (target system):

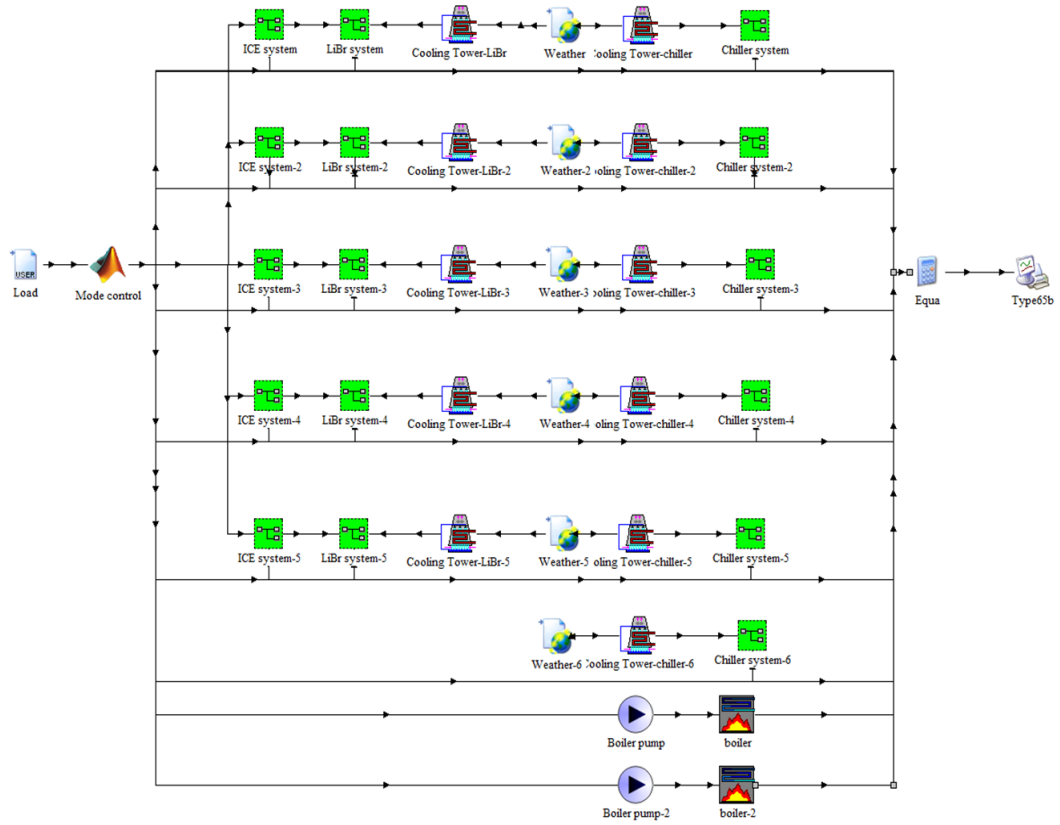

Fig.A6-3 The simulation diagram of System3

The technical parameters of the CCHP system:

1) The ICE

Table A6-1 Technical parameter of the ICE

Parameter	Value	Unit
Intake Air Temperature	20	°C
Jacket Fluid Temperature	74	°C
Jacket Fluid Flow Rate	97800	kg/hr
Oil Cooler Fluid Temperature	20	°C
Oil Cooler Fluid Flow Rate	1	kg/hr
Aftercooler Fluid Temperature	80	°C
Aftercooler Fluid Flow Rate	1	kg/hr
Specific Heat of Jacket Water Fluid	4.19	kJ/kg.K
Specific Heat of Oil Cooler Fluid	3.6	kJ/kg.K
Specific Heat of Exhaust Air	1.007	kJ/kg.K
Specific Heat of Aftercooler Fluid	4.19	kJ/kg.K
Rated Exhaust Air Flow Rate	24126	kg/hr

2) Absorption unit

Table A6-2 Technical parameter of the absorption unit

Parameter	Value	Unit
Chilled water inlet temperature	15.6	°C
Chilled water flow rate	97800	kg/hr
Cooling water inlet temperature	32	°C
Cooling water flow rate	355000	kg/hr
Steam inlet temperature	361	°C
Steam inlet gauge pressure	93.3	kPa
CHW set point	6	°C
Hot water inlet temperature	95.0	°C
Hot water flow rate	978000.0	kg/hr

Output of each equipment simulated in the TRNSYS model:

After setting the parameters, the modular can be connected and simulated to obtain the energy consumption and generation. In order to evaluate the accuracy of the simulation results, we compared the outputs of the CCHP system under full load simulation. In the cooling mode, the ICE is used to supply heat for the absorption unit to cooling, and the electric chiller is configured to supplement the insufficient cooling load. Fig.A6-4 shows the outputs of the CCHP system and the detail output of the absorption unit.

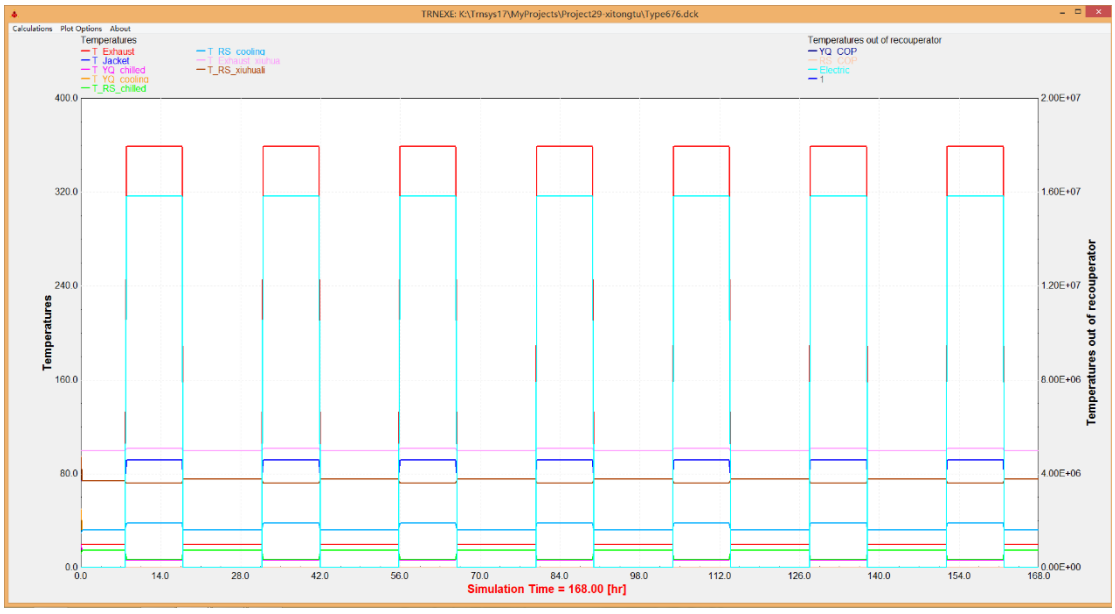

a)

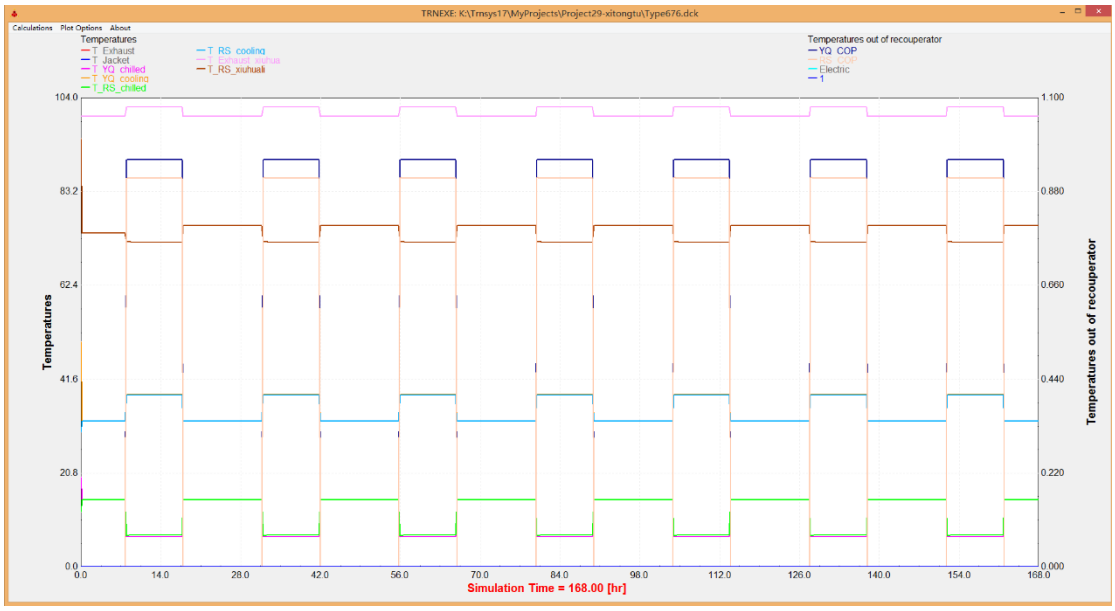

b)

Fig.A6-4 Outputs of the CCHP system under cooling mode: a) the outputs of the CCHP system; b) the outputs of the absorption unit

As the figures indicated, the power generation power of the ICE is 4401kW, and the power generation efficiency is 44.4%. The temperature of the exhaust gas is 359.6°C. The inlet temperature of cylinder liner water is 74°C, and the outlet temperature is 91.7°C. The temperature of exhaust gas after utilizing by the absorption unit is 101.9°C. The inlet temperature of chilled water provided by absorption unit is 15°C, and the outlet temperature is 6.67°C. The inlet temperature of cooling water is 32°C, and the outlet temperature is 38.2°C. The COP of the absorption unit is 0.955. The simulation results of CCHP system under the cooling mode show that all parameters are in reasonable range. It proves that the CCHP system model based on TRNSYS has high accuracy.

References

[1] Abbasi M, Chahartaghi M, Hashemian SM. Energy, exergy, and economic evaluations of a CCHP system by using the internal combustion engines and gas turbine as prime movers. Energy Convers Manag 2018;173:359–74. https://doi.org/10.1016/j.enconman.2018.07.095.

[2] Zhang X, Zeng R, Deng Q, Gu X, Liu H, He Y, et al. Energy, exergy and economic analysis of biomass and geothermal energy based CCHP system integrated with compressed air energy storage (CAES). Energy Convers Manag 2019;199:111953. https://doi.org/10.1016/j.enconman.2019.111953.

[3] Zhu X, Zhan X, Liang H, Zheng X, Qiu Y, Lin J, et al. The optimal design and operation strategy of renewable energy-CCHP coupled system applied in five building objects. Renew Energy 2020;146:2700–15. https://doi.org/10.1016/j.renene.2019.07.011.

[4] Li Y, Tian R, Wei M, Xu F, Zheng S, Song P, et al. An improved operation strategy for CCHP system based on high-speed railways station case study. Energy Convers Manag 2020;216:112936. https://doi.org/10.1016/j.enconman.2020.112936.

[5] Feng L, Dai X, Mo J, Shi L. Performance assessment of CCHP systems with different cooling supply modes and operation strategies. Energy Convers Manag 2019;192:188–201. https://doi.org/10.1016/j.enconman.2019.04.048.

[6] Wang JJ, Jing YY, Zhang CF. Optimization of capacity and operation for CCHP system by genetic algorithm. Appl Energy 2010;87:1325–35. https://doi.org/10.1016/j.apenergy.2009.08.005.

[7] Wu JY, Wang JL, Li S. Multi-objective optimal operation strategy study of micro-CCHP system. Energy 2012;48:472–83. https://doi.org/10.1016/j.energy.2012.10.013.

[8] Xi ZHANG, Ling YANG, Binbin HE, Aiping ZHANG FW. Calculation method of auxiliary power consumption rate for combined heating cooling and power distributed energy system. Therm Power Gener 2017;46:88–92.

[9] Lin B, Jia Z. The energy, environmental and economic impacts of carbon tax rate and taxation industry: A CGE based study in China. Energy 2018;159:558–68. https://doi.org/10.1016/j.energy.2018.06.167.

Chapter 7

PROMOTION AND UTILIZATION OF THE DISTRIBUTED ENERGY SYSTEM: A CASE STUDY OF EMERGENCY POWER SYSTEM

CHAPTER SEVEN: PROMOTION AND UTILIZATION OF THE DISTRIBUTED ENERGY SYSTEM: A CASE STUDY OF EMERGENCY POWER SYSTEM

PROMOTION AND UTILIZATION OF THE DISTRIBUTED ENERGY SYSTEM: A CASE STUDY OF EMERGENCY POWER SYSTEM *7-1*

7.1 Content 7-2

7.2 Reliability and economic analysis of emergency power system integration 7-2

7.2.1 Overview of the Issues 7-2

7.2.2 Methodology of emergency power system optimization 7-3

7.2.3 Application of the emergency power system integration 7-11

7.2.4 Impact of characteristics parameters of EPSs on the total cost 7-16

7.3 Reliability and economic analysis of distributed generation as emergency power ... 7-18

7.3.1 Reliability analysis of power system 7-18

7.3.2 Case comparison 7-19

7.3.3 Results and discussion 7-23

7.4 Summary 7-28

Appendix： 7-29

Reference: 7-32

7.1 Content

The main function of a power system is to supply power to users under optimal operating costs with the assurance of a reasonable quality and continuity at all times [1]. Reliability refers to the probability that a power system will perform its functions correctly within a specific time when it is under normal operating conditions [1,2]. For a regional power system, the utilization of emergency power systems (EPSs) is an effective means to ensure the reliability by installing some small and localized power generators to supply emergency power on the demand side, which are used to avoid an unacceptable impact during power outages. This chapter is aimed to analyze the reliability improvement of the power supply in a building complex with the utilization of the DES as emergency power system. The research on the emergency power system is divided into two parts in this chapter. Firstly, based on the probability of power outage occurrence at each load point in the region, the emergency power system is optimized to improve the regional reliability with the least cost; Secondly, in the case of power failure in the whole region, the distributed energy system is considered as the emergency power and combined with the diesel generators to analyze its impact on reliability and economy.

1) EPSs are essential for buildings to ensure safety and necessary economic activities during power outages. They are usually adopted diesel generators and installed independently in each building. It is found that poor management and maintenance of the separate EPSs will reduce the reliability of the system as well as increase the operating cost. In a building complex, due to the different probability of failure in the distribution network, the time that power outages occur in each building is different. Thus, an emergency power system integration model was analyzed and proposed to improve the reliability of the building complex with the lowest cost. By connecting stand-alone emergency power systems of adjacent buildings with micro-network to form mutual standby system and help each other, the integrated emergency power system was established. The emergency power systems supply the power to their own buildings preferentially according to the reliability requirement and the emergency power demand of the buildings, and the excess power is dispatched to other insufficient buildings through the micro-network. Therefore, the overall reliability and economy can be improved through resource sharing and mutual backup.

2) When all the buildings lose the power source from the utility grid, the building complex relies on the emergency power systems to provide critical load. In this case, the reliability of the emergency power system is the key factor to reduce power outage loss. By “islanding” from the grid in emergencies, the distributed energy system has the potential to improve the reliability of the distribution system, reduce pollution and reduce the energy consumption cost of the diesel generators. The combination of the distributed energy system and the emergency power system using diesel generators can improve the overall reliability of the power supply system, reduce interruption cost and improve system economy. After integrating with the distributed generation, the reliability of the overall power system will be changed. The configurations of distributed generation and the connection modes of the power generators will affect the reliability of the power supply system. This chapter discussed and analyzed the reliability and economic performance of distributed energy systems as emergency power by comparing four case studies with different integrations of diesel generators and the gas internal-combustion engine.

7.2 Reliability and economic analysis of emergency power system integration

7.2.1 Overview of the Issues

The improvement of power supply reliability is a principal issue for modern society [3]. Since the 21st century, the safety and reliability of power system operation have greatly improved. However, power outages still occur occasionally as a result of extreme weather or even equipment and man-made faults [4], such as Italy blackout in 2003, Western Europe blackout in 2006, India power shortage in 2010 and New York blackout in 2019 [5–7]. The power grid is fragile, and various unexpected events can lead to unexpected results and serious losses. Power outages not only cause huge economic losses, but also threaten people's lives. Therefore, improving the reliability and safety of the power system is critical for developing the power grid.

Emergency power systems (EPSs) are a vital part of the power system [8]. Hospitals, airports, industries, transportation centers, commercial facilities, and others rely on the emergency power systems to provide electricity for their critical loads during power outages. Critical load refers to the first level load that will endanger personal safety and significant economic loss when such devices and equipment (e.g. lights, elevators) fail to operation [9]. The diesel generator with the characteristic of power generation stability and fast start is the conventional configuration of emergency power systems. And in the design stage, the emergency power system is stand-alone in the buildings it serves without connecting to other power system, and its installed capacity is usually equal to or larger than the critical load. Because it is a backup power system and only uses when power outages occur in the building, which led to the low utilization rate even idle. During the 2003 blackout in North America’s power system grid, over half of the standby generators in about 58 hospitals in New York failed to start and had to transfer patients to other hospitals [10]. Lessons learned from power outages around the world indicate that the situation of the emergency power system failure will increase as a result of inadequate management and maintenance, operational errors, equipment failures, etc. [11,12]. Therefore, research on the design and management of emergency power systems to improve safety as well as to reduce cost is necessary.

Integration of the stand-alone emergency power systems in a building complex is a way to improve the reliability and reduce the total costs based on the concept of energy network [13–15]. By connecting stand-alone emergency power subsystems to form a micro-network in the building complex, the integrated emergency power system can cooperate and be backup for each other. Because the system cost is growing with the increase of the installed capacity, but the power outage loss is in the opposite. System installed capacity reduction will cause the increase of power outage loss [16]. Therefore, to improve the reliability as well as to minimize cost of the integrated emergency power system is the focus of this section.

To assess the reliability of the power supply of the building complex, the power outage should be simulated firstly. A power outage probabilistic model of the building complex was established by Monte Carlo simulation to calculate the Average Service Availability Index (ASAI) and Expected Energy Not Supplied (EENS), which were used as the power supply reliability evaluation indexes. After that, taking self-priority as the basic dispatch strategy, an integration and dispatch model was simulated in Matlab. The EPSs supply the power to their own buildings preferentially according to

the reliability requirement and the emergency power demand of the buildings, and the excess power is dispatched to other insufficient buildings through the micro network. Thirdly, taking the total cost model including economic loss during power outages and system costs as the objective function, Genetic Algorithm was used to obtain the optimal configuration and dispatch strategy. Comparing the ASAI and total cost of the stand-alone emergency power system (SEPS) and the integrated emergency power system (IEPS), the superiority of the model was indicated. Finally, a sensitivity analysis of some factors influencing the total cost of the building complex was carried out in this paper. The research flow of this paper is shown in Fig.7-1.

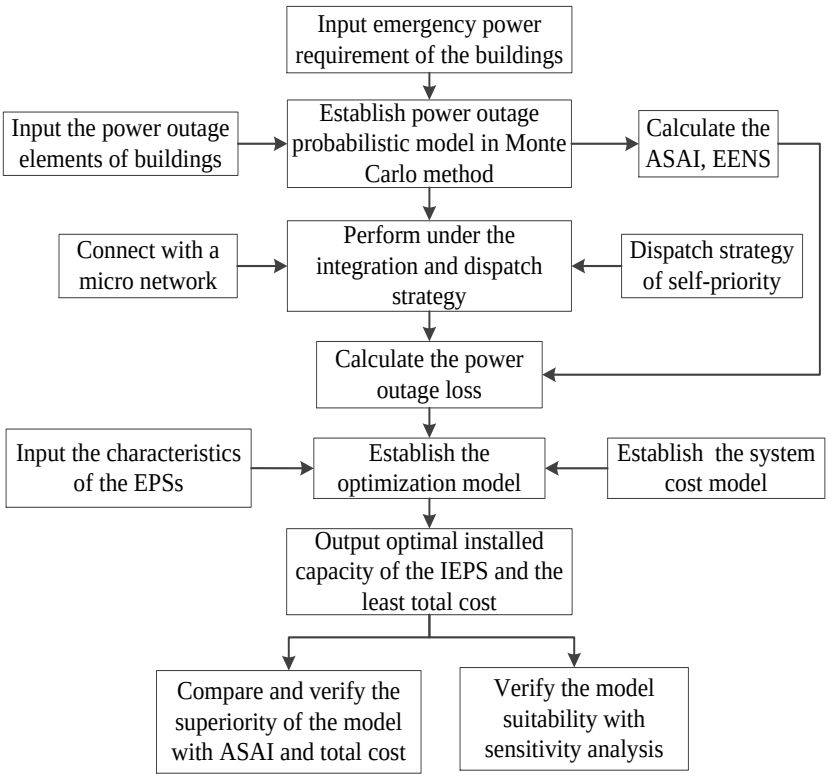

Fig.7-1 The research flow diagram

7.2.2 Methodology of emergency power system optimization

7.2.2.1 Power outage probabilistic model of a building complex

(1) The reliability assessment index of power system

Expected Energy not Supplied (EENS) refers to the expected energy load that is not delivered at the load point in demand side because of unexpected power outages. EENS can be used to evaluate the economy and the reliability of the power system. EENS can be expressed mathematically as Equation (7-1) [24].

$$EENS_k^t = \lambda_k r_k L_k^t \tag{7-1}$$

where, $EENS_k^t$ is the expected energy not supplied of building$_k$, kWh. λ_k is the failure rate of building$_k$. r_k is the power outage duration, hours. L_k^t is average load of the buildings at t-time, kWh.

(2) Power outage loss calculation

The power outage loss is divided into direct economic loss and indirect economic loss. The former refers to losses incurred during and after the actual outage; the latter refers to additional costs incurred by users to reduce the outage, adjust their activities, or adopt standby energy sources [19]. The direct economic loss increased sharply at the instant of power outages and increased with the duration of power outage. However, the growth rate decreases with the duration of outage [20]. The indirect economic loss increases with the duration of the outage, and the growth rate of different types of building losses is different. The composite customer damage function (CCDF) [21] is used to express the relationship between outage loss and outage duration, considering the loss characteristics of different types of users. The composite customer damage function is obtained as follows:

$$f_{CCDF}(T_{outage}) = \sum_{i=1}^{n} \frac{c_i \times k(T_{outage})}{N_i} \tag{7-2}$$

Among them, i is the type i customer (the type of users include residence, industry, government, and so on); n is the number of categories of users, c_i is the proportion of power consumption of the type i customer, k(T_{outage}) is the unit power outage loss of the type i customer, \$/kWh, it can be obtained by investigation [22]. T_{outage} is the duration of power outage, h. N_i is the load rate of the type i customer.

According to the Ref. [23] based on its research data, the function can be estimated as Equation (7-3).

$$f_{CCDF}(T_{outage}) = 18.989{T_{outage}}^{0.4156} \tag{7-3}$$

Therefore, the formula for calculating the annualized power outage loss is calculated as follows:

$$C_{outage_k} = \sum_{t}^{8760} \left[\mathrm{f}_{CCDF}(T_{outage}) \times EENS_k^t\right] \tag{7-4}$$

(3) Monte Carlo simulation

The Monte Carlo simulation (MCS) method is based on the principle of mathematical statistics, also known as the stochastic simulation method. This method uses large-scale stochastic number sequences to simulate complex systems. As the number of simulations increases, a stable conclusion can be obtained by averaging the estimates of each statistic or parameter, thereby receiving certain parameters or important index. Its advantage is that it considers the probability of all situations in which an event may occur. Power outages are unpredictable, but a probabilistic model based on MCS can be established according to the failure rate, failure duration and repair rate of the load point to obtain EENS of the buildings. The Monte Carlo simulation process for this research is as follows:

1) Enter the setting parameters

Input basic data of region, building and each load point, including: The failure rate λ_k, the power outage duration r_k, the average load of load point L_k.

2) Simulated power outage initial time and duration of the load point

In order to ensure the fineness of the analog data, combined with the power emergency device startup characteristics, select the appropriate time interval and split the year into N time segments. Based on the reliability parameters of the load point, the time point at which the power outage occurs will be randomly obtained.

The power outage duration is set to conform to the standard normal distribution, and the corresponding average power outage duration is taken as the expected value of the standard normal distribution. The power outage duration is randomly selected in this distribution.

[0,1] is used to record whether there is power outage in this time interval. 0 means power outage is not happened and 1 is power outage occurrence, shown as Equation (7-5). The power outage state matrix of each load point divided by time interval in a year is obtained. The Fig. 7-2 examples the power outage state matrix of a load point. As the matrix reveals, the power outage occurred at the $2N^{th}$ moment, and the duration of the outage is $x \times N$. The kN^{th} moment also occurred power outage, and the duration of power outage is $y \times N$.

$$i = \begin{cases} 0, \ Power\ supplying \\ 1, \ Power\ outage\ occuring \end{cases} \tag{7-5}$$

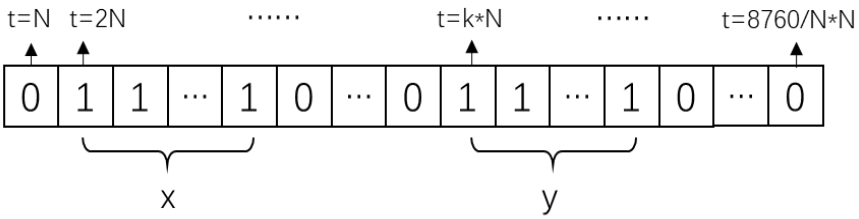

Fig.7-2 The example of power outage state matrix

3) Calculation of power loss load and the power outage duration of the building

According to the last step, the power outage state matrix of each load point is obtained. The matrix is multiplied by the critical load of each load point to obtain the outage load loss of each time interval. The load point outage loss of each time interval is accumulated. When there is outage loss, the power outage status of the building is recorded "1". Therefore, we can obtain the power outage status and power outage load loss of the building, as shown in Fig. 7-3.

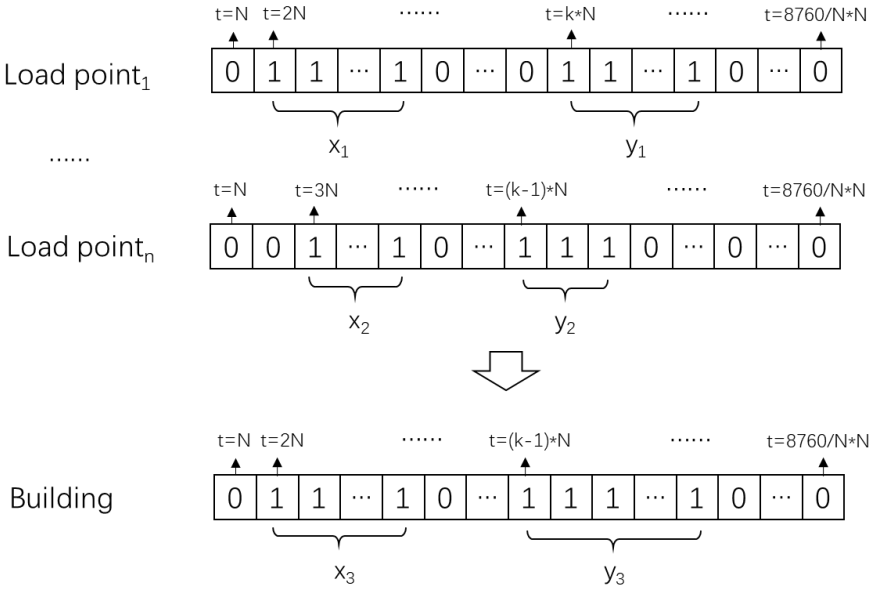

Fig.7-3 The accumulation of power outage state matrix

4) Calculation of EENS and annual outage duration

In the same way, the building outage loss of each time interval is accumulated. When there is outage loss, the power outage status of the building complex is recorded "1". Therefore, we can obtain the power outage status and power outage load loss of the building complex. Then, the EENS for each time interval is obtained. And the cumulative time interval is the annual outage duration, which can be used to calculate the ASAI.

Monte Carlo simulation can simulate all cases of power outage occurred in the building complex and obtain the EENS every simulation interval. Therefore, the results simulated through MCS can be seem to the average EENS of buildings.

7.2.2.2 Emergency power system (EPS) model

(1) Emergency power demand after adopting EPS

The emergency power systems in the buildings are expressed as EPS_1, EPS_2, ..., EPS_i, ..., EPS_k, ..., EPS_p. $EENS_k^t$ is the emergency power demand of $building_k$ at t-timeslot, calculated by the power outage probabilistic model in section 7.2.1.1. The EPS_k will be turned on to satisfy the critical loads of the $building_k$ when the power outages were happened. The remaining loss load ($\Delta EENS_k^t$) can be calculated as shown in Equation (7-6).

$$\Delta EENS_k^t = \begin{cases} 0 & EENS_k^t < Ge_k^t \\ EENS_k^t - Ge_k^t & EENS_k^t \geq Ge_k^t \end{cases} \tag{7-6}$$

where, Ge_k^t is the power supplement provided by EPS_k at t-timeslot. t is the running time of the EPS_k.

The calculation of Ge_k^t is obtained as follows:

$$Ge_k^t = \begin{cases} V_k \times t \times AF_k & t < SD_k \\ Cp_k \times AF_k & SD_k \le t \le CT_k \\ 0 & CT_k \le t \le FRT_k \end{cases} \quad (7\text{-}7)$$

where, V_k is ramping rate of the EPS_k, %. SD_k is the startup time of the EPS_k, hour. Cp_k is the installed capacity of the EPS_k, kW. AF_k is the available factor which is a reliability index of the equipment in EPS_k, %, obtained according to the actual equipment. CT_k is the maximum support time of the EPS_k, hour. The total energy supply time of the EPS does not exceed the support time. If it exceeds the support time, it needs time to refuel. FRT_k is the fuel replenishment time, hours.

(2) The costs of EPS

The costs of the EPS (C_{EPS}) in the building complex is divided into three parts: annualized investment cost (AIC), annualized operation cost (AOC) and annualized maintenance cost (AMC), which are calculated as follows:

$$\mathrm{AIC}_k = Cp_k \times IN_k \times R \quad (7\text{-}8)$$

$$R = \frac{r(1+r)^n}{(1+r)^n - 1} \quad (7\text{-}9)$$

$$\mathrm{AOC}_k = Cp_k \times f_k \times H_k \quad (7\text{-}10)$$

$$\mathrm{AMC}_k = Cp_k \times M_k \quad (7\text{-}11)$$

$$C_{EPS_k} = \mathrm{AIC}_k + \mathrm{AOC}_k + \mathrm{AMC}_k \quad (7\text{-}12)$$

where, IN_k is the investment per unit capacity per year, $\$/\mathrm{kW}\cdot\mathrm{yr}$. R is the capital recovery factor. r is the interest rate, and n is the lifetime of the equipment. f_k is fuel cost per unit capacity per year, $\$/\mathrm{kW}\cdot\mathrm{yr}$. H_k is the utilization hours per year. M_k is the maintenance cost per unit capacity per year, $\$/\mathrm{kW}\cdot\mathrm{yr}$.

7.2.2.3 Integration and dispatch strategy model

In a building complex, by connecting stand-alone emergency power subsystems and being backup for each other, the integrated emergency power system (IEPS) can serve several buildings in a more safe and economic manner. Therefore, a micro-network of the building complex was created to establish the integration and dispatch model of EPSs in a building complex to achieve this purpose. The concept schematic diagram of the stand-alone emergency power system (SEPS) and the integrated emergency power system (IEPS) was displayed in Fig.7-4.

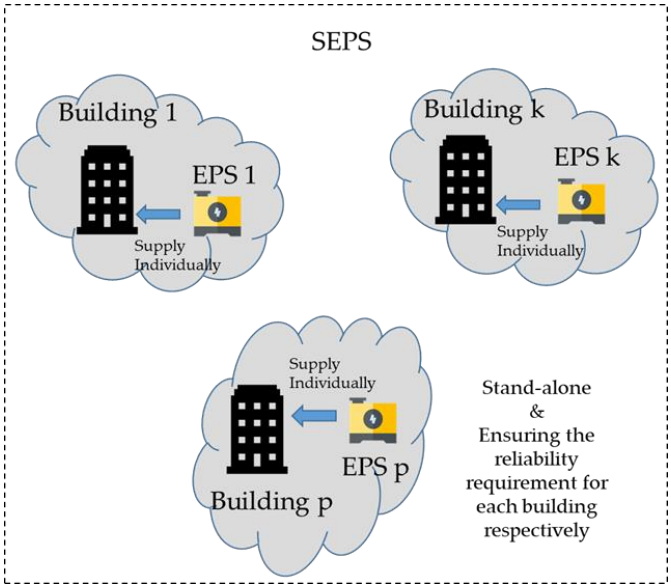

a)

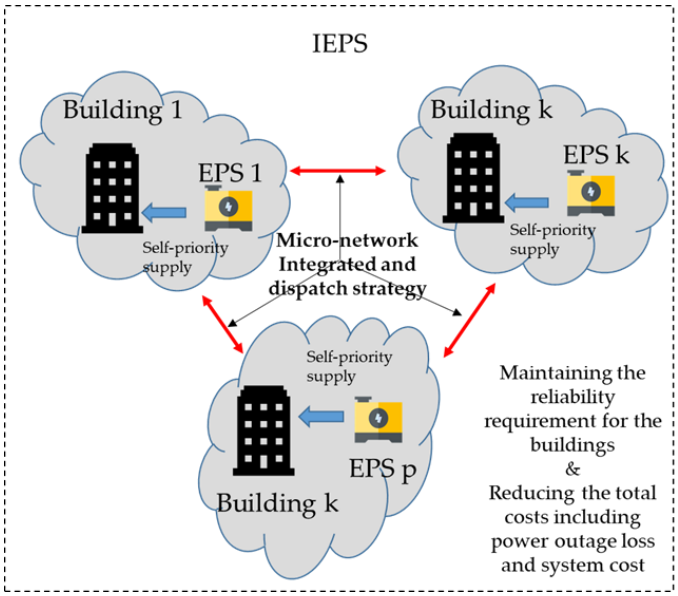

b)

Fig.7-4 The schematic diagram of stand-alone emergency power system (SEPS) and integrated emergency power system (IEPS).

First, taking self-priority as the basic dispatching strategy, EPS_k should guarantee its own emergency power supply of $building_k$. When the Ge_k is more than the power outage demand load of the $building_k$ ($EENS_k$), there is still $rest_k$ remaining available for other buildings. When the Ge_k is less than the power outage demand load of the $building_k$ ($EENS_k$), there is still a lack of $\Delta EENS_k$ that cannot be compensated and it can be provided by other EPSs ($Rest_1'$, $Rest_2'$,…) until $\Delta EENS_k$ is satisfied. The reliability of the micro network $AF_{network}$ also needs to be calculated. Thus, the power outage demand load is reduced to $EENS_k'$ after dispatching the emergency power. Therefore,

after integrating and dispatching the EPSs, the total power outage demand load of the building complex is the sum of the EENS' of all buildings at t-timeslot. The logic diagram of the integration and dispatch model is shown in Fig.7-5.

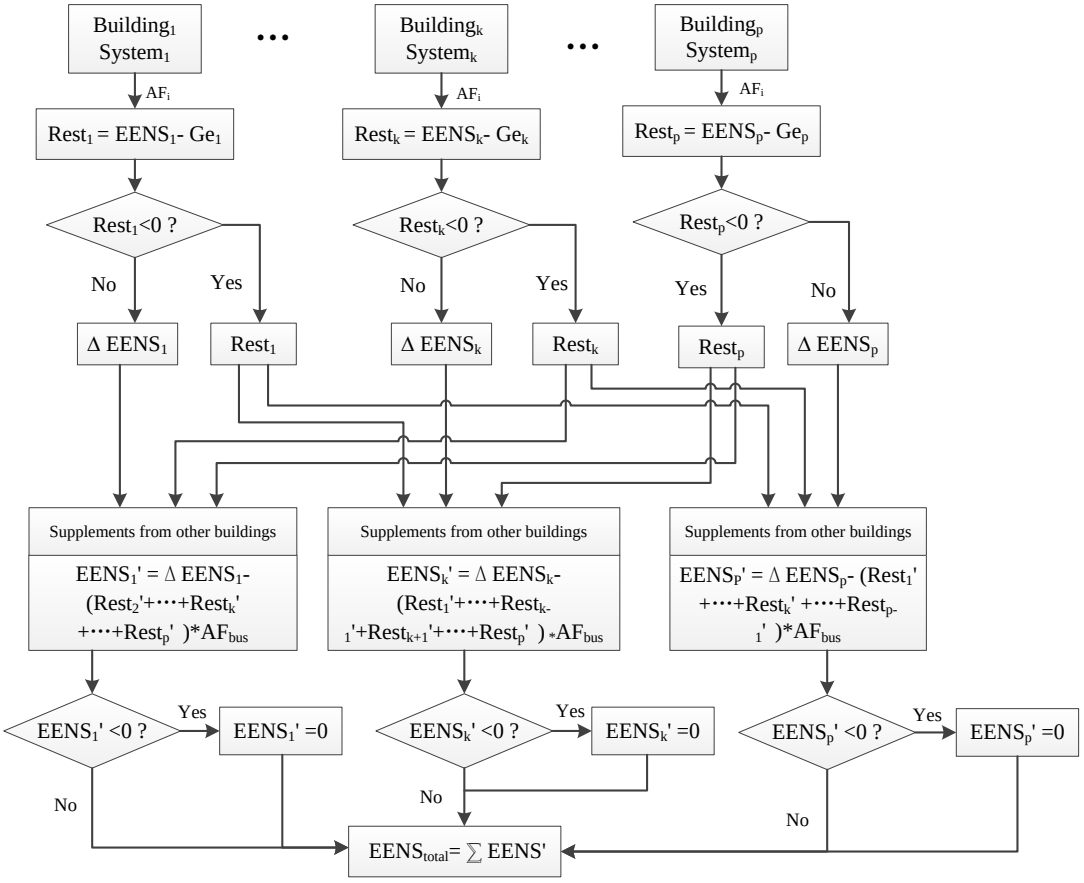

Fig.7-5 The logic diagram of the integration and dispatch strategy model.

And the integration and dispatch process are obtained as followings.

$$Rest_k^t = Ge_k^t - EENS_k^t \tag{7-13}$$

$$\Delta EENS_k^t = \begin{cases} 0 & Rest_k^t < 0 \\ -Rest_k^t & Rest_k^t \geq 0 \end{cases} \tag{7-14}$$

$$EENS_k^{t'} = \begin{cases} \Delta EENS_k^t - AF_{network} \times \sum_{j=1}^{p} Rest_k^{t'} (j \neq k), & EENS_k^{t'} > 0 \\ 0 & EENS_k^{t'} \leq 0 \end{cases} \tag{7-15}$$

$$EENS_{total}^t = \sum_{k=1}^{p} EENS_k^{t'} \tag{7-16}$$

7.2.2.4 The Optimization Simulation

As Fig.7-6 shows [25], an increased level of reliability usually involves significant investments in equipment and infrastructure. And a reduction in reliability involves financial power outage loss of users because of the increase of interruptions. For these reasons, it is essential to figure out the optimal installed capacity of the EPSs, in order to minimize the total cost of reliability (composed by the power outage loss and the necessary cost to improve the level of reliability).

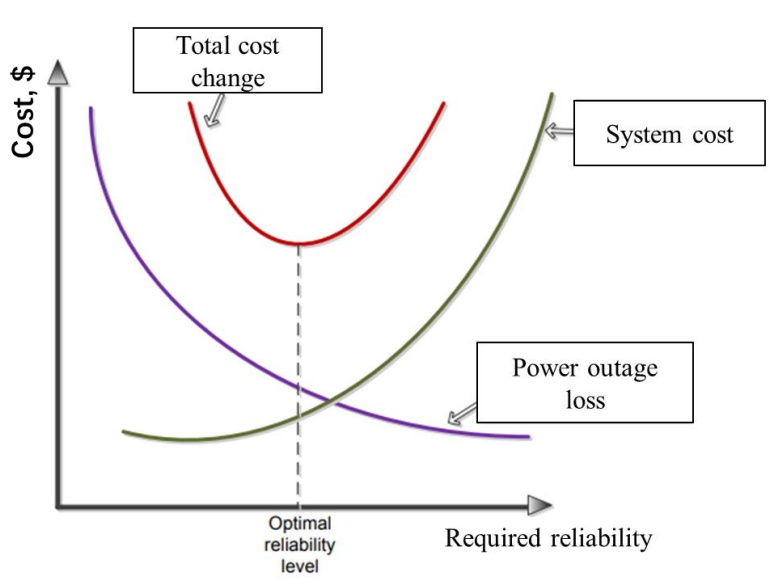

Fig.7-6 Cost changes with the increase of the reliability

The main objective function of this research work is to minimize the total costs while satisfying the power reliability requirements of demand side. Mathematically, the objective function model, the total cost (C_{total}), of the proposed emergency power system can be expressed as follows:

$$\mathrm{F} = \min(C_{total}) = \min \sum_{k=1}^{p} (C_{outage_k} + C_{EPS_k}) \tag{7-17}$$

Based on the above analysis, the installed capacity determines the power supply reliability and system cost of the IEPS. After determining the installed capacity, we can obtain the impact of improvement the power supply safety of the building complex and the reduction of system cost. Therefore, Cp_k are optimized in this model.

There are constrains as follows:

a) To optimize the capacity of the emergency power system, it is necessary to reduce excess investment. Therefore, the total installed capacity of the new scheme, that is, the sum of the installed capacity of each subsystem of the new scheme should be less than or equal to initial installed capacity.

$$\sum_{k=1}^{p} \mathrm{Cp}_k \leq \sum_{k=1}^{p} \mathrm{Cp}_{k,0} \tag{7-18}$$

where, $Cp_{k,0}$ is the initial capacity of EPS_k.

b) The reliability of the building complex should be improved:

$$ASAI^t \geq ASAI_0^t \tag{7-19}$$

where, $ASAI_0^t$ is the initial average service availability index.

In this paper, genetic algorithm is used to solve the optimization model. The genetic algorithm optimization logic diagram is as follows Fig.7-7:

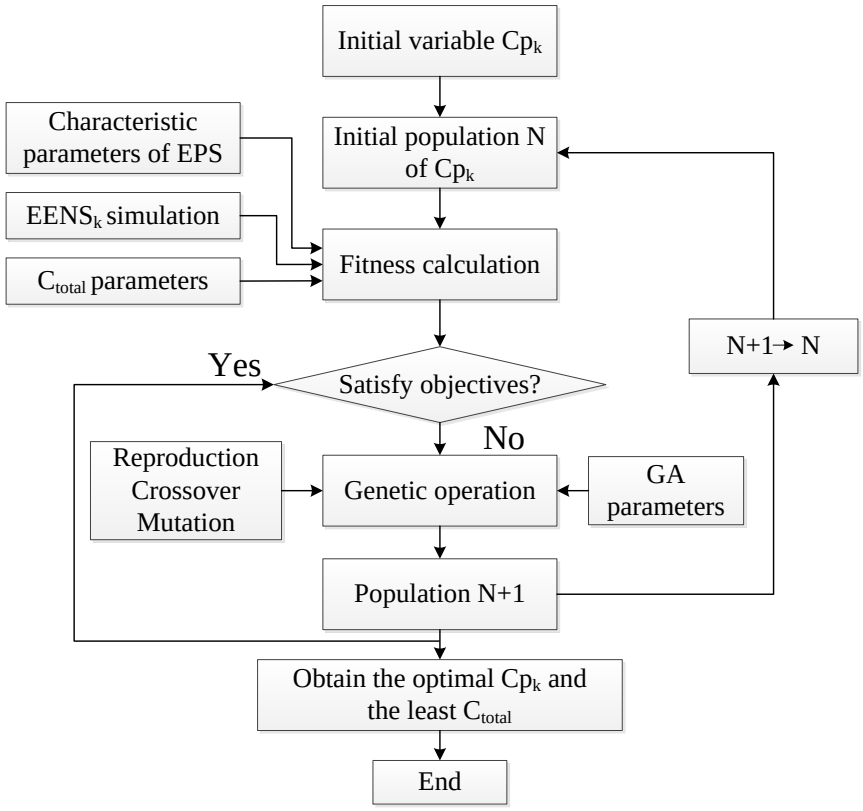

Fig.7-7 Genetic algorithm logic for the optimization model

7.2.3 Application of the emergency power system integration

7.2.3.1 Case study introduction

In this section, the integration and dispatch model was verified in a building complex in a certain region of Shanghai, China. The building complex included three adjacent buildings, which were a commercial high-rise building ($Building_1$), an office high-rise building ($Building_2$), and a central business district building ($Building_3$) (hereinafter referred to as B_1, B_2, B_3). The schematic diagram of the distribution network of the building complex and the reliability parameters are shown in Appendix. The information of the three buildings is shown in Table 7-1 below. To meet the reliability requirements of the critical load of each building, EPSs are stand-alone allocated in each building. Their initially capacity is set as the critical load of its own building, shown as Fig.7-8.

Table 7-1 The information of the building complex

Buildings	$Building_1$	$Building_2$	$Building_3$
The type of building	Commercial	Office	Central business district
Average load	4935kW	4985kW	7298kW
Critical load	1819kW	2165kW	1473kW

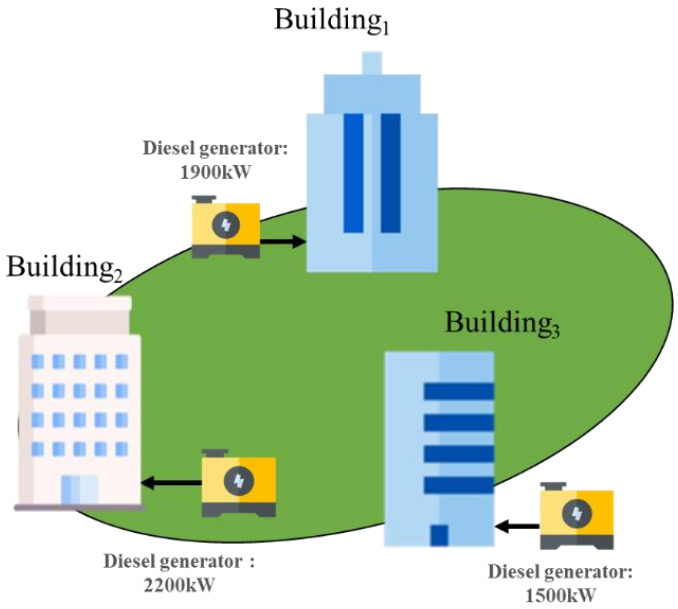

Fig.7-8 Schematic diagram of stand-alone emergency power systems.

The EPSs of these three buildings are adopting diesel generator, which is common form of backup power. According to the investigation, the parameters of the diesel generation are shown in Table 7-2.

Table 7-2 The parameters of diesel generation [8,20]

Parameters	Value
AF_k	99.854%
Failure rate	0.032
Repair rate	21.8920
CT_k (h)	12
SD_k (h)	1/6
IN_k (\$/kW)*	300
f_k (\$/kWh)*	0.23
M_k (\$/kWh)*	0.01258
FRT_k (h)	24

*(The U.S. dollar exchange rate against RMB is 1:7; The U.S. dollar exchange rate against JPY is 1:105).

7.2.3.2 Results of the power outage probabilistic model

In order to simplify the simulation of the startup phase of the emergency system, select 10 minutes as the interval and split the year into 52,560 time periods. According to the power reliability parameters of load point (The information for details of the load point is in appendix), the ASAI and EENS of three buildings simulated in MCS are shown in Fig.7-5. Daily EENS in one month (March) as an example was demonstrated in Fig. 7-9 a).

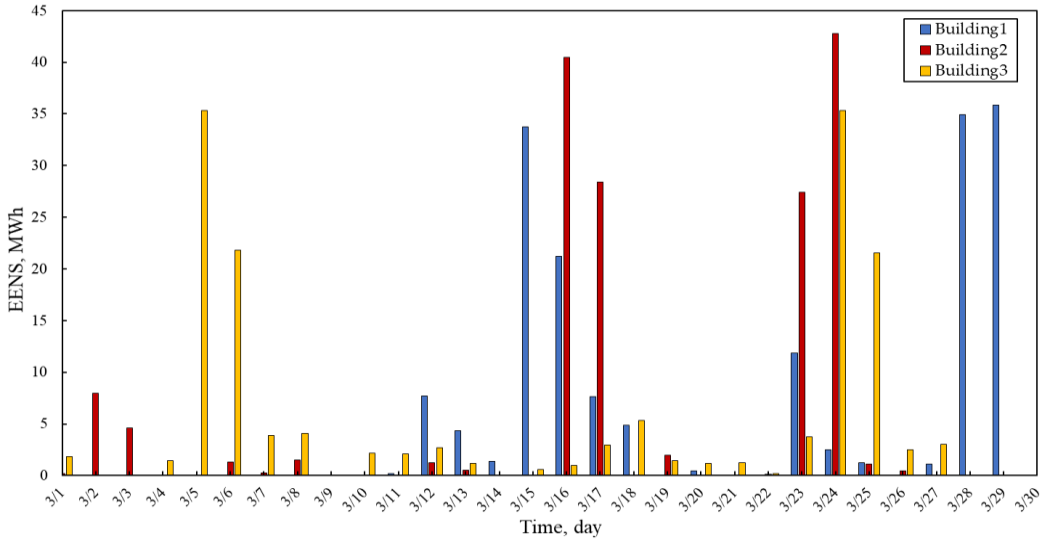

a)

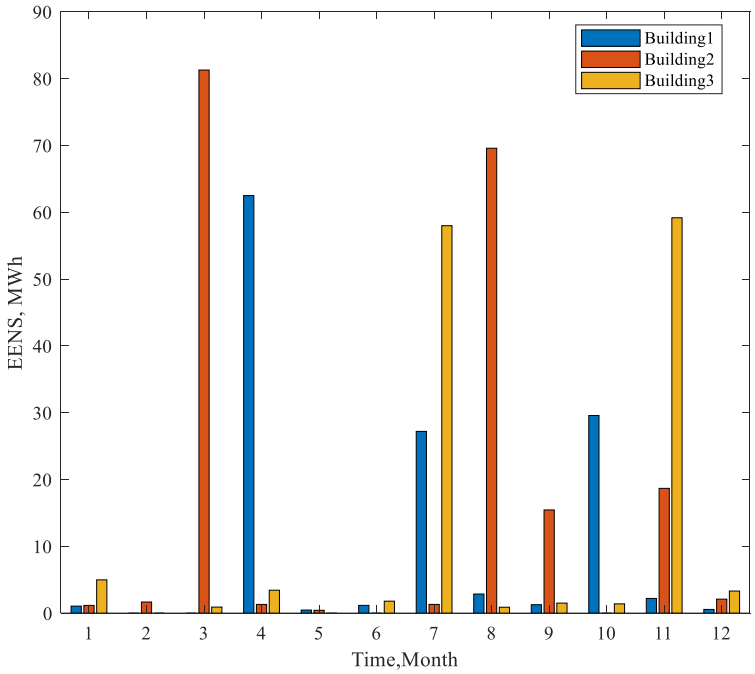

b)

Fig.7-9 EENS of three buildings simulated by MCS: a) every day in one month; b) every month in one year

It indicated that there three situations occur: 1) Only one building occurred power outage in one day (for example, only building$_3$ occurred power outage on 3/1, only building$_2$ occurred power outage on 3/2, only building$_1$ occurred power outage on 3/14); 2) Two buildings occurred power outage at the same time (for example, building$_2$ and building$_3$ both occurred power outage on 3/6, building$_1$ and building$_3$ both occurred power outage on 3/27; 3) All three buildings occurred power outage at the same time (for example, there are power outage in three buildings on 3/16, 3/17, 3/23, 3/24 and 3/25. Due to the different reliability and critical load of distribution network of each building, the power outage duration and power outage loss are also different. Fig. 7-9 b) shows the EENS of three buildings per month in a year.

According to the simulation results of MCS， the ASAI and total EENS of the building complex can be calculated, as listed in Table 7-3.

Table 7-3 The reliability and total power outage loss of the building complex

Reliability index	Data
$EENS_{total}$ (MWh)	457
Total power outage loss (million $)	2.59

7.2.3.3 Results of the integrated emergency power system application

Two systems are compared in this section to analyze the advantage of integrated emergency power system:

SEPS: There are stand-alone EPSs in the three buildings, and they cannot be integrated and dispatched to each other. In SEPS, the $rest_k$ is 0.

IEPS: The EPSs are integrated and dispatched through the micro network in IEPS.

Fig.7-10 and Table 7-4 are obtained after simulating the integration and dispatch model.

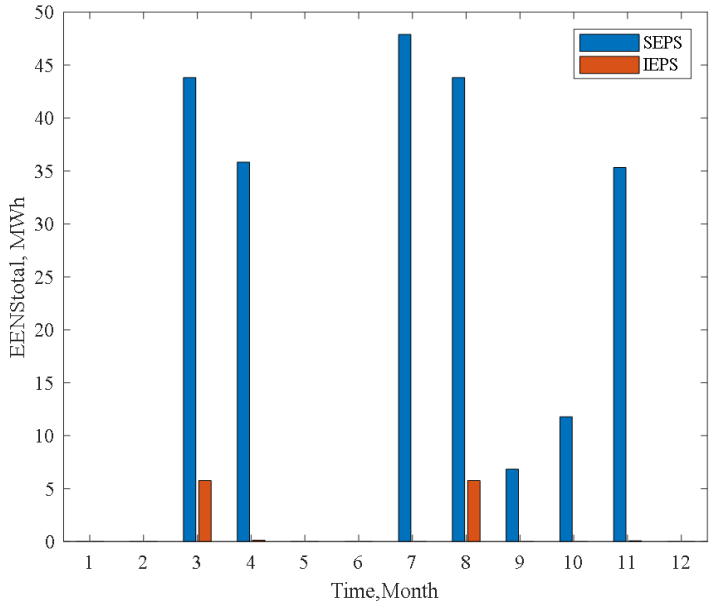

Fig. 7-10 The $EENS_{total}$ of the building complex with SEPS and IEPS

Table 7-4 The comparison of the SEPS and IEPS

Index		Stand-alone emergency power system	Integrated emergency power system	Rate %
Cp_i(kW)	$Building_1$	1900	1900	-
	$Building_2$	2200	2200	-
	$Building_3$	1500	1500	-
	Total	5600	5600	-
Total EENS (MWh)		220.34	8.99	-95.92%
Annual investment cost (million $)		0.134	0.134	0%
Annual operation cost (million $)		0.054	0.102	+89.32%
Annual maintenance cost (million $)		0.003	0.005	+89.32%
Outage loss (million $)		1.249	0.051	-95.90%
Total cost (million $)		1.440	0.293	-79.66%

The results showed that after integrating the emergency power system, the power supply reliability of the building complex improved as the total EENS reduces 95.92% and the total cost was saved by 79.66%. Once the EPSs can integrate with each other, when power outages occur in one of the buildings , not only its own emergency system can provide power, but also the emergency systems of the other two buildings can also be used as a supplement. In this case, the IEPS can make full use of the emergency power systems in the building complex, which increases the support time and capacity compared with the SEPS. Therefore, the total EENS was cut down significantly. It was indicated that the integration of emergency power system had a great effect on improvement of the power supply reliability.

7.2.3.4 Solution of the optimization simulation

Taking the minimum expense of the building complex as the objective function, the optimal configuration of the integrated emergency power system can be obtained using the Genetic Algorithm. It can be seen from Table 7-5 that the optimal installed capacity of the IEPS is 5010kW, which is decreased by 10.54% compared with the initial installed capacity, therefore the investment cost is saved by 10.60%. Under the optimal configuration, the total EENS could decrease by 94.23%, as a result, the total cost of the building complex can be cut down by 95.15%. The results evidently illustrated that the IEPS in the building complex can reduce the system investment cost by maximizing resource utilization. In this way, it can achieve investment cost saving as well as reliability improvement.

Table 7-5 The comparison of SEPS and IEPS with optimal configuration

Index		Stand-alone emergency power system	Integrated emergency power system with optimal configuration	Rate %
Cp_i(kW)	$Building_1$	1900	1860	-2.11%
	$Building_2$	2200	1680	-23.64%
	$Building_3$	1500	1470	-2.00%
	Total	5600	5010	-10.54%
Total EENS (MWh)		220.34	10.65	-94.23%
Annual investment cost (million $)		0.134	0.120	-10.60%
Annual operation cost (million $)		0.054	0.102	+88.62%
Annual maintenance cost (million $)		0.003	0.005	+88.62%
Outage loss (million $)		1.249	0.061	-95.15%
Total cost (million $)		1.440	0.288	-80.03%

7.2.4 Impact of characteristics parameters of EPSs on the total cost

It is of vital need to determine the sensitivity of the final results to the possible variations in the input data. This part mainly studied the impact of characteristics parameters of EPS on the total cost of the building complex. As Equation (7-7) demonstrated, the power outage loss is influenced by the startup time, maximum support time and the fuel replenishment time of the EPS. From Equation (7-8) ~ (7-12), the system cost is influenced by the investment cost, the fuel cost, and the maintenance cost per unit capacity of the EPS. Therefore, these six impact factors are changed in multiples and their impacts on the total cost are investigated.

Results were shown in Fig.7-11. The reduction of startup time or fuel replenishment time can decrease the total cost. On the contrary, the increase of maximum support time will cut down the total cost. And the total cost was sharply mounting with the growth of unit investment cost, unit fuel cost and unit maintenance cost. This is because the power outage duration and EENS of the building complex were lessened with the reduction of startup time or fuel replenishment time and the increase of maximum support time. Thereby, the power outage loss would decrease. In addition, the climbing in unit investment costs, unit fuel costs and unit maintenance cost had led to an increase in the system costs of EPSs, so the total cost of the building complex was rising. The above conclusions verify the correctness and applicability of the optimization model.

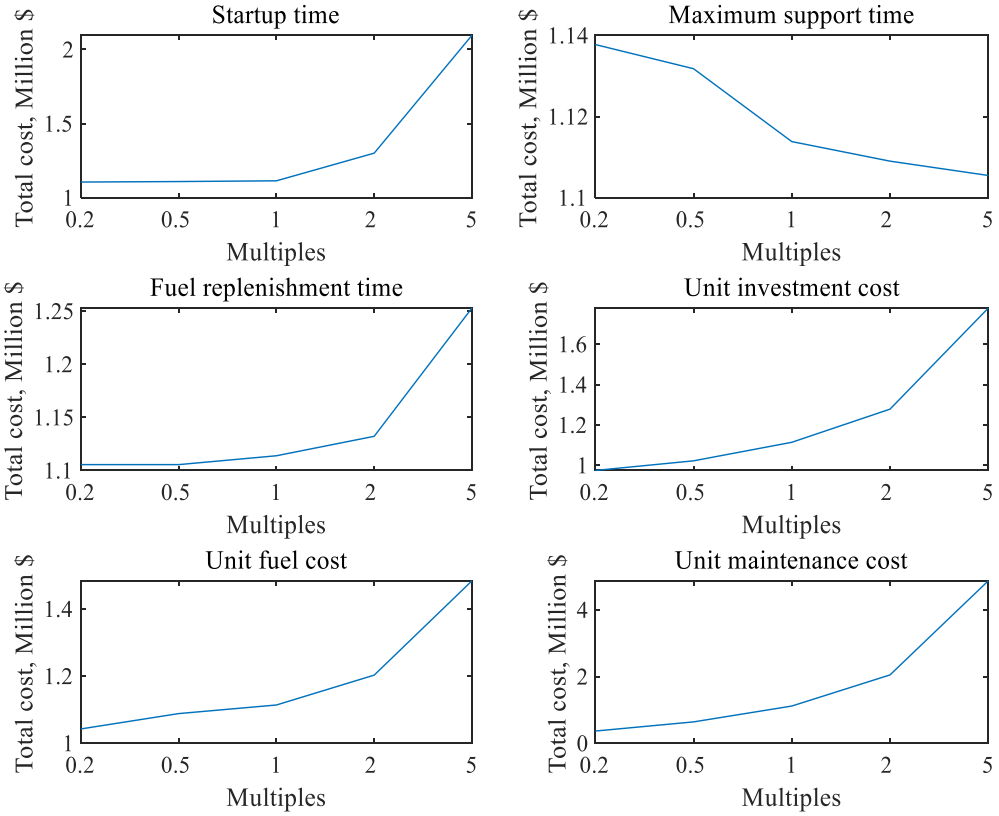

Fig.7-11 The impact of characteristics parameters on the total cost of the building complex

The characteristics of the equipment in EPSs determine the power supply reliability of the building complex. In order to reduce the total cost of emergency power system in the building complex, hybrid emergency power systems that combining diesel generators with other distributed energy system can be considered for power supply, which can save the energy and improve the carbon emission reduction.

7.3 Reliability and economic analysis of distributed generation as emergency power

Diesel generators have several drawbacks to their use as the emergency power generator. Diesel generators rely on a fossil fuel that has seen its retail price increase over 200% in the last five years [28]. Diesel generators are generally noisier and emit more pollutants than technologies relying on distributed energy resources, although both of these negative characteristics have improved-since 1980, diesel engines have reduced emissions of NOx and particulate matter by 90% [29]. Diesel generators also need to be operated approximately once per month if used as standby power, which increases the maintenance cost.

The distributed energy system provides efficient, low-cost, clean energy, enhance local resiliency, and improve the operation and stability of the regional electric grid. The power to isolate from the larger grid makes DES resilient, and the ability to conduct flexible, parallel operations permit the delivery of services that make the grid more competitive. By "islanding" from the grid in emergencies, a DES can both continue serving its included load when the grid is down and serve its surrounding community by providing a platform to support critical services from hosting first responders and governmental functions to providing key services and emergency shelter. Intelligent integration of distributed generator and diesel generator set into emergency power system will reduce the outage duration and the interruption cost and also increase the revenue of the utilities owing to quick power restoration and the improved utilization of the distribution system capacity.

When the utility grid fails, the buildings only rely on the emergency power system for power support. Therefore, the improvement of the reliability of the emergency power system is the key factor to reduce the power outage loss and improve the reliability and economy of power supply. With the access of DESs, the reliability of emergency power system will be changed. And different connection modes of the diesel generators with DES have great influence on the reliability of energy supply system. The reliability and economic performance were analyzed when the integration of the distributed energy system with the emergency power system in this section.

7.3.1 Reliability analysis of power system

The comparison of reliability and availability shows that reliability is only related to failure rate while availability is related to both failure rate and repair rate. For a repairable energy supply system, the repair time cannot be ignored because it affects the calculation of downtime cost. Therefore, despite the EENS, the availability also can be used to present the reliability of the power supply system.

After application of the DESs as emergency power when the power outages occur, a more complex power system is established with diverse power generators. Therefore, the system reliability indices depend on the reliability of each component of the system and their connection modes. The connection modes of the power generators can be divided into series and parallel.

For a series system, the reliability indices can be expressed as follows:

$$\lambda_{system} = \lambda_1 + \lambda_2 + \cdots + \lambda_n \tag{7-20}$$

$$\mu_{system} = \frac{\lambda_1 + \lambda_2 + \cdots + \lambda_n}{\frac{\lambda_1}{\mu_1} + \frac{\lambda_2}{\mu_2} + \cdots + \frac{\lambda_n}{\mu_n}} \tag{7-21}$$

For a parallel system, let $r = 1/\mu$. The reliability metrics can be presented as the following:

$$\lambda_{system} \approx (r_1 + r_2 + \cdots + r_n) \times \lambda_1 \lambda_2 \ldots \lambda_n \tag{7-22}$$

$$\mu_{system} = \mu_1 + \mu_2 + \cdots + \mu_n \tag{7-23}$$

7.3.2 Case comparison

As Section 7.2.2 described, the emergency power system (EPS) adopted the diesel generator is allocated in each building. When the utility grid interrupted, the building complex only relies on the EPSs for power support. During this period, all the sub-EPSs should be turned on to supply the maximum power. Thus, the reliability of the IEPS changes from a parallel system into a series system when the building complex is all in a power outage. The impact of the reliability of the emergency power system (AF and EENS) on the power outage loss of the building complex is significant.

Since the distributed energy systems are set near the demand side, the local load can be maintained by the resources available locally. When the utility grid fails, the distributed generation is also a source of emergency power, which can reduce the cost and pollution of the emergency energy system which adopts diesel generator, improve the reliability of the power supply system and minify the power outage loss. The output of distributed generation and its connection mode of generators will affect the reliability of the power system and outage loss of the building complex. This section proposes four different cases of the emergency power systems integrated with distributed generation, and their reliability and economic performance are calculated and compared.

7.3.2.1 Introduction and reliability indices calculation of proposed cases

As one of the distributed generations, the gas internal combustion engine (ICE) is a high overall efficiency technology, which can supply reliable and controllable energy regardless of time. Therefore, in this research, taking the ICE as an example, four different cases were proposed to analyze the reliability and economic performance of the emergency power system integrated with the distributed energy system.

1) Case 1:

   In Case 1, the ICE is the ICE is in series with diesel generators (DG). The reliability block diagram of the emergency power system is shown in Fig.7-12. DG_1, DG_2, and DG_3 are emergency power systems of $Building_1$, $Building_2$, and $Building_3$, respectively.

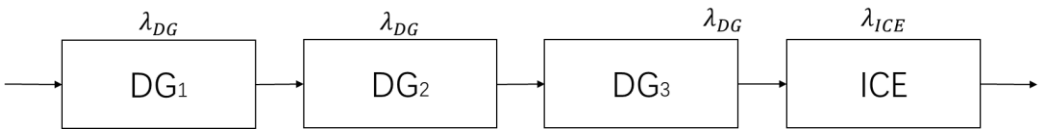

Fig.7-12 Reliability block diagram of Case 1

The diesel generators are in series, so the reliability indices of Case 1 can be expressed as:

$$\lambda_0 = \lambda_{DG} + \lambda_{DG} + \lambda_{DG} + \lambda_{ICE} = 3\lambda_{DG} + \lambda_{ICE} \tag{7-24}$$

$$\mu_0 = \frac{\lambda_{DG} + \lambda_{DG} + \lambda_{DG} + \lambda_{ICE}}{\frac{\lambda_{DG}}{\mu_{DG}} + \frac{\lambda_{DG}}{\mu_{DG}} + \frac{\lambda_{DG}}{\mu_{DG}} + \frac{\lambda_{ICE}}{\mu_{ICE}}} = \frac{3\lambda_{DG} + \lambda_{ICE}}{\frac{3\lambda_{DG}}{\mu_{DG}} + \frac{\lambda_{ICE}}{\mu_{ICE}}} \tag{7-25}$$

2) Case 2:

In Case 2, the ICE is in parallel with DG_3 and in series with DG_1 and DG_2. The ICE can reduce the output of DG_3 to supply emergency power. And when the ICE is failure, the DG_3 is used as a backup system to supplement. The reliability block diagram of Case 2 is displayed in Fig.7-13. The failure rate and repair rate of Case 2 are calculated as follows:

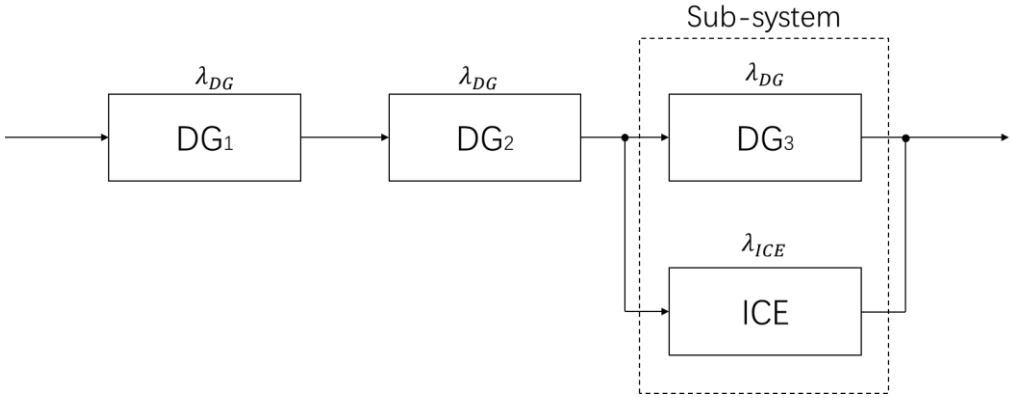

Fig.7-13 Reliability block diagram of Case 2

For a sub-system, the ICE and DG_3 is in parallel, so the reliability indices can be expressed as follows:

$$\begin{cases} \lambda_{SB} \approx (r_1 + r_2) \times \lambda_{DG} \times \lambda_{ICE} = (\frac{1}{\mu_{DG}} + \frac{1}{\mu_{ICE}}) \times \lambda_{DG} \times \lambda_{ICE} \\ \mu_{SB} = \mu_{DG} + \mu_{ICE} \end{cases} \tag{7-26}$$

where, λ_{DG}, μ_{DG} are the failure rate and repair rate of the DG, respectively. λ_{ICE}, μ_{ICE} are the failure rate and repair rate of the ICE, respectively.

The sub-system is in series with DG_1 and DG_2, so the reliability indices of Case 2 can be expressed as:

$$\lambda_1 = \lambda_{DG} + \lambda_{DG} + \lambda_{SB} = 2\lambda_{DG} + (\frac{1}{\mu_{DG}} + \frac{1}{\mu_{ICE}}) \times \lambda_{DG} \times \lambda_{ICE} \tag{7-27}$$

$$\mu_1 = \frac{\lambda_{DG} + \lambda_{DG} + \lambda_{SB}}{\frac{\lambda_{DG}}{\mu_{DG}} + \frac{\lambda_{DG}}{\mu_{DG}} + \frac{\lambda_{SB}}{\mu_{SB}}} = \frac{2\lambda_{DG} + (\frac{1}{\mu_{DG}} + \frac{1}{\mu_{ICE}}) \times \lambda_{DG} \times \lambda_{ICE}}{\frac{2\lambda_{DG}}{\mu_{GD}} + \frac{(\frac{1}{\mu_{DG}} + \frac{1}{\mu_{ICE}}) \times \lambda_{DG} \times \lambda_{ICE}}{\mu_{DG} + \mu_{ICE}}} \tag{4-28}$$

3) Case 3:

In Case 3, the ICE is in parallel with DG_2 and DG_3 and in series with DG_1. The ICE can reduce the output of DG_2 and DG_3 to supply emergency power. And when the ICE is failure, the DG_2 and DG_3 is used as a backup system to supplement. The reliability block diagram of Case 3 is displayed in Fig.7-14. The failure rate and repair rate of Case 3 are calculated as follows:

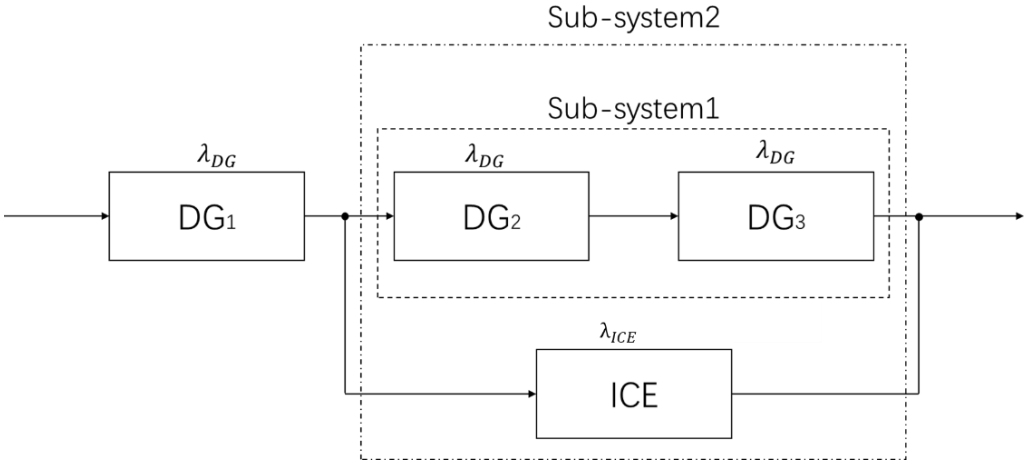

Fig.4-14 Reliability block diagram of Case 3

For a sub-system$_1$, the DG_2 and DG_3 is in series, so the reliability indices can be expressed as follows:

$$\begin{cases} \lambda_{SB_1} = \lambda_{DG} + \lambda_{DG} = 2\lambda_{DG} \\ \mu_{SB_1} = \dfrac{\lambda_{DG}}{\mu_{DG}} + \dfrac{\lambda_{DG}}{\mu_{DG}} = \dfrac{2\lambda_{DG}}{\mu_{DG}} \end{cases} \tag{7-29}$$

For a sub-system$_2$, the ICE is in parallel with sub-system$_1$, so the reliability indices can be expressed as follows:

$$\begin{cases} \lambda_{SB_2} \approx \left(r_{SB_1} + r_{ICE}\right) \times \lambda_{SB_1} \times \lambda_{ICE} = (\dfrac{\mu_{DG}}{2\lambda_{DG}} + \dfrac{1}{\mu_{ICE}}) \times 2\lambda_{DG} \times \lambda_{ICE} \\ \mu_{SB_2} = \mu_{SB_1} + \mu_{ICE} = \dfrac{2\lambda_{DG}}{\mu_{DG}} + \mu_{ICE} \end{cases} \tag{7-30}$$

The sub-system$_2$ is in series with DG_1, so the reliability indices of Case 3 can be expressed as:

$$\lambda_2 = \lambda_{DG} + \lambda_{SB_2} = \lambda_{DG} + (\frac{\mu_{DG}}{2\lambda_{DG}} + \frac{1}{\mu_{ICE}}) \times 2\lambda_{DG} \times \lambda_{ICE} \tag{7-31}$$

$$\mu_2 = \frac{\lambda_{DG} + \lambda_{SB_2}}{\dfrac{\lambda_{DG}}{\mu_{DG}} + \dfrac{\lambda_{SB_2}}{\mu_{SB_2}}} = \frac{\lambda_{DG} + (\dfrac{\mu_{DG}}{2\lambda_{DG}} + \dfrac{1}{\mu_{ICE}}) \times 2\lambda_{DG} \times \lambda_{ICE}}{\dfrac{\lambda_{DG}}{\mu_{DG}} + \dfrac{(\dfrac{\mu_{DG}}{2\lambda_{DG}} + \dfrac{1}{\mu_{ICE}}) \times 2\lambda_{DG} \times \lambda_{ICE}}{\dfrac{2\lambda_{DG}}{\mu_{DG}} + \mu_{ICE}}} \tag{7-32}$$

4) Case 4:

In Case 4, the ICE is in parallel with DG_1, DG_2 and DG_3. The ICE can reduce the output of the diesel generators to supply emergency power. And when the ICE is failure, the diesel generators are used as a backup system to supplement. The reliability block diagram of Case 4 is displayed in Fig.7-15. The failure rate and repair rate of Case 4 are calculated as follows:

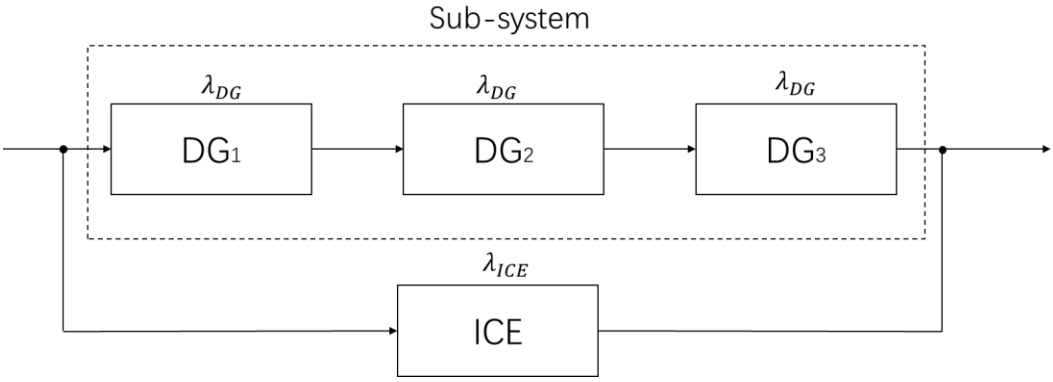

Fig.7-15 Reliability block diagram of Case 4.

For a sub-system, the DG_1, DG_2 and DG_3 is in series, so the reliability indices can be expressed as follows:

$$\begin{cases} \lambda_{SB} = \lambda_{DG} + \lambda_{DG} + \lambda_{DG} = 3\lambda_{DG} \\ \mu_{SB} = \dfrac{\lambda_{DG} + \lambda_{DG} + \lambda_{DG}}{\dfrac{\lambda_{DG}}{\mu_{DG}} + \dfrac{\lambda_{DG}}{\mu_{DG}} + \dfrac{\lambda_{DG}}{\mu_{DG}}} = \mu_{DG} \end{cases} \tag{7-33}$$

The sub-system is in parallel with the ICE, so the reliability indices of Case 4 can be expressed as:

$$\lambda_3 \approx (r_{SB} + r_{ICE}) \times \lambda_{ICE} \times \lambda_{ICE} = (\frac{1}{\mu_{DG}} + \frac{1}{\mu_{ICE}}) \times \lambda_{ICE} \times \lambda_{ICE} \tag{7-34}$$

$$\mu_3 = \mu_{SB} + \mu_{ICE} = \mu_{DG} + \mu_{ICE} \tag{7-35}$$

After calculating the failure and repair rate of each case, the availability factor (AF) of the power supply system can be obtained from the following formula:

$$AF_i = \frac{\mu_i}{\lambda_i + \mu_i} \tag{7-36}$$

From the calculation, we can see that the availability of the system is determined by the failure rate and repair rate of the components and their connection mode, but it is unconcerned with the installed capacity of the power supply system.

7.3.2.2 The parameters of the proposed cases

Four cases are modelled by using the technical specifications, cost parameters and reliability

indices of each component of the system as shown in Table 7-6. And the Table 7-7 shows the configurations of the case study. The technical and cost details as presented in Table 7-6 are used to assess the economic and reliability viability of distributed energy technologies in an emergency power system.

Table 7-6 Technical and cost parameters [20,26,27]

Parameters	Diesel generator	Gas internal-combustion engine
Failure rate	0.032	0.66767
Repair rate	21.8920	31
CT_k (h)	12	Always
SD_k (h)	1/6	2/15
IN_k (\$/kW)	300	971
f_k (\$/kWh)	0.23	0.039
M_k (\$/kWh)	0.01258	0.01143
FRT_k (h)	24	0

Table 7-7 Configurations of the case studies.

Equipment	Case 1	Case 2	Case 3	Case 4
DG_1 (kW)	1860	1860	1860	1860
DG_2 (kW)	1680	1680	1680	1680
DG_3 (kW)	1470	1470	1470	1470
ICE (kW)	500	2000	4000	5500

The reliability and economic performance of these four cases are calculated and compared to assess the benefits of the distributed generations as emergency power.

7.3.3 Results and discussion

7.3.3.1 Reliability performance comparison

Based on the reliability indices, the availability factor (AF) and EENS are used to evaluate the reliability of the four cases with different configurations. The values of several reliability indices parameters for four case studies are presented in Table 7-8. It can be seen from the table that the power supply reliability can be improved with the application of distributed generation. According to the reliability calculation formula in Section 7.3.2, the availability factor is unconcerned with the installed capacity of the power supply system, but the type of generator units and the connection mode of the power supply has a significant impact on the reliability. Compared with Case 1, the availability is improved by 0.143% of Case 2, the availability of Case 3 increased by 0.341% and the Case 4 is 0.429% higher than that of Case 1, as shown in Fig.4-16. Therefore, the connection mode of Case 4 is optimal. Distributed generation and emergency power system can be backup for each other under a parallel connection to improve the overall reliability of power supply.

Table 7-8 Reliability indices of four cases

Case	λ	μ	AF	EENS
Case 1	0.764	29.46	0.97473	218.30
Case 2	0.066	22.22	0.99705	138.02
Case 3	0.035	36.45	0.99903	56.60
Case 4	0.005	52.89	0.99991	4.42

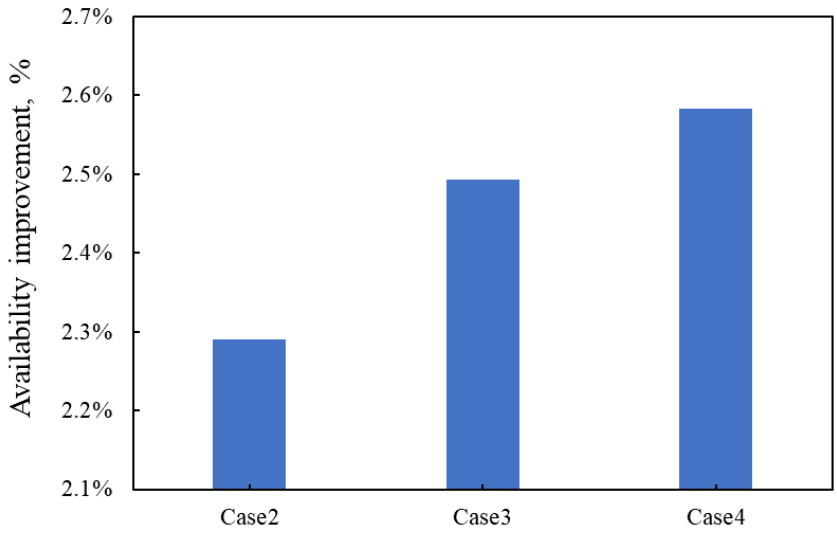

Fig.7-16 Availability improvement with the application of distributed generation.

According to proposed Monte Carlo simulation in Section 7.2, the power outage loss can be calculated. Fig.7-17 demonstrated the EENS and power outage loss of four cases. After the application of distributed generation, the annual EENS and power outage loss are greatly reduced. Because the distributed generation and the diesel generators are in parallel connection to supply power, thus, when the distributed generation fails, the diesel generators can be used as a backup to supplement, which greatly reduces the duration of power outage and the cost of interruption. As Fig.4-18 shows, compared with Case 1, the annual EENS and the power outage loss of Case 2 is reduced by 36.77%. And the annual EENS and power outage loss of Case 3 is 74.07% lower than that of case 1, respectively. The reliability of Case 4 is the best, and the annual EENS and power outage loss is the lowest, which reduce 97.98% comparing with Case 1.

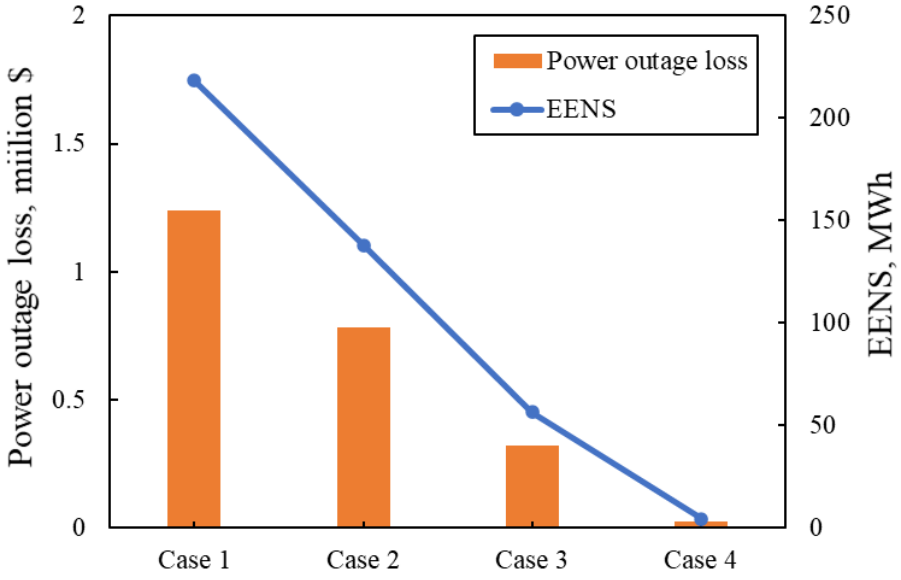

Fig.7-17 Annual EENS and power outage loss of four cases

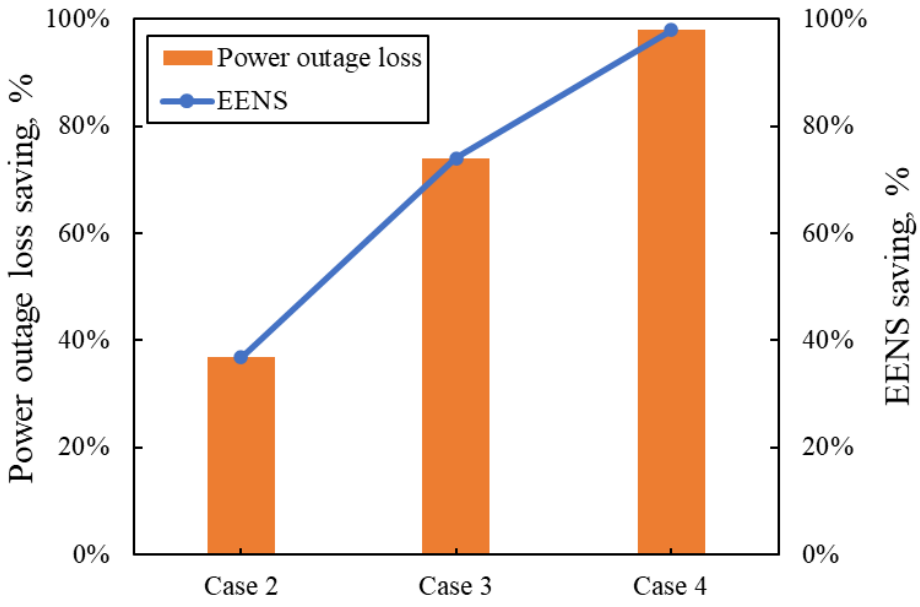

Fig.7-18 EENS and power outage loss saving after application of distributed generation

7.3.3.2 Economic performance comparison

The economic performance is composed of the annualized investment cost (AIC), annualized operation cost (AOC), and annualized maintenance cost (AMC). Fig.7-19 displays the annualized costs of four cases. The total cost of Case 1 is 4.09 million $, of which AIC is 0.23 million $, AOC is 3.26 million $, and AMC is 0.59 million $. The total cost of Case 2 is 3.82 million $, of which AIC is 0.4 million $, AOC is 2.84 million $, and AMC is 0.58 million $. The total cost of Case 3 is 3.47 million $, of which AIC is 0.63 million $, AOC is 2.28 million $, and AMC is 0.56 million $.

The total cost of Case 4 is 3.21 million $, of which AIC is 0.80 million $, AOC is 1.86 million $, and AMC is 0.55 million $. The cost comparison of four cases is shown in Fig.7-20. The AOC saving is the most, because the fuel cost of the ICE is cheaper and the DG. The ICE can used to replace DG for energy supply, which reduces the output of DG. Therefore, the operation cost and maintenance cost of the system are fell down. Compared with Case 1, the installed capacity of the ICE increases gradually, so AIC of Case 2, Case 3 and Case 4 are increased. Overall, although the AIC of Case 4 increases most, the total system cost of Case 4 is the least.

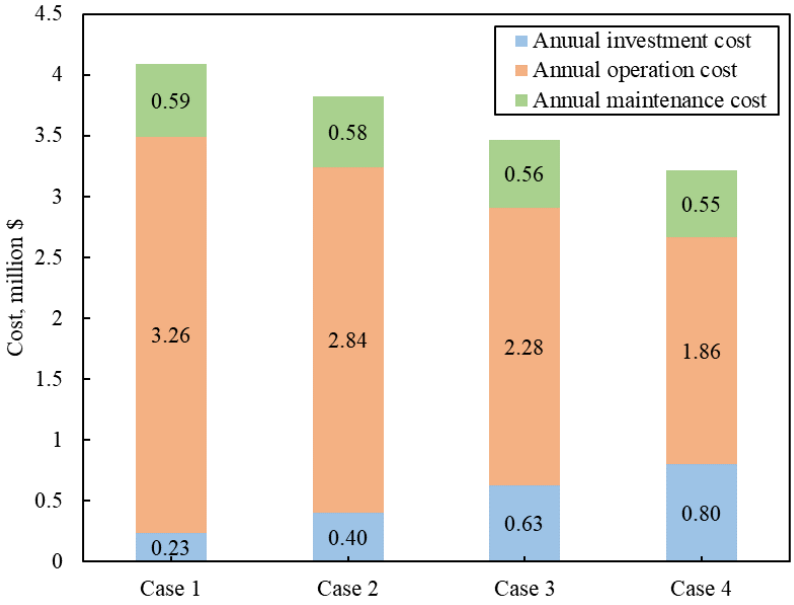

Fig.7-19 Annualized costs of the proposed cases.

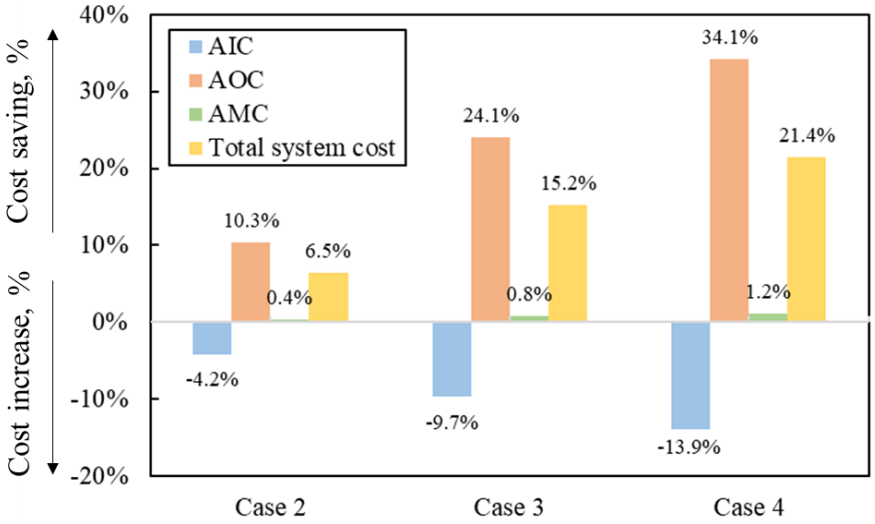

Fig.7-20 Costs comparison of the proposed cases.

Through the comparison of four cases, the results obtained from this study have established that the improvements in the reliability of a power system can be achieved with the incorporation of

distributed generation units. After integrating the DES with the emergency power system, they can be backup for each other in a parallel connection. Thus, the interrupt duration can be reduced. Moreover, with the increase of the ICE configuration, the EENS declines significantly and more power outage loss is avoided. And the integration of DES with the emergency power system has demonstrated its effect on the operating costs of the system. The fuel consumption cost and maintenance cost can be greatly saved as the output of DES increases. The results prove that the DES can greatly save the operation and maintenance costs as well as improve the reliability of the emergency power system.

7.4 Summary

In order to improve reliability and reduce power outage loss, the emergency power system is an indispensable part of regional power supply system. This chapter is divided into two parts to analyze the reliability improvement of the power supply in a building complex with the utilization of the DES as emergency power system.

Firstly, optimize the emergency power system integration. According to the concept of micro-network, the integrated emergency power system (IEPS) can serve multiple buildings more safely and economically in a building complex. Due to the different probability of distribution network failure in each building, the stand-alone emergency power system of each building can integrate and dispatch to maximize the utilization of resources. Therefore, this chapter proposed an integration emergency power system (IEPS) by connecting the stand-alone emergency power subsystems with the micro-network and backing up each other to achieve the purpose of improvement in reliability and economy. And taking the minimum total cost consisted of system cost and power outage loss as the objective function, the optimal capacity and dispatch strategy are obtained by using the Genetic Algorithm. This chapter takes a building complex in Shanghai as an example to verify the superiority of the model. The results show that after application of the proposed model, the EENS is reduced by 92.57%. The total cost is cut down by 69.58%, of which the cost of emergency power systems is reduced by 4.43%, and the power outage loss is reduced by 92.57%. It is indicated that the proposed integration and dispatch model of the emergency power systems can reduce the cost of the emergency systems as well as improve the reliability of buildings.

Secondly, the impact of the combination of the distributed energy system and the emergency power system on system reliability and economy is analyzed. Different configurations of distributed generation and the connection mode of the generators will affect the reliability of the overall power supply system. Therefore, four different configurations of distributed generation and connection modes are proposed to calculate the reliability and economic performance after integrating the distributed generation with the emergency power system. Due to the integration of the DES, distributed generation and the emergency power system can be backup for each other under a parallel connection. The results showed that the availability of the overall power system improved after application of the DES, and the power outage loss of the building complex was declined because of the drop in the EENS. In addition, the AOC and AMC that carry the largest percentage of the total cost of the system have been reduced considerably after the application of the distributed generation. It is obvious suggested from this study that significant savings in operation and maintenance costs as well as a considerable improvement in the reliability of the emergency power system have been achieved with the incorporation of distributed generations.

It can be deduced that the users should encourage the integration of distributed generation into the emergency power system as an alternative way to increase the reliability of power supply under power outage.

Appendix:

In a region, three different kinds of buildings: a commercial high-rise building (Building1), an office high-rise building (Building2), and a central business district building (Building3) (hereinafter referred to as B1, B2, B3) are adjacent buildings. The upper end is led by two 35kV transformer stations. Each building has four 10kV transformers, and each of the two transformers is spared, as shown in Table A7-1. (For example, the transformer of B1 is T1-1, T1-2., T1-3, and T1-4, in which the transformers T1-1 and T1-2 are reserved for each other, and the T1-3 and T1-4 are alternate with each other). The schematic diagram of the distribution network in this region is shown in Fig.A7-1 below. B1, B2 and B3 are all high-rise buildings, where the load is divided into first, second and third levels. The load point distribution and power reliability parameters of the three buildings is shown in Table A7-2 and Table A7-3 as below.

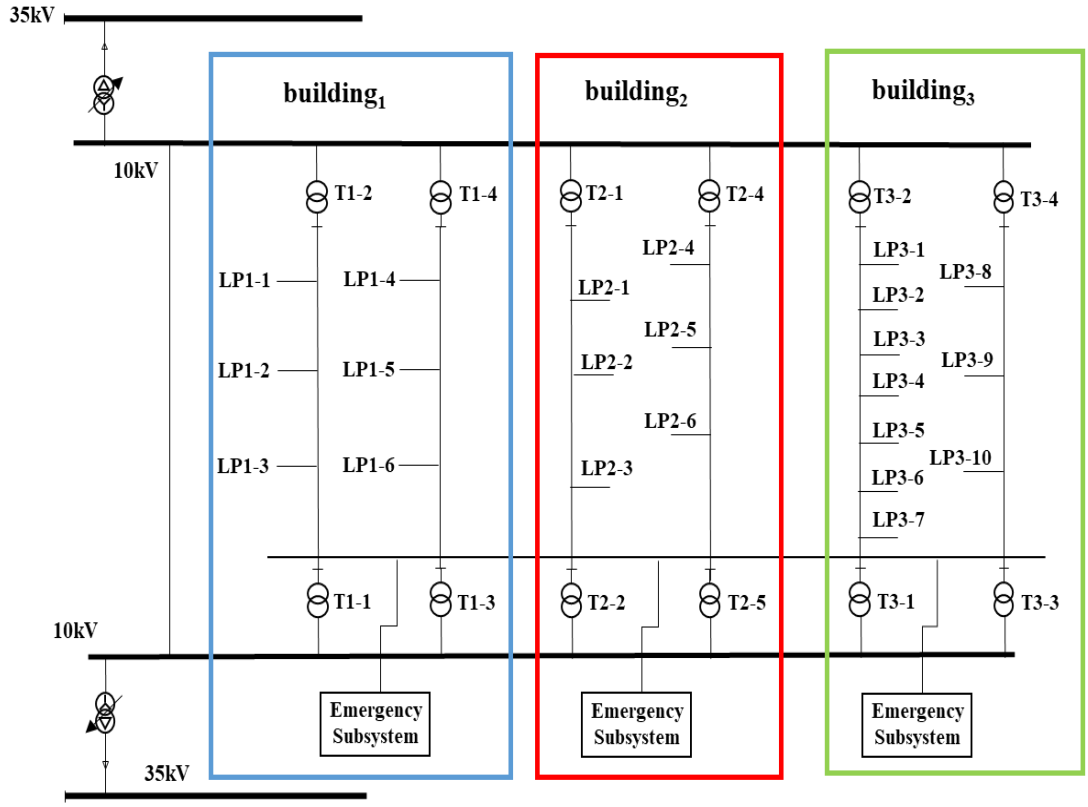

Fig. A7-1 Schematic diagram of the distribution network

Table A7-1 Overview of three buildings' power distribution information

Building name	$Building_1$ (B_1)		$Building_2$ (B_2)		$Building_3$ (B_3)	
The type of building	Commercial		Office		Central business district	
Power load	4935kW		4985kW		7298kW	
First and second-level load	1819kW		2165kW		1473kW	
Transformer sequence number and power	T1-1	1250kW	T2-1	1250kW	T3-1	2000kW
	T1-2	1250kW	T2-2	1250kW	T3-2	2000kW
	T1-3	1250kW	T2-3	1250kW	T3-3	2000kW
	T1-4	1250kW	T2-4	1250kW	T3-4	2000kW

Table A7-2 Transformer and Load Point Distribution in three buildings

Building	Transformer	Load point	Demand load (MW)
$Building_1$	T1-1 T1-2	LP1-1	530
		LP1-2	890
		LP1-3	850
	T1-3 T1-4	LP1-4	1250
		LP1-5	1100
		LP1-6	315
$Building_2$	T2-1 T2-2	LP2-1	630
		LP2-2	910
		LP2-3	850
	T2-3 T2-4	LP2-4	1250
		LP2-5	1000
		LP2-6	345
$Building_3$	T3-1 T3-2	LP3-1	900
		LP3-2	570
		LP3-3	998
		LP3-4	900
		LP3-5	590
		LP3-6	438
		LP3-7	500
	T3-3 T3-4	LP3-8	920
		LP3-9	774
		LP3-10	708

Table A7-3 Power reliability parameters of building loads

Load point	Power consumption	First and second-level load	λ	r	Reliability
Region	17218	5457	-	-	-
T1-1/1-2	3769	1499	0.072	39	0.99989
T1-3/1-4	2985	320	0.072	39	0.99989
T2-1/2-2	4223	1833	0.072	39	0.99989
T2-3/2-4	2927	332	0.072	39	0.99989
T3-1/3-2	6049	1153	0.072	39	0.99989
T3-3/3-4	2722	320	0.072	39	0.99989
LP1-1	1825	1295	0.314	11.17	0.99960
LP1-2	988	98	0.321	10.96	0.99960
LP1-3	956	106	0.321	10.96	0.99960
LP1-4	1400	150	0.241	4.1915	0.99988
LP1-5	1232	132	0.321	10.96	0.99960
LP1-6	353	38	0.3303	11.1	0.99958
LP2-1	769	139	0.269	12.7	0.99961
LP2-2	1030	120	0.321	10.96	0.99960
LP2-3	2424	1574	0.321	10.96	0.99960
LP2-4	1410	160	0.241	4.1915	0.99988
LP2-5	1128	128	0.321	10.96	0.99960
LP2-6	389	44	0.3303	11.1	0.99958
LP3-1	1112	212	0.2437	15.726	0.99956
LP3-2	704	134	0.269	12.7	0.99961
LP3-3	1233	235	0.2437	3.5198	0.99990
LP3-4	1112	212	0.2437	15.726	0.99956
LP3-5	729	139	0.269	12.7	0.99961
LP3-6	541	103	0.269	12.7	0.99961
LP3-7	618	118	0.269	12.7	0.99961
LP3-8	1075	155	0.321	10.96	0.99960
LP3-9	879	105	0.249	14.35	0.99959
LP3-10	768	60	0.249	14.35	0.99959

Reference:

[1] Abdullah MA, Agalgaonkar AP, Muttaqi KM. Assessment of energy supply and continuity of service in distribution network with renewable distributed generation. Appl Energy 2014;113:1015–26. https://doi.org/10.1016/j.apenergy.2013.08.040.

[2] Pagliaro M. Renewable Energy Systems : Enhanced Resilience , Lower Costs 2019;1900791:1–6. https://doi.org/10.1002/ente.201900791.

[3] Larsen PH, Lacommare KH, Eto JH, Sweeney JL. Recent trends in power system reliability and implications for evaluating future investments in resiliency. Energy 2016;117:29–46. https://doi.org/10.1016/j.energy.2016.10.063.

[4] Rusin A, Wojaczek A. Trends of changes in the power generation system structure and their impact on the system reliability. Energy 2015;92:128–34. https://doi.org/10.1016/j.energy.2015.06.045.

[5] Meier A, Ueno T, Pritoni M. Using data from connected thermostats to track large power outages in the United States. Appl Energy 2019;256:113940. https://doi.org/10.1016/j.apenergy.2019.113940.

[6] Pina A, Ferrão P, Fournier J, Lacarrière B, Corre O Le, Andri AI. ScienceDirect ScienceDirect ScienceDirect ScienceDirect Literature Review of Power System Blackouts Literature Review of Power System Blackouts Yuan-Kang Assessing the feasibility of using the a heat demand-outdoor Yuan-Kang Yi-Liang function for a long-t. Energy Procedia 2017;141:428–31. https://doi.org/10.1016/j.egypro.2017.11.055.

[7] Xiang L. Energy network dispatch optimization under emergency of local energy shortage with web tool for automatic large group decision-making. Energy 2017;120:740–50. https://doi.org/10.1016/j.energy.2016.11.125.

[8] Marqusee J, Jenket D. Reliability of emergency and standby diesel generators: Impact on energy resiliency solutions. Appl Energy 2020;268:114918. https://doi.org/10.1016/j.apenergy.2020.114918.

[9] Wang JJ, Fu C, Yang K, Zhang XT, Shi G hua, Zhai J. Reliability and availability analysis of redundant BCHP (building cooling, heating and power) system. Energy 2013;61:531–40. https://doi.org/10.1016/j.energy.2013.09.018.

[10] Zhang P, Li W, Li S, Wang Y, Xiao W. Reliability assessment of photovoltaic power systems: Review of current status and future perspectives. Appl Energy 2013;104:822–33. https://doi.org/10.1016/j.apenergy.2012.12.010.

[11] Xue H, Birgersson E, Stangl R. Correlating variability of modeling parameters with photovoltaic performance: Monte Carlo simulation of a meso-structured perovskite solar cell. Appl Energy 2019;237:131–44. https://doi.org/10.1016/j.apenergy.2018.12.066.

[12] Ahn H, Rim D, Pavlak GS, Freihaut JD. Uncertainty analysis of energy and economic performances of hybrid solar photovoltaic and combined cooling , heating , and power (CCHP + PV) systems using a Monte-Carlo method. Appl Energy 2019;255:113753. https://doi.org/10.1016/j.apenergy.2019.113753.

[13] Kumar R, Saxena D. A Literature Review on Methodologies of Fault Location in the Distribution System with Distributed Generation 2020;1901093:1–12. https://doi.org/10.1002/ente.201901093.

[14] Assessment R. An Analytical Approach for Bulk Power Systems Reliability Assessment 2006;8013:19–25. https://doi.org/10.13334/j.0258-8013.pcsee.2006.05.004.

[15] Zhu J, Zhang Y. A Frequency and Duration Method for Adequacy Assessment of Generation Systems with Wind Farms. IEEE Trans Power Syst 2019;34:1151–60. https://doi.org/10.1109/TPWRS.2018.2872821.

[16] Ali Kadhem A, Abdul Wahab NI, Aris I, Jasni J, Abdalla AN. Computational techniques for assessing the reliability and sustainability of electrical power systems: A review. Renew Sustain Energy Rev 2017;80:1175–86. https://doi.org/10.1016/j.rser.2017.05.276.

[17] Huda ASN, Živanović R. Improving distribution system reliability calculation efficiency using multilevel Monte Carlo method. Int Trans Electr Energy Syst 2017;27:1–12. https://doi.org/10.1002/etep.2333.

[18] Gubbala N, Singh C. Models and considerations for parallel implementation of monte carlo simulation methods for power system reliability evaluation. IEEE Trans Power Syst 1995;10:779–87. https://doi.org/10.1109/59.387917.

[19] Wang L, Singh C, Tan KC. Reliability evaluation of power-generating systems including time-dependent sources based on binary particle swarm optimization. 2007 IEEE Congr Evol Comput CEC 2007 2007:3346–52. https://doi.org/10.1109/CEC.2007.4424904.

[20] Adefarati T, Bansal RC. Reliability and economic assessment of a microgrid power system with the integration of renewable energy resources. Appl Energy 2017;206:911–33. https://doi.org/10.1016/j.apenergy.2017.08.228.

[21] Chao W, Zheng XU, Peng GAO, Yong C, Zhejiang U. Reliability Index Framework for Reliability Evaluation of Bulk Power System 2007;27.

[22] Chowdhury A. Application of customer interruption costs in transmission network reliability planning. IEEE Trans Ind Appl 2001;37:53–60.

[23] The Value of Lost Load (VoLL) in European Electricity Markets : Uses , Methodologies , Future Directions 2019.

[24] Adefarati T, Bansal RC. Reliability assessment of distribution system with the integration of renewable distributed generation. Appl Energy 2017;185:158–71. https://doi.org/10.1016/j.apenergy.2016.10.087.

[25] Vásquez P, Vaca Á. Methodology for Estimating the Cost of Energy not Supplied -Ecuadorian Case-. Proc 2012 6th IEEE/PES Transm Distrib Lat Am Conf Expo T D-LA 2012 2012. https://doi.org/10.1109/TDC-LA.2012.6319047.

[26] Jiang J, Gao W, Wei X, Li Y, Kuroki S. Reliability and cost analysis of the redundant design of a combined cooling, heating and power (CCHP) system. Energy Convers Manag 2019;199:111988.

https://doi.org/10.1016/j.enconman.2019.111988.

[27] Zhang L, Gao W, Yang Y, Qian F. Impacts of investment cost, energy prices and carbon tax on promoting the combined cooling, heating and power (CCHP) system of an amusement park resort in shanghai. Energies 2020;13. https://doi.org/10.3390/en13164252.

Chapter 8

CONCLUSION AND PROSPECT

CHAPTER EIGHT: CONCLUSION AND PROSPECT

CONCLUSION AND PROSPECT 8-1

8.1 Conclusion 8-1

8.2 Prospect 8-5

8.1 Conclusion

The high rate of world energy consumption caused by a growing population and global economic expansion coupled with rapid industrialization has necessitated a massive investment in reliable and efficient energy supply. With the rapid growth in energy demand, concerns about climate change, high prices of fossil fuels, and the depletion of fossil fuels, the countries around the world are changing the focus of the production of electricity from large, centralized power plants to local generation units scattered over the territory. As an ideal system for incorporating renewable energy sources, distributed energy systems (DESs) allow producing energy that is consumed in proximity to the points of production, thus reducing energy costs and carbon emissions, achieving energy self-sufficiency. The outstanding performance of DESs in reliability, economy, and environment is leading to an increased interest in its application. However, the implementation of DESs is still hindered. Lack of a comprehensive evaluation in the design and operation of the DESs is one of the major barriers. At present, the evaluation method of DESs is relatively simple and one-sided, which cannot reasonably and accurately evaluate the comprehensive benefits of DESs. Therefore, this study proposed a DES composed of photovoltaic, energy storage and gas engine, and its grid stabilization and carbon reduction potentials were analyzed. Focusing on these advantages, a multi-criteria evaluation method was established to optimize the system. Finally, different case study scenarios of the DES utilization were demonstrated. It is hoped to improve the core competitiveness of the DES and promote its development.

The main works and results can be summarized as follows:

In chapter one, RESEARCH BACKGROUND AND PURPOSE OF THE STUDY, analyzed the significance of the DES for future energy development. Through the analysis of the advantages of the DES, it shows that DESs have the ability to reduce the energy crisis and environmental pollution as well as increase energy security. In addition, the current development status of DES was investigated and the technologies that can be applied to DESs were introduced. Due to the advantages of energy conservation and environmental protection, DES has been vigorously developed by the government. However, the high investment cost and improper installed capacity are hindering the diffusion of the DES. Moreover, the evaluation method with a single criterion is also an obstacle for its promotion.

In chapter two, LITERATURE REVIEW OF THE DISTRIBUTED ENERGY SYSTEM, is mainly to sort out the research status of the DES. First of all, the research in design and operation strategy of DES were presented. Because the DES is a complex system composed of multiple devices and can supply multiple energy sources, its configuration design and operation strategy determine the achievements of the system, which is the main research focus of the DES. Secondly, the performances of the DES evaluated by previous literatures were reviewed and analyzed. Different evaluation methods will have significant impacts on the configuration and operation strategy of the DES. Trade-offs between different performances can be addressed by the multi-criteria evaluation analysis.

In chapter three, THEORIES AND METHODOLOGY OF THE STUDY, presented the methodological research and established the mathematical model. Firstly, the research motivation

for the research was expounded. Then, the models of energy units and the quantitative analysis of the reliability, economic and environmental performance of the DES were presented. Moreover, the simulation models and algorithms used in the follow-up study are provided.

In chapter four, ECONOMIC AND ENVIRONMENTAL ANALYSIS OF DISTRIBUTED ENERGY SYSTEM FOCUSING ON GRID STABILIZATION, explored the potential of the DES on grid stabilization performance and analyzed its economic and environmental benefits. Based on the actual load data of a Smart Community in Japan, a DES model equipped with PV, gas internal-combustion engine and battery energy storage system was established. Then, the impacts of the DES with different combinations on the proposed grid stabilization indices (independence ratio and peak shaving ratio) were compared. After that, under the objective function of the minimum annualized total cost of the users, the optimal combinations of the DES with different independence ratios and peak shaving ratios were obtained. The results showed that increasing the installed capacity of the gas internal-combustion engine could improve the independence ratio and peak shaving ratio, while the battery energy storage system has no contribution to the independence ratio, and only plays a role in peak shaving. The annualized total cost can be reduced at the low share of independence ratio by introducing the battery system, but it is not economic at high independence ratio. By comparing the investment cost and the annualized total cost of the optimal combinations of the DES under different independence ratios, it was indicated that the effect of the increase in the DES investment cost is small at high independence ratio. In addition, as the increase of independence ratio and peak shaving ratio, the emission reduction of the DES is also improved, which shows that the introduction of the DES is conducive to improving environmental benefits. But from the perspective of economic benefits, the introduction rate of the DES on the demand side has an economic optimal proportion. If continuing to increase the independence ratio, the gains of improving the grid stability and environment came at the expense of economic benefits. It is essential to balance both.

In chapter five, MULTI-CRITERIA ASSESSMENT FOR OPTIMIZING DISTRIBUTED ENERGY SYSTEM, proposed a multi-criteria evaluation method of the DES taking the economy, reliability and environment into consideration, and the effect of different evaluation criteria on the configuration optimization of each equipment in the DES was compared and analyzed. Firstly, the concept of peak load price and carbon tax is introduced, and the grid stabilization and carbon emission reduction effect achieved by the DES are converted into economic benefits and included in the total cost. After that, a configuration optimization model with the objective of minimizing the total cost is established based on the Genetic Algorithm. By comparing the optimization results of different PV penetration scenarios, it is found that with the increase of the PV penetration, the total cost of the DES decreased at the beginning but increased after the PV penetration exceeds 30%. And the installed capacity of the gas internal combustion engine decreases with the growth of PV penetration, but the installed capacity of the battery energy storage system will be improved with the expansion of the PV penetration. In addition, from the comparison of optimization results of different evaluation criteria as objective functions, the economic advantages of the gas internal combustion engine can be improved after adding peak load cost into the objective function of optimization simulation, because of its great contribution to grid stabilization; And carbon emissions have an important impact on the promotion of the PV, but the current level of carbon tax still cannot

reflect the advantages of the DES. When the carbon tax increases, the advantage of environmental benefit can significantly improve the penetration of the PV. Different evaluation criteria represent different achievements of the DES, which has a significant impact on the configuration of the equipment in the DES. Therefore, when optimizing the configuration of the DES, it is necessary to determine the optimization direction according to the evaluation criteria based on the urgent issues of local energy supply and power demand.

In chapter six, PROMOTION AND UTILIZATION OF THE DISTRIBUTED ENERGY SYSTEM: A CASE STUDY OF COMBINED COOLING, HEATING AND POWER SYSTEM, the utilization of the CCHP system and the impact of different factors on promoting the system were discussed. As a typical DES, CCHP system is identified as a sustainable energy development with its high efficiency. In this chapter, a CCHP system in an amusement park in Shanghai, China was used as an example for promotion research. Firstly, according to the actual configuration of the CCHP system, three CCHP systems with different penetration were proposed and simulated by TRNSYS simulation software. Secondly, the economic and environmental performance of these different penetration CCHP systems were evaluated based on the dynamic payback period and carbon dioxide emissions. Then, the impacts of investment cost, energy prices, investment subsidy, and a carbon tax on promotion of the CCHP system was discussed through the sensitivity analysis. According to the results, CCHP system could bring significant environmental benefits, but the economic performance decreases due to the excessive investment cost. In order to expand the application of CCHP system, two aspects in price and subsidy policy could be adjusted. Through calculation, the energy price has a greatest impact on the CCHP system economy. And the current subsidy can reduce the economic gap between the CCHP system and the conventional system, but it still needs to be increased by 1.71 times to achieve market competitiveness of the CCHP system with 100% penetration under the current investment cost and energy prices. In addition, the introduction of a carbon tax could accelerate the promotion of the CCHP system. When the carbon tax reaches $25/ton, the CCHP system becomes the best choice of energy supply system.

In chapter seven, RELIABILITY AND ECONOMIC ANALYSIS OF THE DISTRIBUTED ENERGY SYSTEM AS EMERGENCY POWER SYSTEM, the utilization of the DES as emergency power system under the power outage scenario was analyzed. Firstly, the stand-along emergency power system is optimized to improve the regional reliability with the least cost. To achieve this purpose, an emergency power system integration model was proposed by connecting the stand-alone emergency power subsystems with the micro-network and backing up each other. The superiority of this model was verified through an example of a building complex in Shanghai. The results showed that the proposed emergency power system integration model can reduce the cost of the emergency systems and improve the power supply reliability of the building complex. Secondly, when the power failure in the whole region, the distributed generation was considered as emergency power to integrate with the emergency power system. Four case studies were put forward and compared to analyze the impact of different configurations and connection modes on the reliability and economic benefits of the overall power system. The results showed that the availability of the power system was increased, and the power outage loss was reduced with the output growth of distributed generation. And because of the low fuel consumption cost of the distributed generation, the operation and maintenance costs could be greatly declined. It can be seen

that the application of distributed generations can significantly increase the reliability as well as achieve the operation and maintenance costs saving of the emergency power system.

In chapter eight, CONCLUSION AND PROSPECT have been presented.

To summary, this article evaluated the economic, reliability and environmental performance of a proposed DES composed of PV, BESS and ICE systems. Focusing on the grid stabilization and carbon emission reduction performance, a multi-criteria evaluation method was proposed to optimize the system. The DES can improve the grid stabilization through power supply independence augment and peak shaving. And the effect of the increase in the DES investment cost is becoming small with the growth of the independence ratio. From the perspective of economic benefits, the introduction rate of the DES on the demand side has an optimal proportion. High independence rates can improve power supply reliability and environmental benefits but will result in a loss of economic benefits. Focusing on grid stabilization and carbon emission reduction effect of the DES, a multi-criteria evaluation method considering the economic, reliability and environmental performance is established and proposed to optimize the structure and configuration. From the comparison of optimization results of different evaluation criteria, economic performance will increase the configurations of the PV and the BESS, while the peak shaving ability improves the installed capacity of the ICE. In addition, carbon tax has a significant role in promoting PV penetration. It is suggested that optimizing the configuration with multi-criteria evaluation can maximize the application potential of the DES and improve its market competitiveness. At last, the utilization of the DES was discussed through the CCHP system and emergency power supply system. The impact of different factors on promoting the CCHP system was carried out. It presented that increasing energy prices and subsidy policies could improve the economic benefits of DES. The introduction of carbon tax can effectively accelerate the development of the DES. From the results of analyzing the utilization of the DES as emergency power system, it can significantly increase reliability as well as achieve costs saving of the power system when it is used as emergency power.

This research analyzed grid stabilization effect of the proposed DES and used the multi-criteria evaluation to trade-off these different performances by taking comprehensive advantages of DES. The utilization of the DES as emergency power system to show the reliability improvement was also demonstrated in the research. It is hoped that it can provide theoretical reference and new ideas for the promotion and application research of the distributed energy system.

8.2 Prospect

With the development of the smart grid, DES will integrate more efficient, low-cost and intelligent equipment and technology, such as electric vehicles, hydrogen energy utilization equipment and so on. Therefore, except the grid stabilization and emission reduction, there is still room for further research on the application potentials of the DES.

In addition, when determining the evaluation criteria of DES, we only consider the main influence factor of CO_2 emission in the aspect of environmental indicators in this paper,, and do not consider the influence of SO_2, PM 2.5 and other pollutants. How to establish the calculation model of these pollution factors plays an important role in improving the evaluation system.